

DEVELOPMENT OF A NON-INVASIVE TOOL FOR MAMMALIAN SPERM

Teresa Vilanova Perez

St. Peter's College

University of Oxford

Supervised by: **Dr Kevin Coward**

Co-supervised by: **Dr Helen Elizabeth Townley**

Nuffield Department of Women's and Reproductive Health

Thesis submitted for the Degree of Doctor Philosophy

Trinity Term 2021

Acknowledgements

First and foremost, I would like to thank my supervisor, Dr Kevin Coward, for having trusted my potential and having given me the opportunity to carry out a DPhil in his group, this once in a life-time experience that has above exceeded any imaginable expectations; It has been magic, and deeply inspirational. Thank you Kevin, for having believed in me, having always supported and guided me in this 3 year and a half journey, after which I have seen myself become a proper scientist, and a better person.

Thank you too to my secondary supervisor Dr Helen Townley, whose engineering-like experience and out-of-the-box mindset has helped forge a more practical thinking process for my work, and having always offered her help whenever I needed so. I am also very grateful for having received the big support from one of our collaborators; Prof. Marc Yeste, having welcomed me to carry out a big portion of my work at his lab in Girona (Spain), and continuously given me a hand to more accurately plan my experiments with boar sperm.

Thanks as well to Celine Jones, our devoted lab manager, who has been like my third supervisor always ready and happy to help me out in the lab, having helped me be appointed as the Trainee Representative of the British Andrology Association, but also if I ever needed her for more personal matters. I wish I could ever become as organised, tidy and thoughtful as you are Celine.

A big thanks to my funding bodies; St. Peter's College, for having granted me a Gustav Scholarship, and SRF for their many travelling stipends, having both allowed me to accomplish my DPhil experience to the fullest.

I would also like to thank all my colleagues at my department whom have in a way or another helped me make myself comfortable in the laboratory at the John Radcliffe; Dr Rebecca Dragovic, for her patience with the NanoSight, Neva for transferring me some of her valuable experience with Western Blotting and her friendship, which I worship even more. And Dr Karl Morten, for having trained me to use the ClarioStar, which was an essential tool for my thesis, but also, and most important, for having always been caring about my well-being as a DPhil student.

I would also like to thank my lab colleagues; Xin, Yaqiong, Eissa, Shiyan and Sally, for having made my long stays in the office much more enjoyable, and for those after-work dinner trips to the many restaurants around Oxford.

Moreover, I would like to thank my friends; my Spanish ones that I am so heartfully thankful to have met at Oxford, my dearest friend Angy, my spanish ones ("Mis desfis" Ester, Miren, Javi, Pablo y Gil) y Cindy, Berni y Paula. A mis amigas, cuya amistad se ha reforzado incluso a pesar de la distancia, gracias a las cuales no he perdido la cabeza (Carol, Maria, Cristina, Blanqui desde Noruega, Charmin y Desi, y mi primo Alfonso).

Finalmente, quisiera agradecer con mayor intensidad si cabe, a mis padres, que me han dado la vida, y me han otorgado las mejores enseñanzas, mejores principios y no han dejado de mimarme, incluso siendo como para ellos el irme a vivir fuera haya sido tan duro. And at last but not least, a huge thank you to my life jacket, Oliver, por haber sido una parte esencial del final de esta etapa, por su paciencia e inconmensurable bondad, y hacerme sentir especial cada dia.

This thesis has reused material including figures, and text from an already published article for in which I am the first author.

Index

Glossary of Abbreviations **5**

ABSTRACT **9**

CHAPTER 1 ..... **11**

Mammalian Cell-based Nanotools in Reproductive Biology: A Non-Invasive Approach for Infertility Treatment 11

1.1 Assisted Reproductive Technology for the Treatment of Infertility: Potential Impact upon Gametes and Embryo Development 12

1.2 Nanotechnology for the Treatment of Infertility 24

1.3 Key Features of Extracellular Vesicles and their Potential Role in Infertility Treatment 27

1.4 Extracellular Vesicles in Human Reproduction 35

1.5 Theragnostic Applications of EVs and Future Perspectives in the Fields of Reproductive Biology and Medicine 42

1.6 Aims 51

CHAPTER 2 ..... **54**

The use of HEK293T cells and Mammalian Culture Methods for the Mass Isolation of HEK293T-derived Exosomes 54

2.1 Aim of this Chapter 55

2.2 Background 55

2.3 Hypothesis 59

2.4 Materials and Methods 59

2.5 Results 65

2.6 Discussion 68

2.7 Key findings 73

CHAPTER 3 ..... **74**

Assessment of the Short and Long-term Effects of HEK293T-derived Exosomes upon the Functionality of Mammalian Sperm 74

3.1 Aim of this Chapter 75

3.2 Background 75

3.3 Hypothesis 80

3.4 Materials and Methods 80

3.5 Results 88

3.6 Discussion 97

3.7 Key findings 100

CHAPTER 4 ..... **102**

A Detailed Investigation of the Specific Interaction Between HEK293T-derived Exosomes and Boar Sperm with Particular Focus on Internalization Mechanisms 102

4.1 Aim of this Chapter 103

4.2 Background 103

4.3 Hypothesis 107

4.4 Materials and Methods 108

4.5 Results 118

4.6 Discussion 132

4.7 Key findings 142

CHAPTER 5 ..... **143**

Functionalization of HEK293T-Derived Exosomes and Molecular Cargo Loading 143

5.1 Aim of this Chapter 144

5.2 Background 144

5.3 Hypothesis 149
5.4 Materials and Methods 149
5.2 Results 162
5.3 Discussion 169
5.4 Key Findings 173

CHAPTER 6 175

Final Discussion and Future Perspectives 175
6.1 Biocompatibility of HEK293T-derived Exosomes with Mammalian Sperm 178
6.2 Optimization of HEK293T-derived Exosomes as Efficient Nanocarriers for Drug Delivery 179
6.3 The Impact of HEK293T-derived Exosomes in Fertility and Other Clinical Applications 181
6.4 General Limitations 183
6.5 Conclusion and Next Steps 184

References 187

Appendix I 220

NTA Graphs Displaying the Differences in Size and Concentration Profiles of HEK293T-derived Exosomes Processed in Different Ways 220
I.I The Effect of Freeze/Thaw cycles 220

Appendix II 223

Appendix III 225

Appendix IV 226

Glossary of Abbreviations

AMH	Anti-Müllerian Hormone
ART	Assisted Reproductive Technology
BCA	Bicinchonic acid Assay
BTB	Blood-Testis Barrier
BODIPY	Bio-Maleimide (BODIPY FL N-(2-aminoethyl) maleimide
CASA	Computer Assisted Sperm Analysis
Ca^{2+}	Calcium
CFDA	5(6)-carboxyfluorescein diacetate
CFTR	Cystic Fibrosis Conductance Regulator
CFSE	Carboxyfluorescein Succinimidyl Ester
CMV	Cytomegalovirus
CTL	Non-exosome treated control samples
CPP	Cell Penetrating Peptide
CXS	Connexins
Cx-43	Connexin-43
DMEM	Dulbecco's Modified Essential Medium
dSTORM	Super-resolution microscope for single particle detection
ESCRT	Endosomal Sorting Complex Required for Transport
EV	Extracellular Vesicles
EXO	Exosome-treated samples
FBS	Foetal Bovine Serum
FDA	Food and Drug Administration
FSH	Follicle Stimulating Hormone

GFP	Green Fluorescent Protein
HCO_3^-	Bicarbonate
HEK293T	Human Embryonic Kidney 293T cells
HEPES	4-(2-hydroxyethyl)-1-pipe-razineethanesulfonic acid
HRCM	High-Resolution Confocal Microscopy
ICSI	Intracytoplasmic Sperm Injection
ILV	Internal Luminal Vesicle
ISEV	International Society for Extracellular Vesicles
IVF	*In Vitro* Fertilisation
LAMP2	Lysosomal-Associated Membrane Protein 2
LB	Lysogeny Broth
LH	Luteinizing Hormone
LIN	Linearity
MF	Membrane Fluidity
MHC	Major Histocompatibility Complex
MMP	Mitochondrial Membrane Potential
MISEV	Minimal Information for Studies of EVs guidelines
MSNPs	Mesoporous Silica Nanoparticles
MVB	Multivesicular Bodies
NTA	Nanoparticle Tracking Analysis
NON	Non-capacitating buffer
PBS	Phosphate-buffered Saline
PCR	Polymerase Chain Reaction
PI	Propidium Iodide
PLL	Poly-L-Lysine (PLL)

PMSF	Phenylmethanesulfonylfluoride
PUFA	Polyunsaturated Fatty Acid
P_4	Progesterone
RIPA	Radioimmunoprecipitation Assay
ROS	Reactive Oxygen Species
RT	Room Temperature
R18	Octadecyl Rhodamine B Chloride
R18-EXO	R18-labelled exosomes
SEC	Size-exclusion Chromatography
SEM	Standard Error of the Mean
SMGT	Sperm-mediated Gene Transfer
SMT	Sperm-mediated Transfer
SOC	Super Optimal Broth
SS	Side Scatter
SSC	Spermatogonial Stem Cell
STR	Straightness
TAE	Tris/Acetate/EDTA
TE	Tris/EDTA
TEM	Transmission Electron Microscopy
TIRFM	Total Internal Reflection Fluorescence Microscopy
TMA	Testicular-mediated Administration
TMGT	Testis-mediated Gene Transfer
TMR	Tetramethylrhodamin
UC	Ultracentrifugation
VAP	Smooth Path Velocity

VCL	Track Velocity
VSL	Straight Line Velocity
WB	Western Blotting
WGA	Wheat Germ Agglutinin
WOB	Wobble
ZP	Zona Pellucida
Δψm	Mitochondrial Membrane Potential

ABSTRACT

Background: Male-factor problems are responsible for 50% of all cases of infertility worldwide. With treatment and research skewed towards female infertility, many of the issues responsible for male infertility are not being addressed. The approach used for infertility treatment is crucial not only to the individuals suffering from this condition, but also for future generations. *In vitro* fertilization and intracytoplasmic sperm injection remain the gold standards for assisted reproduction; however, the manipulation of sperm, oocytes, and embryos, can induce structural and functional damage. Moreover, there is no optimal alternative for the introduction of therapeutic compounds into sperm. Therefore, there is an urgent need to develop an effective tool for the delivery of factors that can aid sperm function and help to combat infertility. Exosomes are a subtype of extracellular vesicle secreted by all cells, including commercial cell lines. The proven delivery potential and biocompatibility of exosomes have created a new opportunity for the non-invasive treatment of health conditions, such as male infertility. **Hypothesis**: Exosomes derived from Human Embryonic Kidney 293T (HEK293T) cells provide a safe, efficient, scalable, and versatile approach for the delivery of cargo into sperm, thus, making it possible to tackle sperm-borne deficiencies, which are among the most prevalent causes of male infertility, in a wide range of clinical scenarios. **Aim:** To develop a mammalian-based manufacturing system based on HEK293T cells to obtain highly enriched samples of exosomes for efficient and safe compound delivery into mammalian sperm under conditions that mimic the fertilization scenario *in vitro*. **Results:** The approach used to isolate exosomes from HEK293T cells was scalable and achieved high-yields of exosomes with preserved exosome traits and cell adhesion functions.

Five-hours *in vitro* exposure of boar sperm with HEK293T-derived exosomes under capacitating conditions did not exert a detrimental impact upon various aspects of sperm functionality, including sperm motility, sperm viability, membrane integrity, and mitochondrial membrane potential ($P<0.05$). Visualisation of boar sperm samples treated with HEK293T-derived exosomes revealed a spontaneous interaction within only 10 minutes of *in vitro* co-incubation that was irrespective of the incubation conditions used (capacitating and non-capacitating). Moreover, the proportion of sperm featuring internalized exosomes significantly increased with the time of incubation ($P>0.005$). An enrichment in CONNEXIN-43 (Cx-43) in the HEK293T-derived exosomes was confirmed, and hence, further in-depth analysis may shed light on the specific role of Cx-43-constituted hemichannels in exosome-sperm communication. **Conclusions**: This thesis has proven that HEK293T-derived exosomes may represent a promising research tool for studying sperm biology and provide new options for the intra-gamete delivery of compounds to enhance sperm function, thus creating exciting options for the treatment of infertility. Further work is required before being able to translate this approach to the clinic. Such work may involve the enhancement of targeting efficiency via functionalization of the HEK293T-derived exosomes with cell penetrating peptides, evaluating the delivery efficiency of the cargo of interest, and confirming the safety of this tool with human gametes.

Note to reader: The work presented in this thesis has been heavily impacted by the COVID-19 outbreak and therefore this should be taken into consideration before evaluating the quality and quantity of the experiments described herein.

CHAPTER 1

Mammalian Cell-based Nanotools in Reproductive Biology: A Non-Invasive Approach for Infertility Treatment

1.1 Assisted Reproductive Technology for the Treatment of Infertility: Potential Impact upon Gametes and Embryo Development

1.1.1 Infertility: Understanding the Big Picture

Infertility is the inability to conceive after one year of unprotected sexual intercourse (NICE, 2017) and affects approximately 15% of couples globally (Kumar and Singh, 2015; ESHRE Capri Workshop Group, 2017). Infertility is the result of genetic and environmental factors, or a combination of both and, with a global trend of decreasing fertility (**Figure 1.1**), this has been identified as a public health priority by demographers and policymakers (United Nations, 2019).

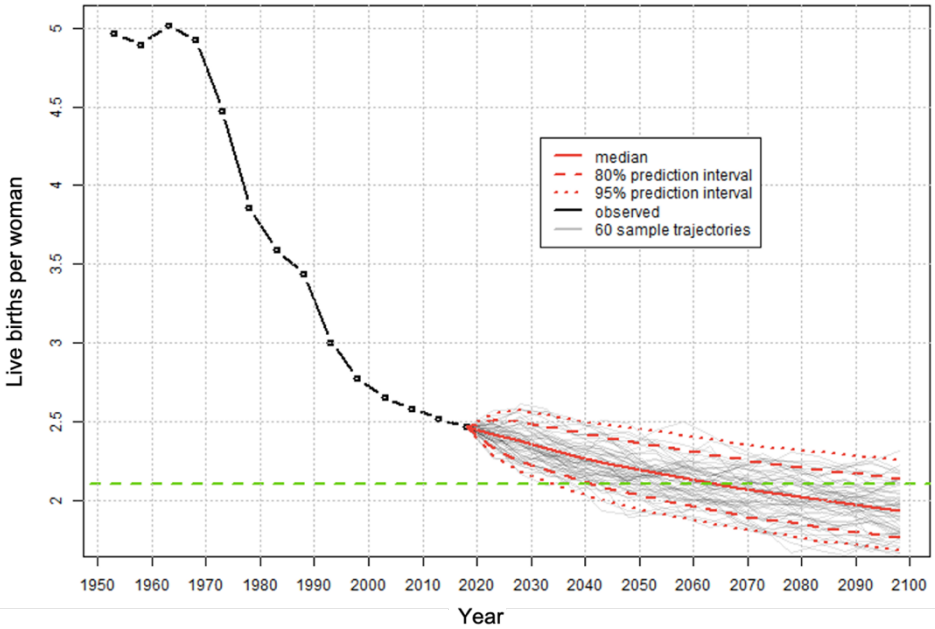

Figure 1.1. Global fertility rates indicated by mean number of live births per woman between 1950 and 2100. Bayesian Hierarchical Modelling was used to produce future fertility estimates (beyond 2020). Only a short period of time is shown for of the sample trajectories of total fertility (grey lines). The median projection is the solid bold red line, with 80% and 95% predicted confidence intervals shown as dashed and dotted red lines, respectively. The replacement-level of 2.1 children per woman is plotted as a green horizontal dashed line is shown for reference, and refers to the number of children birthed per woman for a population to be able to replace itself from one generation to the next. Image acquired from: *United Nations (b), DESA, Population Division. Licensed under Creative Commons license CC BY 3.0 IGO*

Approximately 20% of couples living in developed countries experience either primary infertility, which is the inability to have any children, or secondary infertility – the inability to conceive or carry a pregnancy to term following a previous birth (Population and Fertility, 2018). Infertility is also beginning to affect newly industrialised countries like South Africa (Pantazis and Clark, 2018), though limited access to specialised medical care often results under-diagnosis (Sun et al., 2019).

As a widespread condition, infertility can impact different levels of society, from the psychological and physical distress of the couples involved to the financial burden of governing bodies that are responsible for dealing with such issues (Slade et al., 2007; Zegers-Hochschild, 2009; Greil et al., 2010).

Infertility can arise because of a problem with the female, the male, or both sexes. And to tackle this medical problem assisted reproductive technologies (ART) have been developed. According to the Human Fertilisation and Embryology Authority (HFEA), male-factor infertility accounts for up to 50% of all cases of ART (**Figure 1.2**); 35% being known causes, and the remaining 15% being unexplained infertility coming from the male part. Male infertility affects approximately 12% of all males (Agarwal et al., 2015).

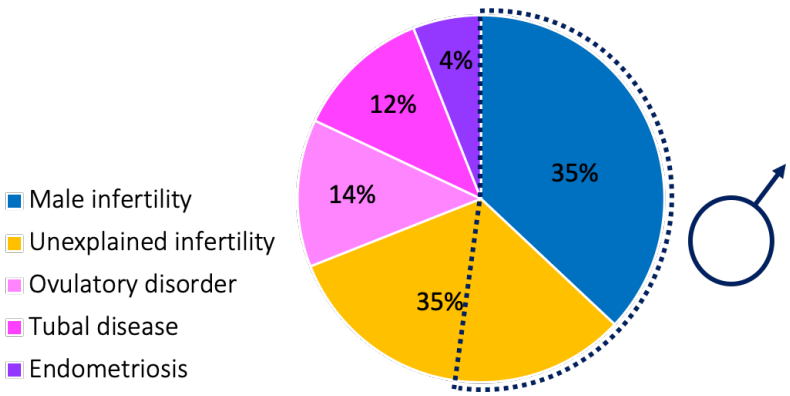

Figure 1.2. The proportions of each main reason for infertile couples undergoing ART treatment. Male-factor infertility (<35%, blue), followed by unexplained infertility (35%, yellow; 50% of which corresponds to male-related infertility), and female-related infertility (including ovulatory disorder, tubal disease and endometriosis) accounting for 30%. (https://HFEA.gov.uk; date accessed: May 2020.)

1.1.2 The Aetiology of Male Infertility

Male fertility has been in steady decline in recent years, particularly in the more developed countries; mean sperm count has reduced by almost 50% in western countries over the last 60 years (Levine et al., 2017). Reasons for such a decline include increased prevalence of obesity, unhealthy lifestyles leading to increased stress levels and cultural shifts that result in higher exposure to toxic agents and endocrine disruptors (Sermondade et al., 2013; Bonde et al., 2016; Khandwala et al., 2017; Skoracka et al., 2020).

Male infertility can be anatomically classified into three different groups; (1) extra-testicular, (2) pre-testicular (or secondary), and (3) testicular (or primary) infertility (**Table 1.1**). Extra-testicular infertility describes either the inability of a male to perform sexual intercourse or ejaculatory dysfunction, which is not directly related to the anatomy of the testes (e.g. retrograde ejaculation, post-surgery complications) (Nieschlag et al., 2010). Pre-testicular or secondary infertility is mainly caused by endocrine disorders due to an impairment of the central nervous system (e.g. hypogonadism) (Nieschlag et al., 2010). Finally, testicular, or primary infertility, takes effect at the cellular level of the testicular tissue (e.g. sperm abnormalities, such as globozoospermia) and is the primary cause of infertility (75% of all male infertility cases; Jungwirth et al., (2012)). In 40–50% of cases involving primary testicular failure; however, the leading cause is unknown and therefore categorised as idiopathic infertility (Pierik et al., 2000; Bhasin, 2007; Nieschlag et al., 2010; Winters and Walsh, 2014). This is mainly due to a lack of understanding of the molecular and genetic mechanisms responsible for male infertility defects.

One of the most common diagnoses in infertile males is azoospermia, clinically defined as the absence of sperm in the ejaculate. Azoospermia is reported in 1% of the overall male population and in 10–15% of infertile men (Oates, 2012).

Table 1.1. Male infertility aetiologies and prevalence in azoospermic males.

CLASSIFICATION	CAUSE	FREQUENCY IN AZOOSPERMIC MALE	KEY REFERENCES
Extra-testicular		**10-15%**	
Infection	Bacteria, viruses, Chlamydia	10.5%	Nieschlag et al., (2010)
Cystic fibrosis	Mutations of the CFTR[1]-gene	3.1%	Nieschlag et al., (2010)
Pre-testicular		**16.4%**	
Hypogonadotropic hypogonadism	Impaired secretion of FSH[2] and LH[3]	2%	Nieschlag et al., (2010)
Klinefelter Syndrome (47, XXY)	Meiotic non-disjunction	13.7%	Van Assche et al., (1996); Nieschlag et al., (2010)
Testicular		**40-50%**	
Varicocele	Vein insufficiency	21-39%	Tulloch, (1955); Sun et al., (2018)
Maldescended testes	Testosterone, AMH[4] deficiency. Congenital, anatomical hindrance	8.4%	Nieschlag et al., (2010)
Molecular abnormalities at the cellular level (e.g. Spermatogenic arrest, globozoospermia)	Multifactorial genetic, and epigenetic mutations	15-30%	Pandiyan and Jequier, (1996); Tournaye., (2012)
Idiopathic infertility	————	**10-50%**	Bhasin., (2007); Cocuzza et al., (2013); Winters and Walsh., (2014)

[1]CFTR: Cystic Fibrosis Transmembrane Conductance Regulator, [2]FSH: Follicle Stimulating Hormone, [3]LH: Luteinizing Hormone, [4]AMH: Anti-Müllerian Hormone

Despite its frequency, little is known about the specific aetiologies underlying male infertility. While there have been advances in the genetic screening of animal models, the scope for clinical genetic testing in human infertile male remains low. Specific mutations have been identified and account for approximately 30% of male infertility cases (Shamsi et al., 2011; Gunes et al., 2016), though the clinical identification of infertile males is not precise.

Up to 40% of men from couples experiencing recurrent pregnancy loss exhibit normal sperm parameters, but also chromosomal aneuploidy in the sperm (Ramasamy et al., 2015). Similarly, traditional semen analysis is problematic as it does not provide enough information on the biological competency of the sperm. Additionally, it is typically only patients with poor semen analysis results that are offered a more detailed examination that could reveal the underlying biological cause for infertility, for example, karyotyping and the evaluation of DNA fragmentation and oxidative stress. As a result, most infertile males remain undiagnosed (Liu and Baker, 2007). It is hypothesised that a large proportion of sperm defects remain unexamined but are potentially treatable by developing more advanced and experimental diagnostic tests (Mortimer, 2018). Hence, more studies to understand sperm biology in the context of male infertility are required.

1.1.3 Sperm Structure

Sperm cells are highly specialised and consist of three differentiated regions; the head containing the nucleus, the mid-piece containing approximately one hundred mitochondria wrapped around the central flagellum, and the sperm tail, which is vital for movement (**Figure 1.3**).

The acrosome, a specialised secretory vesicle, is located close to the anterior end of the nuclear envelope and releases hyaluronidase to break through the thick layer of cumulus cells surrounding the oocyte's zona pellucida (ZP) (Gadella, 2012). Sperm cell components, such as proteins, RNA and centrioles, are key for sperm function, and hence defects in them are a direct causative factor for male infertility (Turner et al., 2020).

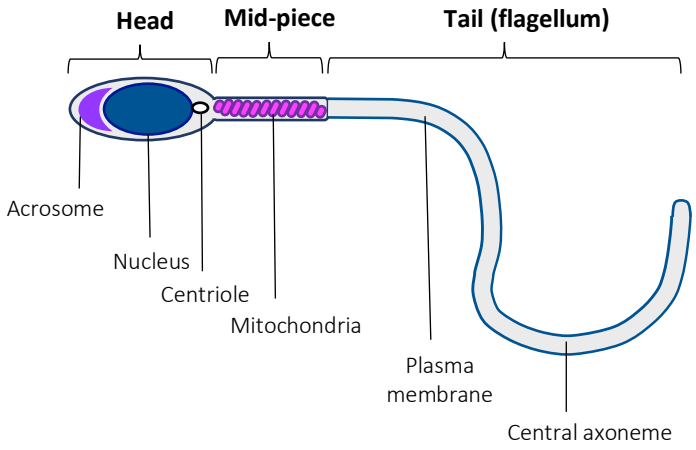

Figure 1.3. The structure of human sperm showing the three main regions; head, mid-piece and tail along with inner structures.

During sperm formation, many of the cellular organelles originating from the spermatogonial stem cells (SSCs) are lost. Lost organelles include the Golgi complexes, endoplasmic reticulum, ribosomes and membrane vesicle transport systems, as they are no longer required for sperm function (Gadella et al., 2008). This loss results in a lack of machinery for *de novo* protein synthesis and protein surface recycling, rendering the sperm unable to repair any damage caused to the nucleic acids and protein cargo. Therefore, the sperm nucleus consists of super-condensed chromatin, combined with protamines instead of histones as to protect the DNA during the maturation process and transit that occurs prior to fertilization (Ward, 2010;Ward, 2011).

1.1.4 Natural Sperm Selection and Post-Fertilization Events

Upon unprotected coitus, around 250 million mature sperm cells previously stored in the epididymis, are ejaculated into the female tract together with secretions from the male accessory gland (Carlson, 2019).

This seminal fluid is rich in factors that mediate sperm motility activation and inhibit premature fertilization-related events. Throughout the whole process, the sperm has to overcome several barriers with the purpose of selecting the most biologically competent sperm cell to fertilize an egg (**Figure 1.5**).

Upon the deposition of sperm into the vagina, the seminal fluid confers protection against the vagina's mucosal immune system and hostile milieu, by neutralizing the acidic pH. Sperm motility is key for migration towards the cervix and out of the cervical mucus, which is released around ovulation (Kanwar et al., 1979). Non-motile sperm, sperm bearing morphological anomalies and those with an excessive content of polyunsaturated fatty acids (PUFA) in their plasma membrane, will remain trapped inside the cervical crypts (Ollero et al., 2000).

Sperm selection mechanisms of the uterus are less clear, though uterine leukocytes have been proposed as an additional selection barrier, as they increase the levels for reactive oxygen species (ROS) harmful to the sperm (Henkel, 2011). Only sufficiently motile sperm will escape this hostile environment and reach the utero-tubal junction (Velando et al., 2008).

The oviductal isthmus confers a protective environment that enhances sperm viability and fertilization ability. At the oviduct, sperm cells undergo capacitation that results in the switching of the sperm's motility into a hyper-activated status, enabling them to reach and fertilize the oocyte. This change of status is also accompanied by an ability to release digestive enzymes at the surface of the oocyte's ZP.

Hyperactivation is required for the sperm cell's detachment from the oviductal epithelium and to increase the chances of encountering the oocyte. Moreover, only capacitated sperm are capable of reacting to the chemotactic and thermal stimuli, that are released to attract the sperm towards the oocyte in the ampulla (Bahat and Eisenbach, 2006; Eisenbach and Giojalas, 2006).

Finally, upon fertilization, the sperm's DNA has to undergo decondensation and replication for the sperm and the oocyte's pronuclei to be able to fuse into one before undergoing mitosis. DNA decondensation kinetics have been correlated with embryo development rates (Cebesoy et al., 2006), with a positive correlation between embryo quality with sperm DNA decondensation velocity in IVF (Galotto et al., 2019). This was first observed in 1998 in humans and was later confirmed in *Rhesus* monkey (Bourgain et al., 1998; Hewitson et al., 1999). These findings suggest that retention of the acrosome may delay DNA decondensation at the nucleus region of the sperm.

It is important to acknowledge the many selection barriers that are bypassed during an ART cycle, especially when using ICSI (as it is based upon the injection of the sperm inside the oocyte), and how this practice may inevitably use non-fully competent sperm for the fertilization of the eggs. In future ART development, more efficient and less invasive alternative techniques should be prioritized, such as nanotools for intra-gamete drug delivery, as to enhance the sperm from infertile men *in vivo* to gain competence to fertilize the oocytes following the natural sperm selection barriers after natural coitus.

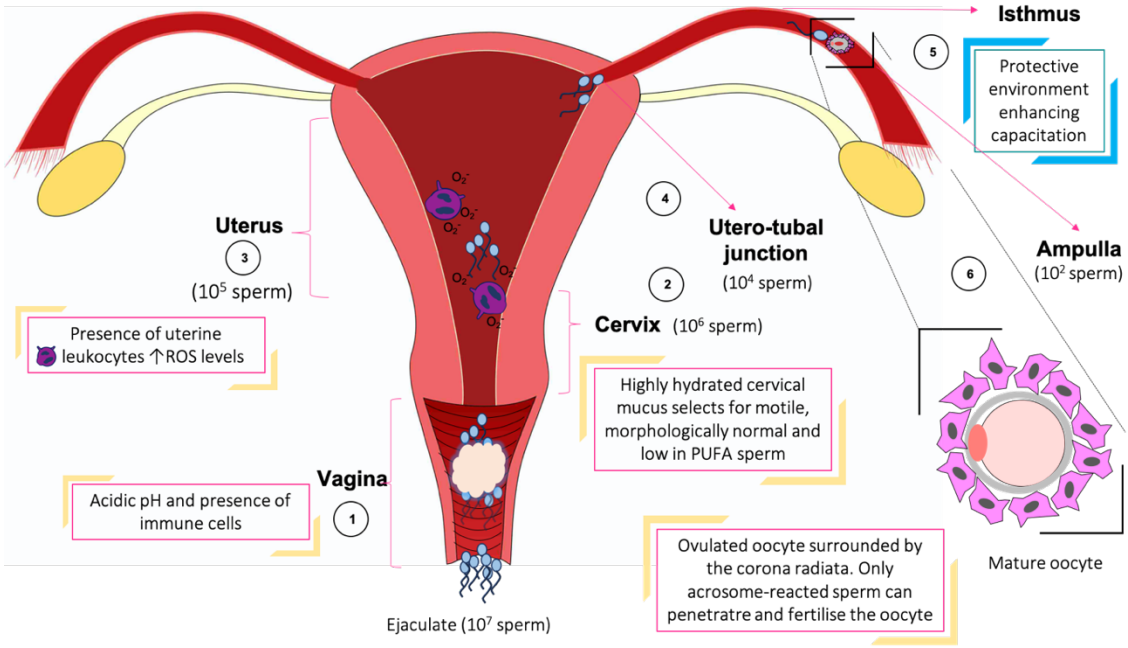

Figure 1.5. The female reproductive tract, and the fertilization events that take place upon the encounter of natural barriers that the sperm is subjected to upon ejaculation. 1) The ejaculated sperm first experience a drop in the pH and encounter the immune cells in the vagina. 2) The conformation of the cervical mucus (only highly hydrated if within the ovulatory period) will allow the passing of morphologically normal and motile sperm towards the uterus. 3) At the uterus the sperm will encounter a high level of ROS and uterine leukocytes. 4) Only 10^4 sperm will then reach the utero-tubal junction. 5) Around 10^2 sperm will then swim along the isthmus and undergo capacitation. 6) Very few acrosome-reacted sperm will reach the ampulla and meet the oocyte via recognition of the chemotactic signals released by the oocyte's cumulus cells, with just one being capable of penetrating the corona radiata and fertilising the oocyte.
ROS: Reactive Oxygen Species, PUFA: Polyunsaturated Fatty Acids.

1.1.5 Current Status of ART and Detrimental Effects of Gamete Manipulation in Embryo Quality

ART remains the gold standard for human infertility treatment, and includes *in vitro* fertilization (IVF) and intracytoplasmic sperm injection (ICSI), which account for one-third and two-thirds of ART treatments, respectively (ESHRE, 2018). ART procedures have been standardised and are widely used in fertility clinics globally, though began with Edwards and Steptoe (1978), who achieved the first successful IVF procedure, culminating in a live birth.

IVF involves the *in vitro* incubation of a concentrated sample of sperm (from 100,000 to 200,000 sperm) with a few oocytes inside a petri dish, and fertilization can then be documented 12-20 hours later (Goldberg et al., 2007).

ICSI was developed a decade after IVF, to expand male infertility treatment (Palermo et al., 1992) and involves manually injecting a single sperm inside the oocyte with a micromanipulator (Goldberg et al., 2007). For both ART procedures, sperm and oocytes are retrieved from patients or donors, and prepared for manipulation; sperm samples are washed and capacitated to select biologically optimum sperm cells and oocytes are washed to remove blood and surrounding cumulus cells (denudation) (Goldberg et al., 2007).

Despite being developed for severe male-related infertility, ICSI is also used to treat mild male factor infertility, unexplained infertility, and mixed male/female infertility. There is a tendency for ICSI treatment to be more prevalent in the Middle East (Dyer et al., 2016) and its widespread use has been criticised as wrongful conduct (Boulet et al., 2015; Chambers et al., 2016).

The American Society for Reproductive Medicine (ASRM) released an official statement (COM017) (Practice Committees of the American Society for Reproductive Medicine and Society for Assisted Reproductive Technology, 2012), concluding that routine ICSI should not be applied for non-male infertility cases if IVF has been proven to be successful. In such cases, IVF should always be considered before ICSI.

Despite the widespread use of ART, successful pregnancy rates remain very low and it is associated with an increased risk of complications for the mother and baby. ICSI success rate represents just 40–45% of the ART cycles, which reduces to 34% per embryo transferred to the mother (ESHRE, 2018).

Health problems associated with ART include pregnancy-related complications in live-births (such as ectopic pregnancies), congenital malformations, fertility problems in the following generations, an increased risk of cancer and delayed psychological and neurological development in the baby (Hansen et al., 2013; Hargreave et al., 2013; Coates et al., 2015; Qin et al., 2016).

Sperm defects have been suggested as the primary factor for increased live-birth health defects (Krawetz, 2005; Aitken and De Iuliis, 2007; Kumar et al., 2013; Coates et al., 2015). As a technique where almost all-natural barriers for sperm selection are deliberately bypassed (Cooper, 2007), ICSI creates a risk of passing on molecular aberrations into the offspring when injecting oocytes with genetically abnormal sperm (Aitken et al., 2013; Crawford and Ledger, 2019).

Health problems may also arise from the manipulation of gametes, as it poses an extra stressor that can result in a detrimental impact on embryo development (Loutradi et al., 2006; Le Bouc et al., 2010). There are major concerns regarding ART, as cellular structures essential for early cell division are potentially damaged when sperm cells with an intact acrosome full content of digestive enzymes, is placed inside the oocyte (Hewitson et al., 1999). Indeed, ART procedures have been shown to induce DNA fragmentation, epigenetic defects, and increase oxidative stress in gametes and the resulting embryo (Agarwal et al., 2006; Kobayashi et al., 2007; Toro et al., 2009; Kumar et al., 2013). Moreover, during the management of the infertile couple at IVF clinics, the treatments are predominantly skewed towards the female partner due to its greater implication, as she is the one who has to go through multiple check-ups, undergo ovarian stimulation with the associated health risks, oocyte retrieval, embryo transfer and ultimately carry the pregnancy. Consequently, remarkable attention is invested in improving embryo quality and pregnancy outcome. However, the value of appropriate male evaluation and treatment is overlooked, as these techniques, especially ICSI, can provide the couple with a baby without the need to explain the nature or cause of a previous pregnancy loss (Turner et al., 2020).

The relatively low rates of ART success are also attributable to multiple factors that can lead to failed embryo development.

The ART procedures themselves have the potential to disrupt successful development, including the medications used for ovulatory stimulation, the composition of the culture media, *in vitro* culture, freezing and thawing processes and changes in the hormonal environment at the time of implantation (or a combination of these factors) can result in earlier or later blockages of the embryo development as reviewed by (Ramos-Ibeas et al., 2019). Additionally, the mechanical strains exerted upon the gametes during manipulation may be carried over to the future offspring. Such mechanical strain can occur with the erroneous insertion of a microinjection pipette during ICSI, thus disrupting the oocyte's spindle apparatus that is essential for chromosome segregation (Nudell and Lipshultz, 2001; Eichenlaub-Ritter et al., 2002; Rienzi et al., 2003). Prior handling of the oocytes, such as during denudation when cumulus cells and corona radiata are removed, may cause a displacement of the first polar body with respect to the meiotic spindle locus (Silva et al., 1999; Wang et al., 2001; Rienzi et al., 2003). Such displacement may lead embryologists to use an incorrect micropipette needle entry position and cause major disruptions to the oocyte's organelles such as the spindle apparatus (**Figure 1.4**). Disruption to the spindle apparatus is detrimental for development rates and it either may be rapidly observed in the embryo's morphokinetics, or result in visibly healthy embryos that are carrying chromosomal disorders with compromised gene expression and/or detrimental epigenetic modifications (Fauque et al., 2007; Song et al., 2015; Swain, 2019).

Development of ICSI-fertilised embryos is slower, especially in the initial phases, than those fertilised by IVF (Speyer et al., 2019). In the study by Speyer, the variation in embryo development rates has been attributed to natural versus artificial sperm selection, with idea that IVF-derived embryos have been fertilised by sperm of better quality. This theory is further supported by an observed development delay in ICSI-derived embryos, mostly during the phases when the paternal genome becomes activated (Shoukir et al., 1998; Miller and Smith, 2001; Speyer et al., 2019).

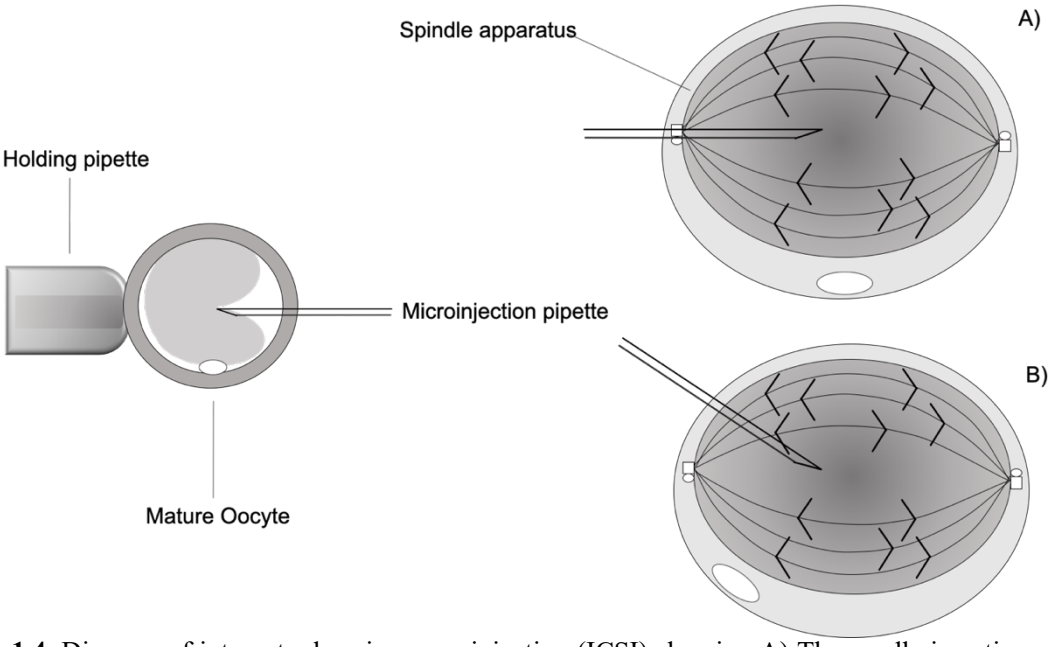

Figure 1.4. Diagram of intracytoplasmic sperm injection (ICSI) showing A) The needle insertion position when the first polar body is located in its normal position. B) Potential damage to the spindle apparatus caused by needle insertion when the first polar body has been deviated due to prior oocyte manipulations. Adapted from: *Nudell and Lipshultz, (2001) under a CC BY 4.0 license.*

Overall, the poor success rates in ART, and the above-mentioned risks from gamete manipulation posed to the mother and the future baby, calls for a need for basic scientific research to address this inefficiency and translate therapeutic improvements, including less invasive techniques, back into the clinical context (Babakhanzadeh et al., 2020; Turner et al., 2020).

1.2 Nanotechnology for the Treatment of Infertility

Nanotechnology has rapidly expanded over the recent years and is now applied in many areas of healthcare. Nanotechnology can be very useful in the development of non-invasive bioimaging, diagnosis, tissue engineering and minimally invasive drug administration for the treatment of infertility-related disorders (Wagner et al., 2006; Kim et al., 2010a; Maeda et al., 2013).

This discipline involves a wide spectrum of inorganic materials (e.g. silica particles, carbon nanotubes and gold nanoparticles) and organic compounds such as liposomal formulations and micelles synthesised from phospholipids (**Figure 1.6**).

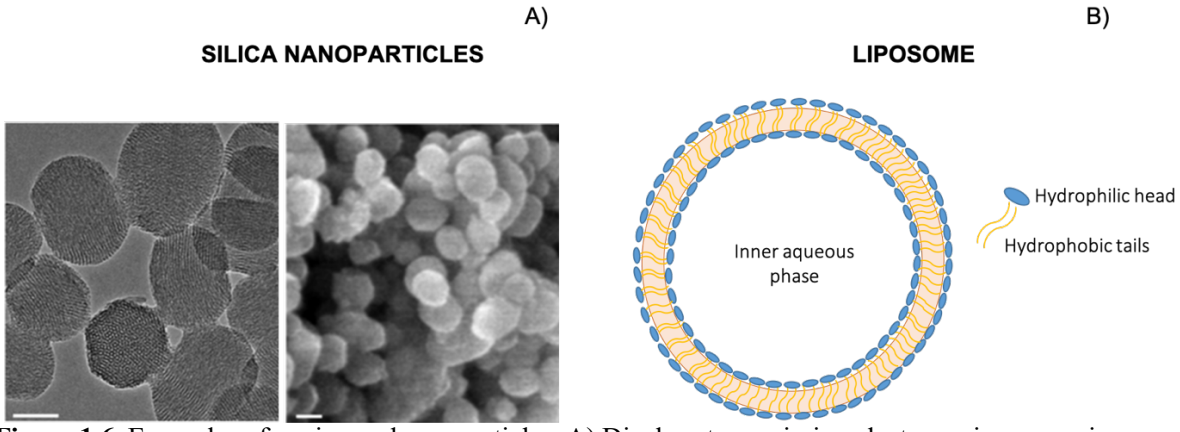

Figure 1.6. Examples of engineered nanoparticles. A) Displays transmission electron microscopy images of mesoporous silica nanoparticles, scale bar = 0.05µm (left image) and 0.1µm (right image). B) Scheme displaying the common structure of a liposome. Adapted from: *Barkalina et al., (2013) under a CC BY 4.0 license.*

In nanomedicine, nanoscale particles are used to optimize drug loading and tissue targeting to ensure the appropriate dose administration. Such technology is particularly useful for specific targeting and overcoming mucus and blood barriers for which pharmacokinetics and medicament design are ineffective.

The blood-testis barrier (BTB) is considered one of the tightest blood-tissue barriers in the mammalian body. Unlike the brain-tissue barrier, which is mainly composed of tight junctions (TJs), the BTB has a complex variety of specialised junctions between apposing Sertoli cells that are adjacent to the membrane of the seminiferous epithelium (**Figure 1.7**). These junctions are comprised of coexisting TJs, gap junctions, desmosomes, basal ectoplasmic specialization and a "testis-specific atypical adherens junction" (Siu and Cheng, 2004). Therefore, entry through the BTB is limited to particles that have specific physicochemical properties (Petros and DeSimone, 2010; Albanese et al., 2012).

Particles for BTB transmission need to be under 95 nm in diameter (Park et al., 2010) and typically use ligand-targeting strategies to further enhance transfer across different structures before reaching their site of action (Snow-Lisy et al., 2015).

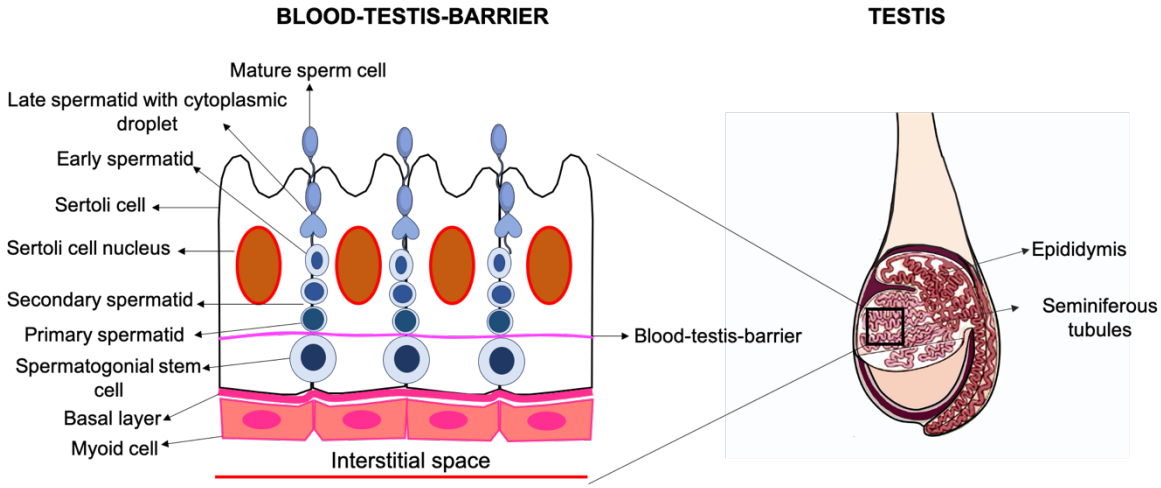

Figure 1.7. The composition of the blood-testis-barrier within the seminiferous tubules in the testicular tissue parenchyma, composed by adjacent Sertoli cells isolating the seminiferous epithelium from the interstitial space. Adapted from: *Schindell et al., (2018) under a CC BY 4.0 license*.

Drug administration for applications such as improvement of post-thawing quality of sperm has been successfully achieved with nanoparticles, displaying an incomparable ability to penetrate the BTB, with both intravenous injection and oral administration (Yoshida et al., 2009; Park et al., 2010; Lankveld et al., 2011; Morishita et al., 2012; Kong et al., 2014; Kielbik et al., 2019; Najafi et al., 2020).

Additionally, the use of mesoporous silica nanoparticles and liposomes have been explored for compound delivery to mammalian sperm (Garcez et al., 2010; Kim et al., 2010b; Campos et al., 2011; Barkalina et al., 2015a; Moretti et al., 2016; Najafi et al., 2019). Such specific and efficient drug delivery systems to the male reproductive tissue stand to revolutionize the field of fertility treatment. The application of artificial nanoparticle systems, however, call into question their safety when used with sperm cells responsible for generating new life.

The non-biodegradability, immunogenic status and possible transgenerational effects of the available nanoparticles, all raise concern (Sasaki et al., 2000; Szebeni, 2001; Kunzmann et al., 2011; Poma et al., 2014; Liu et al., 2016). The fact that these cells will potentially give rise to an embryo is a major factor of consideration when choosing a non-invasive and efficient approach, as the long-term safety for offspring needs to be ensured (Barkalina et al., 2015b; Das et al., 2016).

Beyond the challenges surrounding efficacy and safety, an additional burden for the pharmaceutical industry is the complexity behind the manufacturing process of nanomedicines. Manufacturing concerns were raised when the sole supplier of generic Doxil (Johnson & Johnson) failed to meet the requirements of the Food and Drug Administration (FDA) of Good Manufacturing Practices for the mass production of PEG-liposomal doxorubicin. Set against the manufacture of small molecules, the production of nanosized formulations entails greater expense and more intricate quality control (Siew, 2014; Agrawal et al., 2017).

All these considerations have paved the way to investigate cell-derived alternatives that share common properties with the targeted cells as to ensure a safer and more efficient drug administration. However, finding a biocompatible alternative for drug delivery that is capable of rivalling the efficiency of nanoparticles to cross reproductive tissues remains a significant challenge.

1.3 Key Features of Extracellular Vesicles and their Potential Role in Infertility Treatment

Extracellular vesicles (EVs) are enclosed membrane structures secreted by cells and promote intercellular communication by transferring the metabolites into the recipient cell.

EV metabolites are derived from the cell they were secreted from and consist of proteins, nucleic acids, and lipids, amongst other factors. EVs are secreted by all human tissues and have been isolated from almost all body fluids, including blood, ejaculates, and breast milk (Ronquist and Brody, 1985; Caby et al., 2005; Simpson et al., 2008; Lasser et al., 2011).
EVs mediate a range of processes in cell and tissue biology, including immune responses and pathogenic mechanisms (Théry et al., 2009; Lasser et al., 2011; Lee et al., 2012; Raposo and Stoorvogel, 2013). The cellular mediation of EVs makes them a potential novel diagnostic and therapeutic agents (Lener et al., 2015).

There are several EV subtypes, which differ in terms of their biogenesis pathway, size, and biological properties (Van der Pol et al., 2012) (**Table 1.2**). The four main classes of EVs, as determined by their biogenesis pathway, are exosomes, microvesicles, apoptotic bodies and oncosomes.

Exosomes are one of the best studied EVs, indeed, the most is known about EVs from exosomes (Witwer and Thery, 2019). Exosomes are the smallest EV type with a diameter ranging from 30 to 200 nm (Raposo and Stoorvogel, 2013; Colombo et al., 2014), and thus, present the most optimum size range to traverse the BTB. Exosomes consist of lipidic-bilayer structures that are rich in sphingomyelin, cholesterol, ceramide, and phosphatidylserine (Matsuo et al., 2004) and were first observed in antigen-presenting cells (Raposo et al., 1996; Zitvogel et al., 1998). The metabolite cargo exosomes contain depends on the cell-type and physiological status of the parent cell, as well as the biogenesis mechanism from which they originate (Colombo et al., 2014).

As EV characteristics overlap among subtypes, existing isolation techniques are not refined enough to isolate specific subtypes (Aalberts et al., 2012; Palma et al., 2012; Gould and Raposo, 2013).

This is mostly important to avoid the presence of apoptotic bodies and oncosomes in the sample preparations that are to be used with live cells, as these could alter normal cell function by inducing apoptotic and cancer-related pathways (Eguchi et al., 2020).

Table 1.2. Characteristics and properties of the four main extracellular vesicle (EV) subtypes.

EV SUBTYPES	CHARACTERISTICS				KEY REFERENCES
	BIOGENESIS	DIAMETER (nm)	MARKERS	CONTENTS	
Exosomes	Endolysosomal pathway leading to intraluminal budding of multivesicular bodies and final exocytosis through fusion with the cell membrane	30-120	Tetraspanins (e.g CD9, CD63, CD81) Cytosolic proteins (e.g. ESCRT[1] components, Alix, Flotillin and Syntenin-1)	mRNA, miRNA and other non-coding RNAs, cytoplasmic and membrane proteins, including MHC[2]	Vlassov et al., (2012); Raposo and Stoorvogel, (2013)
Microvesicles	Outward budding of the cell membrane	100-1000	Integrins, Selectins (P-selectin), CD40	mRNA, miRNA and non-coding RNAs, cytoplasmic and membrane proteins	Andaloussi. et al., (2013); Raposo and Stoorvogel, (2013)
Apoptotic bodies	Outward blebbing of the apoptotic cell membrane	500-2000	Phosphatidylserine, Nuclear proteins (e.g Lamin A/C) Mitochondrial proteins (e.g Cytochrome-C), secretory pathway components (e.g. calnexin)	Nuclear fractions, cell organelles	Andaloussi. et al., (2013)
Oncosomes	Membrane shedding of amoeboid cancer cells	1000-10^4	Nuclear proteins (e.g Lamin A/C) Mitochondrial proteins and secretory pathway components	Nuclear fractions, cell organelles	Minciacchi et al., (2015)

1 ESCRT: Endosomal Sorting Complex Required for Transport, [2]MHC: Major Histocompatibility Complex

1.3.1 Exosome Biogenesis and Characterization

Exosome biogenesis has been studied for more than thirty years with several sorting pathways having been identified in exosome production with the use of inhibiting factors (Trajkovic et al., 2008; Hsu et al., 2010; Baietti et al., 2012; Colombo et al., 2013; Hoshino et al., 2013). The most common pathway for exosome origination is firstly through membrane endocytosis of the mother cell, where receptors and lipids present at the endocytosis site are incorporated into the membrane of the newly formed early endosomes (**Figure 1.8**). Early endosomes then develop into late endosomes by following a maturation process, subsequently giving rise to multivesicular bodies (MVBs) containing internal luminal vesicles (ILVs). ILVs are formed by the inward budding of the multivesicular membrane. Budding can either be regulated by the endosomal sorting complex required for transport (ESCRT)-dependent pathway that requires ubiquitination, or by an ESCRT-independent mechanism, which seems to depend upon lipid raft microdomains for the lateral segregation of cargo (Bobrie et al., 2011). Finally, the MVBs fuse with the cell's plasma membrane and ILVs are released into the extracellular media, becoming exosomes.

The exosome biogenesis pathway was first discovered during reticulocyte maturation studies in the 1980s (Harding et al., 1983; Pan and Johnstone, 1983; Pan et al., 1985) and the term exosome was later defined by Rose Johnstone and colleagues (1987) to more specifically refer to this subtype of extracellular vesicle.

The diversity of EVs described so far, together with the inability to distinguish them with the currently available isolation and characterization techniques, has led to confusion in the field regarding exosomes nomenclature.

The lack of a universal marker valid for cell-types specific and exclusive to exosomes confounds the problem (Laulagnier et al., 2005; Oksvold et al., 2014; Smith et al., 2015), though exosome-associated surface markers may help with identification. Exosome-associated surface markers are membrane transport and fusion proteins (e.g. Rab GTPase, ANNEXINS, FLOTILLIN), tetraspanins (e.g. CD9, CD63, CD81), heat-shock proteins (e.g. HSP70, HSP90) and endosome-associated proteins involved in MVE biogenesis (e.g. ALIX, SYNTENIN-1, TSG101) (Van Niel et al., 2006; Vlassov et al., 2012; Kowal et al., 2014).

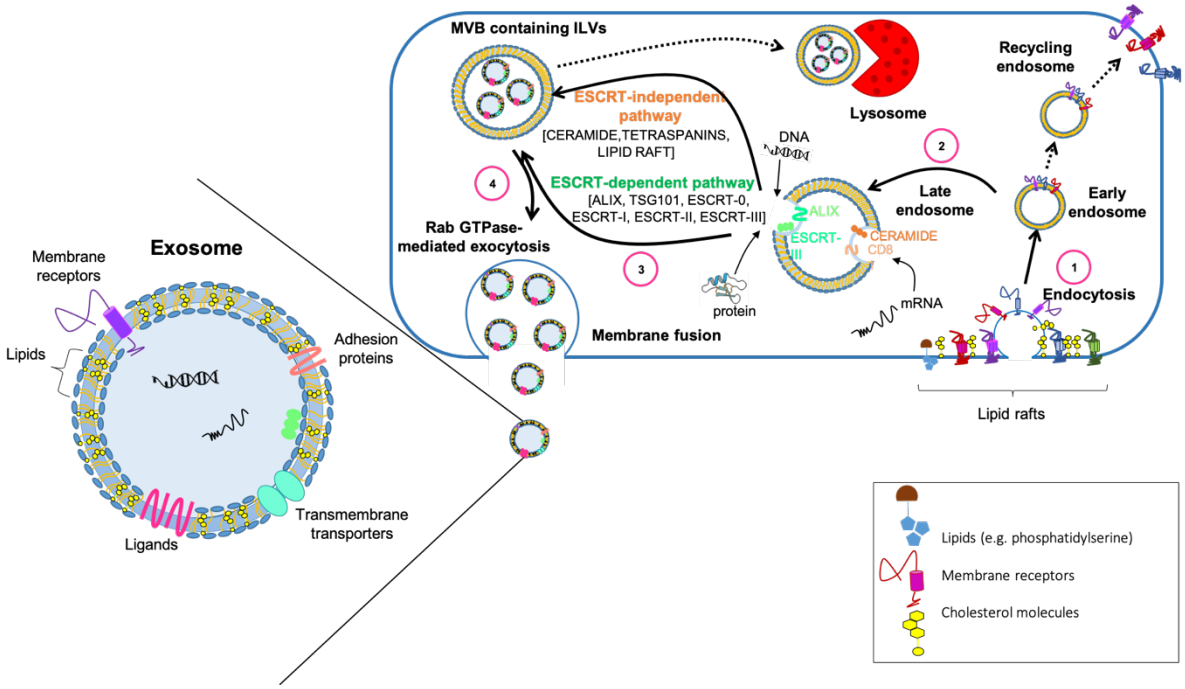

Figure 1.8. Schematic of exosome biogenesis pathways. 1) Exosomes originate by the inward budding of the endosomal membrane of their mother cell by a clathrin or non-clathrin-dependent endocytosis. Endocytosis preferentially takes place in those membrane domains rich lipids, known as lipid rafts, during which the lipids present together with membrane receptors will be incorporated into the membrane of the early endosomes at this point. 2) These early endosomes then become late endosomes following a maturation process involving physiological changes such as acidification, changes in the protein content and tendency to fuse with other membranes, finally giving rise to MVBs. MVBs formed from late endosomes experience a continuous reversed budding of the limiting membrane, during which late endosomes buds into their lumen, resulting in an enrichment of ILVs. 3) This inward budding process can either be ESCRT-dependent with other accessory proteins involved (e.g. ALIX and TSG101) or ESCRT-independent reliant upon other molecules (e.g. ceramide, lipid rafts, tetraspanins). The MVBs either fuse with lysosomes via a ubiquitin-dependent pathway for degradation or follow the endocytic pathway for the generation of exosomes. 4) Finally, the MVB's membrane fuses with the cell's plasma membrane releasing their ILVs to the extracellular media in a process known as exocytosis. MVB: Multivesicular Body, ESCRT: Endosomal Sorting Complex Required for Transport, ILV: Intraluminal Vesicle

To address the issue of EV identification, the International Society for Extracellular Vesicles (ISEV) published a series of criteria for the presumption of the presence of specific EV types.

To establish the presence of exosomes, for example, the ISEV statement recommends confirming the presence of exosome-associated surface markers, as well as the absence of proteins not associated with exosomes (Lötvall et al., 2014; Thery et al., 2018). Additionally, a number of datasets have been developed to collect information relating to the exosomal proteins, RNA, and lipids, that have been described to date (Mathivanan and Simpson, 2009; www.exocarta.org) (**Table 1.3**).

Table 1.3. Key exosomal protein markers, lipids and nucleic acids.

	EXOSOMAL MARKERS	CATEGORY	KEY ROLE	KEY REFERENCES
PROTEINS	CD9, CD63 and CD81	Tetraspanins	Compartmentalization of receptors and cell adhesion. CD81 and CD63 have also been described in ESCRT-independent exosome biogenesis pathways. and cell adhesion.	Hemler, (2005); Perez-Hernandez et al., (2013)
	Flotillin, Syntenin	Signalling protein	Participate in exosome biogenesis and signal transduction	Strauss et al., (2010); Baietti et al., (2012)
	Alix, TSG101	Multivesicular body biogenesis	Involved in the ESCRT-dependent MVB biogenesis pathways	Thery et al., (2001); Vlassov et al., (2012); Colombo et al., (2013)
LIPIDS	Ceramide	Membrane sphingosine fatty acids	Involved in ESCRT-independent MVB biogenesis	Trajkovic et al., (2008)
NUCLEIC ACIDS	mRNA miRNA (e.g. miR-21) lncRNA circRNA	micro RNAs Messenger RNAs Non-coding RNAs circular RNAs	Immune regulation, cell targeting, cell proliferation, gene expression…	Zhang et al., (2015); Fanale et al., (2018)

1.3.2 Mechanisms for Exosome-Mediated Intercellular Communication

Intercellular communication can take place between adjacent cells, for instance through gap junctions, or between distant cells via secreted soluble factors such as hormones and cytokines (Camussi et al., 2010). Recently a role of exosomes in intercellular communication has been recognised, using a form of paracrine communication. This concept was based on the observation that exosomes released by a parent cell are carriers of cell-specific bioactive compounds that interact with target cells and influence their phenotype features and behaviour (Ratajczak et al., 2006b; Camussi et al., 2010; Tian et al., 2010). The efficiency of exosome cargo internalization into a recipient cell relies upon the mechanism by which it takes place.

Once internalised, exosomes may then fuse with limiting endosomal membranes or with other intercellular compartments, resulting in the horizontal transfer of their contents to the cytoplasm and organelles of the target cells, such as the nucleus. Various pathways for exosome uptake have been proposed, including receptor-mediated uptake, direct fusion of membranes, or internalization via endocytosis (Mulcahy et al., 2014; Costa Verdera et al., 2017; Gonda et al., 2019; Gurung et al., 2021) (**Figure 1.9**). The most widely accepted uptake mechanism for EVs, including exosomes, is endocytosis (Costa Verdera et al., 2017; Gonda et al., 2019).

Endocytosis is an umbrella term for many different pathways including clathrin-dependent endocytosis, caveolin-dependent endocytosis, phagocytosis, micropinocytosis, and lipid raft-dependent endocytosis; most of these processes require cholesterol to be present in the plasma membrane (Grimmer et al., 2002; Nabi and Le, 2003). The role of endocytosis in EV uptake has been substantiated by several studies that have revealed the energy-dependent manner of EV incorporation into endosomal compartments (Morelli et al., 2004; Escrevente et al., 2011; Montecalvo et al., 2012).

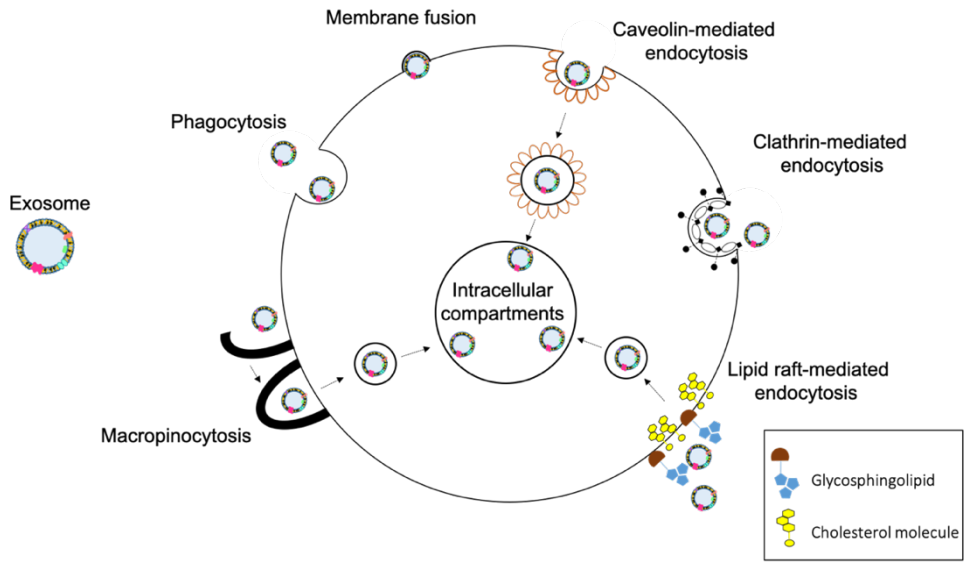

Figure 1.9. Pathways of exosome uptake. Exosomes may be internalised by the target cells through clathrin or caveolin-mediated endocytosis and phagocytosis. Additional evidence supports their interaction with lipid rafts (mainly constituted by glycosphingolipids and cholesterol) resulting in another form of endocytosis. Exosomes can also be internalised by macropinocytosis where membrane ruffles or protrusions extend from the cell enclosing the exosomes into the lumen. Ultimately, internalised exosomes may fuse with the endosomal limiting membrane of different intracellular compartments to enable their cargo to elicit a phenotypic response in the recipient cell. Adapted from: *Mulcahy et al., (2014) under a CC BY-NC 3.0 license.*

Another potential uptake mechanism is through direct membrane fusion, in which the EV membrane comes into direct contact with plasma membrane of the cell (Parolini et al., 2009), and as a result, both hydrophobic cores join to form one structure. Membrane fusion can be observed through fluorescent lipid dequenching and is known to be enhanced by acidic conditions (Peschka et al., 1999; Montecalvo et al., 2012; Schwarz et al., 2013). It has also been suggested that the lipid raft-like composition in the membrane of EV's enhance fusion with recipient cell membranes (Valapala and Vishwanatha, 2011).

Another mechanism for exosome uptake within lipid-raft-mediated mechanisms that has been described is via protein-protein interactions. One of the most common theories involves the role of tetraspanins – these proteins are highly abundant in the membranes of exosomes (Gonda et al., 2019). It has been widely suggested that tetraspanin-enriched microdomains, also known as raft-like clusters in the plasma membrane of exosomes, act as adhesion molecules, and are involved in vesicular and cellular fusion as key exosome-cell binding mediators (Hemler, 2005, Levy and Shoham, 2005; Johnstone, 2006).

Furthermore, recent proteomic studies have identified the presence of connexins; specialised gap-junction proteins in extracellular vesicles, including exosomes. From the 21 different connexin proteins, CONNEXIN-43 (Cx-43) is the most widely expressed, and by consequence, the one that has been studied the most. Cx-43 was first known for its essential role in forming gap-junctions between neighbouring cells (Gago-Fuentes et al., 2014). However, Cx-43 is also implicated in the communication between non-opposed cells through exosomes (Soares et al., 2015; Esseltine and Laird, 2016).

Cx-43 may also have roles beyond cellular communication, such as the regulation of gene expression, the modulation of cell growth and cell death, and mechanical roles (Oliveira et al., 2005; Martins-Marques et al., 2015; Leo-Macias et al., 2016). Such mediation has been proposed as a potential therapeutic mechanism to the extent to be proposed as a mechanism with therapeutic potential itself (Martins-Marques et al., 2016; Ribeiro-Rodrigues et al., 2017). Indeed, the presence of Cx-43 in EVs has been correlated with an enhanced protective effect in cardiomyocytes, alleviation of inflammation and neuronal damage after spinal cord injury, and thus, the presence of Cx-43 in exosomes could also be exploited for other applications such as to protect sperm damage caused by ROS.

1.4 Extracellular Vesicles in Human Reproduction

1.4.1 Extracellular Vesicles from the Male Reproductive System

EVs have been successfully retrieved from all body fluids, including semen (Carlsson et al., 2003; Pisitkun et al., 2004; Caby et al., 2005; Asea et al., 2008; Ogawa et al., 2008; Lasser et al., 2011; Colombo et al., 2014).

Most of the EVs present in the human seminal fluid originate from the epididymis and prostate (Ronquist and Brody, 1985), and are known as epidydimosomes and prostasomes respectively, with an estimated concentration of around $1x10^{12}$ EVs/mL (Rodriguez-Caro et al., 2019). Prostasomes and epididymosomes have been recorded to fuse with sperm (Ronquist et al., 1990; Ronquist et al., 1996; Arienti et al., 1997; Carlini et al., 1997) and to mediate processes relevant to sperm functionality and oocyte fertilization, including sperm maturation, motility and capacitation (**Table 1.4)**.

Seminal plasma protects sperm cells and maintains their fertilization capacity in preparation for their encounter with the oocyte. One of the most important processes that precedes oocyte fertilization, and renders the sperm capable of such an event, is capacitation. Capacitation involves several intracellular pathways that lead to cellular changes such as a decrease in the cholesterol content of the sperm's plasma membrane (Cross, 1998).
Seminal fluid prevents premature capacitation through the presence of "decapacitating" factors that block cholesterol efflux.

Prostasomes and epididymosomes exhibit regulatory effects that can either be inhibitory or stimulatory in terms of the fertilisation capability of sperm. For instance, the main source of cholesterol in seminal fluid comes from prostasomes (Ronquist and Brody, 1985; Arvidson et al., 1989). The high cholesterol/phospholipid ratio stabilizes the sperm plasma membrane in the acidic vaginal environment and confers anti-capacitating properties by inhibiting the tyrosine phosphorylation of two specific proteins (P80 and P110) – the terminal markers of capacitation signal pathways (Cross and Mahasreshti, 1997; Pons-Rejraji et al., 2011).

Table 1.4. Exerted properties of seminal plasma EVs (prostasomes and epididymosomes) upon sperm functionality.

DESCRIBED PROPERTIES OF PROSTASOMES AND EPIDIDYMOSOMES	SPECIES	KEY REFERENCES
Enhancing sperm motility	Human Bovine	Stegmayr and Ronquist., (1982); Park et al., (2011) Martin-DeLeon., (2015)
Prevention of microbial activity	Human	Carlsson et al., (2000)
Immunosuppressive activity of the female reproductive tract	Human	Skibinski et al., (1992); Vojtech et al., (2014)
Aiding post-testicular sperm maturation	Bovine	Caballero et al., (2012)
Inhibition of phagocytosis	Human	Skibinski et al., (1992)
Mediating capacitation and acrosome reaction:		
- Induction of capacitation	Human	Park et al., (2011)
- Inhibition of capacitation	Human	Palmerini et al., (2003)
- Inducing acrosome exocytosis	Human	Cross and Mahasreshti., (1997); Minelli et al., (2002); Pons-Rejraji et al., (2011)
	Boar	Siciliano et al., 2008
Effects on the plasma membrane:		
- Membrane fluidity	Human	Carlini et al., (1997)
- Membrane integrity	Boar	Piehl et al., (2013); Du et al., (2016)
Protective effect against oxidative stress	Human	Skibinski et al., (1992)
Protective effect against freezing/thawing stress	Boar	Fernandez-Gago et al., (2013)

Epididymosomes are involved in fertilization by being brought into contact with immature sperm in the cauda epididymis. These have an important role in the segregation of proteins from their lipid raft domains onto acceptor lipid-raft domains in the sperm's membrane in order to enhance sperm maturation, and also to provide the sperm with the proteins that will enable oocyte-sperm interaction (Cooper, 1998; Sun et al., 2000; Saez et al., 2003; Sullivan et al., 2007; Oh et al., 2009). In contrast, prostasomes first make contact with the sperm cells during ejaculation (Aalberts et al., 2014). This interaction takes place more efficiently under capacitating conditions in the form of binding (Aalberts et al., 2013).

This binding of prostasomes with the sperm has been suggested to occur in the uterus and the oviduct, both sites with a slightly alkali pH and with the presence of bicarbonate (Arienti et al., 1997; Carlini et al., 1997; Schwarz et al., 2013).

Membrane fusion between prostasomes and sperm will then only take place in capacitated sperm under acidic conditions, that further increased the sperm's membrane fluidity rendering it susceptible to interact with the oocyte (Carlini et al., 1997; Ikawa et al., 2010). It has been suggested that prostasome fusion may be enhanced by a reduction in pH at the sperm's entry site between the oocyte's cumulus cells (Aalberts et al., 2014).

Prostasomes are also regarded as precursors for the initiation of capacitation only in capacitating conditions, that takes place under the presence of bicarbonate and at a pH around 7.4-7.5 by increasing intracellular cAMP, the central activator of various capacitation-related processes, once the sperm reaches the oviduct, as these are piggy-backed by the sperm (Pons-Rejraji et al., 2011; Aalberts et al., 2013). It has also been hypothesised that prostasomes are essential for calcium signalling pathways required for the later stages of capacitation, such as the induction of motility hyperactivation and the acrosome reaction (Palmerini et al., 1999; Palmerini et al., 2003; Pons-Rejraji et al., 2011; Park et al., 2011).

The enhancement of sperm physiology and oocyte fertilization are not the only reproductive roles in which EVs seem to be implicated. *In vitro* studies have also correlated the presence of EVs seminal fluid with a high level of decidualisation in the female endometrium (Doyle et al., 2012; Rodriguez-Caro et al., 2019). This suggests a role of seminal fluid EVs in enhancing endometrial receptivity in terms of the morphological and functional changes in the endometrium in preparation for embryo implantation. In addition, a recent study by Chen et al. (2020) suggests that a paternal tRNA implicated in early embryo cleavage may be transferred into the mature sperm by seminal-derived exosomes, thus playing a significant role in preimplantation embryo development.

1.4.2 Extracellular Vesicles from the Female Reproductive System

So far the female EVs have been isolated from the vagina, the uterus and the oviduct (known as uterosomes and oviductosomes respectively), and from the oocyte's follicular fluid. EVs originated from female reproductive tissues also represent a key mediator in the fertilization processes including oocyte-sperm recognition and supporting embryo implantation.

It has been speculated that female fluid EVs also may modulate sperm functions relevant for fertilization (Al-Dossary et al., 2015; Martin-DeLeon, 2016; Fereshteh et al., 2019; Franchi et al., 2020). During the phases prior to fertilization, the female reproductive tract is a hostile environment that promotes selection for high quality sperm, and is only protective in the oviduct beyond the isthmus site, allowing the sperm to fully prepare for fertilization. Correspondingly, EVs from the vagina and the uterine may be associated with sperm physiology and embryo-endometrial interaction among other possible functions (Griffiths et al., 2008; Machtinger et al., 2016; Simon et al., 2018; Fereshteh et al., 2019).

Oviductosomes, on the other hand, may be involved in aiding fertilization processes (Al-Dossary et al., 2013). The oviduct has two main parts; the isthmus, responsible for sperm capacitation, and the ampulla, which provides the environment for oocyte interaction and fertilization. Due to their different functions, it has been proposed that EVs from these two portions have distinct roles (Al-Dossary et al., 2013). Oviductosomes isolated from these two different regions of the bovine oviduct, however, had similar biological effects on sperm functionality *in vitro* (Franchi et al., 2020). Moreover, an increase in the intracellular calcium levels of the sperm treated with EVs isolated from the ampulla indicates that further studies may elucidate distinct roles for EVs within signalling pathways (Franchi et al., 2020).

The EVs that are isolated from follicular fluid are released either by the theca cells, granulosa, cumulus cells and/or the oocyte, and these have been linked with follicular maturation and oocyte competence (Da Silveira et al., 2012; Machtinger et al., 2016; Simon et al., 2018).

Another important fertilization role has been granted to female EVs; During oocyte-sperm fusion events and exocytosis of the sperm's acrosome a specific subset of EV markers, tetraspanins CD9 and CD81, are closely involved with tetraspanin-tetraspanin interaction in what is known as "tetraspanin web formation" (Frolíková et al., 2018). It has also been reported the transfer of these transmembrane proteins into the sperm's membrane occurs via EVs released from the oocyte at the moment of sperm penetration through the egg's perivitelline space (Miyado et al., 2008; Tanigawa et al., 2008; Ohnami et al., 2012). In addition, there is some evidence shedding light to embryo intercommunication taking place via EVs. It has been reported that for different mammalian species the *in vitro* culture of pooled embryos is more successful than when embryos are cultured individually, (Ferry et al., 1994; Hoelker et al., 2009; Ebner et al., 2010; Restelli et al., 2014). Despite being illogical from a physiological point of view, this idea is sustained by the concept that embryos may generate their own microenvironment by secreting growth factors that exhibit autocrine and paracrine effects (Katz-Jaffe et al., 2006; Saadeldin et al., 2014). This secretome has been shown to contain extracellular vesicles that are capable of traversing the ZP to end up being internalised by blastomeres within the embryo (Ratajczak et al., 2006a; Saadeldin et al., 2014).

The most abundant EV subtype to have been characterised within embryonic secretome are exosomes, it has been suggested that these exosomes provide a form of two-way communication in which embryo-derived exosomes are taken up by the maternal counterpart including the endometrium, the epithelial and the stromal cells, as possible mediators for embryo implantation (Giacomini et al., 2017), process which is considered as one of the main causes of failure during ART procedures.

Moreover, uterosomes, as reviewed earlier for their effects upon sperm, may have an additional role in further supporting maternal-embryo cross-talk; It has been hypothesised that both the endometrial epithelial cells and the blastocyst acquire uterosomes, leading to the transfer of signalling molecules and immunomodulating factors. In doing so, the endometrium is prepared for embryo invasion and the maternal immune system is regulated for the entire duration of pregnancy, through the release of uterosomes into the blood (Ng et al., 2013; Braundmeier et al., 2012; Burnett et al., 2012 and Nguyen et al., 2016). Together with embryo and placental-derived EVs, uterosomes constitute a major communication mechanism between the foetus and the mother (Redman and Sargent, 2007; Tannetta et al., 2014; Tong and Chamley, 2015; Nair and Salomon, 2018).

Because of the clear functional roles of EVs as mediators for fertilization processes and pregnancy support, there is significant interest in investigating their potential as a therapeutic tool for reproductive purposes (Barkalina et al., 2015b; Simon et al., 2018).

This is why, when developing a therapeutic approach for male infertility, not only the influence of the EVs derived from the male reproductive tissue, but also that from those female EVs should be examined, as there could be an enhancing or suppressing effect on the desired outcome.

1.5 Theragnostic Applications of EVs and Future Perspectives in the Fields of Reproductive Biology and Medicine

1.5.1 Diagnostic Advances Facilitated by EVs

Due to their ubiquity and specificity, the field study of EVs has become very popular and has grown interest in a wide range of diseases and medical conditions (Andaloussi. et al., 2013; You and Ikezu, 2019). Since exosomes have been discovered in all the human body fluids and carry a specific cargo that is dependent on the cell type and physiological state of the donor cells, they are considered very valuable for minimally invasive diagnosis, for instance, by making it possible to use urine samples instead of having to perform painful biopsies.

EVs are being used in the diagnosis; as biological markers for cancer progression, immune system competence, and disease prognosis (Vlassov et al., 2012; Tan et al., 2016; Bernard et al., 2019). They are helpful for diseases that are largely inaccessible such as pancreatic tumours, and in cases where early diagnosis is crucial for an effective therapeutic outcome (Nilsson et al., 2009; Palanisamy et al., 2010; Spielmann and Wong, 2011; San Lucas et al., 2016). For instance, blood-circulating miRNAs carried in exosomes have been identified as valuable biomarkers for colorectal cancer, lung cancer, and diabetes (Chen et al., 2008; Gilad et al., 2008; Mitchell et al., 2008). Since approximately 2010, several companies have been developing exosome-based diagnostic tests in the oncological space, that rely upon biofluid-based systems to capture and analyse EVs that contain cancer biomarkers. Some of these exosome-based diagnostic tests are commercially available, such as the ADAPT biotargeting system by Caris Life Sciences, which is used for pancreatic and breast cancer diagnosis, and Exosome Diagnostics'ExoDx™ Prostate Test at-home collection kit.

Similar to cancer diagnostics, exosomes have also become a focus for reproductive scientists in identifying conditions that are challenging to diagnose. This is the case for endometriosis; a multifactorial and heterogeneous disease in women that currently lacks suitable diagnostic markers (Khalaj et al., 2019). But also for the non-invasive pre-implantation genetic testing of embryos (carried out at IVF clinics for embryo selection to avoid transferring to the mother's uterus embryos carrying chromosome aneuploidies or disease-related mutations); As it has begun to be developed the genetic screening of embryonic DNA that is secreted onto the culture media through exosomes, instead of using the conventional pre-implantation genetic testing via blastomere biopsies that compromise the embryo's viability and are much more cost-worthy (Galluzzi et al., 2015; Leaver and Wells, 2020; Simon et al., 2020). Therefore, the importance of exosomes as carriers of metabolites and genetic material that can be used for diagnostic and therapeutic applications is becoming increasingly useful to avoid the conventional methods that are invasive and sometimes difficult to perform.

1.5.2 Therapeutic Advances Facilitated by EVs and Clinical Limitations

Exosomes are being developed as a biocompatible approach for drug delivery in a wide range of diseases for a number of reasons;

(1) Exosomes have demonstrated capability to deliver drugs both *in vivo* and *in vitro* (El-Andaloussi et al., 2012) with higher efficacy than that of liposomes and nanoparticles (Fuhrmann et al., 2015; Haney et al., 2015; Ohno et al., 2016; Matsumoto et al., 2017b; Saint-Pol et al., 2020). The first proof-of-concept showing the potential of exosomes as vehicles for compounds was performed to load siRNA to the brain using naturally-engineered exosomes from readily available cell lines (Valadi et al., 2007; Alvarez-Erviti et al., 2011).

Exosomes have been loaded with nucleic acids and biologically active compounds, such as curcumin and catalase, for their subsequent release into human tissues (Sun et al., 2010; Ruiss et al., 2011; El-Andaloussi et al., 2012; Wahlgren et al., 2012; Ohno et al., 2013; Tian et al., 2014; Haney et al., 2015; Liu et al., 2015; Aryani and Denecke, 2016; Ju et al., 2017).

(2) Exosomes can be administered *in vivo* via subcutaneous, intraperitoneal, intranasal, intravenous routes, and even via oral administration; all of the methods have the proven potential to reach different sites of therapeutic action (Burnouf et al., 2019). Interestingly, exosome-formulated drugs such as the chemotherapeutic drug paclitaxel, have been successfully administered orally, and show good stability under the acidic conditions of the digestive system (Agrawal et al., 2017).

(3) The unparalleled internalization of drug-loaded exosomes into specific cells and tissues, such as catalase-loaded exosome accumulation in mice neurones and microglial cells (Haney et al., 2015), highlights the efficacy of crossing the blood-brain barrier (Osorio-Querejeta et al., 2020).

The use of exosomes for drug delivery across biological barriers has implications for male infertility treatment and overcoming the BTB, which presents a major drug administration challenge to the male reproductive tissues (Chen et al., 2016). In addition to BTB challenges for fertility drug administration, intra-sperm delivery of compounds is limited by the high structural compartmentalisation of the sperm's plasma membrane that resists exogenous molecule uptake (James et al., 2004; Tapia et al., 2012) (**Figure 1.10**).

The sperm plasma membrane differs from most other human cell membranes in its higher percentage of fatty acids, consisting of cholesterol, neutral fatty acids, glycolipids and phospholipids. A significant proportion of these phospholipids are plasmalogens, particularly PUFA (Lenzi et al., 1996).

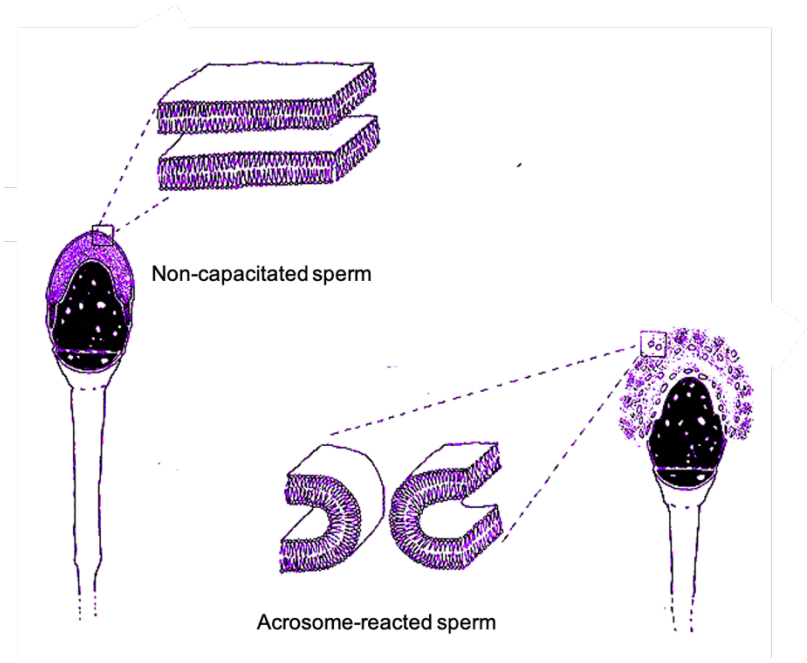

Figure 1.10. Schematic representation of the structure of the plasma membrane displaying high lipidic compartmentalisation in a human non capacitated sperm and disposition of the polyunsaturated phosphatidylethanolamine plasmalogens in an acrosome reacted sperm. Adapted from: *Martinez and Morros, (1996) under a CC BY-NC 3.0 license.*

This network of fatty acids, together with the cholesterol molecules, act as a shield to the sperm by playing a key role in stabilizing the membrane and protecting it against external agents (Tapia et al., 2012). For these reasons, the penetration of this shield remains a challenge that has to be addressed using alternatives other than potentially toxic nanomolecules.

For the development of exosomes for clinical purposes, several considerations need to be taken into account. For instance, there are concerns relating to bioengineering techniques in terms of their clinical safety, since these might be related to the use of vectors with a viral origin, and hence, the associated risk of an undesired integration of viral material (Lenzi et al., 1996).

The challenges encountered in exosome administration that are related to physical barriers, rapid *in vivo* clearance, and immune-dependent phagocytosis necessitate higher administration of doses, thus compromising the safety and clinical applicability of this approach. EV administration poses challenges relating to their fast clearance and short half-life in blood and bioaccumulation.

Exosome administration routes result in their accumulation in preferential organs such as the spleen, the liver, and the kidneys (Matsumoto et al., 2017a), highlighting the importance of choosing an adequate source cell and administration route (Wiklander et al., 2015). Wiklander (2015) compared the distribution sites of exosomes isolated from different cell sources after different systemic administration routes in mice. These authors observed some differences in biodistribution patterns between the different exosome sources, suggesting that exosomes may adopt the homing trends of the maternal cell of origin. They also proved that intravenous injections resulted in significantly higher levels of accumulation in the liver and spleen compared to intraperitoneal and subcutaneous injections. However, in order to increase the likelihood of exosomes accumulating in the desired tissue, EVs can be modified with ligands and cell-penetrating-peptides to target them towards specific tissues and cell-types (Armstrong et al., 2017; Murphy et al., 2019). The clinical relevance for exosomes has rapidly begun to expand since the first assays have demonstrated a true clinical utility, subsequently gaining international and FDA approvals (Castellanos-Rizaldos et al., 2018).

The rise in use of EVs in the laboratory first led to the implementation of guidelines and standardised initiatives, such as the EV Transparent Reporting and Centralising Knowledge (EV-TRACK) and the Minimal Information for Studies of EVs guidelines (MISEV) (Lötvall et al., 2014; Witwer et al., 2017; Thery et al., 2018).

As research moves forward into a clinical context, position statements discussing the clinical requirements for EV-based assays and structured procedures for the pharmaceutical categorization of EV-based therapeutics have been published by the ISEV, together with representatives from the European Network on Microvesicles and Exosomes in Health and Disease, supported by the EU Horizon 2020 program (Lener et al., 2015; Ayers et al., 2019).

An important caveat in the development of EV-based therapeutics is the inherent heterogeneity and biological complexity of these samples since their properties are influenced by their parent cells, as well as by their modification and handling, thus hampering the identification of the therapeutically active component and its mode of action. However, recently a number of academic institutions and hospitals have carried out small scale first-in-human Phase I clinical trials using exosomes (Chen et al., 2019). Publications arising from these trials suggest that exosome treatment is safe and well-tolerated (Shigemoto-Kuroda et al., 2017; Du et al., 2018; Yin et al., 2019). The first-ever reported clinical trial using exosome-based therapies was conducted in France by Escudier et al., (2005), using EVs from dendritic cells to investigate their antitumor effects in patients with melanoma. This study, together with another Phase I trial that was conducted simultaneously in the US in patients with advanced non-small cell lung cancer, revealed promising results regarding the safety and feasibility of EV administration (Morse et al., 2005). Such success led to a Phase II clinical trial (NCT01159288) that was conducted ten years later to treat non-small cell lung cancer patients (Viaud et al., 2011). However, in this study, EV-treatment did not induce an adaptive T cell anti-tumour response in the patients, possibly due to their late metastatic stage at the moment of the treatment (Besse et al., 2015; Lener et al., 2015). Despite the steady increase in the number of clinical trials registered in international databases, very few of these incorporate ongoing studies that investigate the potential of exosomes as therapeutics.

Since the beginning of 2020, with the emergence of the SARS-CoV-2 viral infection, the field of EV therapy is experiencing an increase as novel therapies to tackle this worldwide pandemic are explored. This is the case of a Phase I clinical study sponsored by Ruijin Hospital (NCT04276987), to test an inhalator in patients with severe acute respiratory syndrome caused by the SARS-CoV-2 virus.

This device delivers exosomes that are derived from mesenchymal stem cells via the intranasal airway since previous research work has shown their significant ability to reduce lung inflammation and pathological impairment (Liu et al., 2020).

Some biotechnology companies are also reaching the pivotal point of testing exosome-based products in humans. Earlier this year and Australian company Exopharm, announced the first dosing in its first human clinical trial to test the wound healing potential of platelet-derived exosomes. This Phase I study will test Exopharm's product Plexaris; a cell-free exosome formulation. Preclinical animal studies have already shown a regenerative effect for wounds and scars (Exopharm, 2021). The clinical application of exosomes is still very premature, and further investigations will need to identify cost- and time-effective procedures to allow the mass production of exosomes to achieve realistic batch sizes for therapy in a clinical setting. This is one of the biggest issues for drug manufacturing and development, as discussed in the international harmonisation guidelines published by the International Council for Harmonisation of Technical Requirements for Pharmaceuticals for Human Use (ICH) (www.ICH.org). In order to deal with this problem, some academic groups have recently begun to investigate ways of amplifying the enrichment or purification strategies for exosome production; Some of these techniques focus on the enrichment of EVs from cell culture supernatants by using plastic adherent cultures and bioreactors of different types, similar to those used for tissue engineering (Teixeira et al., 2017; Watson et al., 2018; Yan et al., 2018). Ideally, this process should be scalable in the future and be able to accommodate large volumes of cell culture media in order to circumvent and reduce the costs of production (Gimona et al., 2017).

Research and development of exosome-based strategies for human infertility remain scarce, yet the advancements achieved for the therapies used in other fields of medicine make a big contribution to the field, by learning from the successful practices.

1.5.3 EV-Applied Therapy for Reproductive Medicine

As already mentioned, despite the generalised increase in research and applications of EVs into a large number of diseases, the field of reproductive medicine remains far from any clinical or preclinical studies. With regards to the therapeutic potential of this tool, very few studies have purposely isolated exosomes for their directed use as molecular carriers to treat infertility-related problems. The ideal use-case for this kind of therapy would be infertile male patients, whose infertility problem is caused by a lack or deficit of molecular cargo in the mature sperm, for instance, those patients lacking sperm-borne oocyte-activating factor PLCζ, resulting in oocyte activation failure post-fertilization, even following the intracytoplasmic injection of sperm into oocytes (ICSI) (Amdani et al., 2013), and hence, these tools could be used in applied ART to supplement gametes with fertility-enhancing compounds, either promoting sperm motility or protecting gametes from deterioration during long-term culture *in vitro* (Barkalina et al., 2015b).

EVs have been isolated from female and male reproductive fluids, and their potential use in embryo implantation and gamete maturation explored (Sohel et al., 2013; Vilella et al., 2015; Rodriguez-Caro et al., 2019). In these studies, exosomes that are already present in the physiological environment where fertilization and embryo development takes place have been isolated, and their transporting role of these molecular mediators tested, and hence no modifications nor exogenous cargo has been introduced into these nanocarriers for these assays. More precisely, for mammalian sperm several studies have experimented with prostasomes that have been previously isolated from semen ejaculates by incubating them with sperm cells (Siciliano et al., 2008; Fernandez-Gago et al., 2013; Piehl et al., 2013; Mogielnicka-Brzozowska et al., 2015; Du et al., 2016; Zhou et al., 2019). Piehl et al. (2013) reported successful transfer of proteins from prostasomes into sperm; the largest natural protein to be transferred to the sperm membrane was actin (42 kDa of molecular weight).

Sperm present an advantage for the transfer of molecular cargo as they are more abundant than oocytes and can be used as a vector for the transfer of therapeutics or metabolites into the oocyte upon fertilization. The mechanism by which sperm is used for the transfer of genetic material is known as sperm-mediated gene transfer (SMGT) (Smith and Spadafora, 2005; Coward et al., 2007; Moisyadi et al., 2009; Parrington et al., 2011), but this concept may be used more broadly as sperm-mediated transfer (SMT) to refer to any EV cargo intended for its incorporation into the resulting embryo. This method of sperm cell delivery would avoid embryo manipulation, and hence, avoid harming the embryo. Furthermore, when looking to go one step further in the indirect cargo transfer, this can also be carried out via testicular-mediated administration (TMA), initially developed as a method for the creation of transgenic animals, which offers the advantage against SMT that is allows the mass transfer of the cargo (Muramatsu et al., 1997). TMA is also of special importance for gene-editing purposes, which in such case can be referred to as testicular-mediated gene transfer (TMGT). Many groups have targeted SSCs for the introduction of CRISPR/Cas9 gene-editing machinery in order to correct paternal mutations at the level of this precursor stem cell and hence prevent them from being passed on to the future generations. So far, this has not been attempted *in vivo* via testicular administration, but rather *in vitro* using techniques such as electroporation (Wu et al., 2015; Sato et al., 2015; Sato et al., 2020), to ensure the loading of these constructs into the cultured SSCs.

In the past, for TMGT several strategies have been used including viral, non-viral, physical, and chemical methods (Sehgal et al., 2011). Due to safety reasons, non-viral methods such as lipofection- and electroporation-based TMGT have become preferred methods (Dhup and Majumdar, 2008; Pramod and Mitra, 2018).

Exosome-aided TMA, as a non-invasive approach for cargo transfer into SSCs has not been thoroughly investigated, nor with exosomes previously isolated from an external source, for the transfer of exogenous cargo into mammalian gametes *in vitro*. TMA aided with exosomes isolated *in vitro* is of particular relevance for the treatment of mammalian sperm since there are certain clinical scenarios where it is not possible to collect or use seminal fluid-derived EVs from those male patients with testicular cancer or those suffering from obstructive or ejaculatory problems (Shin et al., 2005; Carpi et al., 2009). Therefore, there is an urgent need for further research evaluating whether cell line-based exosomes can be used to deliver compounds into gametes in a safe manner considering the clinical setting.

To conclude this chapter, I believe exosomes derived from a mammalian cell line will offer a non-invasive alternative for compound delivery into sperm from patients with a wide spectrum fertility problems. Cell line-derived exosome delivery of therapeutics will rival current techniques, such as artificial nanocarriers, in biocompatibility, scalability and efficiency and enhance successful fertility outcomes without the use of ART.

1.6 Aims

Advances in nanomedicine have led to the targeted delivery of imaging and therapeutic agents to tissues or cell-types, creating a non-invasive diagnostic and treatment approach that rivals the ability of engineered nanomaterials. Such a biocompatible approach to fertility treatment is of urgent need, as gametes that underpin human development are susceptible to damage with traditional fertility treatments and problematic nanomaterials.

Exosomes are being developed in many fields of medicine as nanocarriers capable of rivalling artificial systems for their similarities with cell-derived structures in terms of size, surface area, loading capabilities, for their robustness concerning ease for mass production and stability within body fluids, and finally, for their versatility in terms of physicochemical properties allowing their adjustment to a specific function and target.

Exosomes as a versatile delivery tool can also be deployed for the transfer of genetic material, lipids, proteins, and exogenous agents, in various reproductive contexts; either for the direct supplementation of gametes or the indirect enhancement of fertility-related processes including loading of blocking agents or inhibitors for research purposes into the better understanding of human infertility. This approach may improve our ability to perform intra-gamete delivery in an efficient and non-invasive manner towards achieving or improving sperm functionality and indirect loading of therapeutics into the oocyte upon its fertilization. Therefore, enhancing the advancement of infertility treatment. However, the safety and reproducibility for the use of this biocompatible alternative remains to be examined with sperm, characterised by its highly specialised morphology and function, thus comprising a challenging target for the loading of cargo, in a way that can be used for as many clinical patients as possible.

I aim to develop a versatile, mammalian-based manufacturing system for the isolation and exploitation of exosomes for a non-invasive *in vitro* approach that can serve as a future proof-of-concept for drug delivery into sperm for male fertility treatment, and evaluate its safety and reproducibility for future development in a research and clinical contexts.

1.6.1 Objectives

The following study objectives will be pursued to achieve the study aim:

1. To develop a mammalian-based high yield and scalable system using HEK293T cells for the isolation of exosomes with exosomal traits and preserved functional integrity. Sample characterisation techniques recommended by the ISEV will be used to assess exosomes due to compatibility with live mammalian sperm.

2. To evaluate the short-term and long-term effects of the exposure of HEK293T-derived exosomes upon sperm functionality. HEK293T-derived exosomes will be co-incubated *in vitro* with boar sperm under conditions mimicking the fertilization setting and appropriate exosome doses and incubation times will be determined through the safety, reproducibility and efficacy perspectives.

3. To evaluate exosome-sperm interaction efficiency using different labelling strategies, including surface binding and intracellular uptake in a qualitative and quantitative manner, and an in-depth analysis of the potential uptake mechanisms.

4. To develop a proof-of-concept for exosome functionalization to enhance specific sperm targeting and test different strategies for loading molecular cargo into the exosomes, for future high efficiency drug delivery into the recipient sperm.

CHAPTER 2

The use of HEK293T cells and Mammalian Culture Methods for the Mass Isolation of HEK293T-derived Exosomes

2.1 Aim of this Chapter

This chapter aims to develop and test a protocol for the mass isolation of exosomes from a mammalian-based system using HEK293T cells, in a consistent, reproducible and scalable manner, to further exploit their delivery potentials for reproductive purposes.

2.2 Background

2.2.1 HEK293T Cells as a Source of EVs for Reproductive Purposes

Researchers have been studying how to isolate EVs for their potential to deliver drugs. EVs are secreted by all human tissues and researchers have described a vast number of methods for their successful retrieval from a number of different sources (Gandham et al., 2020).

Reproductive scientists have described the properties of EVs isolated from reproductive fluids, more specifically, prostasomes from the seminal fluid have been widely used for different reproductive outcomes (Fernandez-Gago et al., 2013; Piehl et al., 2013; Mogielnicka-Brzozowska et al., 2015; Du et al., 2016; Rodriguez-Caro et al., 2019; Zhou et al., 2019). Nonetheless, this is not the only source from which exosomes or other types of EVs can be isolated from for their use with mammalian gametes.

When considering certain clinical scenarios, the retrieval or use of seminal fluid is not necessarily an option. This is the case for patients with ejaculatory problems, or those suffering from testicular or other forms of cancer (Shin et al., 2005; Carpi et al., 2009). For these patients *in vitro* cultured cell lines may represent a unique source for exosome-based therapies.
Many researchers are now considering HEK293T cells as the commercial cell line of choice for the production of exosomes.

The main reasons to consider HEK293T cells as an ideal source of exosomes is because these cells lack cancer-related and immunogenic mechanisms and are regarded safe to work with under *in vitro* and *in vivo* conditions (Li et al., 2016; Rosas et al., 2016; Zhu et al., 2017). Li and colleagues (2016) profiled the protein, RNA, and miRNA cargo contained in the exosomes derived from HEK293T cells. These authors used Gene Ontology and the Kyoto Encyclopedia for Genes and Genomes databases, and concluded that very few pathways were disease-related or cancer-related in the exosomes derived from these cells when characterizing the proteins and RNA present within them. In another study, Zhu et al (2017) dosed mice with HEK293T-derived EVs both intravenously and intraperitoneally for 3 weeks and then evaluated the EV-induced immune response and toxicity levels. Blood samples were collected and analysed from each mouse and no signs of toxicity were detected either with regards to cell populations, chemical composition, or immune markers. Moreover, EVs derived from HEK293T cells have also been shown to exhibit significant versatility in terms of their targeting ability; HEK293T-derived exosomes have successfully been used to deliver anticancer drugs to hematopoietic cells such as myeloid cells, B cells, and have the capability to cross the blood-brain barrier in both *in vitro* and *in vivo* mice models (Sun et al., 2010; Alvarez-Erviti et al., 2011; Ruiss et al., 2011; Corso et al., 2019; Osorio-Querejeta et al., 2020). Li *et al* (2016) also reported protein content in HEK293T-derived exosomes directly related with various tissues including placenta, skin, liver, uterus, muscle, lymph, lung, and hepatocytes, suggesting their ability to interact specifically with such tissues. Finally, HEK293T cells also allow a versatile manufacturing system for the mass production of exosomes as proven by El-Andaloussi et al (2012) when they developed a protocol with mammalian-cell transfection for the mass engineering of HEK293T-derived exosomes containing the cargo and a cell-penetrating peptide (CPP) of interest.

Indeed, *in vitro* cultured cell lines are considered to be the only efficient approach for the manufacture and large scale production of modified EVs. This is important when considering the further development of these nanotools in an industrial context (Gimona et al., 2017), also for the application of exosomes with reproductive cells and tissues, something yet to be explored.

2.2.2 Techniques for the Isolation of Exosomes

Exosomes are the smallest EV subtype. The size of exosomes (between 30 nm and 120 nm) and their physicochemical properties including their buoyant density, overlap between different EVs, thus posing a significant challenge when trying to purify specific subtypes from one another (Carpintero-Fernández et al., 2017).

The gold standard technique for the isolation of exosomes is differential ultracentrifugation (UC). Differential UC consists of a low-centrifugation step to remove cell debris and large EV subtypes, followed by a high centrifugation step of at least 110,000×*g* to pellet the exosomes (Thery et al., 2006). Differential UC was the first extended technique for exosome isolation and is therefore most commonly reported in the literature (Gudbergsson et al., 2016). In this thesis, a slightly different UC protocol was used for the isolation of HEK293T-derived exosomes, as described in Dragovic et al (2015). This protocol was purposely established to pose a lower detrimental impact on exosomal integrity since this method only incorporates one single round of UC (Gudbergsson et al., 2016). Following isolation, there are a series of characterization techniques that have to be carried out to be able to confirm the enrichment of a particular EV subtype.

This also applies to the isolation of exosomes from HEK293T cells, for which the ISEV, a consortium of long-term experts in the field of EV biology, has published a series of guidelines to standardise a common protocol for sample identification that takes into account the different sources and methods that exist for exosome isolation (Thery et al., 2018). The minimal criteria to be followed by researchers isolating exosomes from cell media include: (1) the quantification of enrichment in terms of the concentration of exosomes in a volume of sample, (2) characterization of the size distribution of the samples using a system such as Nanoparticle Tracking Analysis (NTA), (3) the visualisation of the exosome's morphology with Transmission Electron Microscopy (TEM), and (4) a semi-quantitative analysis of the protein expression levels as specific markers for exosomes by comparing their expression levels with those from the cell lysate the exosomes were isolated from. Such markers need to be a minimum of three proteins that are expected to be enriched in exosomes, especially transmembrane and cytosolic proteins; this will ensure the integrity of the exosomes at the time of sample processing by Western Blotting (WB). It is also important to include negative controls; that are proteins not to be expected in exosomes, such as proteins that are enriched in larger EV subtypes (e.g. apoptotic bodies and oncosomes). Such controls are vital because it ensures the absence of contaminant vesicles and cellular organelles such as mitochondrial, and endoplasmic reticulum, and thus, further confirms the lack of cancer-related or apoptotic-inducing factors that can be detrimental to mammalian sperm.

2.3 Hypothesis

I hypothesised that extracellular vesicle samples obtained from this commercial cell line and in following optimum UC-based protocols will allow the enrichment of exosomes in high concentrations, with a preserved and functional status compatible for their use with mammalian sperm.

2.4 Materials and Methods

2.4.1 The Mass Production of Exosomes from HEK293T Cells

HEK293T cells were cultured in Dulbecco's modified essential medium (DMEM) supplemented with 10% foetal bovine serum (FBS), 1% v/v penicillin and streptomycin, and 4mM glutamine. Cells were incubated at 37°C with 5% CO_2 for 24 hours to 70% confluency. DMEM was replaced by serum-free expression media (Expi293) (Life technologies, California, US) supplemented with penicillin and streptomycin (1% v/v), and kept for a further 48 hours at 37°C with 5% CO_2 by slightly modifying the protocol by Thery et al (2006). To achieve high exosome concentrations, HEK293T cells were cultured in 24 flasks (175 cm^3). A total of 600 mL of culture media from HEK293T cell culture was collected; this was centrifuged (5000×*g* at 4ºC for 10 min) and the resulting supernatant was filtered through a filter with a 0.20 μm pore-size (VWR, UK). The filtrate was then centrifuged at 150,000×*g* for 2 h at 4ºC in a Beckman Coulter L-80 UC ultracentrifuge equipped with an SW 32 Ti Swinging-Bucket Rotor (Beckman Coulter, UK).

The pellet was resuspended in phosphate-buffered saline (PBS), as previously described (Dragovic et al., 2013) (**Figure 2.1**). Samples were stored at –80°C for no longer than 3 months to avoid structural damages (See **Appendix I.I**).

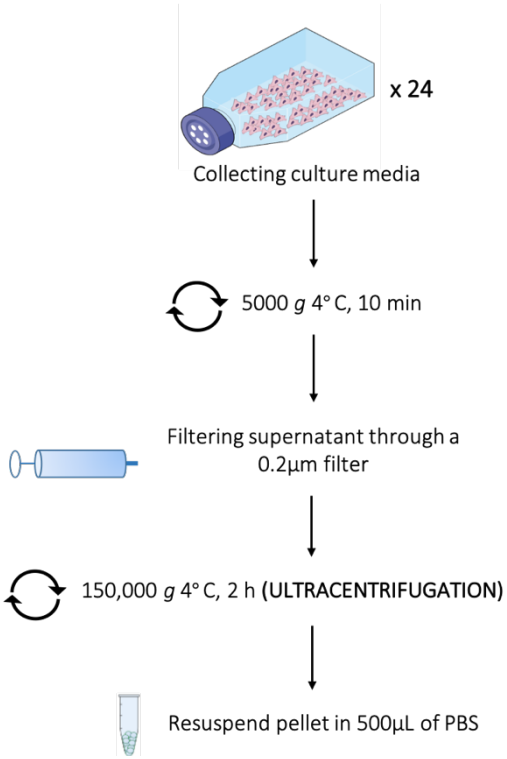

Figure 2.1. Differential ultracentrifugation-based protocol for the isolation of HEK293T-derived exosomes from the culture media of HEK293T cells cultured in 24 flasks (175 cm^3).

2.4.2 Sample Characterization Techniques

Several techniques were carried out to prove that the samples were enriched with exosome-like vesicles, including; NTA, the bicinchonic acid assay (BCA) for total protein quantification, WB, and TEM. These techniques were carried out in strict accordance with the Minimal Information for Studies of Extracellular Vesicles 2018 (MISEV2018) guidelines to ensure that each sample was evaluated accurately with regards to sample purity and exosome integrity (Thery et al., 2018).

Nanoparticle Tracking Analysis

The concentration and size profiles of each exosome sample (n = 3) were determined with a NanoSight NS500 equipped with a 488 nm laser (Malvern, UK), by following a previously described protocol (Carnell-Morris et al., 2017). A sample volume of at least 0.5 mL was loaded into the system using a 1 mL syringe at an infusion rate of 1000. Sample analysis was carried out with the NTA set up for the parameters displayed in **Table 1.1,** as per the manufacturer's recommendations. Video recordings were analysed using NTA 3.1 software, as carried out by other authors (Sokolova et al., 2011; Gardiner et al., 2013).

Table 2.1. Settings used for the Nanoparticle Tracking Analysis of the HEK293-derived exosome samples.

NTA SETTINGS	
PARAMETERS	VALUE
Infusion rate	15
Flow speed	5-10s
Camera level	12
Camera detection level	5
Video recordings	5 x 60s/video
Minimum number of completed tracks	200/video
Shuttler speed	30 * 8 ms
Camera gain	219

Protein quantification by a bicinchonic acid protein assay

The BCA protein assay kit (Pierce, Paisley, UK) was used to determine the total protein content in each exosome sample, and each assay was performed in triplicate. Protein concentrations were extrapolated from a standard curve using a linear equation.

Western Blotting

Western Blotting was carried out by loading exosome samples in triplicate alongside their source material lysate (HEK293T cell lysate). Each sample contained an equivalent amount of total protein (10 μg) to allow the comparison of different markers between the exosome samples and the cells from which they were derived. Protein extracts were mixed with radioimmunoprecipitation assay (RIPA) buffer (Sigma-Aldrich, US) supplemented with protease inhibitor tablets (Roche, Germany). Samples were then loaded onto a 10% Nu-PAGE gel (Novex, UK) with 1X Nu PAGE MES SDS running buffer (Novex, UK) and run at 160 V for 1 h. Protein bands generated by Western blotting were identified and manually selected for quantification on chemiluminescent blots using the GBOX Chemi XX6/XX9 (Syngene, Cambridge, UK) equipped with GeneTools software (Syngene, Cambridge, UK). Membranes were incubated with primary antibodies against specific exosome markers (Alix, Syntenin-1 and CD9). As negative controls, membranes were also incubated with primary antibodies against other cellular compartments (Calnexin, Cytochrome-C and Lamin-A). Further details relating to these protein markers are given in **Table 2.2**.

Table 2.2. Function and molecular weight of protein markers for exosome characterization: Alix, Syntenin-1, CD9, Calnexin, Cytochrome-C and Lamin-A.

MARKER	FUNCTION	MOLECULAR WEIGHT (KDA)	REFERENCES
Alix	**Cytosolic proteins involved in MVB[1] biogenesis** (Both these markers demonstrate the presence of EVs enclosing intracellular material)	95-110	(Baietti et al., 2012)
Syntenin-1		37-40	
CD9	**Transmembrane protein involved in cell targeting or cell adhesion** (This marker demonstrates the presence of EVs with a lipid-bilayer structure)	25-27	(Andreu and Yáñez-Mó, 2014)
Calnexin	**Protein involved in the ER[2] secretory pathway** (This marker serves as a negative control to discard the presence of larger EV subtypes like oncosomes)	90-95	(Andaloussi. et al., 2013; Thery, 2018)
Cytochrome-C	**Protein associated with mitochondrial compartment** (This marker serves as a negative control to discard the presence of larger EV subtypes like oncosomes)	12-14	
Lamin-A	**Protein associated with the cell nucleus** (This marker serves as a negative control to discard the presence of larger EV subtypes like oncosomes)	69-80	

[1]MVB: Multivesicular Body [2]ER: Endoplasmic Reticulum

Specific details for the primary and secondary antibodies are detailed in **Table 2.3**. The relative amount of protein in each lane was normalized against the band intensities obtained in cell lysates.

Table 2.3. List of primary and secondary antibodies used for Western blotting.

NAME	SPECIES	WORKING CONCENTRATION	MANUFACTURER
Primary antibodies			
Alix	Mouse	1:1000	AbCam
Syntenin-1	Rabbit	1:1000	AbCam
CD9	Rabbit	1:1000	AbCam
Calnexin	Rabbit	1:1000	Cell Signalling Technologies
Cytochrome-C	Rabbit	1:1000	Cell Signalling Technologies
Lamin A/C	Mouse	1:200	Santa Cruz
Secondary antibodies			
Anti-mouse	Goat	1:1000	Dako
Anti-rabbit	Swine	1:1000	Dako

Transmission Electron Microscopy

HEK293T-derived exosome samples were sent to Errin Johnson at the Electron Microscopy Facility (Sir William Dunn School of Pathology, University of Oxford) where 20 μL of undiluted exosome samples were stained by following a standard negative stain protocol and placed onto lacey carbon copper grids (300 mesh). High-resolution TEM images were then acquired with a FEI Tecnai 12 microscope operating at 120 kV, and equipped with a Gata OneView camera.

2.5 Results

2.5.1 Sample Characterization Techniques

NTA, BCA, Western blotting, and TEM were used to quantify and determine the quality and efficiency of the isolation protocols designed for the isolation and enrichment of HEK293T-derived exosomes.

Nanoparticle Tracking Analysis

Size profiles for the samples of HEK293T-derived exosomes were obtained by NTA with a lower size limit of detection of 70nm, and are shown in **Figure 2.2**. In all three profiles, the larger peaks showed a mean modal size of 167.1 nm (153.7 ± 6.6 nm, 176.7 ± 8.1 nm and 171 ± 6.0 nm); on average, 72.3% of particles were < 200 nm in size.

Additional smaller peaks, representing larger particle sizes, were also apparent, and most likely represent aggregates of exosomes. The total mean concentration represented by the area under all three curves was 8.63 x 10^{10} EV/mL.

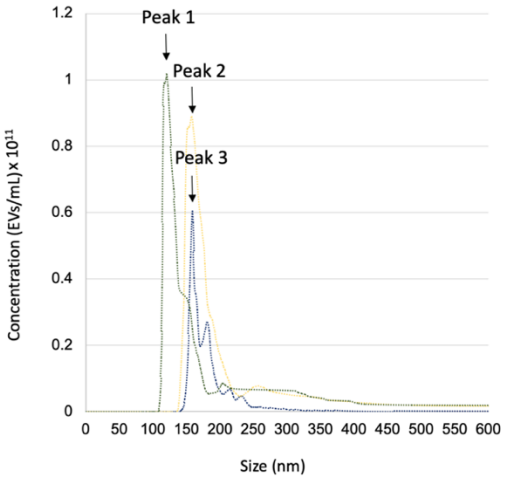

	SIZE MODE	CONCENTRATION
Peak 1	153.7 ± 6.6nm	1.14 x10^{11} ± 1.03 x 10^{10} EVs/mL
Peak 2	176.7 ± 8.1nm	8.42 x10^{10} ± 3.03 x 10^{9} EVs/mL
Peak 3	171 ± 6.6nm	6.07 x10^{10} ± 3.33 x 10^{9} EVs/mL
Total mean	167.1nm	8.63 x10^{10} EVs/mL

Figure 2.2. Size and concentration profiles, as determined by NTA, showing three peaks with a modal size of 153.7 ± 6.6 nm, 176.7 ± 8.1 nm and 171 ± 6.6 nm (n = 3).

It is worth noting that storage conditions including freeze-thaw cycles have an impact in the profile of HEK293T-derived exosomes as described in **Appendix I.I**

Protein Quantification by a Bicinchonic Acid Protein Assay

Protein assays showed a mean total protein concentration of 0.26 mg/mL. These results, together with the total concentration of exosomes obtained by NTA, were then used to determine the degree of purity of the exosome samples, as described by Webber and Clayton (2013). These authors concluded that ratios > 3×10^{10} EV/mg equate to high vesicular purity, ratios of 2×10^{10} to 2×10^{9} EV/mg represent low purity, and any ratios below 1.5×10^{9} EV/mg represent samples that are not pure. The EV:protein ratio for my HEK293T-derived exosome samples was determined to be 3.33×10^{11} EV/mg, indicating that my samples had high vesicular purity.

Transmission Electron Microscopy

TEM revealed the presence of multiple vesicle populations in the HEK293T-derived samples (**Figure 2.3**), with the most frequent ones (27 out of 31 total vesicles; 87%) being small round membranous vesicles of a size ranging between 30-100 nm (white arrows) as measured with the Image J software. Moreover, in both images two other vesicle morphologies are present in these samples; intermediate-sized oval vesicles (black arrowheads) with a size ranging from 150-250 nm in the left image, and a larger double vesicle (300 nm) resembling a rose in the right image (white circle) with another vesicle inside. Overall, no aggregation can be seen, as well as very little cell-debris contamination.

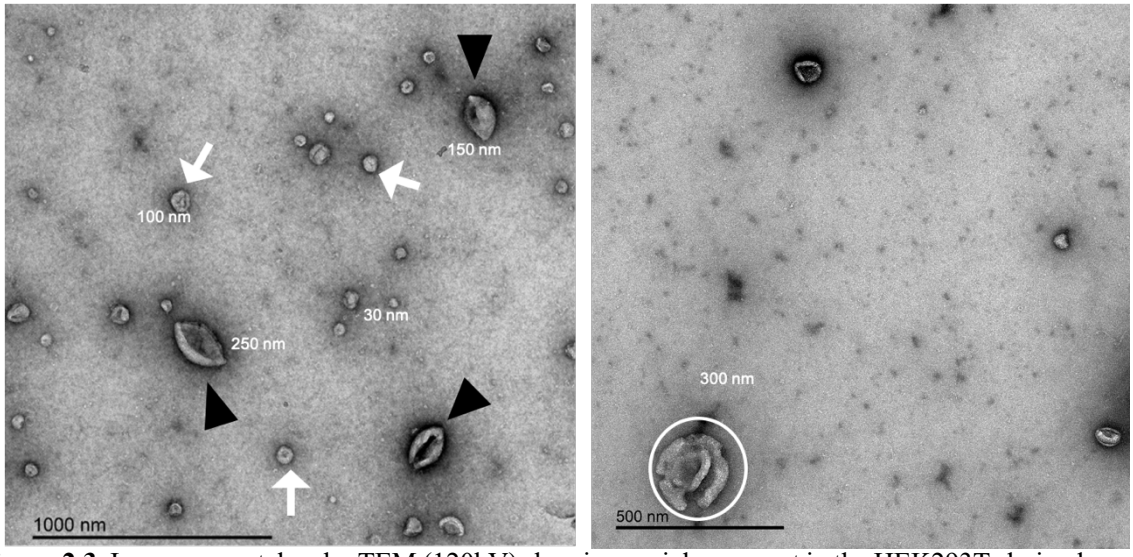

Figure 2.3. Images were taken by TEM (120kV) showing vesicles present in the HEK293T-derived samples with size ranging from ~ 30 to 300 nm. Left image displays small-rounded vesicles (white arrows) of ~ 30 nm to 100 nm in size, and oval vesicles (black arrowheads) of ~ 150-200 nm in size (scale bar = 1000 nm). Right image displays a large double vesicle (white circle) of ~ 300 nm diameter (scale bar = 500 nm).

Western Blotting

Western blotting was performed with 10 µg of total protein and used to determine the relative expression levels of protein markers in my HEK293T-derived exosome samples. The mean density of each band was quantified from chemiluminescent blots using the GeneTools software.

The analysis showed that specific-exosomal protein markers (Alix, Syntenin-1 and CD9) were expressed in all exosome samples (**Figure 2.4A**); lane 1 shows that there were no bands in the HEK293T cell lysate for either Alix or Syntenin-1. There was a weak band for CD9 in the HEK293T cell lysate (lane 1); the mean band density for this protein marker in exosome lysates (lanes 2, 3 and 4) was 0.20 fold higher that in the HEK293T cell lysate. The negative control markers (Calnexin, Lamin-A and Cytochrome-C) were all expressed in the HEK293T cell lysates. However, no bands for Cytochrome-C and Lamin-A were present in the exosome lysates (**Figure 2.4B**). While Calnexin was present in both HEK293T cell lysates and exosome lysates, the mean band density corresponding to this protein was 0.36 fold higher in cell lysates than in the exosome lysates.

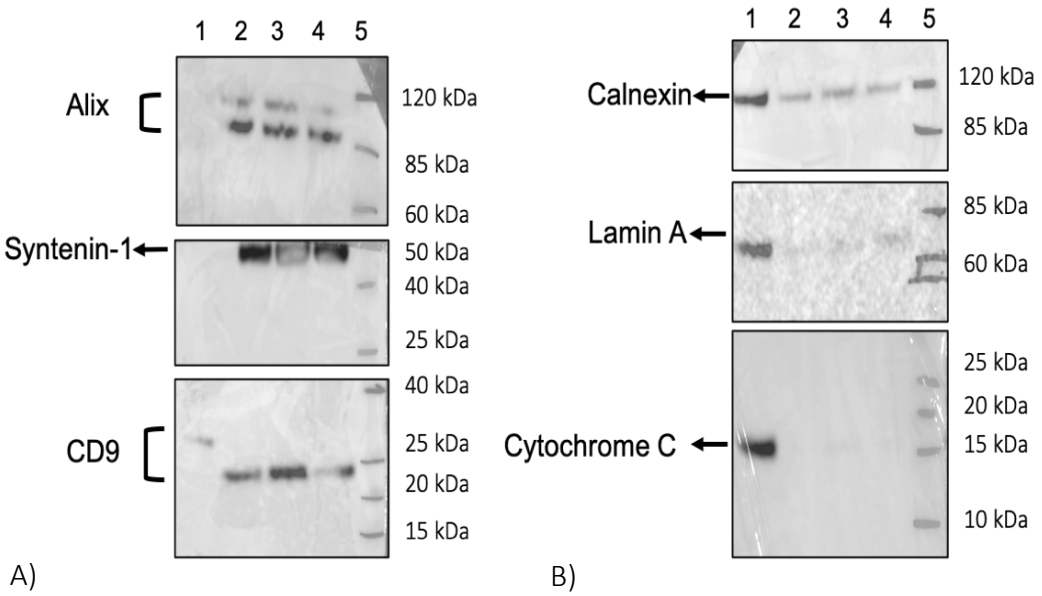

Figure 2.4. Western blotting images of the protein expression levels for A) the exosomal markers (Alix, Syntenin-1 and CD9) at ~ 97 kDa, ~ 35 kDa and ~ 25 kDa and B) negative control markers (Calnexin, Lamin-A and Cytochrome-C) at ~ 90 kDa, ~ 69 kDa and ~ 12 kDa respectively. Lane 1 corresponds to HEK293T cell lysates, lane 2-4 correspond to exosome samples (n = 3), and lane 5 corresponds to the protein marker. The density of protein bands was identified and manually selected for quantification on chemiluminescent blots using GBOX Chemi XX6/XX9 equipped with GeneTools software, by normalizing the relative protein amount in each lane against the band intensities obtained from HEK293 T cell lysates. No bands are visible for Alix and Syntenin-1 in the HEK293T cell lysates shown in lane 1, and stronger bands can be seen for exosome lysates (lanes 2, 3 and 4). CD9 was evident in lane 1; the mean band density for this protein marker in the exosome lysates (lanes 2, 3 and 4) was 0.20 times higher than in the HEK293T cell lysates. With regards to the negative markers, strong bands can be seen for Cytochrome-C and Lamin A in HEK293T cell lysate (lane 1), while no bands are present in the exosome samples shown in lanes 2, 3 and 4. Calnexin expression can be seen as fainter bands in the exosome lysates (lanes 2, 3 and 4) with a mean band density that is 0.36 times lower when compared to the HEK293T cell lysate (lane 1).

2.6 Discussion

When researchers first start working with EVs, some considerations need to be taken into account; at present, there is no specific consensus with regards to the size range, morphology, or specific markers. Indeed, these parameters depend on both the source and EV biogenesis pathway. There are several theories regarding the synthesis of exosomes, and different molecular machinery may be involved in different pathways (Raposo and Stoorvogel., 2013; Colombo et al., 2014; Kowal et al., 2014; Thery et al., 2018). Moreover, several previous studies have shown that exosomes are associated with high levels of morphological heterogeneity (Poliakov et al., 2009; Hoog and Lotvall., 2015; Zabeo et al., 2017).

Despite this variability, most authors recognize exosomes as small, round and membrane-bound vesicles, that are 30–200 nm in size (Thery et al., 2018). According to this size range, and by using existing isolation techniques, it is impossible to solely purify or isolate one single subtype of EV, due to common physical and biological properties (Carpintero-Fernández et al., 2017). The data drawn from the TEM imaging revealed that the most abundant vesicles present in my samples where indeed exosome-like vesicles, with a single-rounded structure, and 30-100 nm, yet, the two other vesicle morphologies (oval and double) present in the images correspond to already described categories of microvesicles (Smith et al., 2015; Zabeo et al., 2017). This is the first time that such categories have been identified in HEK293T-derived samples, and thus, this illustrates a higher complexity in my samples than expected.

When it comes to isolation techniques, there are many options to choose from other than differential UC. These include precipitation-based techniques, immunoaffinity methods and fluidic-based techniques (Monguió-Tortajada et al., 2019). However, these methods are not as scalable as UC and often compromise on purity for specific EV-subtypes. Furthermore, the most common strategy remains UC as it represents one of the most accessible options for laboratories (Gudbergsson et al., 2016), and this is especially important in a field where standardisation is essential for research reproducibility and validation (Gandham et al., 2020). However, as EV identification techniques have improved, it has been acknowledged that there are some drawbacks associated with differential UC that relate to EV aggregation and rupture (Linares et al., 2015).

Researchers have also reported that such high yields may represent artefacts due to the presence of contaminants (Gudbergsson et al., 2016). For this reason, Webber and Clayton (2013) suggested a method, that was accepted by the ISEV, to quantify sample purity relating to the particle-to-protein ratio that has since been widely used in many publications (Faruqu et al., 2018; Gudbergsson et al., 2016).

Nonetheless, EV researchers are beginning to orientate towards the use of an alternative technique to differential UC. Over the last few years, size-exclusion chromatography (SEC) has gained significant attention (Gudbergsson et al., 2016; Davis et al., 2019; Lee et al., 2019; Monguió-Tortajada et al., 2019). SEC was first applied for EV isolation in 2014 and is based on the differential elution profiles of different EV subtypes, by running the liquid sample through a column containing a porous polymer (or stationary phase) (Böing et al., 2014). This method is gaining significant popularity for Researchers claim that SEC protocols can more efficiently distinguish soluble proteins from EV-proteins, and enable specific biomarker screening for EVs. In this sense, SEC can be used to decipher the functional capacities of EVs (Monguió-Tortajada et al., 2019). Nonetheless, the purest elution fraction of vesicles obtained by SEC has a very low yield in comparison to those obtained from UC (Böing et al., 2014; Davis et al., 2019; Monguió-Tortajada et al., 2019). Indeed, the yield obtained is inversely proportional to and dependent upon the level of purity, and additional filtering steps lead to a count decrease in the proportion of exosomes (see **Appendix I.II** for further reference).

Despite the clear drawbacks of UC, the quality validations described in this chapter using standardized techniques for the post-UC isolation of HEK293T-derived exosomes revealed high concentrations of functional and intact exosomes as per the confirmation of the presence of CD9, Alix and Syntenin-1. These exosome samples were also confirmed to be of high purity in terms of the absence of malignant vesicles. Therefore, for the scope of this research mainly focusing into developing a nanocarrier for therapeutic purposes may not be as important to identify and select between different EV categories, but rather to ensure high quantities of competent EVs in the sample volume including microvesicles.

It is also worth mentioning that the size difference of the exosomes as determined by TEM compared to NTA (~30 nm and ~170 nm, respectively) may be due to the fact that NTA can only detect particles above 70 nm (Carnell-Morris et al., 2017), but may also be due to the shrinkage of exosomes, a potential artefact from TEM processing (Raposo and Stoorvogel., 2013). Furthermore, the absence or reduced quantities of other cellular compartments (endoplasmic reticulum, nucleus and mitochondria) in the samples used for WB eliminates the possibility of the presence of larger extracellular vesicle subtypes that are not desired, such as oncosomes and apoptotic bodies, thus, further confirming the high enrichment of these samples with regard to exosome-like vesicles. Finally, the increased expression levels of the cytosolic exosomal markers *Alix* and Syntenin-1 are informative of the exosome's preserved membrane integrity (Baietti et al., 2012; Thery et al., 2018), while the increased expression levels of the tetraspanin CD9 can be used as a biomarker of exosomal cell targeting and cell-adhesion properties (Andreu and Yáñez-Mó., 2014; Thery et al., 2018), and thus, confirming these traits in the exosomes present in my samples.

When exploiting the therapeutic potential of exosomes a thorough understanding of their composition is required at both the individual and population levels. The heterogeneity found in my HEK293T-derived exosome samples has to be critically analyzed with regard to the limitations of isolation techniques as described above.

Exosomes secreted from the same cells have traditionally been expected to contain similar molecular composition to that of the parental cell. However, as already discussed, their cargo is not only cell-type dependent but can differ even between exosomes originated from the same cell due to different biogenesis pathways, and therefore, such a distinct morphology makes it apparent to expect molecular heterogeneity as well in my samples, as it has already been reviewed by Ferguson et al (2016).

For this reason, the majority of studies use exosomes as bulk isolates when evaluating their efficacy as therapeutic carriers in preclinical studies (Alvarez-Erviti et al., 2011; Liu et al., 2015; Faruqu et al., 2018; Watson et al., 2018).

With regards to the mass production of exosomes, in this chapter, I described a very simple method to obtain large quantities of exosomes. This consisted of a batch culture for HEK293T cells, by growing the cells in 24 large flasks (175 cm^3) at a time. This approach requires no additional equipment nor extensive training and is therefore highly reproducible. Nonetheless, when discussing the available options for the mass production of EVs, there exists the possibility of using bioreactors that resemble those for tissue engineering. These bioreactors have been specifically designed for the cell culture and further collection of larger volumes of culture media (Yan et al., 2018). In fact, some of the studies developing exosome-treatments in bulk have used this method to obtain high yields of exosomes from HEK293T cells (Faruqu et al., 2018; Watson et al., 2018). Therefore, when thinking of going one step further in the manufacturing of exosomes on an industrial scale, the implementation of this technology may be considered for their clinical application for the treatment of infertility, as long as previous extensive evaluation proves the safety of the HEK293T-derived exosomes for their use with live sperm even with the existing heterogeneity in the samples obtained in bulk.

2.7 Key findings

- A versatile mammalian manufacturing system based on a commercially available cell line (HEK293T cells) was developed for exosome enrichment. The rationale behind choosing this specific source for exosome isolation was based upon its well-established properties and the simplicity of scaling-up when considering future clinical and industrial applications.
- HEK293T cells were demonstrated to be a robust and efficient source for the mass production of exosomes by following a standardised protocol that allows the assessment and recognition of exosome-like populations present in a specific sample in an accurate and reproducible manner.

- NTA, WB, TEM, and BCA confirmed the high enrichment for exosome-like vesicles preserving their cell-tethering properties. Moreover, having described for the first time up to two other distinct microvesicle categories, in terms of morphology, in the HEK293T-derived samples, showing that this mammalian-based manufacturing system may be further developed and scaled-up for the production of biologically-competent nanocarriers, as far as it can be proved that the heterogeneity found in these samples does not compromise mammalian sperm functionality.

CHAPTER 3

Assessment of the Short and Long-term Effects of HEK293T-derived Exosomes upon the Functionality of Mammalian Sperm

3.1 Aim of this Chapter

This chapter aims to test for the first time the effects of short and long-term co-incubation of HEK293T-derived exosomes with mammalian sperm *in vitro* under capacitating conditions, by assessing sperm motility, sperm viability, membrane fluidity and mitochondrial membrane potential. These are informative of the sperm's functionality and ability to undergo capacitation, process which is essential for the fertilisation of the oocyte, and in this way will be used to evaluate the safety of this treatment for future reproductive purposes.

3.2 Background

3.2.1 Animal Models for Research in the Reproductive Sciences

For the majority of ART studies, boar and cattle have been used the most commonly as animal models. While a vast number of experimental publications across the life sciences use rodents as experimental models, particularly, in the field of reproduction and more specifically for sperm-based research, the porcine model is considered as being the most suitable choice for its translation into the human context (Barkalina et al., 2016). The porcine model presents several advantages over murine or rat models, since boar sperm share morphological and physiological similarities with human sperm. In terms of cell structure, the head of rodent sperm has a hooked shape, while boar and human sperm cells have similar paddled and oval head shapes respectively (**Figure 3.1**).

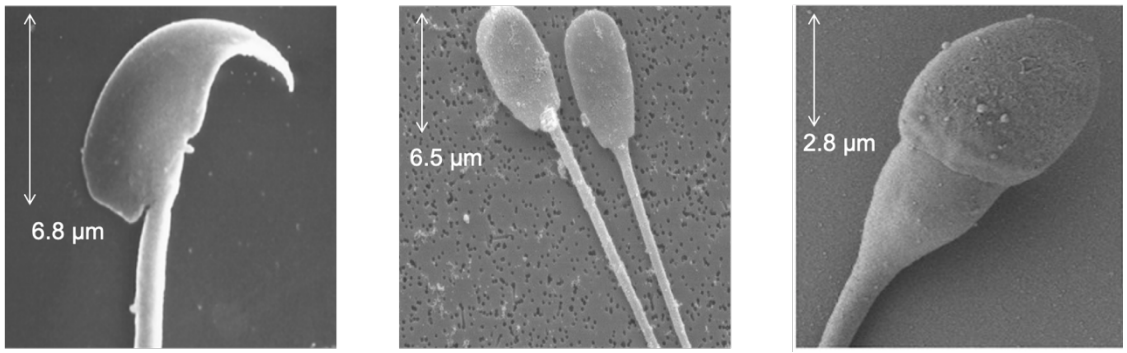

Figure 3.1. TEM images displaying from left to right; mice sperm head with a hook morphology and length ~ 6.8 µm, boar sperm heads with paddled morphology and length ~ 6.5 µm and human sperm head with oval morphology and length ~ 2.8 µm. From left to right, images were adapted from: *Piomboni et al., (2014), Bonet et al., (2018) and Chakraborty et al., (2014) under a CC BY 4.0 licence.*

With regard to reproductive physiology, there are also similarities between boars and humans in terms of hormonal homeostasis and testicular descent (McMahon et al., 1995), but also in the timing of zygotic and pre-embryonic development (Zigo et al., 2020). Moreover, there is a similarity in the mechanisms of testicular thermoregulation when comparing humans and boars (Dadoune and Demoulin., 1993). Thus, boar sperm is an excellent model for studies focusing on biological phenomena that exert an influence on sperm quality. For these reasons, I opted to use boar sperm as a translational research model for male human infertility in this thesis.

3.2.2 Sperm Capacitation and Acrosome Reaction

For fertilisation to take place, the sperm has to undergo a series of structural and metabolic changes that render it capable of recognising, penetrating, and fertilising the oocyte (Yanagimachi., 1994). This activation process is known as capacitation, and takes place inside the female oviduct, at the ampulla. Capacitation *in vivo* is the result of the exogenous signals received by the sperm from the specialised environment in the female reproductive tract. These include an increase of the pH inside the oviduct that varies across different species (Mata-Martinez et al., 2018).

In boar, this pH rise is accompanied by increased levels of bicarbonate (HCO_3^-); this triggers the activation of several signalling pathways and the re-organisation of proteins and lipids in the plasma membrane (Harrison., 1996; Harrison., 2004). This change leads to cholesterol-efflux that is facilitated by acceptor proteins and results in a more fluid membrane with increased permeability to calcium ions (Ca^{2+}) (**Figure 3.2**). Eventually, when spermatozoa are fully capacitated, a destabilisation of the acrosomal sperm head membrane (AR), takes place. This allows sperm to bind to the ZP of the oocyte (Breitbart., 2002).

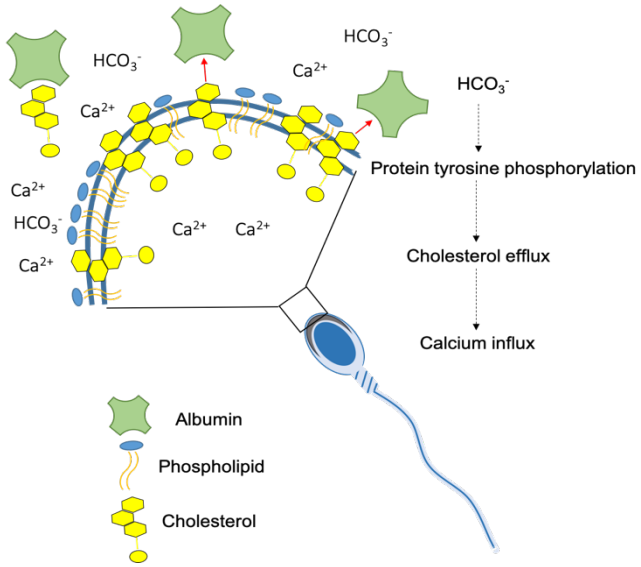

Figure 3.2. Cholesterol efflux from the sperm plasma membrane during sperm capacitation. In sperm capacitated in the presence of albumin and calcium, bicarbonate activates the protein kinase-A signalling pathway inducing protein tyrosine phosphorylation. As a result, the phospholipids asymmetry of the plasma membrane collapses and this permits an albumin-mediated efflux of cholesterol making the membrane more permeable for calcium influx.

Capacitation is difficult to study *in vivo* because it occurs in the female reproductive tract. However, many studies have been conducted *in vitro* to identify indicators for both capacitation and AR. These have been carried out through the use of dyes that bind specifically to the sperm's lipidic membrane and nucleus, thus providing information relating to membrane disorders and sperm viability (Bussalleu et al., 2005; Yeste et al., 2015).

In addition, the mitochondrial membrane potential (Δψm) is a sensitive indicator of the mitochondrial respiratory chain activity, electrogenic transport systems, and the activation of the mitochondrial permeability transition (Ly et al., 2003). A correlation exists between poor sperm mitochondrial function (characterised by a reduction of Δψm), diminished motility, and reduced fertility (Troiano et al., 1998; Donnelly et al., 2000; Wang et al., 2003). This process can also be easily investigated with fluorometric methods by the application of cationic lipophilic dyes (Marchetti et al., 2004; Yeste et al., 2015).

To enhance sperm capacitation and AR *in vitro*, the sperm is subjected to certain conditions and the presence of molecular triggers in the culture media. Boar sperm cells are incubated in capacitation media or buffer (pH of 7.4), containing HCO_3^- and Ca^{2+} that will activate a protein kinase A-dependent pathway for protein phosphorylation. This pathway ultimately induces changes in the sperm motility and membrane lipid architecture (Harrison., 2004). This lipidic restructuring is further enhanced by the presence of BSA as an acceptor protein. BSA acts to sequester cholesterol molecules from the sperm membrane, thus aiding the plasma and outer acrosomal membranes to become docked (Tsai et al., 2010; Yeste., 2013). Subsequently, progesterone hormone (P_4) is introduced to the buffer containing capacitated sperm to induce the AR in a process known as *in vitro* induction of AR (Harper et al., 2003; Witte and Schäfer-Somi., 2007). This is carried out to mimic the high P_4 signals received by the sperm from oocyte cumulus cells once it reaches the ZP, ultimately leading the sperm to become hyperactive and acrosome-reacted as shown in **Figure 3.3** (Osman et al., 1989; Campbell et al., 2013).

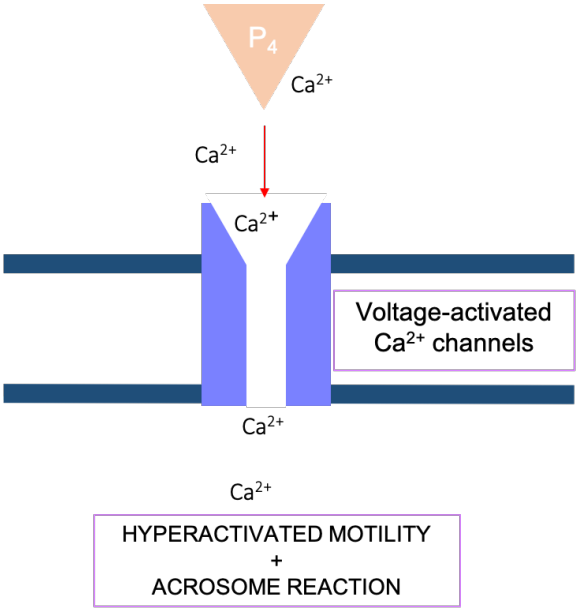

Figure 3.3. Schematic representation of the sperm membrane's signal transduction triggered by P_4. Little is known about the specific mechanisms regulating progesterone-induced AR in boar, yet it is known that after capacitation, the conformational changes in the sperm's membrane lead to an increased sensitivity for progesterone. Recent research has suggested that this hormone subsequently activates a voltage-dependent calcium channel (CatSper) in a similar way to that in humans leading to an increase in calcium influx (Vicente-Carrillo et al., 2017), ultimately triggering hyperactivation of the sperm flagellum and the acrosome reaction (Campbell et al., 2013).

3.2.3 Semen Quality Assessment

Classical methods for the evaluation of boar semen generally involve subjective microscopy and the evaluation of ejaculate volume and concentration, sperm morphology and motility. These methods are used to select upon semen with good quality for artificial insemination (Jung et al., 2015). However, very few of these standard procedures are directly related to fertility; hence, more objective and quantifiable forms of analysis are also needed to establish more accurate criteria. With this regard, computer-assisted sperm analysis (CASA) is often incorporated to examine sperm motility in a more robust and detailed manner. CASA allows the determination of sperm motility via the acquisition of brief video recordings followed by an objective mathematical analysis of various parameters that describe the motion and trajectory of sperm within a given sample (Didion, 2008).

Since any of these parameters can influence the fertilization process, prospective research studies are now using CASA as an informative tool to evaluate a range of factors that can influence sperm function.

For the assessment of the effects caused by the HEK293T-derived exosome treatment, sperm motility and additional assessment of the sperm's functionality can be carried out. These consist of sperm viability, membrane lipid disorder or membrane fluidity (MF) and mitochondrial membrane potential (MMP) as to ensure a specific evaluation of the sperm's capacitated status under *in vitro* capacitating and acrosome inducing conditions as described by Ramió-Lluch (2011) and Covarrubias (2015).

3.3 Hypothesis

I hypothesised that HEK293T-derived exosomes will not cause any detrimental impact upon sperm functionality in any of the parameters tested, and hence that it is a safe tool for its use *in vitro* with live mammalian sperm.

3.4 Materials and Methods

3.4.1 In Vitro Incubation of Boar Sperm Samples with HEK293T-derived Exosome Treatment

All boar semen samples were obtained from two suppliers; Servicios Genéticos Porcinos; (Barcelona, Spain) and JSR Genetics (Cambridge, UK).

Semen samples were provided in a commercial extender and were cooled and stored for no longer than four days at 17°C before use. On the day of an experiment a total of ten semen samples from ten different boars were collected. For each replicate, two different ejaculates were pooled together to reduce the effect of inter-individual variation, resulting in five different replicates (**Figure 3.4**).

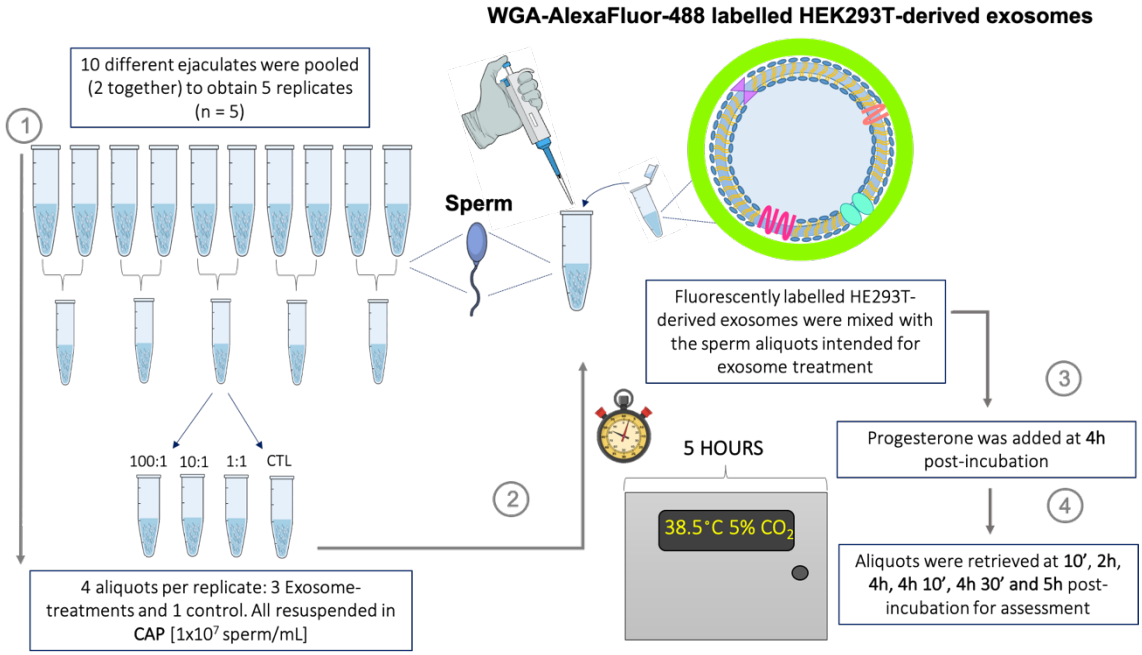

Figure 3.4. Diagram displaying the steps followed for the co-incubation of HEK293T-labelled exosomes with boar ejaculates (n =5). 10 ejaculates from different boars were pooled in pairs to obtain 5 biological replicates. Each replicate was split into four aliquots, 3 for different exosome treatments (exosome to sperm ratios; 100:1, 10:1 and 1:1) and one untreated control (CTL). Sperm aliquots were diluted to a working concentration of $1x10^7$ sperm cells/mL in capacitating buffer (CAP). The aliquots for exosome incubation were mixed with exosomes at different concentrations (10^7, 10^8 and 10^9 EVs/mL) and were placed inside the incubator together with the control for incubation 5 hours. Aliquots were retrieved at 10', 2h, 4h, 4h10', 4h30' and 5h post-incubation for their analysis with CASA and flow cytometry.

Before carrying out any experiment, the quality of the semen samples was assessed by investigating the main semen parameters; concentration and appearance in a Bürker-Turk haemocytometer at 40-x magnification (Nikon Eclipse E200 light microscope) under bright field.

Total motility was assessed with CASA, after having activated sperm motility in a water bath at 35 °C for 15 minutes, as recommended by the supplier. The standard observations for each parameter are defined in **Table 3.1.**

Table 3.1. Basic semen parameters to evaluate the quality of boar sperm. An example of abnormal morphology, abnormal concentration and abnormal progressive motility ranges are shown as well as the expected measurements as discussed in Bonet et al., (2013).

PARAMETERS	MORPHOLOGY	SPERM CONCENTRATION (sperm/mL)	PROGRESSIVE MOTILITY (% sperm)
Abnormal		< 10 x 10^6	< 70%
Expected		20 x 10^6 - 50 x 10^6	70 – 95%

Semen samples were then washed from the commercial extender and from any traces of seminal plasma by centrifugation (< 500×*g* at 17°C for 10 minutes). Sperm-rich fractions were manually collected and subsequently diluted to a final concentration of 1×10^7 sperm/mL in capacitating buffer. Sperm samples were then incubated *in vitro* inside an incubator at 38.5°C and 5% CO_2. To enhance AR in the capacitated sperm, 10 µg/mL of P_4 was added exogenously, as previously described (Jimenez et al., 2003; Ramio et al., 2008).

Exosomes were previously derived and isolated from the mass culture of HEK293T cells, as described in **Chapter 2.4.1**. The HEK293T-derived exosomes were fluorescently labelled with 2 µg/mL of wheat germ agglutinin WGA-AlexaFluor488 conjugate (Thermo Fisher Scientific, UK).

The WGA/exosome mixture was incubated in the dark at room temperature for 30 min and then filtered through a Nanosep® centrifugal device 300K (Pall corporation, US) to remove excess dye. WGA-labelled samples were stored at -80°C for no longer than 24 h.

A negative control, phosphate buffered saline (PBS), was stained and washed in parallel. Size and concentration profiles were determined with NTA. Different exosome to sperm ratios (1:1, 10:1 and 100:1) were tested in order to detect any detrimental effects caused by exosome dosage. The five semen samples were then split into four aliquots of no less than 2 mL. One served as a control, whereas the other three represented different exosome treatments: 10^7, 10^8 and 10^9 EVs/mL (exosome to sperm working ratios of 1:1, 10:1 and 100:1, respectively). Incubation was carried out for 5 h and P_4 was added 4 h after incubation began. Sperm motility, viability, MF and MMP were then analysed at 10', 2 h, and 4 h after incubation began and at 10', 30' and 60' after the addition of progesterone (4 h 10', 4 h 30' and 5 h after incubation began, respectively). These parameters provided key indicators of sperm function and capacitation status.

Composition of the Capacitating Buffer

The capacitating buffer used for the *in vitro* incubation of boar sperm samples was prepared fresh on the same day of the experiment with 20mM 4-(2-hydroxyethyl)-1-piperazineethanesulfonic acid (HEPES), 112mM NaCl, 3.1mM KCL, 5mM glucose, 21.7mM L-lactate, 1mM sodium pyruvate, 0.3mM Na_2HPO_4, 0.4mM MgSO4, 4.5mM CaCl, 19mM of $NaHCO_3$ and 5 mg/mL of BSA (pH = 7.4) in a similar way as described previously (Yeste et al., 2015).

3.4.2. Assessment of Boar Sperm Functionality following Treatment with HEK293T-derived Exosomes

Analysis of Sperm Motility

Sperm motility was assessed using a Hamilton Thorne CASA system (software version 12.3; Hamilton-Thorne Research, USA) equipped with a Nikon Eclipse 80i microscope (Nikon, Japan). This system allowed the objective classification of individual sperm according to different kinematic parameters that were measured from digital images extracted from recorded sperm tracks (Verstegen et al., 2002). For this study, I considered the parameters assessed by the system that are descriptive of sperm motion and trajectory (**Figure 3.5**). These parameters are: total motility (%), progressive motility (%), smooth path velocity (VAP, μm/s), straight-line velocity (VSL, μm/s), track velocity (VCL, μm/s), straightness (STR: VSL/VAP, %), linearity (LIN: VSL/VCL, %) and wobble (WOB: VAP/VCL, %) detailed in **Table 3.2**.

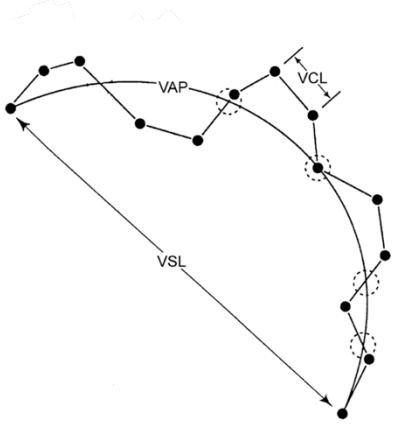

Figure 3.5. Schematic representation of some of the motility patterns measured by the CASA system (Boyers et al., 1989). Black circles represent successive images of the head of motile sperm and are joined by straight path lines. Curved line indicates a smoothed path fitted through sperm track. VAP: average path velocity, VCL: curvilinear velocity, VSL: straight-line velocity. Figure reproduced from: *Rurangwa et al., (2004) under a CC BY 4.0 licence.*

A sperm was considered motile when its VAP was higher than 15 μm/s and progressively motile when its STR was higher than 45%.

Samples were loaded into a 20-µm Leja chamber (Leja, Netherlands) and placed on a heated stage (37°C) for analysis. Images were acquired with the photometer set at 50, with a 100-x objective and negative contrast phase.

A minimum of 1,000 sperm cells were evaluated per sample, and two technical repeats were assessed per sample.

Table 3.2. Motility parameters measured by Computer Assisted Sperm Analysis and their definition.

CASA MOTILITY PARAMETERS	DEFINITION
Percentage of motile sperm (%)	Percentage of sperm that show any type of motility
Percentage of progressively motile sperm (%)	Percentage of sperm that show progressive motility
Path velocity (VAP) (µm/s)	The distance along a 5 point mathematically smoothed path that the sperm travels over time
Straight-line velocity (VSL) (µm/s)	Measures the straight trajectory of the spermatozoa per unit time
Curvilinear velocity (VCL) (µm/s)	Measures the straight trajectory of the spermatozoa per unit time
Linearity (LIN) (%)	VSL/VCL x 100
Percentage of straightness (STR) (%)	The ratio of straight-line velocity* to average path velocity
Wobble (WOB) (%)	VAP/VCL x 100

*Straight-line velocity represents the straight line distance between the position of the sperm head in the first frame of analysis and the position of that sperm head in the last frame of analysis over the fixed time of analysis

Flow cytometry analysis

To further assess any changes upon sperm functionality, flow cytometric analysis was carried out to analyze sperm viability, MF and MMP with the supervision of Dr. Marc Yeste at the TechnoSperm laboratory (Department of Biology, Institute of Food and Agricultural Technology, University of Girona). Samples were determined by a Cell Laboratory QuantaSC™ cytometer (Beckman Coulter; Fullerton, CA, USA; Serial Number: AL300087) using single-line visible light (488 nm) from an argon laser.

Sperm viability was assessed using a SYBR-14/Propidium Iodide (PI) assay according to the protocol described by Garner and Johnson (1995). SYBR-14 is a permeable dye that will stain the nucleus of live cells, whereas PI is an impermeable dye that will only stain the nucleus of those cells that present a disrupted membrane, and hence are recognised as dead cells.

Samples were incubated with each dye, at final concentrations of 100 nm and 12 μM, at 38°C for 10 and 5 minutes, respectively. Sperm that were positive for SYBR-14 and negative for PI (SYBR-14^{+}/PI^{-}) were classified as viable.

MF was evaluated by co-staining with Merocyanine 540 (M-540) and YO-PRO®-1, as described by Harrison et al., (1996). M-540 and YO-PRO®-1 dyes were used at final concentrations of 2.6 μM and 25 nM, respectively, at 38°C for 10 min in the dark. Sperm that were negative for M-540 and YO-PRO (M-540^{-}/YO-PRO^{-}) were classified as viable but had low levels of membrane lipid disorder. M-540 stain capacitated sperm since it fills up the gaps in the sperm's membrane that have been created as a consequence of cholesterol loss during sperm capacitation.

MMP was analysed by incubation with JC-1 (Guthrie and Welch, 2006). Two emission filters (FL-1 and FL-2) were used to detect and differentiate two sperm populations; JC-1 aggregates (JC-1_{agg}) and JC-1 monomers. JC-1 (5,5',6,6'-tetrachloro-1,1',3,3' tetraethylbenzimidazolylcarbocyanine iodide was used at a final concentration of 0.3 μM, at 38°C for 30 min in the dark. Sperm from the JC-1_{agg} population were classified as presenting with high MMP. JC-1 stains the mitochondria in live cells, and the different mitochondrial membrane potential (low and high) can be distinguished with this dye as JC-1 can be in the form of monomers (low MMP) emit a green fluorescence, and this dye will experience a change in conformation to form aggregates together with a monochromatic shift to emit an orange fluorescence when mitochondria exhibit a high MMP.

A minimum of 10,000 events per replicate were evaluated, and data was collected as List-mode Data files (.LMD). Data were analysed using Cell Lab Quanta®SC MPL Analysis Software (version 1.0; Beckman Coulter). Information relating to flow cytometry analyses where given according to the recommendations of the International Society for Advancement of Cytometry (ISAC) (Lee et al., 2008). The sheath flow rate was set at 4.17 µL min-1 in all analyses, and EV and side scatter (SS) were recorded in a linear mode (in EE *vs*. SS dot plots) for a minimum of 10,000 events per replicate. The analyser threshold was adjusted on the EV channel to exclude subcellular debris (particle diameter < 7 µm) and cell aggregates (particle diameter > 12 µm) (Ramió-Lluch et al., 2011).

Each assessment for each sample and parameter was repeated thrice in different tubes, prior to calculating the corresponding mean ± standard error of the mean (SEM). Optical filters were FL1, FL2 and FL3. In this system, the optical characteristics for these filters were: FL1 (green fluorescence): Dichroic/Splitter, DRLP: 550 nm, BP filter: 525 nm, detection width 505 nm - 545 nm; FL2 (orange fluorescence): DRLP: 600 nm, BP filter: 575 nm, detection width: 560 nm - 590 nm); and FL3 (red fluorescence): LP filter: 670 nm/730 nm. Signals were logarithmically amplified and photomultiplier settings were adjusted to particular staining methods. FL1 was used to detect green fluorescence (SYBR-14, YO-PRO and JC-1 monomers), FL2 was used to detect JC-1_{agg} and FL3 was used to detect red fluorescence (M540 and PI).

Data was corrected by determining the percentage of non-DNA-containing particles to avoid an overestimation of sperm cells, as described by Petrunkina et al., (2010), except for the assessment of SYBR-14/PI.

Statistical Analysis

Results from CASA and flow cytometry were analysed using the SPSS statistical package for Windows (Ver. 25.0; Armonk, NY, USA).

Prior to analysing, data were first evaluated for normality (Shapiro-Wilk test) and homogeneity of variances (Levene test). Following this, a mixed model (between-subjects factor: treatment; within-subjects factor: incubation time) was applied followed by a post-hoc Sidak test for pair-wise comparisons. Each sperm parameter was considered as an independent variable. The level of significance was set at $P \leq 0.05$ and data are shown as mean ± SEM.

3.5 Results

3.5.1 Assessment of Boar Sperm Functionality following Treatment with HEK293T-derived Exosomes

Boar sperm were exposed to different concentrations of HEK293T-derived exosomes and the sperm/exosome mixture was co-incubated *in vitro* under capacitating conditions for up to 5 hours. Exogenous progesterone was added to the mixture at 4 h post-incubation to mimic the environment experienced by sperm in the female reproductive tract. Short and long-term exposure effects caused by the HEK293T-exosome treatments upon the biological function of sperm were evaluated through a range of key parameters including motility by CASA and viability, MF and MMP by flow cytometric analysis at 10', 2 h, 4 h, 4 h 10', 4 h 30' and 5 h post-incubation.

Analysis of sperm motility

With regards to sperm motility, none of the exosome treatments had any significant effects upon total sperm motility when compared to the control. However, a slight, but non-significant, increase in sperm motility was observed for the lowest exosome treatment (1:1); this was the case at all time points except at 4 h 30' post-incubation (**Figure 3.6A**). This effect was even more pronounced with the 1:1 treatment for progressive motility, which was significantly higher when compared to the 100:1 treatment ($P<0.01$) at 10' post-incubation (**Figure 3.6B**). At this particular time point, the progressive motility in the 100:1 treatment was also significantly lower than that of the control ($P<0.05$). Moreover, this analysis showed that in the highest exosome treatment (100:1), LIN was significantly lower than in the 1:1 treatment after 4 h 30 min of incubation ($P<0.05$) (**Figure 3.6C**).

After 4 h 10 min of incubation, WOB was significantly higher in the 100:1 exosome treatment than in the rest of the treatments including the control ($P<0.01$ when compared to the control; $P<0.01$ when compared to the 1:1 treatment; and $P<0.05$ when compared to 10:1). WOB was inversely proportional to the concentration of exosomes at 4 h 10 min (**Figure 3.6D**).

On the other hand, there is a decreasing trend in all the treatments and the control, for most sperm kinematic parameters as the period of incubation progressed. However, LIN was seen to increase after 4 h 10 min of incubation, in both the control and all treatments; this increase was more pronounced with the 1:1 ratio (**Figure 3.6C**).

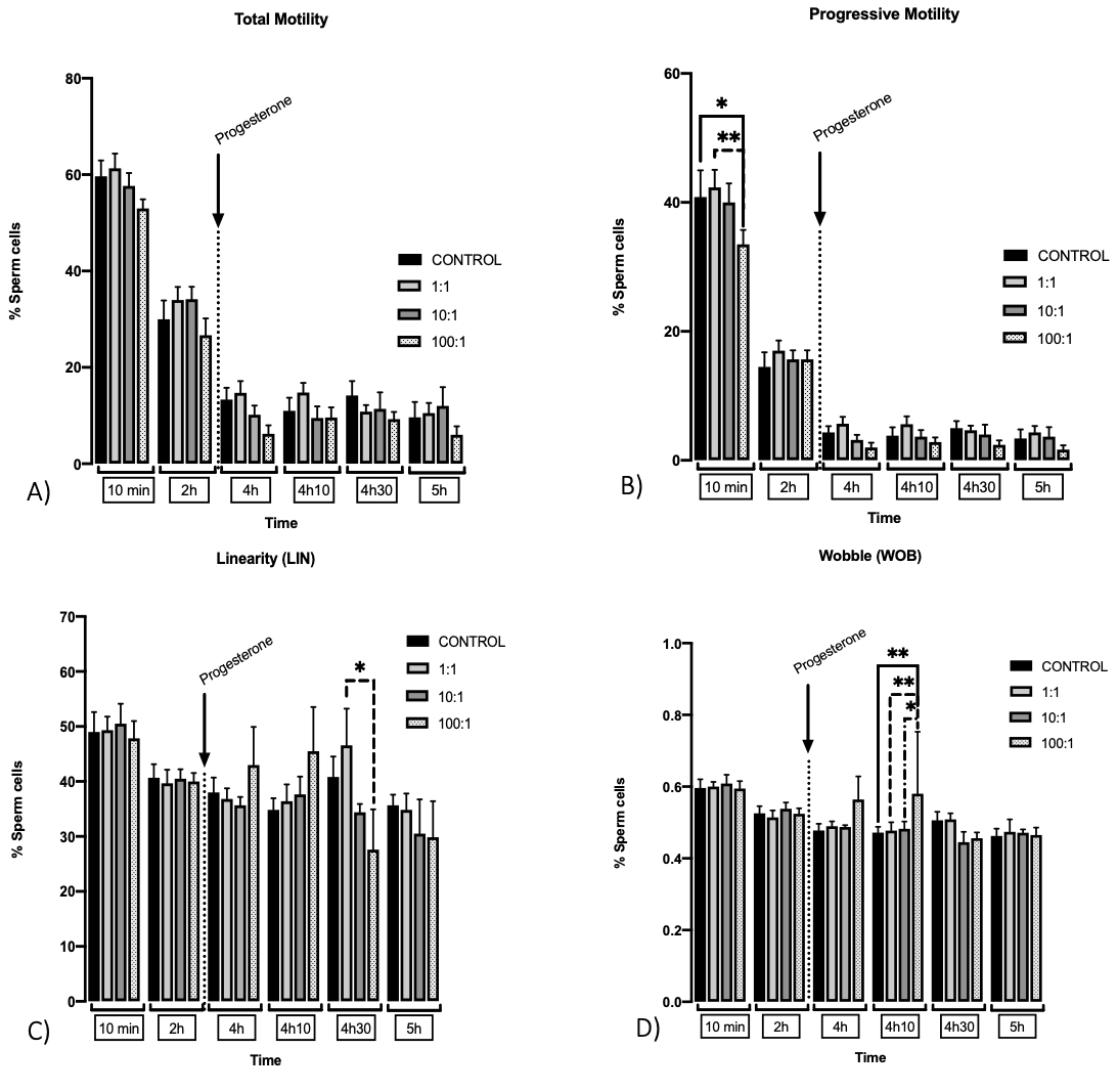

Figure 3.6. Motility parameters of boar sperm, as determined by CASA after in vitro co-incubation with different HEK293T-derived exosome treatments (1:1, 10:1, and 100:1 exosome to sperm ratios) compared to controls. Data are shown as means ± SEM from 5 replicates in the control and treatment groups, (n = 5). Progesterone was added at 4 h post-incubation. A) Total motility declines over time in all the treatments including the control with no significant differences between them (P>0.05). B) Progressive motility is significantly lower for the 100:1 treatment when compared to the time-matched control and 1:1 treatment (P<0.05; and P<0.01, respectively) at 10' post-incubation. C) Linearity was significantly lower for the 100:1 treatment when compared to the time-matched 1:1 treatment at 4 h 30' post-incubation (P<0.05) and finally wobble. D) was significantly increased for the 100:1 treatment when compared to the time-matched control, 1:1 and 10:1 treatments at 4 h 10' post-incubation (P<0.01, P<0.01 and P<0.05, respectively). (*P<0.05, **P <0.01).

As far as the other kinematic parameters are concerned, no significant differences were observed between the controls and the exosome treatments at any given time point (**Table 3.3**), except for LIN and WOB. Furthermore, 30 min post-addition of P4 there can be seen an increase in all the motility parameters as expected in capacitated boar sperm (Ramio et al., 2008).

Table 3.3. Descriptive data of smooth path velocity (VAP), straight-line velocity (VSL), track velocity (VCL) and straight-line velocity (VSL) evaluated by CASA for the different treatments (control, 1:1, 10:1 and 100:1 exosomes to sperm cell ratios) at different incubation times (n = 5).

		TIME POINTS					
		10 min	**2h**	**4h**	**4h10**	**4h30**	**5h**
		Mean ± SEM* (%)	**Mean ± SEM (%)**	**Mean ± SEM (%)**	**Mean ± SEM (%)**	**Mean ± SEM (%)**	**Mean ± SEM (%)**
VAP (µm/s)	CTL †	88.8 ± 3.2	69.1 ± 3.0	50.5 ± 3.3	50.1 ± 2.6	52.7 ± 3.1	57.2 ± 6.6
	1:1	88.1 ± 2.9	73.2 ± 2.0	60.0 ± 2.9	57.0 ± 0.6	54.4 ± 3.6	59.5 ± 5.1
	10:1	87.3 ± 2.1	73.5 ± 1.1	56.0 ± 2.8	67.4 ± 8.4	53.6 ± 6.8	53.6 ± 8.4
	100:1	85.5 ± 1.5	69.1 ± 2.5	48.7 ± 4.9	65.5 ± 11.4	42.3 ± 12.1	42.8 ± 9.9
VSL (µm/s)	CTL	69.9 ± 4.2	49.4 ± 2.3	34.8 ± 2.7	32.8 ± 1.5	37.5 ± 2.3	37.9 ± 3.9
	1:1	70.2 ± 3.1	51.4 ± 2.7	38.3 ± 3.3	37.8 ± 1.4	39.6 ± 2.0	39.7 ± 4.0
	10:1	70.6 ± 3.7	51.6 ± 1.3	35.7 ± 1.3	47.1 ± 8.7	35.3 ± 4.4	31.3 ± 7.5
	100:1	66.2 ± 3.7	48.3 ± 2.1	32.6 ± 2.6	50.9 ± 13.8	30.3 ± 7.8	27.4 ± 6.0
VCL (µm/s)	CTL	149.7 ± 6.6	132.7 ± 8.6	106.6 ± 7.5	106.6 ± 6.2	105.9 ± 9.2	123.8 ± 13.0
	1:1	146.9 ± 4.9	143.0 ± 4.9	116.5 ± 6.1	120.4 ± 6.5	107.6 ± 8.1	125.8 ± 7.7
	10:1	144.2 ± 5.0	137.1 ± 5.0	115.0 ± 6.2	122.0 ± 18.2	117.8 ± 9.7	94.3 ± 23.5
	100:1	144.4 ± 4.2	132.7 ± 7.7	93.7 ± 13.7	111.1 ± 16.0	102.2 ± 27.5	94.2 ± 23.6
STR (%)	CTL	74.2 ± 3.1	66.7 ± 2.5	66.5 ± 2.5	63.0 ± 2.4	70.3 ± 4.7	66.5 ± 3.5
	1:1	74.7 ± 2.0	64.0 ± 2.2	65.0 ± 2.6	64.4 ± 2.9	71.2 ± 3.9	67.0 ± 4.2
	10:1	75.8 ± 3.0	65.3 ± 1.8	63.5 ± 2.9	68.0 ± 5.3	63.3 ± 1.9	54.8 ± 11.1
	100:1	72.5 ± 2.9	64.5 ± 1.5	67.8 ± 4.3	71.5 ± 6.5	52.7 ± 10.7	51.7 ± 10.6

*SEM (Standard error of the mean) † CTL (Control)

Flow cytometry analysis

Flow cytometric assays were used to evaluate sperm viability, membrane lipid disorder, and mitochondrial membrane potential. There were no significant differences between the control and the treatments (100:1, 10:1 and 1:1) at any of the tested time points (**Table 3.4**, **Table 3.5** and **Table 3.6**).

As expected, there was a reduction in the proportion (%) of viable spermatozoa (SYBR-14^+/PI^-), viable spermatozoa with low membrane lipid disorder (M540$^-$/YO-PRO-1^-), and viable spermatozoa exhibiting high mitochondrial potential (JC-1_{agg}), in both controls and treatments as the incubation time progressed and the sperm became increasingly dead. Moreover, in **Table 3.5** it can be seen how P4 induces the late stages of capacitation, from the visible increase of sperm cells with high membrane fluidity.

Table 3.4. Descriptive data for the population of viable sperm (SYBR-14^+/PI^-) by flow cytometry for the different treatments (control, 1:1, 10:1 and 100:1 exosomes to sperm cell ratios) at different incubation times (n = 5).

VIABLE SPERM (SYBR-14^+/PI^-)					
Treatment		**Control**	**1:1**	**10:1**	**100:1**
		Mean ± SEM (%)	**Mean ± SEM (%)**	**Mean ± SEM (%)**	**Mean ± SEM (%)**
Incubation time	10 min	55.61 ± 6.32	54.32 ± 6.65	52.58 ± 5.79	41.70 ± 10.59
	2h	29.19 ± 9.40	13.03 ± 5.71	25.71 ± 3.41	19.67 ± 4.77
	4h	23.08 ± 3.67	22.42 ± 1.79	24.41 ± 4.06	25.93 ± 3.51
	4h10	13.28 ± 2.80	10.97 ± 2.94	17.40 ± 3.94	14.73 ± 6.36
	4h30	15.98 ± 2.35	14.84 ± 3.23	13.18 ± 2.73	13.18 ± 2.95
	5h	14.81 ± 3.11	13.90 ± 1.45	20.34 ± 1.68	16.44 ± 2.04

Table 3.5. Descriptive data for the population of viable sperm with low membrane fluidity (M-540^-/YO-PRO^-) by flow cytometry for the different treatments (control, 1:1, 10:1 and 100:1 exosomes to sperm cell ratios) at different incubation times (n = 5).

VIABLE SPERM WITH LOW MEMBRANE FLUIDITY (M-540-/YO-PRO-)					
Treatment		**Control**	**1:1**	**10:1**	**100:1**
		Mean ± SEM (%)	**Mean ± SEM (%)**	**Mean ± SEM (%)**	**Mean ± SEM (%)**
Incubation time	10 min	58.18 ± 10.77	57.17 ± 11.03	60.19 ± 10.61	57.39 ± 10.10
	2h	33.30 ± 5.78	29.93 ± 6.58	27.30 ± 6.20	30.12 ± 5.15
	4h	19.19 ± 2.70	18.79 ± 3.08	17.68 ± 4.36	16.08 ± 2.69
	4h10	15.41 ± 4.10	13.82 ± 4.75	16.61 ± 1.94	12.90 ± 4.18
	4h30	26.78 ± 14.40	29.55 ± 14.80	28.53 ± 14.85	28.70 ± 14.60
	5h	24.88 ± 12.70	30.93 ± 11.34	25.53 ± 13.28	25.06 ± 12.93

Table 3.6. Descriptive data for the population of sperm exhibiting high mitochondrial membrane potential ($JC\text{-}1_{agg}$) by flow cytometry for the different treatments (control, 1:1, 10:1 and 100:1 exosomes to sperm cell ratios) at different incubation times (n = 5).

VIABLE SPERM EXHIBITING HIGH MITOCHONDRIAL MEMBRANE POTENTIAL ($JC\text{-}1_{AGG}$)

Treatment		Control	1:1	10:1	100:1
		Mean ± SEM (%)	**Mean ± SEM (%)**	**Mean ± SEM (%)**	**Mean ± SEM (%)**
Incubation time	10 min	65.46 ± 6.86	63.55 ± 5.29	55.19 ± 10.42	61.95 ± 6.16
	2h	50.16 ± 1.25	53.25 ± 1.80	51.85 ± 5.29	47.49 ± 7.27
	4h	44.80 ± 8.46	42.82 ± 7.40	45.13 ± 9.76	43.31 ± 7.91
	4h10	34.15 ± 4.67	41.06 ± 14.21	38.16 ± 9.85	39.56 ± 12.4
	4h30	43.65 ± 17.50	55.17 ± 13.18	42.89 ± 14.41	31.68 ± 8.53
	5h	31.85 ± 6.24	26.01 ± 7.09	33.33 ± 5.55	32.15 ± 5.03

Figures 3.7, **3.8** and **3.9** show the different sperm populations detected by flow cytometry after 10 minutes and 4 h 10 min as examples of short-term incubation and long-term incubation, respectively, following the addition of progesterone.

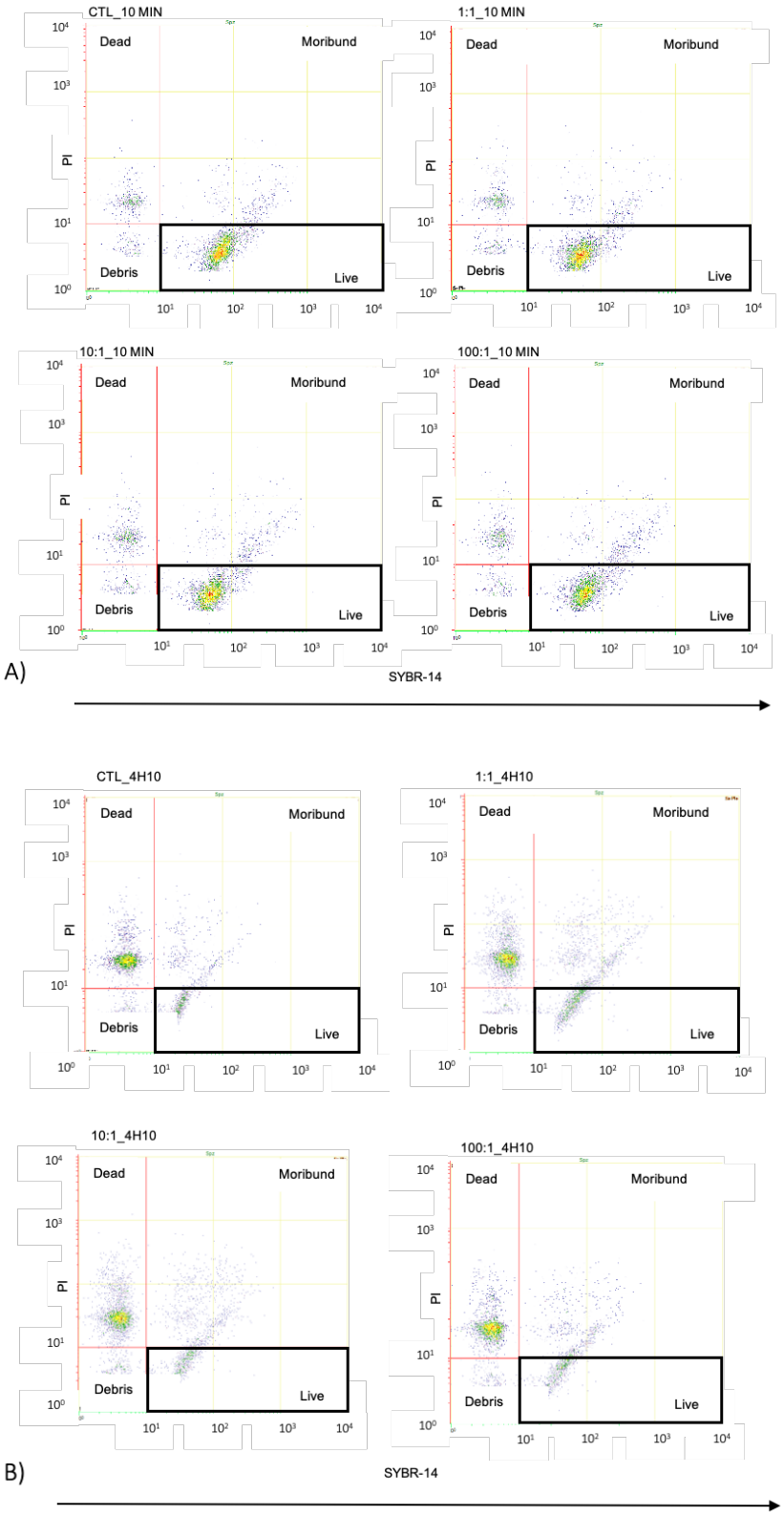

Figure 3.7. Viable sperm population ($SYBR\text{-}14^{+}/PI^{-}$) by flow cytometry for the different treatments (control, 1:1, 10:1 and 100:1 exosomes to sperm cell ratios) A) at 10 minutes post-incubation and B) at 4 h 10 minutes post-incubation.

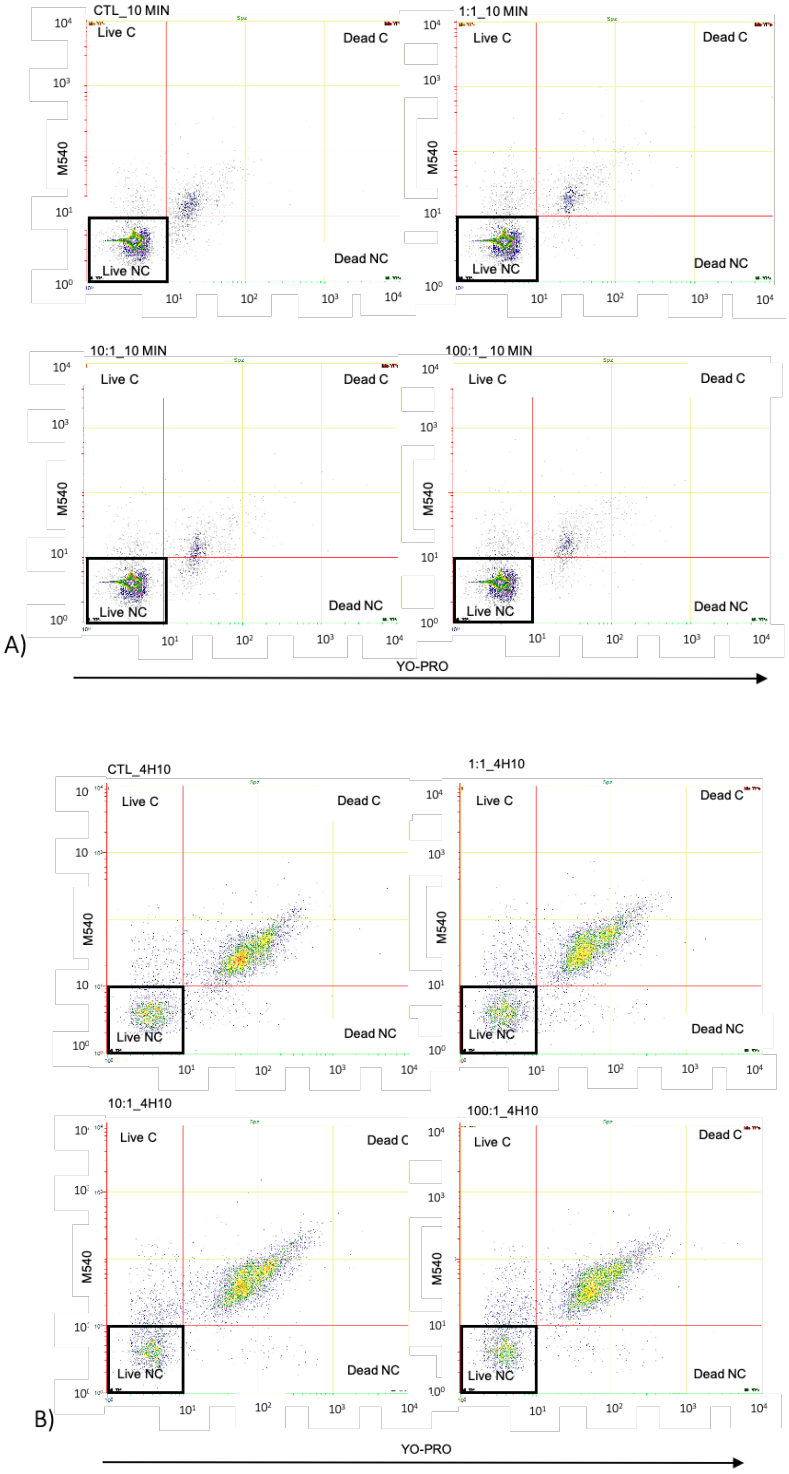

Figure 3.8. Viable sperm population with low membrane fluidity ($M540^{-}$/$YO\text{-}PRO^{-}$) by flow cytometry for the different treatments (control, 1:1, 10:1 and 100:1 exosomes to sperm cell ratios) A) at 10 minutes post-incubation and B) at 4h10 minutes post-incubation. C = Capacitated, NC = Non-capacitated.

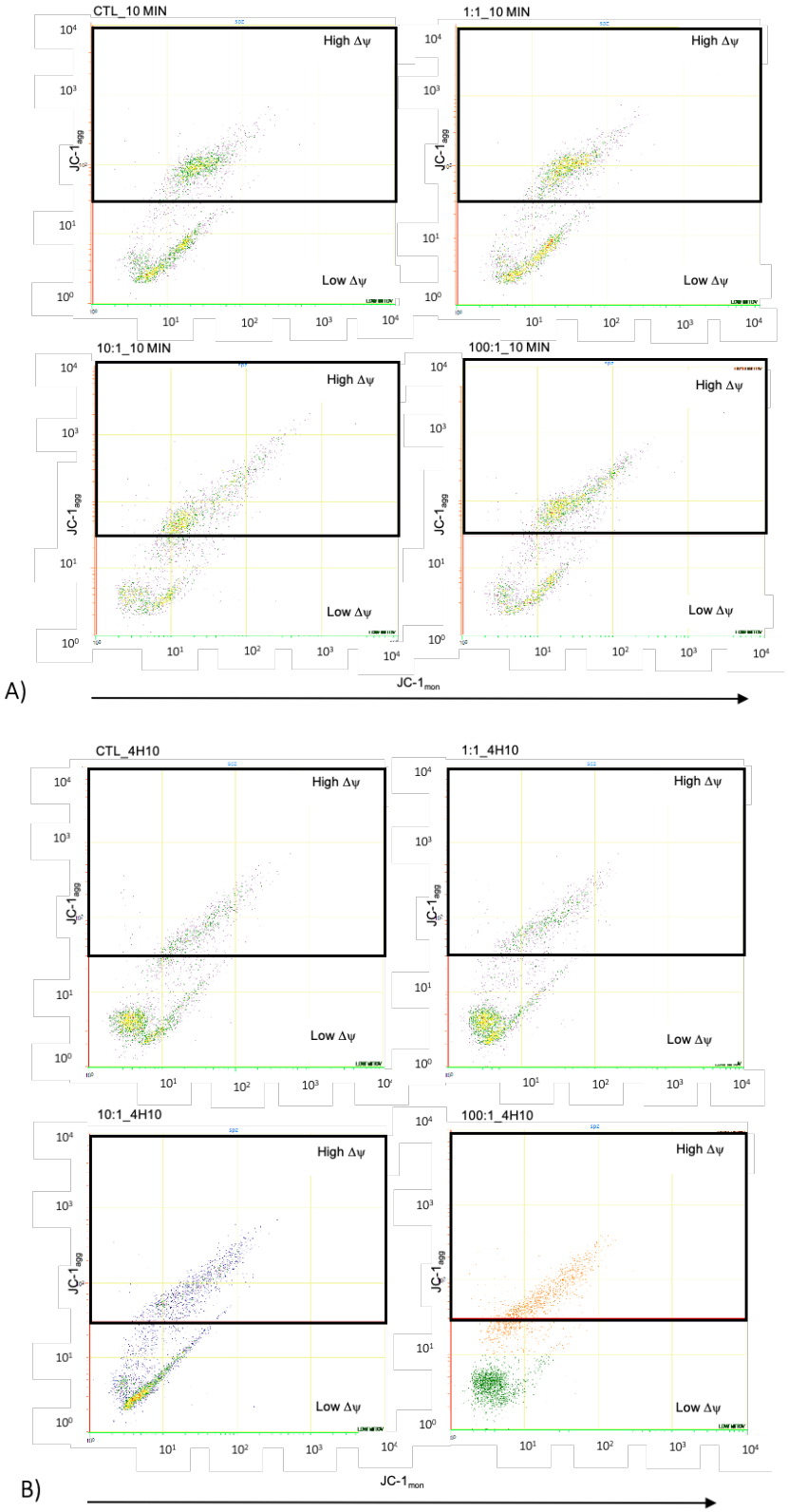

Figure 3.9. Sperm population exhibiting high mitochondrial membrane potential (JC- 1_{agg}) by flow cytometry for the different treatments (control, 1:1, 10:1 and 100:1 exosomes to sperm cell ratios) A) at 10 minutes post-incubation and B) at 4h10 minutes post-incubation. ΔΨ = membrane potential.

3.6 Discussion

This chapter evaluated HEK293T-derived exosomes for their potential as a non-invasive delivery system for mammalian sperm. This assessment was carried out through the *in vitro* co-incubation of previously isolated HEK293T-derived exosomes with boar sperm. Short and long-term exposure effects of increasing exosome treatments were tested (exosome to sperm ratios; 1:1, 10:1 and 100:1). The detrimental impact upon sperm functionality was evaluated by CASA (motility) and flow cytometry for the sperm viability, lipid membrane disorder, and mitochondrial membrane potential. These experiments were carried out under capacitating conditions, with a pH of 7.4, and the exogenous addition of progesterone to induce the acrosome reaction, thus triggering the sequence of structural and metabolic changes that sperm must undergo in order to be able to fertilize the oocyte.

The results described in this chapter revealed that the incubation of boar sperm with exosomes at the highest exosome to sperm ratio (100:1) led to a significant reduction in progressive motility after just 10 min of incubation. This effect was even more apparent when compared to the lowest exosome:sperm ratio (1:1) at this time point, which appeared to have a positive effect upon progressive motility compared to the untreated control. This effect may not be taken as deleterious since this reduction in progressive motility turned out to be transitory as this returned to normal throughout the rest of the incubation period. Instead, I hypothesised that this could be an effect caused by the spontaneous interaction between the HEK293T-derived exosomes and sperm. Moreover, as expected, LIN, which should increase in response to capacitation, showed an increasing trend for treatments, particularly after the addition of progesterone (Garcia Herreros et al., 2005).

Nonetheless, LIN was significantly lower in the 100:1 treatment than in the 1:1 treatment when tested 30 min after the addition of progesterone, thereby suggesting that such a high exosome concentration might have detrimental effects on sperm with regards to capacitation. However, it was interesting to observe that with the highest treatment (100:1), WOB was significantly higher than the control and the other treatments; in fact, the pattern at 4 h 10 min increased proportionally with the concentration of exosomes. While no previous studies have correlated WOB with capacitation, an increase in WOB, depicting a smoother and more curvilinear sperm motion, has been previously described for fresh human and boar sperm samples in response to capacitating conditions (Ramió et al., 2008; Boryshpolets et al., 2015). This data suggest that sperm with the highest exosome treatment (100:1) achieved a higher capacitation status 10 minutes after the addition of progesterone than the control or other treatments, but this contradicts with the LIN observations, hence why it is not ideal to measure sperm motility only to describe the capacitation status in sperm.

In the last part of this study, sperm viability, membrane lipid disorder, and mitochondrial membrane potential were investigated to gain a more reliable prediction of the ability of sperm to undergo capacitation when subjected to different exosome treatments. Remarkably, the exposure of boar sperm to HEK293T-derived exosomes did not affect these three parameters, at least when evaluated by flow cytometry; this effect was evident when comparisons were made between the control and treatments for all the sperm: exosome ratios. Consequently, despite the effects observed in some of the sperm motility parameters for the lowest and highest treatments (1:1 and 100:1 respectively), the co-incubation of high concentrations of HEK293T-derived exosomes with boar sperm did not interfere with their ability to undergo the functional changes that occur during capacitation (for further visual proof that the sperm underwent acrosome reaction refer to **Appendix II**).

These results differ from previous studies, which found that cholesterol from prostasomes was transferred to the sperm membrane, thereby reducing the level of lipid disorder, and thus the membrane's fluidity during the process of capacitation (Carlini et al., 1997; Caballero et al., 2012), resulting in a reduction in the proportion of capacitated sperm (Cross, 1996). Furthermore, others have found that prostasomes stimulate the AR when they fuse with sperm, thus rendering them to be more sensitive to progesterone (Arienti et al., 2002; Palmerini et al., 2003; Bechoua et al., 2011). In this study, however, there was no evidence for such an impact when using HEK293T-derived exosomes. These discrepancies may be related to the biological differences between HEK293T-derived exosomes and prostatic extracellular vesicles, which are more sperm-specific. That being said, this effect could also be explained by the fact that other seminal components could inevitably be carried, together with EVs, by sperm, as other studies have reported that such changes take place when adding seminal plasma to frozen-thawed boar sperm (Garcia et al., 2010; Fernandez-Gago et al., 2013). In any case, further studies should now investigate the extent to which the particular nature of EVs, whether derived from epithelial cell lines, such as HEK293T, or the male reproductive tract, has a specific impact upon the ability of sperm to capacitate and undergo AR. Furthermore, this data warrants further research on the effects upon sperm capacitation that are closely related with sperm motility, such as any changes in the phosphorylation patterns of tyrosine residues in sperm tail proteins, and the capacity of treated sperm to fertilise an oocyte. This may reconcile the differences observed between sperm motility and the other sperm parameters.

Although some studies have successfully used HEK293T-derived exosomes *in vitro* and *in vivo* on a variety of different tissues from several animal species (Sun et al., 2010; Alvarez-Erviti et al., 2011; El-Andaloussi et al., 2012), it is worth considering whether the application of exosomes may evoke an immune response when applied to a boar animal *in vivo*.

Consequently, it must be remembered that the boar model is not entirely representative of the human, particularly with regards to the physiological response.

3.7 Key findings

- For the first time, data were generated to describe the effects of *in vitro* short-term and long-term exposure of exosomes previously isolated from a human cell line for their use with mammalian sperm under conditions that mimic the fertilisation scenario *in vitro*.

- CASA showed that 5-hour *in vitro* exposure of HEK293T-derived exosomes did not significantly impact the motility of boar sperm, rather suggesting a successful capacitation status was achieved by boar sperm and that a spontaneous interaction occurred between the exosomes and the sperm from the beginning of incubation. Moreover, it is likely that exosome interaction more effectively took place in capacitated sperm that present a higher membrane fluidity, and therefore different interaction rates should be looked at between capacitated and non-capacitated conditions.

- Flow cytometry assays revealed that 5-hour *in vitro* exposure of HEK293T-derived exosomes did not significantly impact boar sperm viability, membrane fluidity nor mitochondrial membrane potential.

- The data generated in this chapter demonstrates that exosomes derived from HEK293T cells can be used *in vitro* with mammalian sperm without causing detrimental effects on key functionality parameters. Collectively, these factors are informative of the ability of sperm to undergo *in vitro* capacitation, and that HEK293T-exosomes may be developed further to deliver selective compounds into mammalian sperm.

CHAPTER 4

A Detailed Investigation of the Specific Interaction Between HEK293T-derived Exosomes and Boar Sperm with Particular Focus on Internalization Mechanisms

4.1 Aim of this Chapter

This chapter aims to investigate the capability of HEK293T-derived exosomes to interact with live mammalian sperm with powerful and resolutive fluorescence microscopy techniques and kinetic assays for a qualitative and quantitative analysis that includes an in-depth analysis on the mechanisms governing this interaction.

4.2 Background

4.2.1 EV Labelling and Visualisation Techniques

The direct observation of EV-cell interaction has enabled researchers to track EV movements throughout cells and probe for the co-localisation with cellular components. This has made a significant contribution to our understating of payload delivery and distribution. Fluorescence microscopy is an invaluable tool in the EV field thanks to its ability to specifically visualise the vesicles of interest. However, due to the fundamental barrier created by the limit of light diffraction, the resolution of conventional microscopy is limited to ~ 200 nm in the horizontal/vertical plane (XY) and ~ 600 nm along the optical axis (z) (Nieuwenhuizen et al., 2013). Hence, the analysis of exosomes with a size under 200 nm and the study of individual sites of exosome-cell interaction is impossible with conventional microscopy. Therefore, the comprehensive visualisation of exosomes has mainly been performed via electron microscopy, although, this approach requires laborious sample preparation, thus making it unsuitable for the study of dynamic processes.

This technological limitation changed dramatically with the development of new fluorescence microscopy techniques that have evolved to the extent of allowing the imaging of EVs at single-particle level beyond the diffraction limit of light thus highly improving resolution (Balzarotti et al., 2017). These capabilities represent a powerful approach that combine a higher throughput, multiplexed labelling, and specific labelling approaches.

To allow visualization by fluorescence microscopy, exosomes can be labelled with a range of specific dyes. The most common dyes are lipophilic to stain the exosomal membrane. A typical example is the case of Bio-Maleimide (BODIPY FL N-(2-aminoethyl) maleimide), a thiol-reactive dye that has been previously used to stain several different types of EVs (Enjeti et al., 2008; Dragovic et al., 2013; Dragovic et al., 2015).

Exosomes can also be labelled with dyes based on Wheat Germ Agglutinin (WGA). These dyes consist of a fluorophore that is covalently conjugated to WGA and specifically binds to lectin receptors which are enriched in the exosome surface (Batista et al., 2011, Milutinovic et al., 2016).

Membrane-permeable chemical compounds, including carboxyfluorescein succinimidyl ester (CFSE) and 5(6)-carboxyfluorescein diacetate (CFDA), have also been used for this purpose (Temchura et al, 2008, Escrevente, 2011), since they can be retained in the vesicle membranes for longer periods due to a covalent coupling reaction to lysine residues and other amine sources of membrane proteins via their succinimidyl group (Parish, 1999).

Exosomes can also be visualized in a more specific way via the use of fluorescent proteins to tag specific exosomal markers. For instance, CD9 and CD63 are tetraspanin proteins that are known to be enriched in exosomes. These can be labelled with a fluorophore via specific antibodies or transfection protocols that involve the expression of a green fluorescent protein (GFP) covalently bonded that acts as a reporter (Corso et al., 2019).

In this way, researchers can choose from a wide range of labelling methods thus allowing the acquisition of visual evidence for exosome uptake and exosome processing mechanisms in recipient cells (Mulcahy et al., 2014). Nonetheless, there are technical considerations when choosing the appropriate method. For instance, when specifically labelling or tagging transmembrane proteins, there is a caveat that relies upon the assumption that the fluorescent tag can potentially alter the trafficking behaviour of the exosomes; more specifically, this tagging could alter the membrane docking and cell adhesion roles of the exosomal tetraspanins (CD9, CD63 and CD81) (Hemler, 2005; Levy and Shoham, 2005).

4.2.2 EV-Cell Interaction Mechanisms

Tetraspanin-mediated tethering is not the only mechanism by which exosomes are internalised by target cells. Recent publications highlight another protein-mediated interaction mechanism, based on connexins and integrins (Shimaoka et al., 2019). Integrins primarily act as cell-adhesion molecules by mediating cell-to-cell and cell-to-extracellular matrix adhesive interactions (Shimaoka et al., 2002). Connexins (CXS) on the other hand, are integral components of gap-junctional channels between opposing cellular membranes and mediate the intercellular exchange of small molecules (Brink et al., 2012; Maes et al., 2014). These channels can either be in the form of hemichannels; one hexameric connexon assembly between the cell membrane and the extracellular space, or as gap junction channels; as two sets of connexons connecting two individual cell membranes (reviewed by Goodenough and Paul, (2003)).

The most abundant connexin, and the one that has been studied the most, is CONNEXIN-43 (Cx-43) (Ribeiro-Rodrigues et al., 2017). Cx-43 was initially identified as a protein that is required for gap junction-mediated intercellular communication.

However, pioneer studies have demonstrated that Cx-43 can also mediate communication between non-opposed cells via tunnelling nanotubes and extracellular vesicles (Wang et al., 2010; Soares et al., 2015). Indeed, Soares *et al,* (2015) showed that Cx-43 assembles into functional channels at the EV membrane and, more importantly, facilitates the release of cargo (Soares et al., 2015). Thus, this study revealed a new mechanism for efficient cell-cell communication through EVs that is facilitated by the docking of Cx-43 hemichannels (**Figure 4.1**).

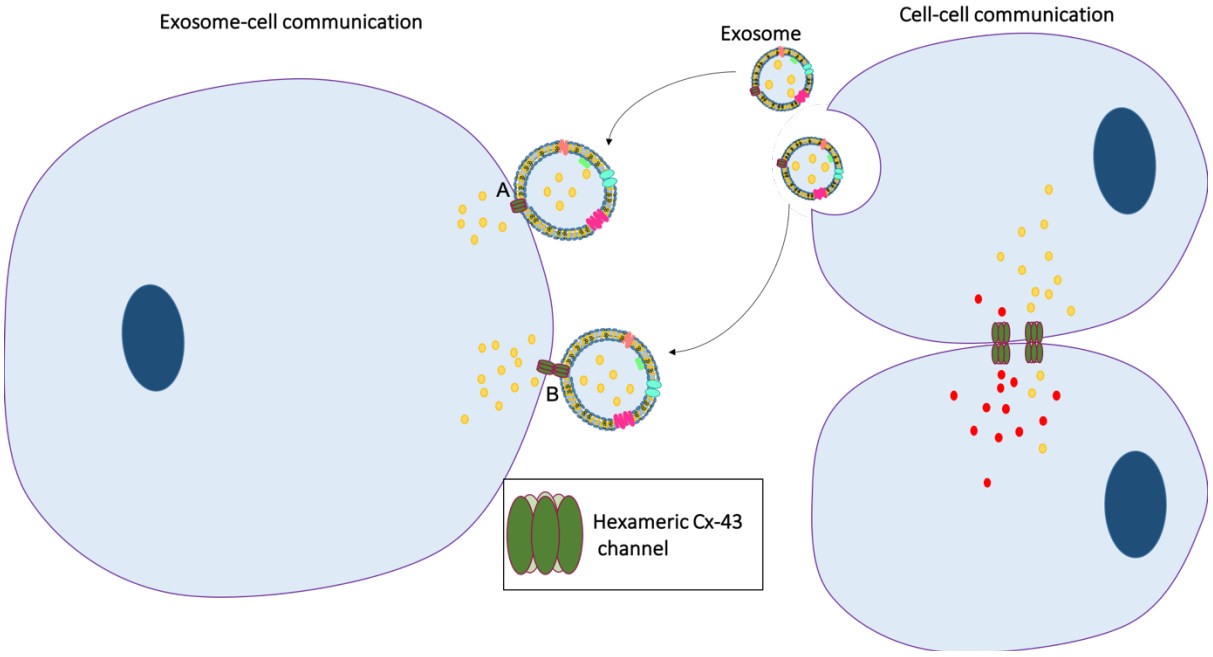

Figure 4.1. Diagram showing paracrine communication through Connexin-43 based channels. Transfer of small molecules can take place through connexon channels either cell-cell or through exosome-cell communication. A) The delivery of the exosomal cargo into the recipient cell can take place through a hexameric channel in the exosomal surface in the form of one single connexon consisting of six subunits of Connexin-43 or B) through gap junctional channels in the form of two assembled connexons at the surface of both membranes.

Membrane fusion as a result of exosome-cell interaction can easily be monitored via the use of membrane dyes. More specifically, there is a fluorescent cationic/lipidic amphiphile probe, octadecyl Rhodamine B chloride (R18) that was first used by Hoekstra et al., (1984) to stain artificial and biological membrane systems and measure the kinetics of membrane fusion. This system is based on the relief of self-quenching of R18 when both membranes come into contact.

The fluorophore is first incorporated into a lipid bilayer where the self-quenching efficiency is proportional to the fluorophore's surface density. As a result of membrane fusion, the probe's surface density decreases, thus leading to a proportional increase in fluorescence intensity, thus allowing quantitative measurements of this process. The versatility of this system has allowed its wide application across different membrane systems including EVs (Srinivasakumar et al., 1991; Arienti et al., 1997; Schwarz et al., 2013; Tian et al., 2013). Exosome-sperm membrane fusion has also been effectively quantified through this system (Carlini et al., 1997; Schwarz et al., 2013).

4.3 Hypothesis

In the previous chapter, I evaluated the *in vitro* treatment of boar sperm with HEK293T-derived exosomes by measuring different functional parameters in the sperm over a long period of incubation. I did not find any significant differences with the non-treated control, thus suggesting that HEK293T-derived exosomes are not detrimental and therefore safe to use with mammalian sperm *in vitro*. Nonetheless, there was a slight motility reduction after 10 minutes of incubation, thus suggesting that this was associated with exosome interaction. In this chapter I investigated exosome-sperm interaction both qualitatively with the use of microscopy techniques and quantitatively with kinematic-based assays to measure the rate of fusogenic events at different conditions.

I hypothesised that HEK293T-exosomes spontaneously interact with boar sperm with 10 minutes of co-incubation, including internalisation across the membrane, especially when sperm are capacitated, representing a suitable membranous systems for their further development as delivery tools.

4.4 Materials and Methods

HEK293T-derived exosomes were isolated and purified as described in **Chapter 2.4.1** and **Appendix I.II**. HEK293T-derived exosomes then were processed accordingly for visualisation techniques and fusion assays, that allow the detailed assessment of exosome-sperm interaction.

4.4.1 Qualitative and Semi-Quantitative Assessment of the Exosome-Sperm Interaction by Fluoresce Microscopy

To visualise exosome-sperm interaction two different fluorescent microscopy approaches were used; I opted for high-resolution confocal microscopy (HRCM) through Airyscan, and super-resolution microscope for single particle detection (dSTORM) (paired with Total Internal Reflection Fluorescence Microscopy (TIRFM)), both of which have different technical advantages and limitations (**Table 4.1**).

Table 4.1. Technical specifications in HRCM and superresolution microscopy.

SPECIFICATIONS	HIGH-RESOLUTION CONFOCAL MICROSCOPY	SUPER-RESOLUTION MICROSCOPY
Resolution	100-150 nm	<100 nm
Labelling dyes	Any fluorescent dye	Stochastic fluorophores only
Ease of use	High	Low
Cost	Low	High

Exosome-sperm association, including both the binding and internalisation of exosomes within sperm cells, were visualised with fluorescent dyes to allow specific qualitative determination by Airyscan and TIRFM. Before visualisation, fluorescently labelled samples were fixed with 10% formalin. Only the sperm cells exhibiting at least one exosome, either bound or internalized were imaged.

HRCM Imaging

Airyscan was used to image boar sperm that had been previously co-incubated *in vitro* with BODIPY-labelled HEK293T-derived exosomes; HEK293T-derived exosomes were labelled with the lipophilic membrane dye BODIPY (Molecular Probes, UK) as previously described by Dragovic et al., (2013). An aliquot of 1 mL of PBS containing 50 μM of BODIPY was centrifuged at 500 x *g* for 3 minutes through a 20 μm filter column Nanosep MF centrifugal device (Pall, USA) to remove dye aggregates. In order to stain HEK293-derived exosomes, the BODIPY filtered through was mixed at a final concentration of 2 μM, and then incubated for 30 min in the dark at room temperature (RT).

To remove free BODIPY, the BODIPY-labelled exosomes were passed through an EXO-spin™ midi SEC column (Cell Guidance Systems, UK), previously equilibrated with PBS, by collecting serial column fractions with 500 μL of PBS. The size and concentration profiles of the BODIPY-labelled HEK293T-derived exosomes were then assessed by NTA as described in **Chapter 2.4.2**. Subsequently, 10 different boar ejaculates were obtained and manipulated as described in **Chapter 3.2.1**. The resulting 5 sperm replicates were each divided into two portions, one aliquot for exosome-treatment and the other to act as an untreated control. Both of these portions were then re-suspended in non-capacitating buffer (pH <7) and diluted to a final concentration of $1x10^7$ sperm/mL.

Non-capacitating buffer was freshly prepared with the same composition as the capacitating buffer described in **Chapter 3.2.1** except that bicarbonate ($NaHCO_3$) and BSA protein (capacitating agents) were not added to the buffer to avoid triggering sperm capacitation. The aliquots destined for exosome treatment were mixed with BODIPY-exosomes to a final concentration of $1x10^8$ EV/mL. The working exosome:sperm cell ratio was 10:1. All samples, including controls, were placed inside an incubator at 37 °C, 5% CO_2. Incubation was performed for up to 4 hours during which aliquots from the exosome-treated samples (EXO) and non-exosome treated control samples (CTL) were collected at 0 h, 2 h, and 4 hours post-incubation (**Figure 4.2**).

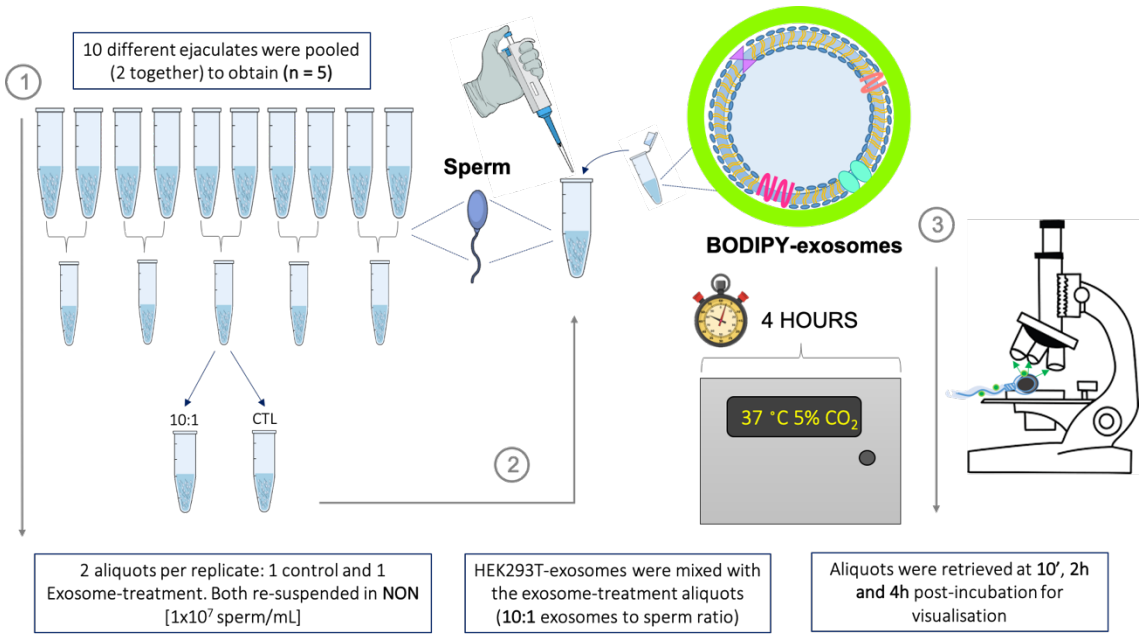

Figure 4.2. Diagram displaying the steps followed for the co-incubation of BODIPY-labelled HEK293T-derived exosomes with boar ejaculates (n =5). 10 ejaculates from different boars were pooled in pairs to obtain 5 biological replicates. Each replicate was split into two aliquots, one exosome treatment (exosome to sperm ratios 10:1) and one untreated control (CTL). Sperm aliquots were diluted to a working concentration of $1x10^7$ sperm cells/mL in the non-capacitating buffer (NON) and placed inside the incubator for incubation up to 4 hours. Aliquots were retrieved at 10 min, 2h and 4h post-incubation for their visualisation with high-resolution confocal microscopy.

Prior to fixation, sperm samples were co-labelled with 2-(4-amidinophenyl)-1H -indole-6-carboxamidine (DAPI) to better visualise the sperm nucleus.

Samples were then sent for imaging to Alan Wainman at the light microscopy facility (Sir William Dunn School of Pathology, University of Oxford). Sperm cells were imaged at 21°C using an inverted Zeiss 880 microscope fitted with an Airyscan detector. The system was equipped with a plan-Apochromat 63 ×/1.4-NA oil lens.

488-nm argon and 405-nm diode lasers were used to excite BODIPY and DAPI respectively (sequential excitation of each wavelength was switched per line to ensure green and blue channels respectively were aligned).

Sections of five slices (at 0.2-µm-thick intervals) were collected every 1 min with a zoom value of 20 pixels/µm. Images were then transformed into maximum Z-stack projections and processed with ImageJ.

Super-resolution imaging

TIRFM incorporated to dSTORM was carried out to visualise the HEK293T-derived exosomes labelled with WGA-AlexaFluor488 at a single level in the boar sperm samples after their *in vitro* co-incubation with boar sperm. HEK293T-derived exosomes were fluorescently labelled with 2 µg/mL of wheat germ agglutinin (WGA)-AlexaFluor488 conjugate (Thermo Fisher Scientific, UK). The WGA/exosome mixture was then incubated on a shaker in the dark at RT for 30 min. After incubation, the WGA/exosome mixture was passed through a SEC column (300 KMWCo Nanosep® device (Pall corporation, US)) and centrifuged at 5000 ×*g*, at 4 ºC for 10 minutes to remove excess dye. This process was repeated three times in total by discarding the filtered-through liquid and topping up the column with fresh PBS. The size and concentration profiles of the labelled HEK293T-derived exosome samples were then re-evaluated by NTA as described in **Chapter 2.4.2**.

Simultaneously, a negative control as to discard any false-positive interaction events from loose dye binding into the sperm, consisting of an aliquot of the same volume of PBS (instead of exosomes) and WGA-AlexaFluor488 dye, was prepared and washed.

For TIRFM imaging, sperm samples were incubated with pre-labelled WGA-AlexaFluor488 exosomes as described in **Chapter 3.4.** and were plated onto 0.01 % Poly-L-Lysine (PLL) coated 8-well IBIDI chambers (Ibidi GmbH, Germany) for 15 min before further processing. After fixation, sperm were labelled for 10 min with 10 µg/mL of WGA-AlexaFluor647 conjugate to visualize the exosomes and sperm membrane. This protocol allowed me to identify exosomes that had been internalized by the sperm; the WGA-AlexaFluor4647 label stained the exosomes that had been previously labelled with WGA-AlexaFluor488 by filling up the gaps on the surface of exosomes, but only those that had not been internalized inside the sperm, thus exhibiting both red and green fluorescence. Samples were then mounted in mounting solution and imaged at 21°C using an inverted TIRFM (Zeiss 880) and dSTORM.

The system was equipped with a Plan-Apochromat 63×/1.4-NA oil lens; 488 nm argon and 647 nm diode lasers were used to excite WGA-AlexaFluor488 and WGA-AlexaFluor647, respectively (sequential excitation of each wavelength was switched per line to ensure green and red channels were aligned). Sections of five slices (0.2µm in thickness) were collected every 1 min with a zoom value of 20 pixels/µm. TIRFM imaging was performed with an Olympus IX83 inverted microscope (Olympus) equipped with a 150×1.45 NA oil-immersion objective at RT.

Fluorescent emission was collected by the same objective onto an electron-multiplying charge-coupled device camera (Evolve Delta, Photometrics). Images were transformed into maximum Z-stack projections and processed with ImageJ (National Institute of Health).

Exosome internalisation was determined at different time points by counting only those sperm cells previously imaged by TIRFM that exhibited at least one exosome (either attached or internalised (regarded as positive)), as described in **Appendix III** of this thesis. A total of 20, 22 and 50 sperm cells were quantified at 10 min, 2 hours, and 5 hours respectively. The statistical significance of internalisation was evaluated with a chi-squared test (GraphPad Prism 8.1.0).

dSTORM imaging (pilot study)

1. Membrane labelling – WGA-AlexaFluor647

dSTORM was initially tested in the absence of TIRFM in an initial pilot study where HEK293T-derived exosomes and boar sperm samples were labelled with WGA-AlexaFluor647 upon their co-incubation for 5 hours;

Sperm sample preparation and co-incubation with the non-labelled HEK293T-derived exosomes was carried out in the same way as for TIRFM, at an exosome to sperm ratio of 100:1. A single sperm aliquot retrieved at 5 hours post-incubation was fixed for visualisation, and to visualised the HEK293T-derived exosomes attached to the sperm another staining was carried out with 2 µg/mL WGA-AlexaFluor647 for 10 minutes in the dark.

2. Exosome uptake labelling – CD9

Additional specific labelling was carried out with a CD9 antibody to discriminate between exosomes and other membranous artefacts that may have been present in the preparation and perhaps provide further insights on the intercommunication mechanisms taking place between the exosomes and the boar sperm. For this, I labelled the fixed samples with a CD9 antibody (antibody dilution 1:50) (Catalogue number: ab92726) followed by an anti-rabbit secondary antibody conjugated with the AlexaFluor488 fluorophore.

Both TIRFM and dSTORM imaging were carried out by Dr Stefan Balint in Professor Michael Dustin's group (The Kennedy Institute of Rheumatology, University of Oxford).

4.4.2 Assessment of the Mechanisms Associated with Exosome-Sperm Interactions

Further analysis of the mechanisms involved in the interaction between HEK293T-derived exosomes and the boar sperm was carried out through a qualitative approach that specifically evaluated Cx-43 as a possible protein-mediated pathway, and a quantitative approach testing membrane-membrane fusion events under different incubation conditions.

Detection of CONNEXIN-43 in HEK293T-exosomes by WB

Semiquantitative analysis by WB was carried out to assess the expression levels of Cx-43 in HEK293T-exosome lysates (in triplicate). These were then compared to the expression levels in a HEK293T cell lysate. The conditions and reagents used for the WB were the same as those described in **Chapter 2.4.2**. The anti-Cx-43 antibody was purchased from Abcam (Catalogue number: ab11370; host animal: rabbit) and was used in with a dilution factor of 1:1000.

Detection of CONNEXIN-43 in HEK293T-derived exosomes by nanogold TEM

Nanogold TEM was carried out to visually detect the location of the Cx-43 protein in HEK293T-derived exosomes. For this, two different antibody strategies were used; In the first, the same Cx-43 antibody used for WB (Catalogue number: ab11370) was applied an incubated (1:50 dilution). This was followed by incubation with a secondary anti-rabbit antibody conjugated with a nanogold particle of size 5 nm in a 1:20 dilution.

In the other strategy, samples were first mildly treated with saponin (0.1%) to allow the entry of the antibody into the inner side of the exosomal membrane by following an established protocol (Soares et al., 2015). For this experiment I purchased the same antibody that had been used in Soares' paper (Catalogue number: sc-271837; Santa Cruz, US). The primary antibody was applied at a 1:5 dilution. This was followed by the same secondary antibody as described for the previous strategy.

For both strategies, a non-saponin treatment, as well as a negative control consisting of the secondary antibody only (dilution 1:20), were tested in parallel. Finally, 20 µL of the undiluted HEK293T-derived exosome samples were sent to Errin Johnson at the Electron Microscopy Facility (Sir William Dunn School of Pathology, University of Oxford) where they were placed onto lacey carbon copper grids (300 mesh) after staining.

High-resolution TEM images were then acquired with an FEI Tecnai 12 microscope operating at 120 kV and equipped with a Gata OneView camera.

Detection of CONNEXIN-43 interaction sites in boar sperm samples co-incubated with HEK293T-derived exosomes by TIRFM

Next, I investigated the role of Cx-43 during the interaction between HEK293T-derived exosomes and boar sperm samples. The exosomes and sperm were co-incubated for 5 hours and labelled post-fixation with WGA-AlexaFluor647 to stain the mammalian membranes. The Cx-43 protein was specifically labelled with a Cx-43 primary antibody (Catalogue number: ab11370) followed by an anti-rabbit secondary antibody conjugated with an AlexaFluor488 fluorophore.

A negative control was also included; for this, the sample was incubated with the secondary antibody only. Samples were then visualised in 8-well IBIDI chambers as described previously for dSTORM .

A quantitative assay for exosome-sperm membrane fusion

The real-time evaluation of membrane fusion kinetics between HEK293T-derived exosomes and boar sperm was carried out under different incubation conditions by using the self-quenching R18 fluorescent probe system. The labelling procedure was carried out by slightly modifying the protocol used by Tian et al., (2013); A concentration of 40 μg/mL of R18 was dissolved in ethanol and used to label 200 μg of total protein from the HEK293T-derived exosome suspension. This mixture was then incubated for 30 min on a shaker at 37 ºC in the dark. Excess dye was then removed by passing the exosome suspension through a 300 KMWCo Nanosep® device (Pall corporation, US) and centrifuged at 5000 ×*g*, at 4 ºC for 10 minutes.

This process was repeated three times in total by discarding the filtered-through liquid and topping up the column with fresh PBS. The size and concentration profiles of the labelled HEK293T-derived exosome samples were then re-evaluated by NTA, as described in **Chapter 2.4.2**.

A negative control was also included. This consisted of an aliquot of the same volume of PBS (instead of exosomes) labelled with the R18 dye; this was processed in the same way.

Different conditions were tested in parallel in a round 4titude black 96-well plate with a clear bottom (BGM Labtech, Madrid). This included different pH levels (pH 5.0, pH 6.8 and pH 7.4) in capacitating and non-capacitating conditions, and the presence and absence of BSA, in the condition media (**Figure 4.3**).

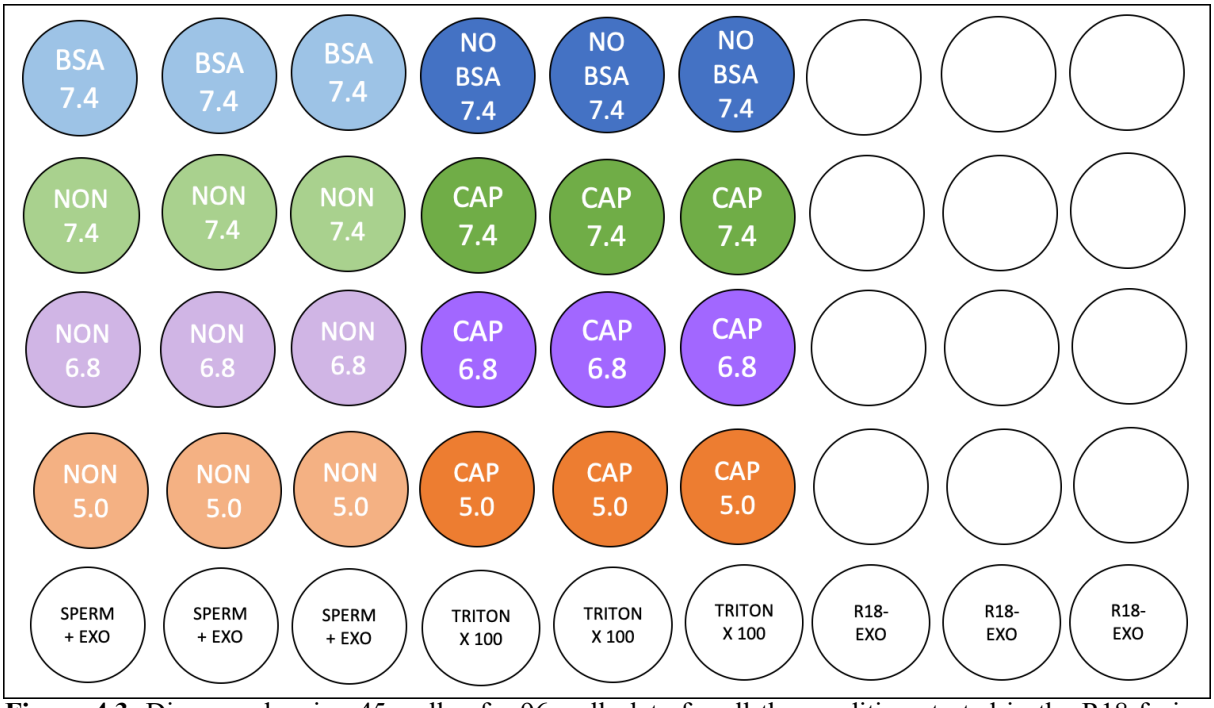

Figure 4.3. Diagram showing 45 wells of a 96-well plate for all the conditions tested in the R18-fusion assay. For the reaction to take place boar sperm at a concentration of 1 x 10^7 sperm/mL were co-incubated for 2 hours while fluorescence intensity was evaluated at real-time throughout at 38.5 °C, 5% O_2 and 5% CO_2 in the presence of R18-labelled HEK293T-derived exosomes at the exosome to sperm ratios of 10:1 and 100:1. In the first row of the plate, the fusion rate influenced by the presence and absence of BSA (light blue and dark blue respectively) in the condition media were compared for a pH of 7.4. In the second row, the next two rows the effect of capacitating and non-capacitating conditions as the absence of BSA and bicarbonate were evaluated upon the fusion rate at pH 7.4, 6.8 and 5.0 (green, purple and orange respectively). Finally, two negative controls and one positive control were also included in the plate consisting of sperm and exosome mixture (SPERM + EXO) and R18-labelled exosomes (R18-EXO) as the negative controls and the sperm/R18-EXO mixture reaction with 0.1% Triton X-100 as the positive control.

Measurements were carried out using a spectrophotofluorimeter ClarioStarPlus (BMG Labtech, Germany) equipped with O_2 and CO_2 tanks every 10 min throughout a total incubation period of 2 hours. The R18 dye was excited with a Rhodamine B excitation wavelength range of 550 – 580 nm, and an emission filter for 605 – 640 nm.

Incubation of the sperm samples was carried out prior to the addition of the R18-labelled HEK293T-derdived exosomes (R18-EXO) in the plate inside of an incubator at 38.5ºC, 5% CO_2 and 5% O_2 for 1 hour to allow equilibration of the sperm in the condition media and to enhance capacitation of the sperm within the wells featuring capacitating conditions.

Further incubation was then carried out by placing the plate into the ClarioStar at 38.5 ºC and a controlled gas tension of 5% CO_2 and 5% O_2 to mimic the environment inside the oviduct (Morin, 2017) for up to 2 hours. Measurements were carried out every 10 minutes throughout, and 10 µg/mL of P_4 was added half-way through the incubation, as described in **Chapter 3.4.1** to promote the acrosome reaction.

All of these different experimental conditions were carried out for two different exosome to sperm ratios; 10:1 and 100:1, as to observe any differences regarding the exosome concentration.

To calibrate the system before conducting the measurements, two negative controls were used as blanks. These consisted of boar sperm that had been co-incubated with unlabelled HEK293T-derived exosomes and R18-EXO only (both in capacitating buffer at 7.4), to remove any background signal caused by the sample composition. Moreover, a positive control was used as a reference for 100% fusion. This was set as the maximum threshold or gain, and consisted of an experimental sample in capacitating and 7.4 pH conditions, with triton x-100 treatment to permeabilise the exosomal membranes and liberate the R18 dye. This achieved the highest signal level that could be obtained with the exosome to sperm ratio of 10:1 and 100:1 used in the different experimental samples.

Finally, the MARS Analysis Software Module (BMG Labtech, Germany) was used to visualise the signal curves in each well of the plate reader and to evaluate and analyze data.

4.5 Results

To visualise exosome-sperm interaction and assess the possible mechanisms involved in such communication, different qualitative and quantitative assays were carried out in boar sperm samples previously treated with HEK293T-derived exosomes.

4.5.1 Qualitative and Semi-Quantitative Assessment of Exosome-Sperm Interactions by Fluorescence Microscopy

Different fluorescence-based microscopy techniques are available to visualise exosome-cell interactions. For exosome-sperm specific interaction, HRCM and super-resolution- based visualisation and labelling techniques were carried out. These were tested in boar sperm samples treated with HEK293T-derived exosomes via the use of different fluorescent labelling strategies.

<u>HRCM imaging</u>

For HRCM with the Ayriscan microscope, HEK293T-derived exosomes were labelled with the lipophilic dye BODIPY. After incubation and washing off the excess dye through SEC, individual column fractions were collected; and their concentration was determined by NTA to select those that were enriched with exosomes (**Figure 4.4**).

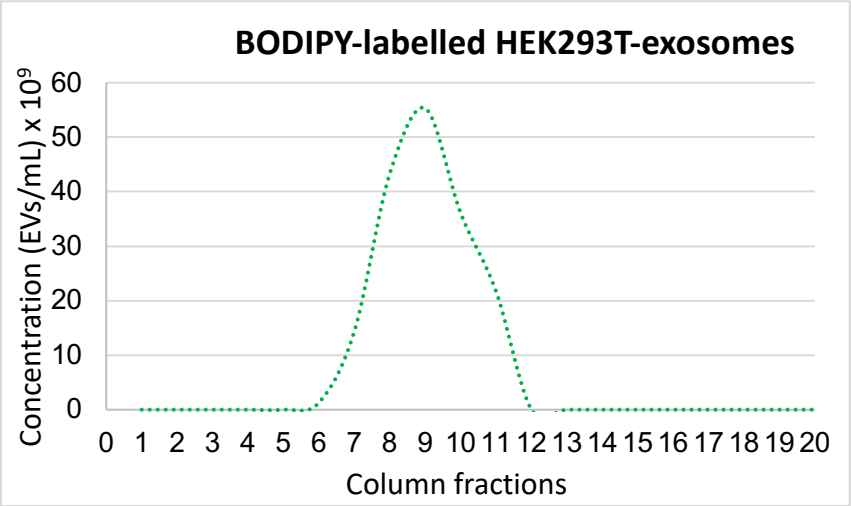

Figure 4.4. Graph showing the concentration determined by NTA for each column fraction collected from SEC. Fractions 6-11 had a concentration between 1 x 10^7 and 55 x 10^9 EVs/mL. Fractions < 6 and > 11 had a concentration below the limit of detection of the machine.

Fractions 6 to 11 showed the highest exosome concentrations. These concentrations ranged from 1 x 10^7 to 5.5 x 10^{10} EVs/mL. Once selected, these fractions were mixed into one single aliquot; the size and concentration profiles were then re-determined by NTA (**Figure 4.5**).

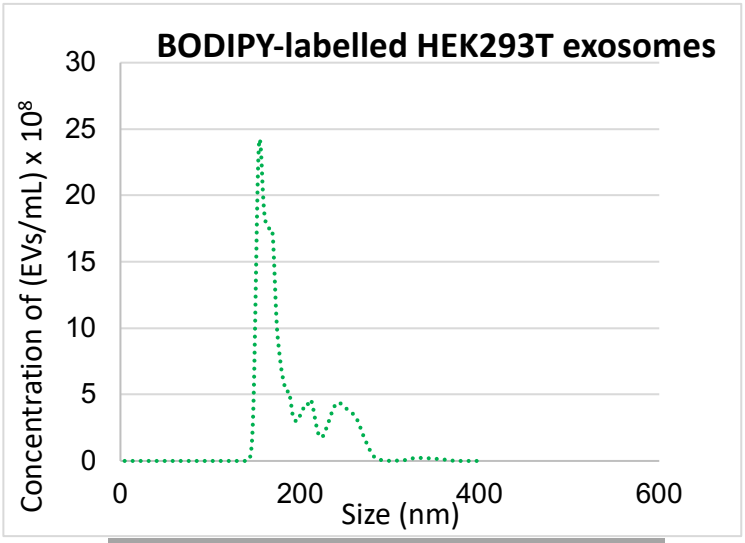

SIZE MODE	CONCENTRATION
140 nm	2.47 x 10^9 EVs/mL

Figure 4.5. Graph showing the size and concentration profile determined by NTA of the BODIPY-labelled HEK293T-derived exosomes. The modal size mode was 140 nm while the total concentration of the sample was 2.47 x 10^9 EVs/mL.

NTA revealed a total concentration of 2.47 x 10^9 EVs/mL and a modal size of 140 nm in the resulting combination of fractions of the BODIPY-labelled HEK293T-derived exosomes. The BODIPY-labelled exosome sample was co-incubated with boar sperm at an exosome to sperm ratio of 10:1, and aliquots at 10 min, 2h and 4h post-incubation were fixed and visualised with Airyscan. This revealed green fluorescent particles that were approximately 500 nm in size (measured by ImageJ). These were attached to the sperm head, mid-piece and tail (**Figure 4.6**). Moreover, up to two exosomes per sperm cell were observed at 2 h and 4 h post-incubation.

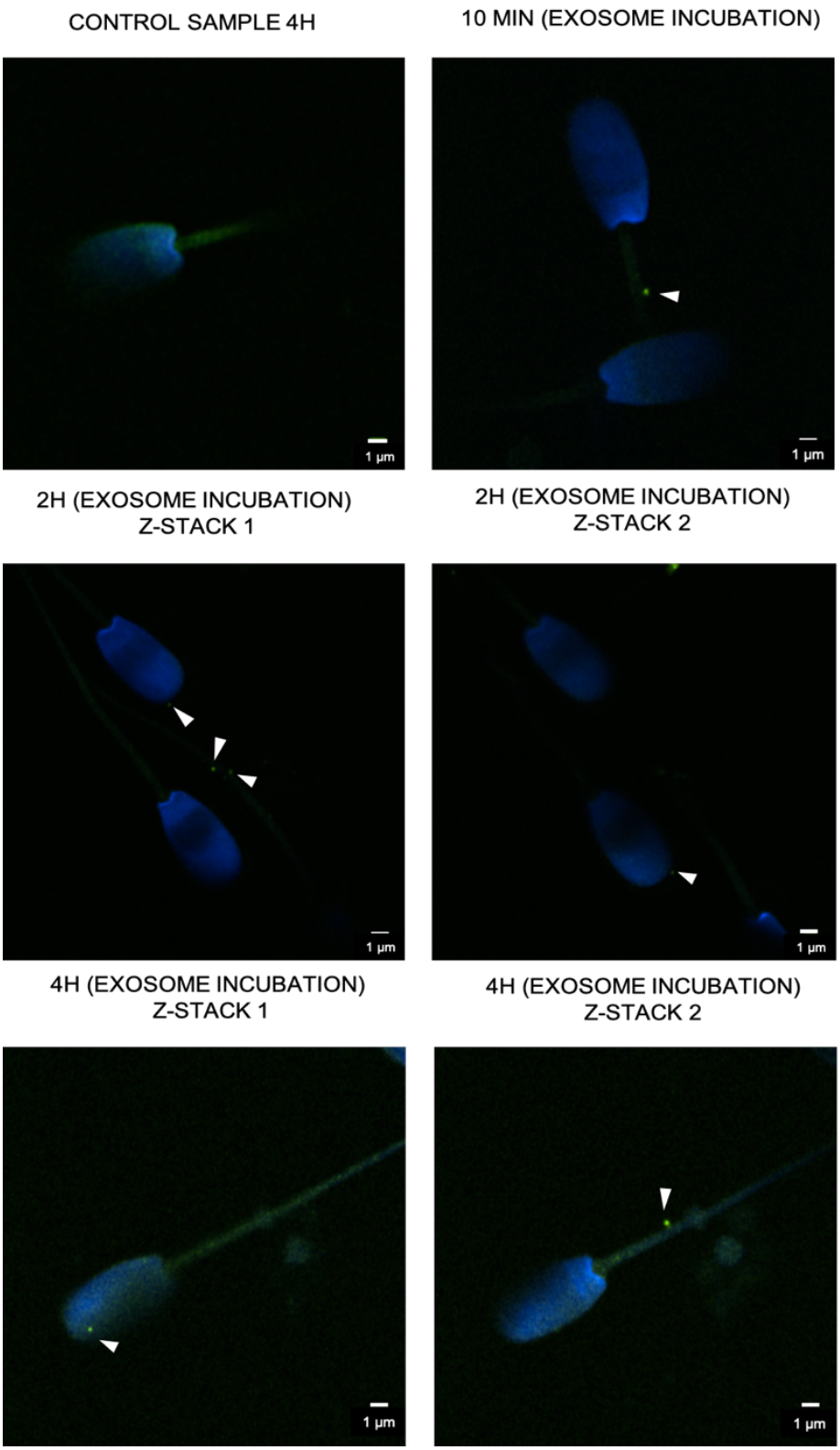

Figure 4.6. Airyscan images showing boar sperm samples after their *in* vitro co-incubation with BODIPY-labelled HEK293T-derived exosomes in an exosome to sperm ratio of 10:1 sperm cells. Images were obtained with a magnification of 600-X, and control and exosome-treated samples (10 min, 2 h and 4 h) were visualized using DAPI-overlaid background. BODIPY-labelled exosomes exhibited green fluorescence (white arrows). Images show different sperm cells. Scale bar = 1µm.

Super-resolution imaging

TIRFM paired with dSTORM was carried out as an enhanced fluorescence microscopy technique to visualise exosome-sperm interaction at the single-particle level in boar sperm samples that had been previously co-incubated with WGA-AlexaFluor488-labelled HEK293T-derived exosomes *in vitro*.

The characterisation and profiling results for the WGA-AlexaFluor488-labelled HEK293T-derived exosome samples are shown in **Chapter 2.5.1**. Images acquired by TIRFM showed the HEK293T-derived exosomes as green fluorescent particles that were either attached to the surface or internalised inside different regions of the sperm being observed that such an association is more localised in the sperm tail and mid-piece at 10 min, 2 h, 4 h 30 min and 5 h post-incubation (**Figure 4.7**).

Exosomes associated with sperm exhibited both green and red WGA labelling; thus producing a slightly orange signal (yellow arrowheads). Exosomes that had been internalised only exhibited green WGA labelling (white arrowheads).

The untreated control at 5 h post-incubation showed no evidence of green WGA-AlexFluor488 dye. At 10 min post-incubation, both surface-bound and internalised exosomes (in orange and green fluorescence respectively) were evident. Moreover, at this time point, green fluorescence was observed along the inner lining of the membrane (white bracket).

In addition, during this analysis I paid particular attention to exosome internalization. **Figure 4.8** shows two TIRFM images presenting two distinct sperm cells at 5 h post-incubation; the exosomes are shown within the white squares.

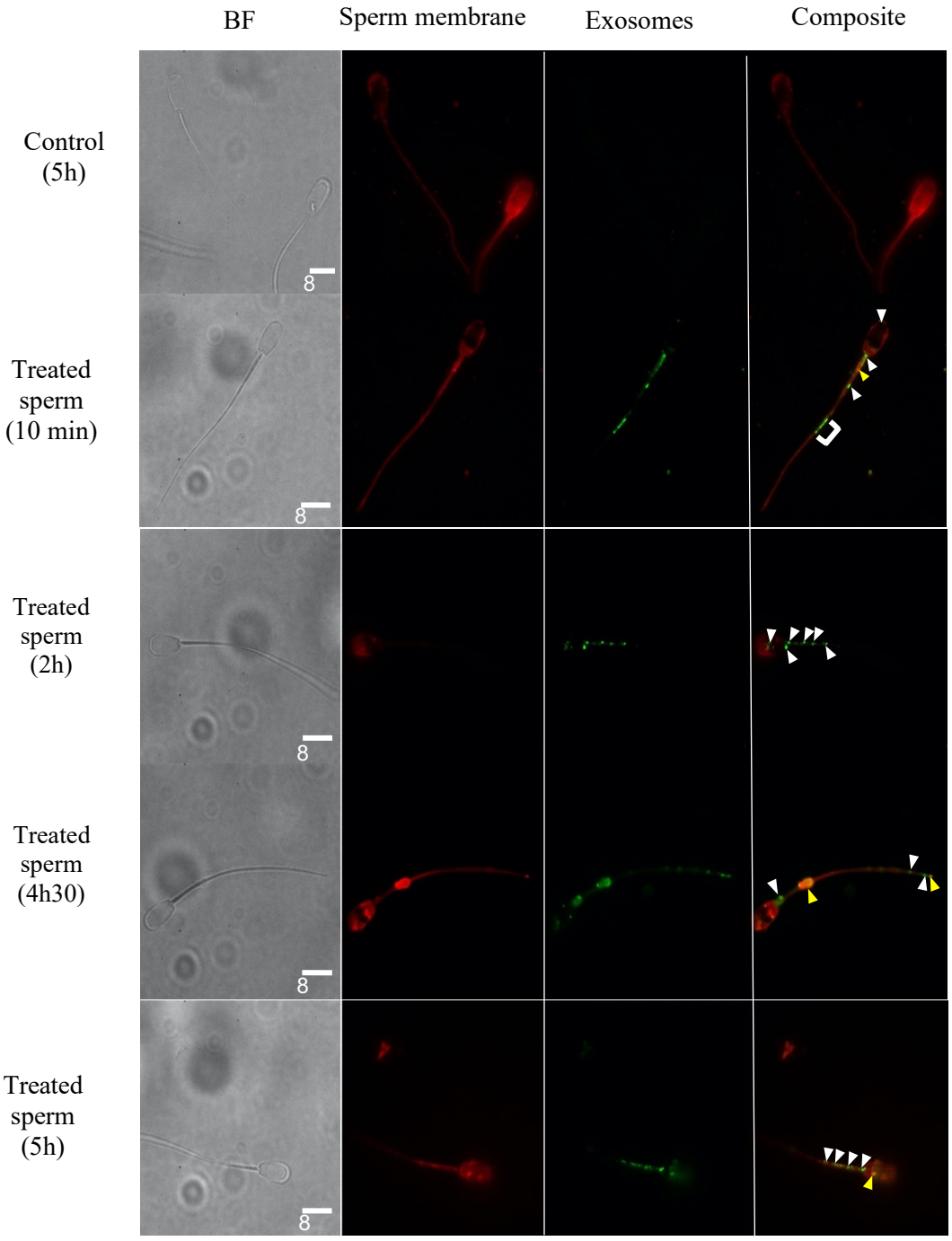

Figure 4.7. Visualization of exosome-sperm interaction after *in vitro* co-incubation of boar sperm with 100:1 HEK293-derived exosome treatment using Total Internal Reflection Fluorescence Microscope (TIRFM). TIRFM images of exosome samples (WGA-AlexaFluor488, green) that were incubated with sperm samples for the indicated times. After fixation, sperm were labelled with wheat germ agglutinin (WGA-AlexaFluor647, red) to visualize the sperm membrane. The presence of an intact sperm is indicated by the bright field image (BF). Images show different sperm cells. Control sperm samples at 5 h post-incubation and exosome treated samples at 10 min, 2 h, 4 h 30 min and 5 h post-incubation. White arrowheads indicate internalised exosomes within the sperm cells, yellow arrowheads indicate attached exosomes outside the sperm cells. Scale bar = 8 µm.

Figure 4.8A is a high-resolution image and shows attached exosomes as an orange-like colour; this is due to the combination of the red and green signals in the composite channel that can also be seen individually in the WGA-AlexaFluor647 (white arrows) and WGA-AlexaFluor488 channels, respectively.

Similarly, **Figure 4.8B** shows a close-up of a signal display for internalized exosomes; here, only the green dye is evident, both in the composite and WGA-AlexaFluor488 channels. The size of these green-particles ranged from 280 nm to 670 nm, as determined by ImageJ.

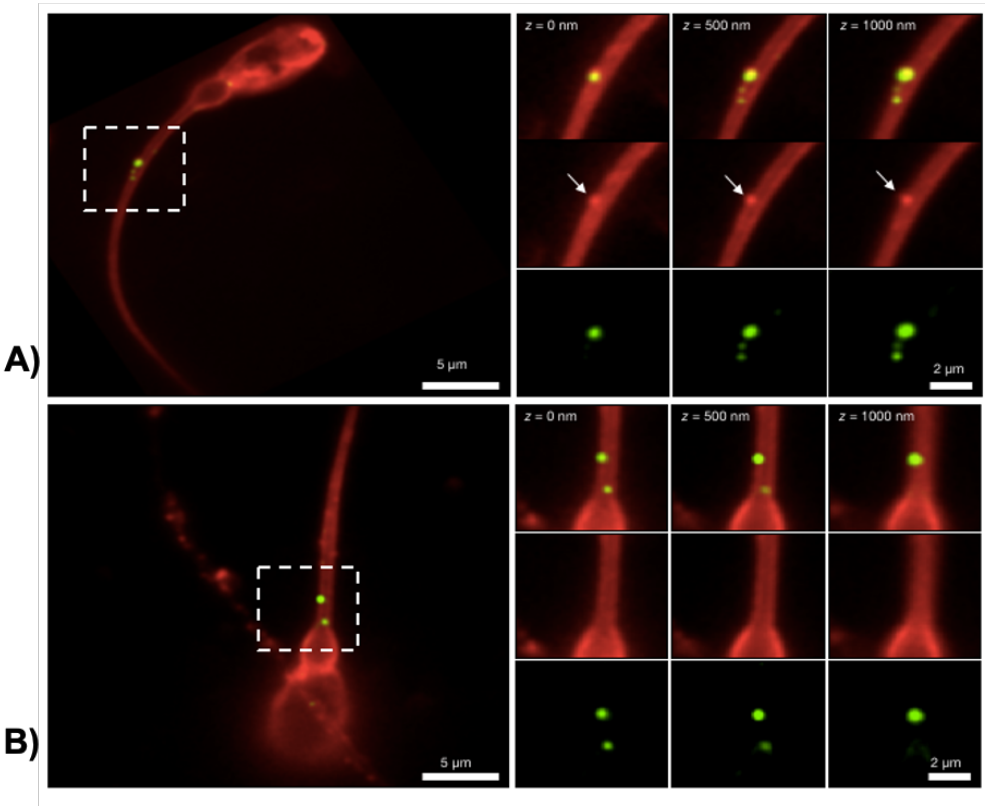

Figure 4.8. Images were taken with TIRFM for a magnified visualisation of exosome-sperm interaction. Regions delineated by white squares have been magnified (z = 0, 500 and 1000 times) to show signal displays in the composite, WGA-AlexaFluor647 (red) and WGA-AlexaFluor488 (green) channels. **A)** and **B)** TIRFM images show two different sperm cells treated with exosomes after 5 h incubation. **A)** Shows a sperm representative to those sperm with an attached exosome; note the green and red signals that are evident in the red (white arrows) and green channels respectively. **B)** Shows a sperm representative to those sperm with internalized exosomes, as it is visible from only a green signal display in the green and composite channels. Scale bars are 5 µm and 2 µm.

The rate of exosome internalisation was quantified at 10 min, 2 hours, and 5 hours (**Figure 4.9**). The proportion of positive sperm cells (those internalised exosomes) was 20%, 50%, and 68% respectively; this increasing trend was positively significant ($P > 0.005$).

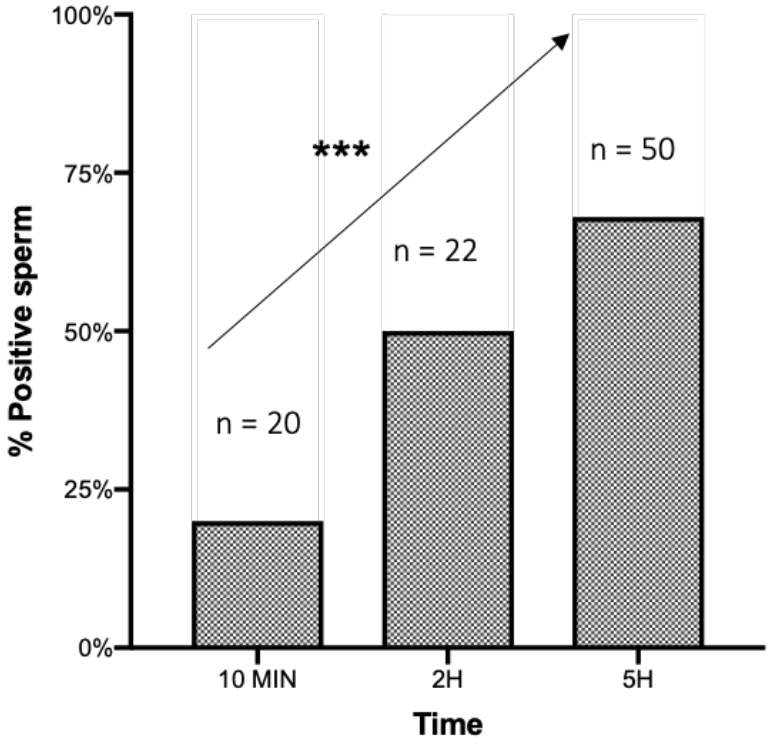

Figure 4.9. Bar graph displaying the proportion (%) of sperm with internalized WGA-AlexaFluor488-HEK293T-derived exosomes with time of incubation. Only those sperm cells displaying at least one exosome were regarded as positive. Internalisation was determined by calculating the percentage of positive sperm cells with at least one exosome internalised within them. Different time points were evaluated, revealing 20% of positive sperm at 10 min, 50% of positive sperm at 2 h and 68% of positive sperm at 5 h post-incubation. A total of 20, 22 and 50 sperm cells (sample size = n) were quantified at each time point, respectively. The data show a significantly increasing trend with incubation time (***$P < 0.005$).

<u>dSTORM imaging (pilot study)</u>

1. Membrane labelling – WGA-AlexaFluor647

dSTORM imaging was used in a pilot study to visualise the internalisation of single exosomes with boar sperm.

After co-incubation for 5 hours, boar sperm samples were labelled with WGA-AlexaFluor488 to visualise interactions between sperm and exosomal membrane, as be seen in **Figure 4.10** (white circle).

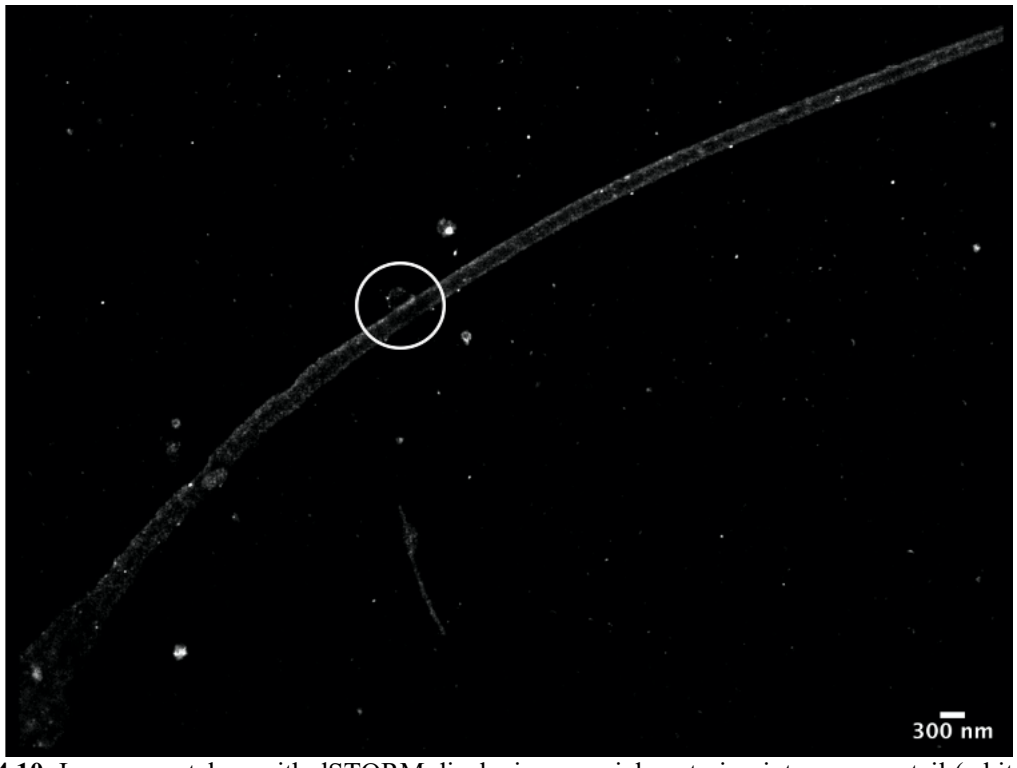

Figure 4.10. Image was taken with dSTORM displaying a vesicle entering into a sperm tail (white circle). Samples were labelled with WGA-AlexaFluor647 to stain all membranes (sperm and exosomes). Scale bar = 300 nm.

2. Exosome uptake labelling – CD9

Anti-CD9 was used to specifically label HEK293T-derived exosomes and any interaction site through this transmembrane protein also present in the boar sperm cell (**Figure 4.11**).

Figure 4.11 shows a sperm cell and exosomal membranes in red (WGA-AlexaFluor647) and the CD9 signal in cyan blue (AlexaFluor488). Despite membrane labelling of a good standard, the CD9 signal can be observed labelling some spots of the boar sperm membrane with high levels of background field. This indicated non-specific binding.

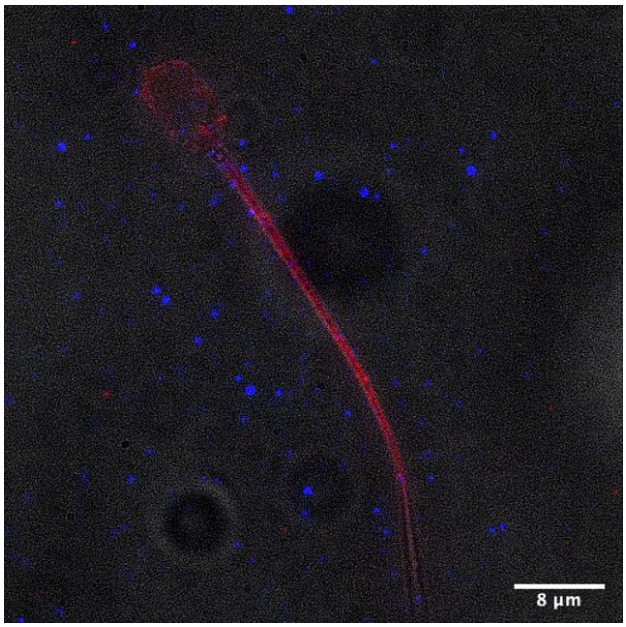

Figure 4.11. Image was taken with dSTORM displaying a boar sperm co-incubated with HEK293T-derived exosomes for 5 hours. Post fixation, the sample was labelled with WGA-AlexaFluor647 (red) to stain the boar and the exosomal membranes and CD9-AlexaFluor488 to stain the exosomes and the interaction sites at the sperm cell membrane (cyan blue). Scale bar = 8 µm.

4.5.2 Assessment of the Mechanisms Underlying Exosome-Sperm Interactions

Next, I investigated the mechanisms underlying the interactions between HEK293T-derived exosomes and boar sperm; Particularly the protein-mediated pathway involving Cx-43. This was carried out by evaluating the expression levels of Cx-43 in HEK293T-derived exosome preparations by WB, nanogold TEM (for the visual localisation of this protein) and dSTORM (to image the protein-mediated channels between the HEK293T-derived exosome and boar sperm membranes).

A quantitative fluorometric assay was carried out to compare different incubation conditions and identify the optimal conditions to enhance exosome-sperm membrane interaction or fusion.

Detection of CONNEXIN-43 in HEK293T-derived exosomes by WB

A semiquantitative WB assay was performed with 10 µg of total protein and used to determine the relative expression levels of Cx-43 in the HEK293T-derived exosome preparations; these were then compared to the HEK293T cells from which they were derived. The mean density of each band was quantified using GeneTools software. Cx-43 was expressed at much higher levels in the exosomal lysates compared to the HEK293T cell lysate (**Figure 4.12**). No bands were seen in the HEK293T cell lysate, while two distinct bands (with molecular weights of 60 and 48 kDa) were evident in all three exosome lysate replicates. The mean band density for the 60 kDa band was 0.5 times higher than that of the 48 kDa band.

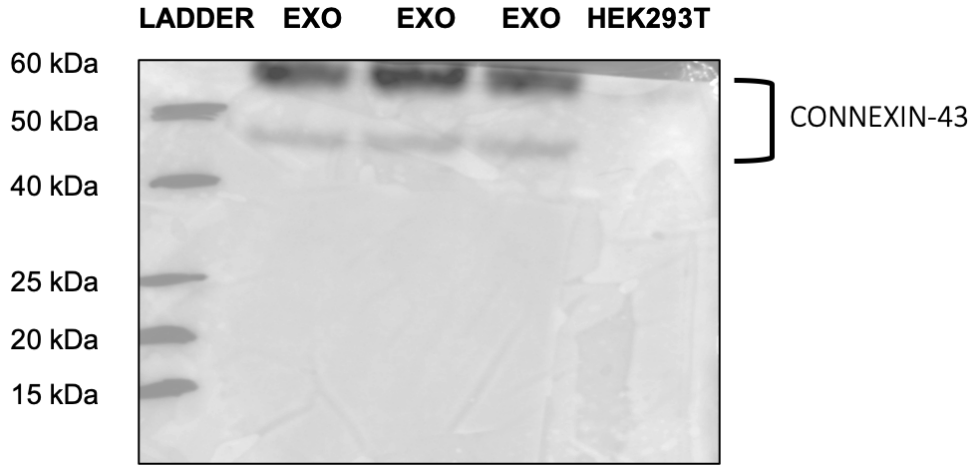

Figure 4.12. Western blotting images of the protein expression levels for Cx-43 in three HEK293T-exosome sample replicates (n = 3) and the HEK293T cell lysate for reference, showing two different bands corresponding to two different Cx-43 isoforms in the exosome lysates of 60 and 48 kDa in size. The density of protein bands was identified and manually selected for quantification on chemiluminescent blots using GBOX Chemi XX6/XX9 equipped with GeneTools software, by normalizing the relative protein amount in each lane against the band intensities obtained from HEK293 T cell lysates. No bands are visible in the HEK293T cell lysate, and in average the 60 kDa band was 0.5 times higher than the 48 kDa band in the exosome lysates. The upper half of this blot was used for another antibody staining and hence why it can be seen cut out right above the Cx-43 band.

Detection of CONNEXIN-43 in HEK293T-derived exosomes by nanogold TEM

Nanogold TEM was carried out to detect Cx-43 protein labelling in HEK293T-derived exosome preparations.

The first attempt was carried out by labelling the HEK293T-derived exosome sample with a primary Cx-43 antibody (Catalogue number: ab11370) in a 1:50 dilution (**Figure 4.13**). Multiple nanogold particles (white arrowheads) were evident (**Figure 4.13A**), yet there were none attached to the exosomes. **Figure 4.13B** shows the negative control in which labelling was only carried out with the secondary antibody; the same labelling pattern was evident, thus confirming that labelling had been unsuccessful.

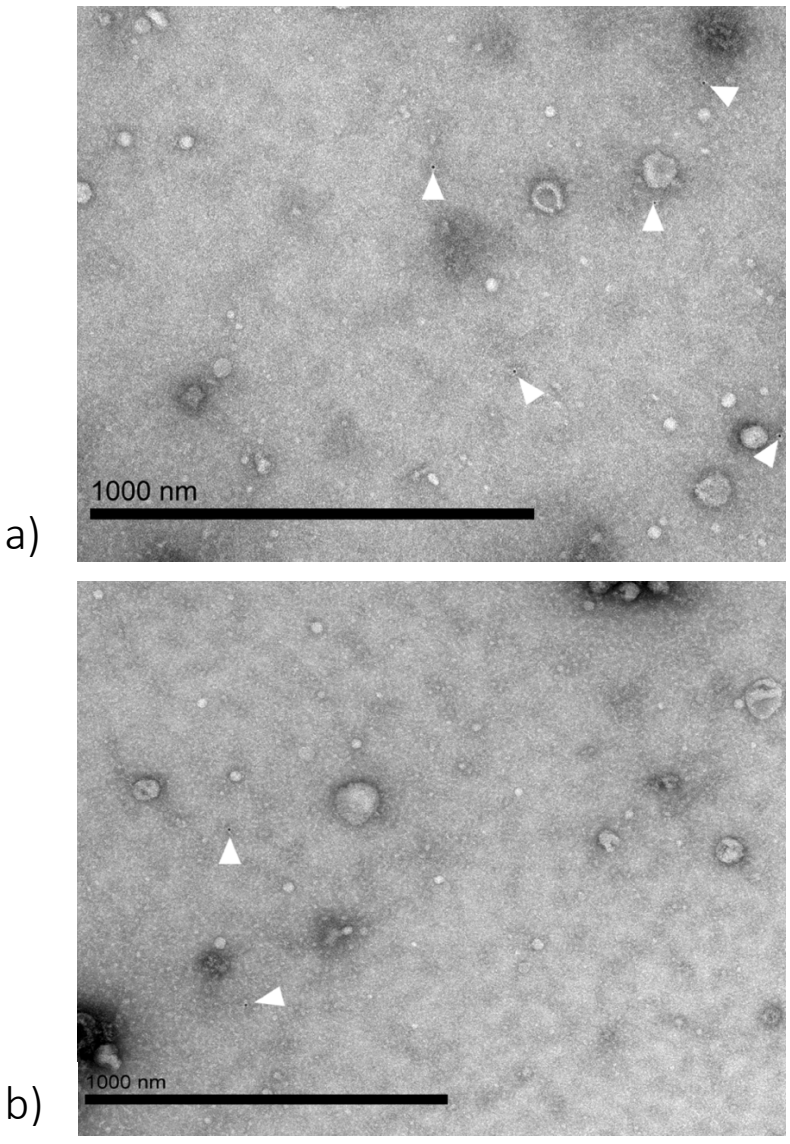

Figure 4.13. Nanogold TEM images of the HEK293T-derived exosomes. a) First attempt labelling the HEK293T-derived exosome samples with anti-Cx-43 as a primary antibody (reference ab11370) in a 1:50 dilution. 5nm nanogold particles (white arrowheads) can be seen unspecifically bound to the surface instead of the exosomes. b) Negative control consisting of the secondary antibody only (1:20) dilution. Scale bar = 1000 nm.

In the second attempt, prior to the labelling, the HEK293T-derived exosomes were treated with 0.1% saponin and a different primary antibody was used (Catalogue number: sc-271837) in a 1:5 dilution (**Figure 4.14**).

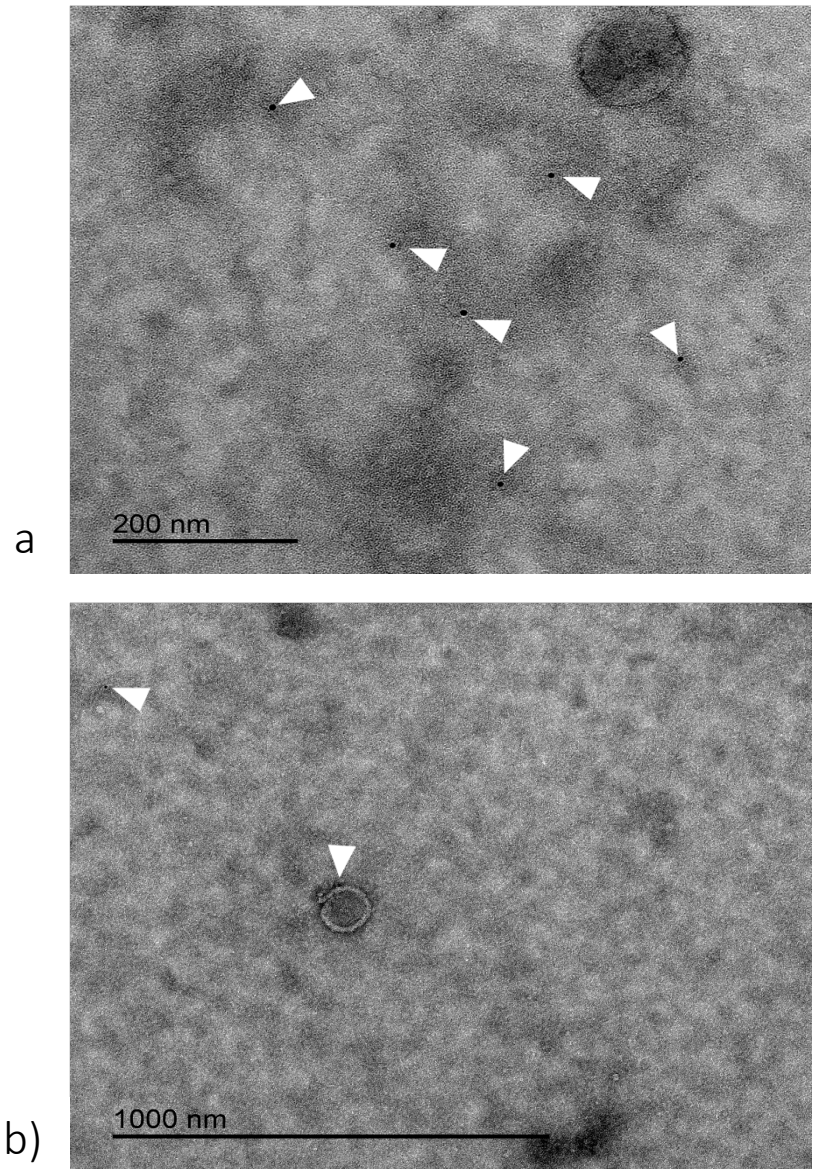

Figure 4.14. Nanogold TEM images of the HEK293T-derived exosomes. a) Second attempt labelling the HEK293T-derived exosome samples with anti-Cx-43 as a primary antibody (Catalogue number: sc-271837) in a 1:5 dilution. Nanogold particles (white arrowheads) can be seen unspecifically bound to the surface instead of the exosomes. b) Negative control consisting of the secondary antibody only (1:20) dilution. Scale bar = 1000 nm

Figure 4.14A shows multiple nanogold particles (white arrowheads) everywhere except around the exosomes; this was the same pattern that can be seen for the negative control in **Figure 4.14B.** Thus, labelling with Cx-43 antibodies failed in both attempts.

Detection of CONNEXIN-43 interaction sites in boar sperm samples co-incubated with HEK293T-exosomes by TIRFM

TIRFM was used to visualise the localisation of Cx-43 protein during the interaction between HEK293T-derived exosomes and boar sperm (**Figure 4.15**). In **Figure 4.15A**, the Cx-43 label (magenta) was mainly localised to the sperm head, but is also clearly evident as background on the slide. **Figure 4.15B** shows the negative control a similar pattern in which the secondary antibody has labelled the entire sperm head.

A) 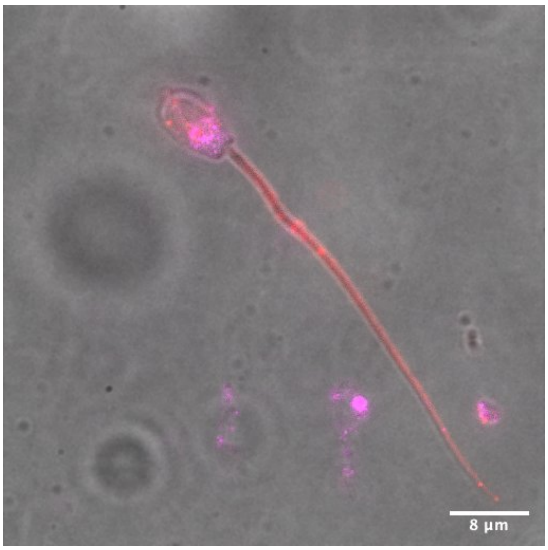

B) 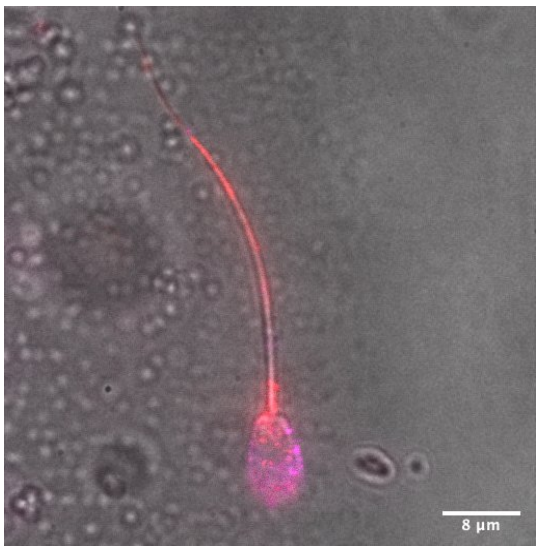

Figure 4.15. Image was taken with TIRFM displaying boar sperm samples co-incubated with HEK293T-derived exosomes for 5 hours. Post fixation, the samples were labelled with WGA-AlexaFluor647 (red) to stain the boar and the exosomal membranes, and specific Cx-43 labelling was carried out through incubation with anti-Cx-43 and anti-rabbit-AlexaFluor488 primary and secondary antibodies respectively to stain the localisation of this protein during the interaction between HEK293T-derived exosomes and the boar sperm (magenta). Scale bar = 8 µm.

Quantitative assay for exosome-sperm membrane fusion

A quantitative fluorometric assay for the real-time evaluation of membrane fusion events between HEK293T-derived exosomes and boar sperm was conducted by testing different incubation conditions (pH 5.0, 6.8 and 7.4) in either capacitating or non-capacitating media. Moreover, the presence and absence of BSA at pH 7.4 was also tested to evaluate the influence of this protein during the membrane fusion process. This was carried out by labelling the membranes of HEK293T-derived exosomes with a self-quenching dye (R18) that can emit a fluorescence signal upon its release from the membrane in which it is contained. These measurements took place throughout the incubation of the R18-EXO with the boar sperm every 10 minutes for a maximum of 2 hours. Unfortunately, this assay was not successful in any of the five optimisation attempts. The background signal was too high and the reaction that took place in the sample wells emitted a fluorescence signal that was too low for its detection. This was the case for all of the conditions tested.

4.6 Discussion

In the present chapter, a range of different fluorescence microscopy techniques were used to visualise the interaction between HEK293T-derived exosomes and boar sperm *in vitro*. This evaluation was then followed by a deeper investigation into the mechanisms involved. Collectively, these experiments provide a qualitative and quantitative assessment regarding the nature and efficiency of this process.

When studying EV uptake, it is essential to involve EV-cell interaction as proof-of-concept to encourage the further development of this tool for delivery purposes. In general, EV visualization is a challenging practice.

EVs with a diameter larger than the diffraction limit of light (~ 200 nm) can potentially be visualized by regular fluorescence microscopy and regular flow cytometry (Thery et al., 2018). However, for EVs smaller than this limit, such as exosomes, high-resolution techniques or bead-assisted multiplexed systems have to be used (Chen et al., 2016, Koliha et al., 2016, Suárez et al., 2017).

In this chapter, two fluorescence techniques were used to compare the visualisation of interactions between HEK293T-derived exosomes and boar sperm cells: HRCM and super-resolution microscopy. These have different technical advantages and limitations.

The most-straightforward and most accessible technique is Airyscan. This is a variation of high-resolution confocal microscopy and offers a 1.5-2 fold improvement of spatial resolution (down to 100–150 nm) when compared to conventional wide-field or laser scanning confocal microscopy. This technique was used to observe the interactions between exosomes and sperm, making it possible to visualise exosomes labelled with BODIPY as a fluorescent lipophilic dye bound to different regions of the sperm. Indeed, the images taken clearly showed BODIPY-labelled exosomes attached to all 3 portions of the sperm; the head, mid-piece and tail. Interestingly, the binding ratio was of up to 2 exosomes per sperm cell despite the low ratio of incubation (10 exosomes to 1 sperm) at 2 hours, thus suggesting a high affinity of the HEK293T-derived exosomes towards boar sperm. Nonetheless, these were visualised as large green dots (~ 500 nm). Hence, this technique is not suitable to discriminate between very bright vesicles with a diameter smaller than 200 nm and exosome clusters or small dim vesicles. Moreover, it was not possible to visualise exosome internalisation with this technique most probably due to a limit in sample depth penetration. Nonetheless, lipophilic dyes are not suitable for uptake experiments since it has been shown that they can form dye aggregates or micelles in aqueous solutions, thus increasing background effects.

This can also be misleading as these can leach off from the exosome membrane and relocate onto the cellular organelles (Tario et al., 2012; Mulcahy et al., 2014). For these reasons, super-resolution microscopy, a technique based on visualisation at the single-particle level under 100 nm, can provide a higher level of accuracy. To make best use of the TIRFM, samples have to be labelled with stochastic fluorophores that can switch between on and off states such as AlexaFluor dyes. Consecutive images were then taken with only a small portion of the fluorophores allowed to fluoresce, thus allowing the localisation of activated fluorophores at any given moment. This, combined with knowledge of the precise position of these fluorescing molecules, allows for the generation of an image that is no longer restricted by the limit of light diffraction (Rust et al., 2006; Heilemann et al., 2008). Indeed, the visualisation of exosome-sperm interaction was achieved at higher resolution with TIRFM, in which images showed WGA-labelled HEK293T-derived exosomes both attached and internalised into all sperm regions at all time points (10 min, 2 h, 4 h 30 min and 5 h).

Both exosome binding and internalisation were observed after only 10 minutes of incubation, thus confirming that exosome-sperm interaction is a rapid and effective process, as previously suggested in the HRCM experiment irrespective of the capacitating status of sperm, and as highlighted by a previous study (Zhou et al., 2019). This observation is also in line with the motility effects seen at this time point and reported in **Chapter 3.4.2** in that there was a spontaneous interaction. Interestingly, with this technique, I also demonstrated an interaction in all three regions of the sperm with a potential preference towards the tail and mid-piece. However, it is most probable that this effect was due to the larger surface area of the sperm tail compared to the head (Curry et al., 1996). In addition, the sperm flagellum beats with a higher frequency and larger amplitude and is, therefore, more prone to make contact with the exosomes on its path.

The number of positive sperm exhibiting at least one internalised HEK293T-derived exosome increased significantly with time of incubation; This was caused by a steady interaction rate. However, this quantification analysis should be taken with caution given the low sample size that was inevitable due to the technical limitations encountered (refer to **Appendix III**). Collectively, my observations of exosome-sperm interaction, both with HRCM and TIRFM, showed a pattern that seemed to contradict previous theories proposed previously by reproductive scientists in 1997; Carlini et al., (1997) and Arienti et al., (1997) showed for the first time, that seminal prostasomes fuse with human sperm cells under acidic conditions. Later on, Aalberts et al., (2013) observed that prostasome binding takes place under capacitating conditions, thus leading to the hypothesis that binding of seminal prostasomes to the sperm takes place under the capacitating conditions present in the seminal fluid and uterus (slightly alkaline and under the presence of HCO_3), which then subsequently fuse with the sperm membrane under the acidic conditions encountered in the vagina and at the site of oocyte fertilisation (Aalberts et al., 2014). Thus, in the first experiment carried out with HRCM at slightly acidic and non-capacitating conditions, I did not expect to see HEK293T-derived exosomes bound to the boar sperm. Moreover, in the experiment carried out with TIRFM, capacitating conditions and a pH of 7.4 should have only enhanced the internalisation of prostasomes or other seminal EVs already attached to the sperm, that had been carried over from the ejaculates, instead of prompting the binding and internalisation of the WGA-labelled HEK293T-derived exosomes that were only co-incubated with the boar sperm at such conditions. Nonetheless, more recent literature has reported the internalisation of prostasomes into mammalian sperm under capacitating conditions (Piehl et al., 2013; Zhou et al., 2019), while another study has even proven exosome internalisation by incubating sperm in extender media (pH 7.2) (Du et al., 2016).

Collectively, this evidence, along with my current results suggest that exosome-sperm interaction has a spontaneous nature that can take place irrespective of pH or the presence of capacitating agents (BSA and bicarbonate) in the incubation media. Furthermore, my exosome preparation was derived from HEK293T cells; Therefore, specificity towards mammalian sperm should not be expected, instead it is, more than reasonable to infer that HEK293T-derived exosomes interact with boar sperm in a spontaneous and stochastic manner, and that for therapeutic purposes we should consider loading cargo into the sperm nucleus via the functionalisation of exosomes.

The dSTORM pilot studies were carried out before the TIRFM experiment so as to ensure optimal sample visualisation. This technique has not been used previously to visualise the interaction of exosomes with boar sperm that are 50 times larger in size. Moreover, as explained further in **Appendix III**, in the TIRFM and dSTORM studies, only sperm cells that were lying flat on the slide during fixation could be imaged, hence reducing the number of sperm presenting with visible exosomes. Despite this technical handicap, it was possible to capture boar sperm with what appeared to be a single exosome going through the sperm tail via membrane fusion or any other internalisation mechanisms that necessitate of membrane contact. However, it was not possible to identify the specific entry mechanism followed by these vesicles from such images. It is also important to mention that the WGA-AlexaFluor647 labelling was carried out only after the fixation of the preparations. This may have stained all of the mammalian-based membranes present in these samples in a non-specific manner, hence including those EVs that may have been carried over from the seminal fluid. Nonetheless, prior to co-incubation with exosomes, the boar sperm samples were washed, pelleted and diluted in capacitating buffer.

An additional washing step is recommended by the manufacturer to help remove seminal fluid for its replacement with commercial extender, for this reason, the likelihood that the one vesicle captured with the dSTORM had been of seminal origin is very low, but rather there is a higher chance that this had indeed been one of the many HEK293T-derived exosomes that had been introduced in the boar sperm samples at a ratio of 100:1.

With regards to the molecular mechanisms in the sperm that may underline the uptake of exosomes, several studies appear to support endocytosis as the main pathway by which exogenous molecules gain entry into most of the mammalian cells (Mulcahy et al., 2014). However, sperm cells lack endocytic pathways and there is some evidence for membrane fusion as the preferred mechanism of interaction between seminal EVs and sperm (Aalberts et al., 2014; Zhou et al., 2019). Overall, there is very limited information of more active entry pathways, especially where the exosomes may be triggering these signals. Indeed, since exosomes lack protein-assembling machinery, scientists have been more inclined to investigate a process that may rather be governed by the sperm. However, when considering the proteins present within the exosomal membrane, these might play a more active role than expected; It has previously been discussed how tetraspanins (CD9, CD63 and CD81) enhance cellular invasion and fusion, it is also known that these can also mediate sperm-oocyte recognition. Indeed, the presence of these proteins at the exosomal surface may explain why exosomes derived from HEK293T cells interact with boar sperm in such an efficient manner. For this reason, a CD9 antibody was used to specifically label the exosomes present in the samples. Unfortunately, the images obtained showed non-specific labelling of the CD9 antibody. If this staining had been successful, it may have been possible to visualise specific interaction sites taking place via this mechanism at the sperm membrane. Moreover, as to facilitate visualization of exosomes, bead-based assisted visualization methods should be considered.

The gap junctional protein Cx-43 has also been suggested as a key mediator in EV internalisation (Soares et al., 2015). In an attempt to prove that this protein could enhance HEK293T-derived exosome/boar sperm interaction I assessed and encountered an enriched expression level for this protein in HEK293T-derived exosome lysates when compared to the HEK293T cell lysate, which has also been reported previously by Soares et al., (2015). In this article, the authors shed light on the importance of Cx-43-based hemichannels and gap junctions either at the exosomal membrane or both in the exosomal and the acceptor membrane respectively, for the transfer of exosomal cargo into the acceptor cell in a fast and effective manner. Indeed, this work demonstrated the involvement of Cx-43 in facilitating the transfer of luciferin and a plasmid in what appeared to be two different mechanisms by which this protein may be operating for each of them. Firstly, luciferin transfer was achieved at a higher level when mutant exosomes were constitutively expressing a Cx-43 isoform that has been described to form constitutively open channels (Soares et al., 2015). Moreover, these authors tested if exosomes lacking Cx-43 protein could transfer a GFP-encoding plasmid. It was then observed that plasmid transfer was indeed achieved at a much higher level when exosomes were expressing Cx-43. However, as discussed by the authors, the transfer of such a large molecule through this channels is unlikely. Consequently, the authors suggested that Cx-43 may indirectly mediate other pathways for the entry of molecules through the membrane. In my experiments, both attempts failed to further confirm and visualise the presence and localisation of Cx-43 in the exosomal membrane by TEM and TIRFM. This may have been due to a lack of accessibility of the primary antibody in labelling the epitope of the Cx-43 proteins. This is supported by the fact that Cx-43 loops into the middle and internal spaces of the exosomal membrane (Ponsaerts et al., 2010), thus, making it difficult for antibodies to conjugate with intact exosomes despite saponin treatment before the TEM nanogold evaluation.

If this assay was to be repeated, perhaps more stringent permeabilisation should be considered, either with saponin or triton. Moreover, WB revealed a different pattern to that seen in Soares' paper. Unlike theirs, my WB shows two different bands of different size and intensity. When looking into previous research, it appears that most enriched band in the HEK293T-derived exosome samples (with a size of 60 kDa) coincides with the mono or poly-ubiquitylated Cx-43 isoforms that have been reported previously (Leithe et al., 2009). This, of course, should be further confirmed by using a specific antibody for the detection of ubiquitylated proteins. Nonetheless, the ubiquitylation of Cx-43 is expected as this is merely a post-translational modification at the cellular level where these proteins were originated to signal their endocytic internalisation from the cell membrane into exosomal membranes (Sigismund et al., 2005, Girão et al., 2009).

The enrichment of Cx-43 in the HEK293T-derived exosome preparations previously linked with exosome uptake leads to hypothesise the active role of this transmembrane protein in the specific intercommunication between HEK293T-derived exosomes and any cell. Further studies will help elucidate the role of the exosomal proteins such as Cx-43 and CD9 in mediating HEK293T-derived exosome uptake by sperm, that most likely will vary with the source used for exosome isolation, and further quantitative analysis on the influence of particular incubation conditions upon the efficiency of such mechanisms may be useful for the optimisation of cargo delivery.

There might also have been fusion events taking place in our samples. Because the conditions at which these are enhanced are not clear, I decided to carry out a quantitative assay based on the real-time evaluation of the fusion kinetics between exosomes and boar sperm membranes by using a simple approach that has been used before in many other membranous systems. This strategy was based upon quantifying the fluorescence signal released by R18 upon the contact of both membranes and is therefore proportional to the number of membrane fusion events

taking place in the sample. It is worth discussing that each of the conditions tested was chosen because of a specific biological reason. The most obvious condition was capacitating condition at a pH of 7.4, since this represents the optimal environment for sperm to become capable of fertilising the oocyte, including enhancement of the acrosome reaction via the addition of P_4 to the incubation media.

The acrosome reaction is a process during which the membrane of the acrosome vesicle is fused with the plasma membrane of the sperm to release the enzymes that will digest the oocyte's ZP. This may also facilitate membrane fusion with the HEK293T-derived exosomes. Moreover, many existing publications describe a low pH as being a confounding factor for the enhancement of membrane fusion (Parolini et al., 2009, Schwarz et al., 2013, Tian et al., 2013). Therefore, more acidic pH conditions were also tested, including a pH of 6.8 to mimic the vagina milieu of the porcine model (Lorenzen et al., 2015) and a pH of 5.0 as a further acidic condition to investigate whether there is a proportional relationship between acidity and the level of membrane fusion.

A similar array of pH conditions were tested by Carlini et al., (1997), who showed higher levels of membrane fusion between prostasomes and human sperm taking place at a lower pH than at a pH above 7.0. It has to be emphasised that sperm do not survive at a pH lower than 6.0 (Makler et al., 1981), and thus this study is merely useful in an academic rather than a clinical context. Moreover, in light of the contradictory observations of a potential exosome binding at slightly acidic and non-capacitating conditions in the HRCM experiment, and both binding and exosome internalisation in slightly alkali and capacitating media from the TIRFM images, it was important to include both sets of incubation buffers. This study was also carried out to test the possibility that membrane fusion may be influenced by the higher membrane fluidity presented in capacitated sperm, mainly caused by the presence of BSA and bicarbonate (only present in the capacitating media).

In addition, a repeat of the 7.4 pH in capacitating conditions was also included with and without BSA. I did this given that this protein acts by sequestering the cholesterol molecules in the sperm membrane increasing its fluidity, and so to test if it would all the more influence as well the fluidity of the exosomal membrane which content is more enriched in cholesterol, thus resulting in a much higher fusion rate when BSA is present. Unfortunately, despite many attempts changing the conditions for this experiment (by increasing the exosome concentration 10 times) this assay did not show any results worthy of discussion. In all cases, the background signal was too high, and the signal emitted by the fusion reactions were too low to be measured by the ClarioStar. Further optimisations of this assay should include a range of exosome to sperm ratios including 100:1, 1000:1 and 10000:1 exosomes to sperm, as well as an increase in the concentration of both the sperm and the HEK293T exosomes in the samples. This may help to achieve a detectable signal.

If this assay would have been successful, I would have also measured sperm viability with the SYBR-14 probe, particularly for the acidic conditions. I would also have made a proteinase K treatment to degrade membrane proteins in the surface of the HEK293T-derived exosomes to assess the extent to which membrane-membrane interactions take place via protein interactions, as such a mechanism to enhance membrane fusion has been proposed by experts in the field (Carlini et al., 1997), also in line with the observations made so far. Either way, it is undeniable that an interaction between the HEK293T-derived exosomal vesicle and mammalian sperm takes place via a mechanism that is governed by the contact of both membranes. Therefore, a deeper study is of great importance, especially when considering future therapeutic approaches; the uptake mechanism may be heavily influenced by the source cell used for exosome isolation, and thus it is key to identify the array of exosomal proteins involved and a route of entry that can ensure a more efficient delivery of the payloads.

4.7 Key findings

- Super-resolution microscopy techniques were used for the first time to observe exosome interaction, at the single level, with mammalian sperm. This revealed that HEK293T-derived exosomes efficiently interact with boar sperm. Internalisation was proven in all of the sperm regions within 10 minutes of simple *in vitro* co-incubation.

  Internalisation increased significantly with time of incubation and followed a spontaneous pattern since there was no specificity towards a particular sperm region and occurred irrespective of the incubation conditions. Most of the HEK293T-derived exosomes were seen either attached or inside of the sperm tail due to its large surface area and active movement. Future work should aim to functionalize the HEK293T-derived exosomes so that they can target the sperm head, and also consider the generation of exosomes from prostate or epididymis cell lines as to compare if they can more efficiently target sperm.

- Clear membrane-membrane contact between a vesicle and a sperm was observed with dSTORM. This suggested that membrane fusion is the main mechanism involved in the uptake of HEK293T-derived exosomes by the sperm, which lack endocytic pathways.

CHAPTER 5

Functionalization of HEK293T-Derived Exosomes and Molecular Cargo Loading

5.1 Aim of this Chapter

This chapter aims to develop and test different approaches to load molecular cargo in the form of DNA and proteins into the HEK293T-derived exosomes, as well as to use a mammalian transfection method for the functionalisation of the HEK293T-derived exosomes with a cell penetrating peptide, to more efficiently target the sperm head as a way to increase cargo loading efficiency in this region of the sperm where the nucleus and other key molecules that mediate fertilization such as oocyte-sperm fusion are present.

5.2 Background

Exosomes are generally rich in metabolites, especially RNAs that they are able to transfer to recipient cells to regulate various physiological processes (Valadi et al., 2007). Therefore, their innate capability to deliver compounds with therapeutic implications makes exosomes highly suitable candidates for drug delivery.

Exosome-based treatments are being developed with exosomes in their native state, as they are secreted from their maternal cell. Indeed, this practice has been performed in most studies in the male fertility field, where native prostasomes isolated from seminal fluid have been used to enhance sperm functionality (Bechoua et al., 2011; Pons-Rejraji et al., 2011; Fernandez-Gago et al., 2013; Piehl et al., 2013; Mogielnicka-Brzozowska et al., 2015; Du et al., 2016). However, an increasing number of publications in other areas of medicine have opted for bioengineered exosomes to boost their therapeutic potential, either through the loading of bioactive cargo or by anchoring cell-targeting moieties into the exosomal surface.

Table 5.1 shows examples of publications where exosomes have been loaded with drugs for a clinical purpose such as cancer therapy.

Table 5.1. Examples where exosomes have been used to deliver drugs with a clinical purpose.

DRUG LOADED	THERAPEUTIC AIM	REFERENCE
AntagomiRs	To target viral and cellular microRNAs for the inhibition of cancer angiogenesis	(Wang et al., 2020)
Paclitaxel and Doxorubicin	To abolish tumor growth with chemotherapeutic agents in triple negative breast cancer	(Haney et al., 2020)
siRNA	To regulate expression of the *TPD52* gene in breast cancer cells	(Limoni et al., 2019)
TPP1	To treat a lysosomal storage disorder or Batten disease by the delivery of a lysosomal enzyme	(Haney et al., 2019)
miR-128-3p	To improve oxaliplatin response for colorectal cancer treatment	(Liu et al., 2019)
ADAM10	To promote angiogenesis in nasal polyps	(Zhang et al., 2018)
Iron oxide	Facilitate targeted tumour cell ablation via magnetically induced hyperthermia	(Altanerova et al., 2017)
siRNA	To target Huntington mRNA	(Didiot et al., 2016)
Catalase	To provide neuroprotective effects in Parkinson's disease	(Haney et al., 2015)
Porphyrins	To improve cellular uptake and induce a phototoxic effect in cancer cells	(Fuhrmann et al., 2015)
Curcumin	To help recover endothelial cell layer permeability in hyperhomocysteinemia	(Kalani et al., 2014)
miRNA	To deliver antitumor miRNA to breast cancer cells	(Ohno et al., 2013)
Heat shock proteins	To enhance natural killer antitumor response against hepatocellular carcinoma	(Lv et al., 2012)
Anti-inflammatory drugs	To induce apoptosis for the treatment of brain inflammatory-related diseases	(Zhuang et al., 2011)

In addition to developing anticancer therapies, exosomes are being explored for other therapeutic avenues. Recent developments include their application to deliver gene editing machinery (CRISPR/Cas9) to recipient cells to knock down specific genes (Lainscek et al., 2018; Li et al., 2019).

5.2.1 Drug Loading by Direct and Indirect Approaches

So far drug loading methods have been developed to ensure encapsulation efficiency of the desired cargo into the exosomes. Like with other nanoparticles, pharmaceuticals can be loaded into EVs by indirect or direct approaches (**Figure 5.1**).

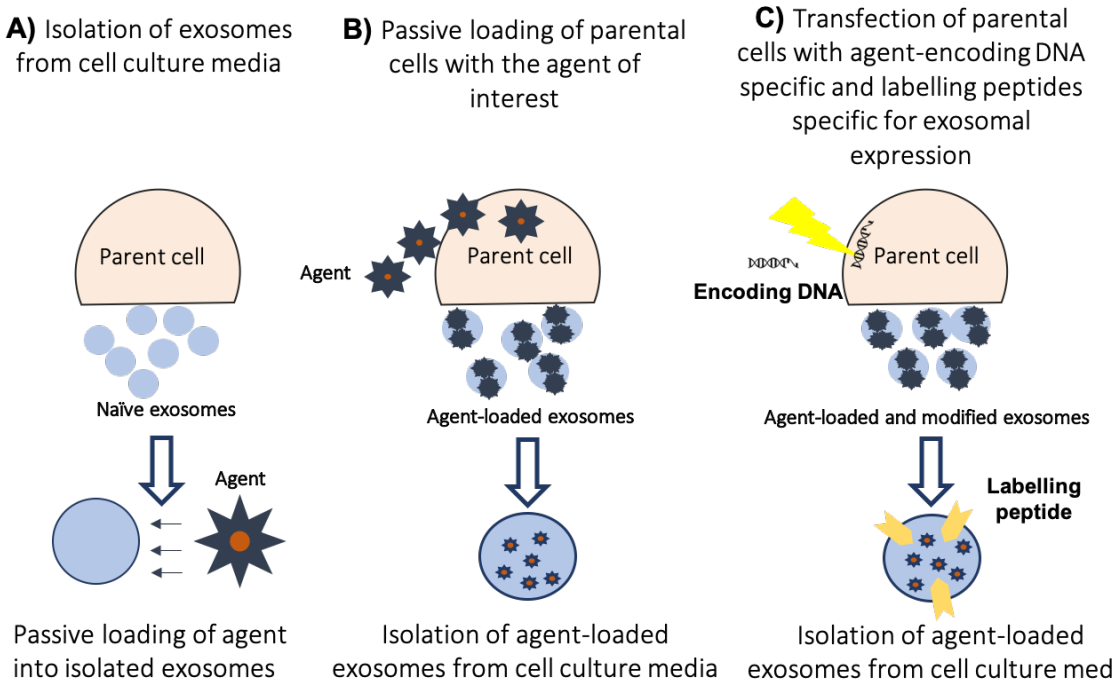

Figure 5.1. Diagram showing different loading approaches of the desired agent into exosomes. A) Direct loading approach. B) Indirect loading approach. C) Indirect loading approach using transfection mechanisms.

Direct approaches involve loading the agent *ex vitro* into the exosomes upon their isolation from the parental cells' culture media (**Figure 5.1.A**). This concept can be subdivided into techniques that are non-disruptive or disruptive to the exosome's integrity; an example of a non-disruptive alternative is incubation at room temperature (Sun et al., 2010).

More aggressive treatments are required to enhance the entry of larger molecules, including electroporation (used to load nucleic acids) (Alvarez-Erviti et al., 2011), sonication and permeabilization of the exosomal membrane with a detergent (Jamur and Oliver, 2010).

Haney and colleagues (2015) compared different techniques to load catalase, a large protein with a molecular weight of 240 kDa; the most effective methods were found to be permeabilization and sonication.

With regards to indirect methods, there are two options. The first involves the loading the loading of compounds into parental cells by following previously described techniques, in the hope that the molecules of interest will be also incorporated and released by the exosomes generated by these cells (Jang et al., 2013; Pascucci et al., 2014) (**Figure 5.1.B**). In one study, researchers carried out the loading of hydrophobic agents via synthetic-membrane fusogenic liposomes into parent cells (Lee et al., 2015). This approach has the advantage that it does not alter the exosome's physicochemical properties, yet it has the disadvantage of lower and less predictable yields since the parent cells may degrade or not release the total amount of cargo initially loaded. The alternative option to this indirect strategy is carried out via the transfection of parental cells using plasmids encoding the genetic sequence of interest followed by an expression sequence specific for the release of the molecules into the endocytical pathway that gives rise to exosomes (El-Andaloussi et al., 2012; Marcus and Leonard, 2013) (**Figure 5.1.C**). This method has the advantage that the constructs can be tailored to also include a cell-penetrating or targeting peptide in order to enhance a specific interaction with the cells or tissues of interest.

5.2.2. The Functionalisation of Exosomes by Mammalian Cell Transfection

The *in vivo* clearance of exosomes is very rapid following their administration, and therefore, work is ongoing to improve the efficiency of drug delivery into the cells of interest. A common way to achieve this is through exosome functionalisation by anchoring special molecules into their surface.

These surface modifications are intended to extend the biodistribution, stability, and pharmacokinetic profiles of the exosomes, thereby facilitating the proposed drug delivery. El-Andaloussi and colleagues (2012), were among the first to publish a protocol for the engineering of exosomes bearing the cell penetrating peptide (CPP) RVG for specific neurone targeting. The RVG peptide sequence contained in an expression plasmid was introduced into dendritic cells with a mammalian transfection protocol, where the peptide's sequence contained in the plasmid's backbone was fused with the exosomal membrane protein product of the gene lysosomal-associated membrane protein 2 (*Lamp2*), required for the incorporation of the RVG peptide onto the exosomal membrane during multivesicular body formation. In this way, the exosomes isolated from the dendritic cell's culture media featured the peptide on their external membrane surface. Moreover, these researchers loaded the engineered exosomes with synthetic siRNA using electroporation. Intravenously injected RVG-tagged exosomes efficiently delivered the siRNA specifically to the brain cells, resulting in the specific knockdown of *BACE1*, the therapeutic target in their mouse model of Alzheimer's disease. A similar approach has been developed to enhance molecule loading into mammalian sperm cells, since these cells possess an intrinsically complex membrane that represent a barrier to the influx of agents (Barlina et al., 2015a). In this sense, synthethic CPP's that have been tested as loading vectors for mammalian sperm can also be used to more efficiently aid the exosomes to deliver bioactive molecules across the sperm plasma membrane.

5.3 Hypothesis

In the previous chapter, the uptake of the HEK293T-derived exosomes by boar sperm was visualised with 10 minutes of co-incubation suggesting high affinity between both systems. Nonetheless, this spontaneous process was mostly taking place in the sperm tail due to its larger surface area and undulating movement. In the present chapter I looked at improving sperm-head targeting through the functionalisation of the HEK293T-derived exosomes with the cell penetrating peptide (C105Y). I hypothesised that an increased efficiency of payload delivery at the sperm nucleus, as the location that contains the proteins that are key to sperm capacitation, oocyte fusion, fertilisation process and as it will be passed on to the oocyte. In addition, different approaches will be used to load molecular cargo into the HEK293T-derived exosomes, as a proof-of-concept for future drug delivery to treat sperm abnormalities.

5.4 Materials and Methods

5.4.1 Transfection of HEK293T Cells with a pcDNA 3.1+/C-(K)- Lamp2a-DYK Plasmid Encoding a C105Y Peptide Sequence

Functionalisation of HEK293T-derived exosomes was carried out with CPP C105Y to enhance mammalian sperm targeting. I did this by transfecting HEK293T cells with a DNA expression plasmid containing the C105Y genetic sequence by adapting the protocol by El-Andaloussi et al. (2012). A pcDNA3.1+/C-(K)/ Lamp2a-DYK plasmid was purchased from GenScript (US) encoding two restriction sites for the insertion of the peptide sequence next to a *Lamp2a* sequence (**Figure 5.2**).

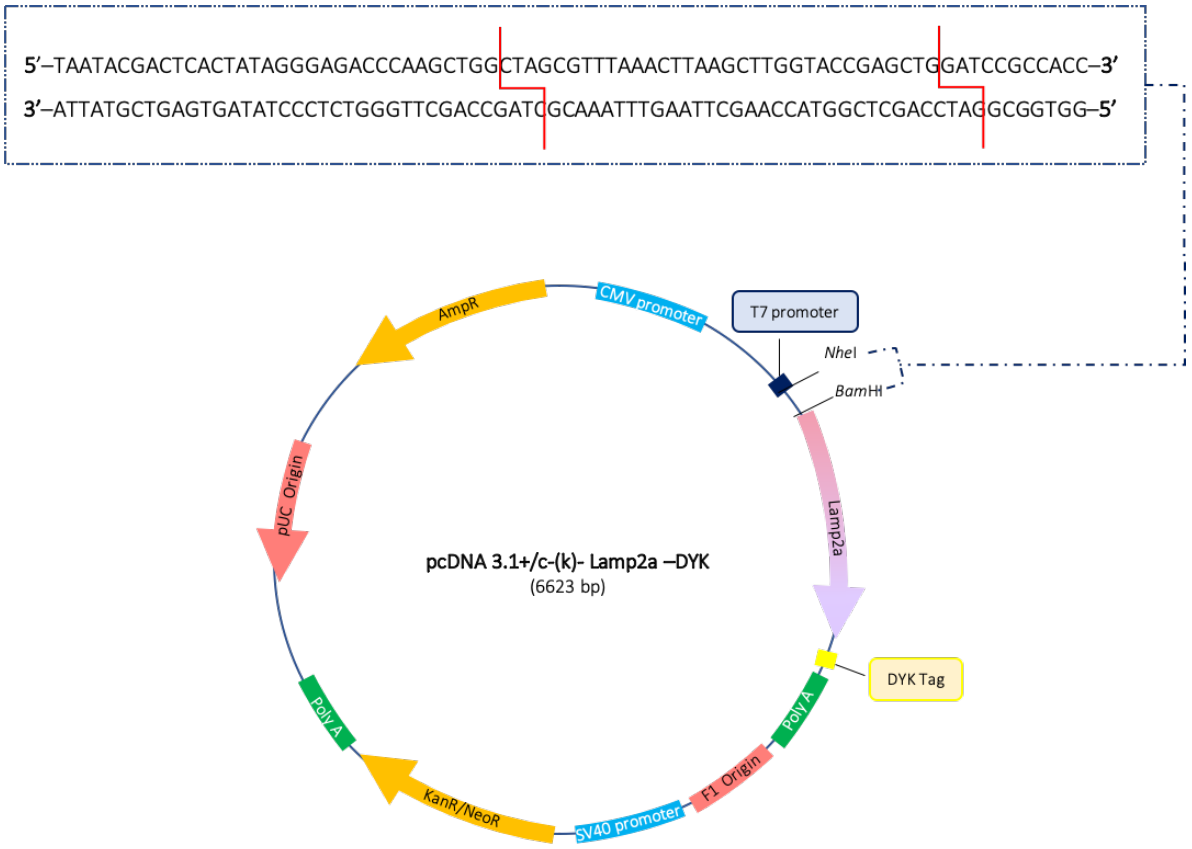

Figure 5.2. Map of the pcDNA 3.1+ plasmid (6623bp) containing a Lamp2a sequence followed by a DYK tag, and the restriction sites for *NheI* and *BamHI* enzymes flanked by the Kozak sequence and T7 promoter. The *Lamp2a* sequence is under the constitutive control of a cytomegalovirus (CMV) promotor. DYK tag represents the sequence motif that codes for an artificial antigen with high affinity for monoclonal antibody. The Kozak sequence is a consensus sequence involved in the initiation of mRNA translation. Neomycin resistance gene (NeoR) enables positive selection of transfected HEK293T cells. Ampicillin resistance gene (AmpR) enables positive selection of transformed *E.coli* bacteria colonies.

This allows the transcription of a Lamp2a-C105Y transmembrane protein that is expressed on the exosomal membrane surface (**Figure 5.3**).

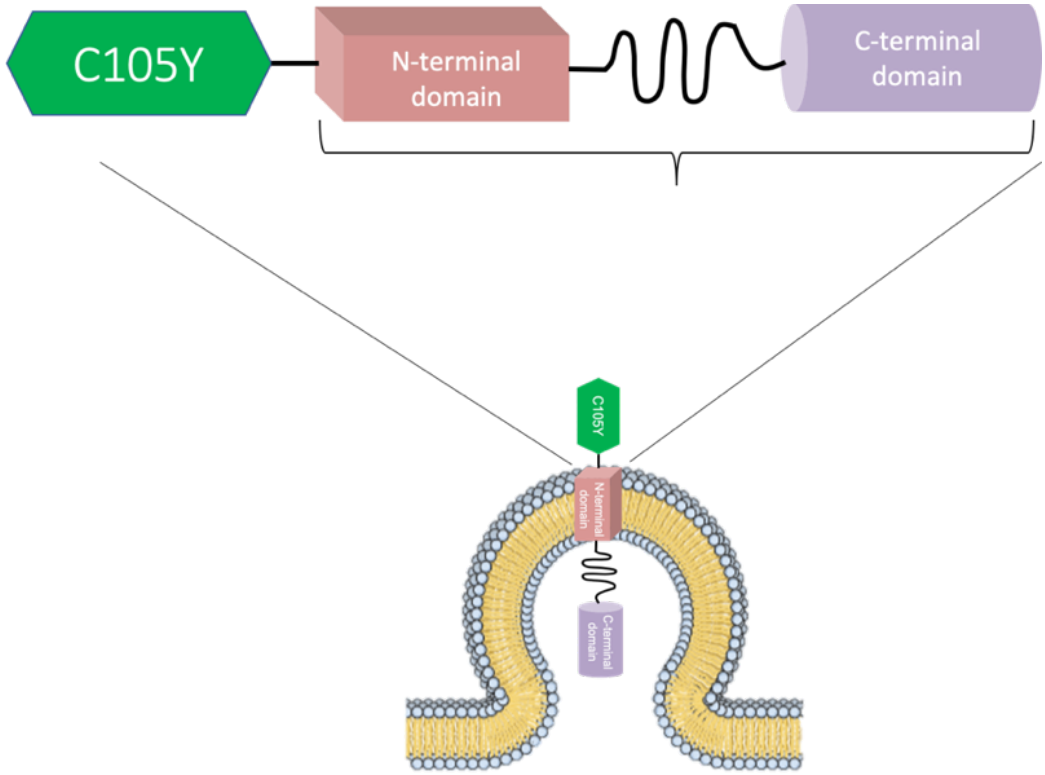

Figure 5.3. Diagram displaying the resulting recombinant protein; the C105Y peptide in the external surface of the membrane fused to the N-terminal domain of the *Lamp2a* protein transmembrane protein.

pcDNA 3.1+/C-(K)- Lamp2a-DYK plasmid amplification

The plasmid was amplified by transforming One ShotTM Top10 Chemically Competent *Escherichia coli* (Thermo Fisher Scientific, UK). Frozen bacteria were thawed briefly on ice, 5 µL of the ligation reaction mix was then introduced to the bacteria and mixed gently. The bacteria were further incubated in ice for 30 min. Plasmid uptake was enhanced by 30-second heat-shock at 42°C followed by 2 minute incubation in ice. Transformed bacteria were then mixed with 600 µL of Super Optimal Broth (SOC) medium (Thermo Fisher Scientific, UK) and were incubated at 37°C at 220 rpm for 1 hour. To positively select the transformed bacteria, the mixture was transferred to a Lysogeny Broth (LB) agar plate containing 100 mg/mL ampicillin (Sigma-Aldrich, United State) and cultured overnight at 37°C.

After the overnight incubation, colonies with well-defined boundaries were transferred to 14 mL tubes containing 100 mg/mL ampicillin LB broth (Sigma-Aldrich, US). The tubes were then cultured for a further 16 hours at 37°C at 220 rpm. Plasmid extraction was performed with the Plasmid Mini Kit (Qiagen, Germany) following the manufacturer's protocol. Plasmids were eluted in 30 µL of nuclease-free water and DNA concentration was measured by optical density at 260 nm in a spectrophotometer.

Annealing of C105Y primers

Complementary primers (forward and reverse) encoding the C105Y targeting peptide (**Table 5.2**) were supplied by Thermofisher scientific, UK. The complementary oligonucleotides were designed to produce an annealed construct with appropriate sticky ends that were complementary to the *Nhe*I and *Bam*HI restriction sites in the plasmid's backbone.

Table 5.2. C105Y amino acid composition and nucleotide sequence of forward and reverse primers

C105Y amino acid sequence	CSIPPEVKFNKPFVYLI
C105Y Forward primer	5'-TCGATGCAGCATCCCCCCCGAGGTGAAGTTCAACAAGCCCTTCGTGTACCTGATC-3'
C105Y Reverse primer	5'-ACGGTCGTAGGGGGGGCCTCTTCAAGTTGTTCGGGAAGCACATGGACTAGAGGCC-3'

Primer annealing was carried out with a reaction mix formula (**Table 5.3**) and the primer annealing program specified in **Table 5.4**.

Table 5.3. Primer annealing reaction mix

REAGENT	VOLUME	CONCENTRATION
T4 DNA ligase buffer	5 µL	1 ×
C105Y Forward primer	1 µL	2 µM
C105Y Reverse primer	1 µL	2 µM
T4 Polynucleotide Kinase	1 µL	400U
Nuclease-free water	42 µL	—

Table 5.4. Thermocycler programme for primer annealing

DENATURATION	95°C; 5 minutes
TOUCHDOWN ANNEALING	Temperature increasing rate; 0.5°C per 10 seconds

Plasmid digestion with restriction enzymes *Bam*HI and *Nhe*I

For the insertion of the C105Y primers into the pcDNA3.1^{+}/C-(K)- Lamp2a-DYK plasmid, the plasmid backbone was linearized by digesting the plasmid with *Bam*HI and *Nhe*I enzymes. The digestion reaction was carried out with a reaction mix (**Table 5.5**) that was incubated at 37°C for 2 hours. The digested vector was then purified using the QIAquick polymerase chain reaction (PCR) purification Kit (Qiagen, Netherlands).

Table 5.5. Plasmid digestion reaction mix

REAGENT	VOLUME	CONCENTRATION
NEBufferTM 1.1	2.5 µL	1×
*Bam*HI Enzyme (10,000U/mL)	2 µL	10U
*Nhe*I Enzyme (10,000U/mL)	2 µL	10U
Calf intestinal alkaline phosphatase (10,000U/mL)	1 µL	10U
Lamp2a pcDNA3.1+/C-(K)-DYK plasmid (325 ng/µL)	17.5 µL	5 µg
Nuclease-free water	5 µL	—

Gel electrophoresis

The products of the digestion were then separated on an electrophoresis gel to assess the efficiency of the digestion reaction. The digested plasmid, together with three negative controls (undigested, single-digested with *Bam*HI and single-digested with *Nhe*I plasmid) were run in parallel. This was performed with a 1.5% agarose gel (Promega, Spain) w/v in Tris/Acetate/EDTA (TAE) (Fisher Scientific, US) buffer solution. Ethidium bromide (Amresco, UK) was added to the agarose gel at a concentration of 1 µg/mL, thus allowing visualisation of DNA fragments under ultraviolet light with a GelDoc-IT TS imaging system (UVP, UK). The samples were mixed with 6x-orange DNA loading dye (Thermofisher scientific, UK). Gel electrophoresis was conducted at 110V for 60 minutes.

Plasmid ligation

Once digested, the plasmid's backbone ends were ligated with the C105Y annealed primers using a ligation reaction mix (**Table 5.6**) that was incubated at RT for 5 minutes. The ligation reaction was set up for 1:1 to 1:10 plasmid to insert ratios.

Table 5.6. Plasmid ligation reaction mix for 1:1 plasmid to insert ratio

REAGENT	VOLUME	CONCENTRATION
Digested pcDNA3.1+/C-(K)-Lamp2a-DYK plasmid (60 ng/µL)	1 µL	1 µg
C105Y annealed primers	0.5 µL	250 ng
T4 DNA ligase buffer (10×)	1 µL	1×
T4 DNA ligase (5U/µL)	1 µL	5U
Nuclease-free water	6.5 µL	—

pcDNA 3.1+/C-(K)-DYK- Lamp2a-C105Y plasmid amplification

Bacterial transformation with Top10 *E. coli* competent cells was carried out in the same way as described above, except that the transformation was carried out with 5 μL of the ligation reaction products. This was performed in order to amplify the plasmid pcDNA 3.1+/C-(K)-DYK- Lamp2a-C105Y containing the insert after the ligation.

Sequencing of the pcDNA 3.1+/C-(K)-DYK- Lamp2a-C105Y plasmid

The insertion of the C105Y sequence onto the pcDNA 3.1+/C-(K)- Lamp2a-DYK plasmid was confirmed by Sanger sequencing (Source Bioscience, UK). The product of the plasmid digestion was predicted with A Plasmid Editor (ApE) software. The insertion of the C105Y sequence into the plasmid was confirmed through sequence alignment with a template of the pcDNA 3.1+/C-(K)-Lamp2a-C105Y-DYK plasmid obtained with the clustalW-multiple alignment tool of the BioEdit software (version 7.0.5.3) (Ibis Therapeutics, California).

5.4.2 Loading of HEK293T-derived Exosomes with Exogenous DNA Cargo (mCherry Plasmid) via Electroporation

mCherry plasmid loading

As a way to test the efficiency of DNA loading, an exogenous gene for the mCherry protein not present in mammalian cells was used. More specifically a mammalian expression plasmid pHL-FcHis-mCherry of 5.4kb in size containing the mCherry protein sequence (437bp) was loaded onto the HEK293T-derived exosomes by following an electroporation approach adapted from Lamichhane *et al.* (2015). To load DNA cargo into exosomes, electroporation DNA reaction mix (**Table 5.7**) was prepared and subjected to two electric pulses at 400 V for 125 μS.

Table 5.7. Electroporation reaction mix formula

REAGENT	VOLUME/CONCENTRATION
HEK293T-derived exosomes	1 x 10^9 EV/mL
pHL-FcHis-mCherry plasmid	5 µg
Gene Pulse Electroporation buffer	Top up to 50 µL

To prevent nucleic acid aggregation 1 mM EDTA was added to the reaction mix that was then incubated at RT for 15 min. The reaction mix was then filtered through a Nanosep column with a 300KDa molecular weight cut-off (Pall Corporation, US) by centrifugation at 500×*g* for 5 min (three times). To remove unbound DNA, 100 µL of DNase I (50 U/µL) (Thermo Fisher Scientific, US) was added to the reaction mix followed by incubation for 20 minutes at 37°C. Then 20 mM of EDTA was added to the mix to inactivate DNase I,. The sample was then washed three times with 500 µL of 1×Tris/EDTA (TE) buffer by centrifugation at 500×*g* for 5 min. After the last centrifugation, the exosomes remaining on the filter membrane of the Nanosep device were suspended in 100 µL of PBS. To ascertain that no unincorporated DNA was carried forward into the final exosome suspension, the optical density (260 nm) of the final sample was determined using an Eppendorf bio-photometer. Only samples without unincorporated DNA were used in the subsequent experiments. To assess the loading efficiency of the plasmid into the exosomes in this step, half of the volume of loaded exosomes was lysed, and PCR followed by gel electrophoresis was performed on the resulting lysate as described below.

Exosome lysis and DNA extraction

DNA was extracted using a modified Qiagen miniprep kit (Qiagen, UK). The mCherry-plasmid-loaded exosome suspension was then mixed with 250 µL of P1 buffer, 250 µL of P2 buffer and incubated at room temperature for 5 minutes. Subsequently, 350 µL of N3 buffer was added and the mixture was then centrifuged at 17900×*g* at RT for 10 min.

The supernatant was added to a Qiaprep 2.0 spin column and centrifuged at 500×*g* for 5 min, followed by a washing step with 500 µL of PB buffer and another round of centrifugation. The column was subsequently washed with 750 µL of PE buffer followed by a third round of centrifugation before eluting the DNA with 30 µL of nuclease-free water. The optical density of the extracted DNA was used to estimate the concentration of incorporated mCherry-plasmid DNA.

Co-incubation of DNA-loaded exosomes with boar sperm *in vitro*

The remaining volume of mCherry-plasmid-loaded exosomes were co-incubated *in vitro* with boar sperm to evaluate DNA delivery. This was carried out for 2 hours and an exosome to sperm ratio of 100:1 (exosomes concentration $1x10^8$ EV/mL and sperm concentration of $1x10^6$ cell/mL), at two different incubation conditions; one at 17°C in the extender medium in a water bath, and the other at 38.5°C inside an incubator (5% CO_2) in non-capacitating buffer. In parallel, two untreated controls with the same amount of boar sperm were co-incubated in the same way for both conditions, resulting in a total of 4 negative controls.

Sperm lysis and DNA extraction

To prepare sperm samples for DNA extraction, spermatozoa were first pelleted by centrifuging at 14,000×*g* for 15 minutes; the unbound exosomes were then removed by one wash with 100 µL of PBS followed by 14,000×*g* centrifugation for 15 min. DNA samples were extracted from the sperm samples via the use of cell lysis buffer solution (4.24 M guanidine chloride; 10mM sodium chloride; 1% N-lauroylsarcosine; 150 mM dithiothreitol; 200 µg/mL proteinase K (Life Technologies, UK); all other reagents were sourced from Sigma-Aldrich, US), the sperm pellet was resuspended in 100 µL of cell lysis buffer and incubated at 57°C for 1 hour.

Extracted DNA was then precipitated by the addition of 200 µL of isopropanol, and resuspended with 14,000×*g* centrifugation for 10 min. The DNA was then purified with the addition of 100 µL 70% ethanol followed by 14,000×*g* centrifugation step for 10 min. The supernatant was removed, and the pellet was left to dry at RT. DNA samples were eluted in 20 µL of purified water. DNA concentration was determined by measuring the optical density at 260 nm.

PCR and gel electrophoresis

Purified DNA extracted from the treated sperm samples and the mCherry-loaded exosomes was amplified by PCR (**Table 5.8** and **Table 5.9**). A set of primers for the mCherry sequence was used as well as a set of primers for the amplification of swine leptin (a protein intrinsic in boar sperm) (**Table 5.10**). This was also performed for the DNA lysates obtained from the untreated sperm and mCherry plasmid to serve as a negative and a positive control, respectively.

Table 5.8. PCR master mix formula

REAGENT	VOLUME
High fidelity PCR master mix (Sigma Aldrich, UK)	25 µL
C105Y forward primer (50 nM/mL)	1 µL
C105Y reverse primer (50 nM/mL)	1 µL
Lamp2a pcDNA3.1+/C-(K)-DYK plasmid (325 ng/µL)	1 µL
Purified water	22 µL

Table 5.9. PCR thermocycler program

Initial denaturation	(94°C; 4 min)
Phase I amplification (10 cycles)	
DENATURATION	94°C; 10 secs
ANNEALING	68°C; 1 min 10 secs
ELONGATION	78°C; 2 min
Phase II amplification (10 cycles)	
DENATURATION	94°C; 15 secs
ANNEALING	68°C; 1 min 10 secs
ELONGATION	78°C; 2 min
Final Elongation	(78°C; 2 min)

Table 5.10. Nucleotide sequence of the mCherry and swine leptin sets of primers

mCherry primers	
mCherry F	5'-ACCGCCAAGCTGAAGGTGACCA-3'
mCherry R	5'-TGCACGGGCTTCTTGGCCTTGT-3'
Swine leptin primers	
Swine leptin F	5'-GACTGTCCCCTGAGCCAGGTAGTGT-3'
Swine leptin R	5'-ACAAAACAGCCTCCTTCCAGGA-3'

The presence of the mCherry and swine leptin sequences were then verified by a gel electrophoresis, as described in **Section 5.4.1**.

5.1.1 Loading of HEK293T-derived exosomes with protein cargo (recombinant mCherry) via saponification

Recombinant mCherry protein was purified from the pHL-FcHis-mCherry mammalian expression plasmid and loaded into HEK293T-derived exosomes via saponification treatment using an established protocol with modifications (Haney et al., 2015).

pHL-FcHis-mCherry plasmid amplification

Plasmid amplification was carried out in the same way as described in **Section 5.4.1**.

Expression of recombinant mCherry protein

HEK293T cells were cultured under standard conditions and seeded into 175 cm^3 tissue culture flasks at a confluency of 30–50%. Transfection with pHL-FcHis-mCherry was performed at 50–70% confluency using the jetPEI DNA transfection kit (Polyplus-transfection SA, France) according to the manufacturer's protocol. Cells were cultured in DMEM supplemented with 10% FBS, 1% v/v 5000U penicillin, 5mg/ml streptomycin, 2 mM L-glutamine and sodium pyruvate (all reagents sourced from Sigma-Aldrich, UK) for 24 hrs, after which the medium was changed to FBS-free medium Expi293.

Purification of recombinant mCherry protein and total protein determination

Culture media was collected on day six of culture, supplemented with phenylmethanesulfonylfluoride (PMSF) (Sigma-Aldrich, UK) and EDTA (Sigma-Aldrich, UK) to a final concentration of 1 mM, and centrifuged at 6,000×*g* for 30 min at 4°C. The supernatant was filtered through a 0.45 μm polyethersulfone membrane filter, and passed through a column containing Protein A Sepharose beads (GE Healthcare Lifesciences, UK) to bind the Fc-tag. The column was then washed with 20 column volumes of PBS, followed by 10 column volumes of TNED buffer (50 mM Tris (pH 8.0), 150 mM NaCl, 10 mM EDTA, and 1mM diothiothreitol; all reagents from Sigma-Aldrich, UK). The enzyme 3C protease was added in one column volume of TNED buffer and left to shake overnight to cleave the Fc-tag. Finally, protein was eluted with TNE buffer (50 mM Tris (pH 8.0), 150 mM NaCl, 10 mM EDTA) in four times, collected four fractions. Total protein content was determined with BCA for 20 μL of each of the fractions collected, and the fraction with the highest protein concentration was used. Protein lysates were stored at –80°C.

Qualitative analysis for mCherry protein purification with SDS-PAGE electrophoresis

The presence of the purified mCherry protein was verified by running 25 µL of the protein lysates collected from the affinity column with SDS-PAGE for protein separation. This was carried out by loading the protein lysates onto 4-12% NuPAGE Novex Bis-Tris minigel (Life Technologies, UK).

To achieve denaturing and reduced conditions, the protein lysate was mixed with an equal volume of 2×Laemmli loading buffer (Life Technologies, UK), and the mixture was denatured at 95°C for 5 minutes. The lysate was then loaded onto the gel that was run in NuPAGE MES SDS running buffer (Sigma Aldrich, Germany) at 160V for approximately 1 hour. After electrophoresis, the gel was placed in a plastic tray with Coomassie solution, and was left on a rocking table to stain the gel for 2-4 hours. After the staining step, the gel was washed several times with distilled water to remove excess stain. To verify column filtering, a small volume of non-filtered supernatant was also loaded onto the gel.

mCherry protein loading into HEK293T-derived exosomes and sample purification

Fraction 2 (with the highest mCherry protein content) was used for the loading of protein into the HEK293T-derived exosomes; The concentration of protein was determined by BCA. The appropriate volumes for each sample were adjusted for a final working protein:exosome ratio of 2:1; 1000 µg of protein was loaded into 500 µg of exosomes. The protein/exosome mixture was diluted in PBS containing 0.1% of saponin (Sigma Aldrich, Germany). The mixture was then left to incubate for 30 min on a shaker at RT. To remove excess protein, the protein-loaded exosomes were washed through an Exo-spin SEC (CELL guidance systems, UK) from which 20 fractions were collected by elution with 500 µL of PBS.

NTA and BCA assessment of SEC column fractions

Finally, for each of the fractions collected from the SEC column, exosome concentration and total protein content of the exosome lysates were assessed with NTA and BCA protein assay respectively.

5.2 Results

To enhance exosome/sperm-head targeting, the functionalisation of HEK293T-derived exosomes was carried out using a transfection protocol to engineer the production of exosomes from the transfected HEK293T cells to feature the CPP C105Y attached to the exosomal membrane. In addition, cargo loading into HEK293T-derived exosomes via direct approaches was attempted as a proof-of-concept for the use of these nanocarriers to deliver therapeutic cargo into mammalian sperm. Both DNA (in the form of an expression mammalian plasmid), and protein (in the form of a recombinant mCherry protein) were used as molecular cargo to be loaded into exosomes using different strategies. Finally, the DNA transfer from the DNA-loaded exosomes into the sperm was assessed by PCR and gel electrophoresis, whereas mCherry protein loading was only evaluated at the level of the HEK293T-derived exosomes with NTA and BCA total protein quantification.

5.2.1 Transfection of HEK293T cells with a pcDNA 3.1+/C-(K)- Lamp2a-DYK Plasmid Encoding the C105Y Peptide Sequence

Functionalisation of the HEK293T-derived exosomes was attempted through a routine transfection protocol.

Prior to transfection, the C105Y peptide was inserted into the mammalian expression plasmid pcDNA3.1+/C-(K)/Lamp2a-DYK with the aim of creating a *Lamp2a*-C105Y fusion transmembrane protein. This would ensure the attachment of the C105Y peptide onto the external surface of the exosomal membrane.

Plasmid digestion with restriction enzymes *BamHI* and *NheI*

Before the insertion of the C105Y insert onto the pcDNA3.1+/C-(K)/Lamp2a-DYK plasmid, a digestion step with *Bam*HI and *Nhe*I restriction enzymes was carried out. This was required to cut the plasmid's backbone in order to create a complimentary ligation site for the C105Y insert. To validate whether the digestion had been successful, the products of this reaction, together with three negative controls (consisting of undigested plasmid and two single-digestions of the plasmid with each of the enzymes) were examined in parallel by electrophoresis (**Figure 5.4**).

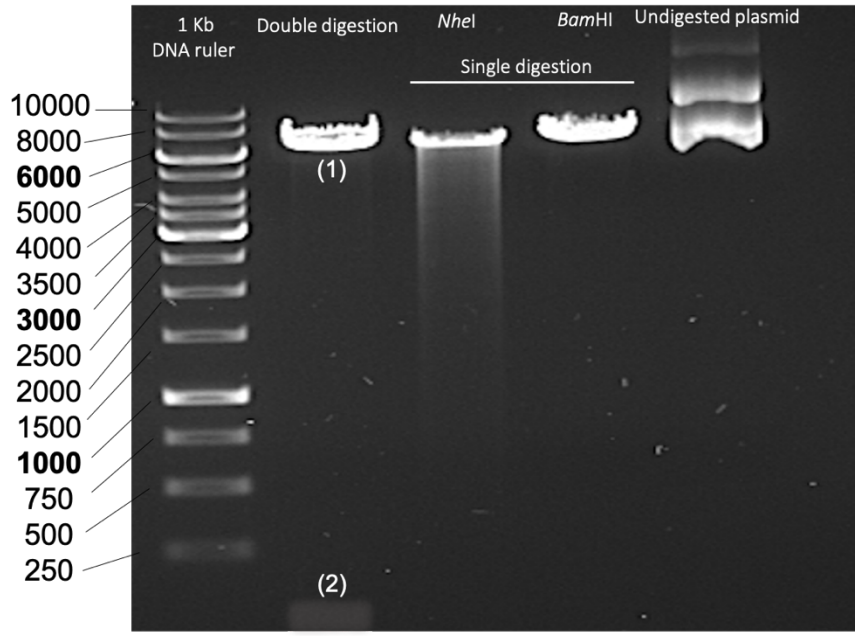

Figure 5.4. Agarose gel displaying the DNA digestion products ran with electrophoresis. From left to right; the 1Kb DNA ladder, undigested pcDNA 3.1+ plasmid and the products of single digestion with *Nhe*I and *Bam*HI enzymes. A faint DNA fragment (~34bp, marked by (2)) can be seen in the well for the double digestion that corresponds to the plasmid's backbone fragment that has been cut-off. All of the controls, including the undigested plasmid verify plasmid digestion for the *Bam*HI/*Nhe*I double digestion only. 1% Agarose gel, electrophoresis was run at 120V for 45 min.

As seen in **Figure 5.4**, the *Bam*HI/*Nhe*I double digestion produced two fragments; a larger one of approximately 6550bp (marked by (1)) and a smaller faint band of ~34bp (marked by (2)) that was not seen in any of the negative controls. Both *Nhe*I and *Bam*HI and single digestion lanes display the linearized plasmid. Finally, the lane corresponding to the undigested plasmid (serving as another negative control) showed a larger band at 6589 bp, with several fainter bands of larger size (<1Kb) that represented different configurations of the circular vector.

Plasmid sequencing

The plasmid sequencing results following plasmid ligation with the C105Y insert showed no alignment with the template pcDNA 3.1+/C-(K)-C105Y-Lamp2a sequence from positions 902 to 950, at the expected site of the C105Y insertion. Instead, the sequence showed perfect alignment with the template of the undigested pcDNA 3.1+/C-(K)-Lamp2a-DYK plasmid backbone due to the mutual absence of the C105Y sequence (**Figure 5.5)**.



Figure 5.5. Nucleotide sequence mapping displaying positions 836 and 1020 of the ligated pcDNA 3.1+ plasmid. The top strand sequence corresponds to the undigested pcDNA 3.1+ plasmid's backbone serving as a control template, the middle strand sequence corresponds to the expected template of the C105Y-Lamp2a pcDNA 3.1+ plasmid, and the third strand corresponds to the sequencing results. *: indicates nucleotide alignment. -: indicates absence of nucleotides.

5.2.2 Loading of HEK293T-derived Exosomes with DNA Cargo (mCherry Plasmid) via Electroporation

The mammalian plasmid pHL-FcHis-mCherry was used to investigate the efficiency of DNA loading into HEK293T-derived exosomes via electroporation, as well as the cargo delivery by the exosomes into the boar sperm. The presence of the genetic mCherry sequence was evaluated in the loaded HEK293T-derived exosomes and in the treated boar sperm by PCR followed by gel electrophoresis for both lysates. These lysates were simultaneously compared to a positive control for the presence of mCherry sequence; mCherry plasmid, and two negative controls consisting of untreated boar sperm DNA lysate incubated at both conditions (17°C and 37°C) as well as water. PCR was carried out for samples and controls with two sets of primers in different wells; for the specific amplification of the mCherry sequence (437bp), and for swine leptin (150bp) that is intrinsically present in boar sperm (**Figure 5.6**).

In **Figure 5.6.A** there was one band of 437 bp in one of the untreated sperm controls (untreated boar sperm at 17°C) as well as in **Figure 5.6.B,** in the lane with the untreated boar sperm at 37°C revealing amplicon contamination. Moreover, in **Figure 5.6.B**, the same band is present in the lane corresponding to the loaded-exosomes lysate; this matched the size of the mCherry sequence that was observed in the lane with the pHL-Sec-mCherry plasmid lysate used as a positive control. This gel also revealed three other larger bands at the top corresponding to the plasmid's different circular conformations (~ 5Kb), as well as an unexpected smaller band (~300 pb). Moreover, swine leptin bands (150 bp) expected in all those wells containing sperm DNA lysate that had been amplified with the swine leptin primers were missing (**Figure 5.6.A**). Finally, the smaller bands (<50 bp) present in all of the wells represent

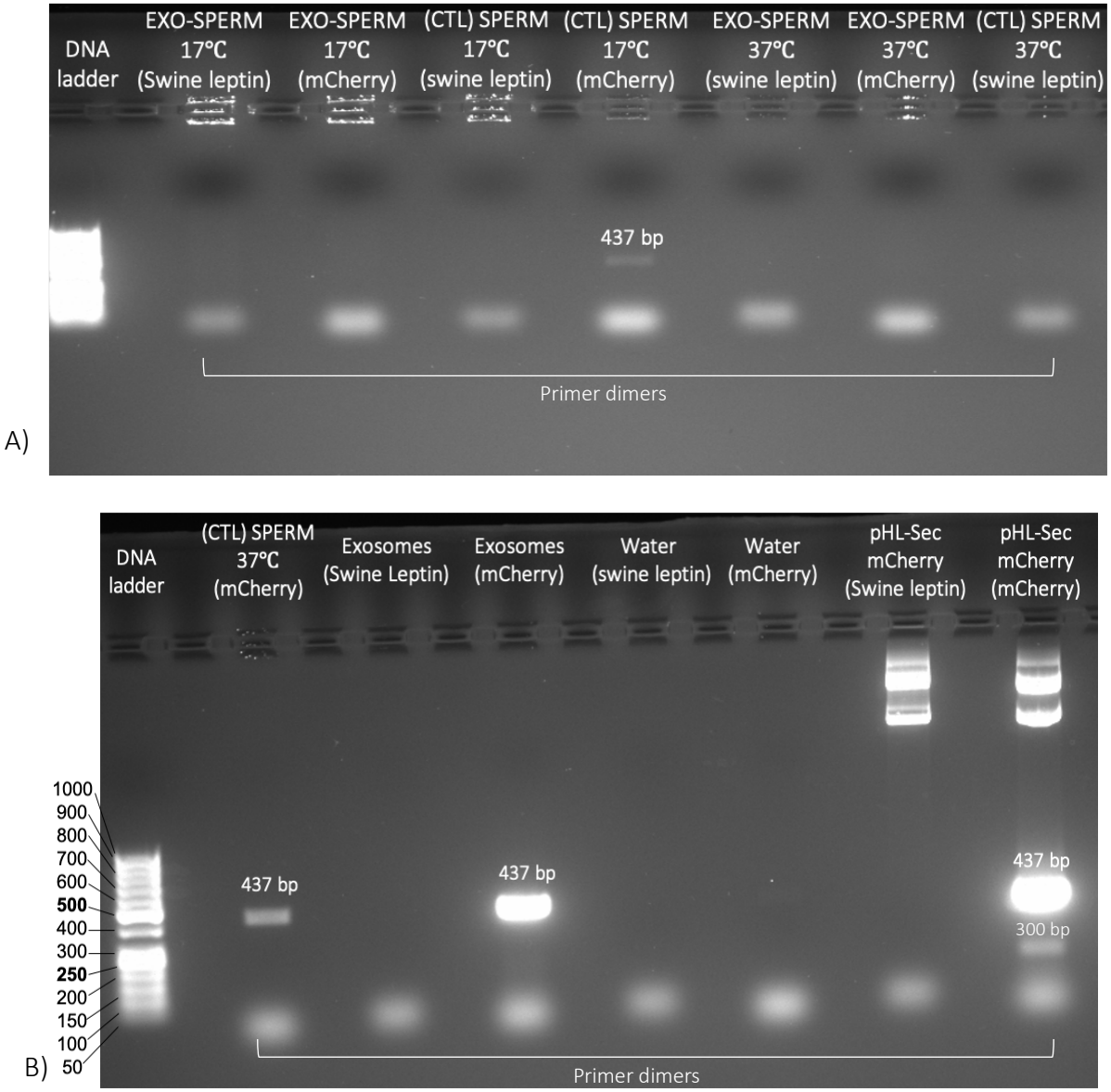

Figure 5.6. Electrophoresis gel displaying the DNA bands product of the PCR amplification. A) Gel 1 displaying all of the exosome-treated sperm samples as well as most of the untreated sperm controls. B) Gel 2 displaying the untreated sperm control (37°C) as well as the exosome lysates and the negative and positive controls with water and mCherry plasmid respectively. Each sample and control were assessed for mCherry amplification and swine leptin amplification, with mCherry and swine leptin primers.

5.2.3 Loading of HEK293T-derived Exosomes with Protein Cargo (Recombinant mCherry) via Saponification

Protein cargo loading of mCherry into HEK293T-derived exosomes was attempted using a mild saponification treatment (0.1%).

Qualitative analysis of mCherry protein purification by SDS-PAGE electrophoresis

The recombinant mCherry protein was expressed with a pHL-FcHis-mCherry mammalian expression plasmid. The purified protein via column filtering obtained from the culture of transfected HEK293T cells was then evaluated by SDS PAGE (**Figure 5.7**).

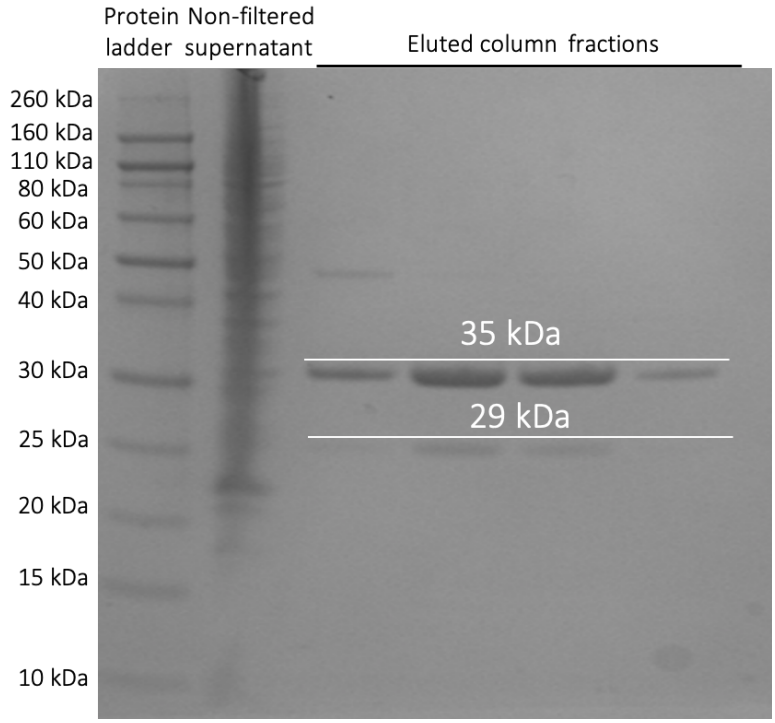

Figure 5.7. SDS-PAGE revealed different bands that represent the proteins collected in the unfiltered supernantant compared to the eluted fractions collected from the affinity column previously functionalised with Sepharose beads. A dense strip with multiple bands can be seen in the lane for the unfiltered supernantant, whereas very obvious 35 kDa and 29 kDa bands can be seen in the four lanes for the column fractions consisting of mCherry protein and Fc tag respectively.

A strong 35 kDa band can was evident in all four lanes of the eluted column fractions corresponding to the mCherry protein, as well as a fainter 29 kDa band corresponding to the Fc tag. The unfiltered supernatant lane shows all of the proteins present in the supernatant before filtering through the affinity column.

mCherry protein loading into HEK293T-derived exosomes and sample purification

From all the eluted fractions, fraction 2 presented the highest total protein content (1384 µg/mL) as determined by BCA assay. The total protein determination in all of the HEK293T-derived exosome samples was 2768 µg/mL.

NTA and BCA assessment of column fractions

Each of the 20 eluted column fractions were evaluate by NTA to determine exosome concentration, as well as with a BCA protein assay for total protein content (**Figure 5. 8**).

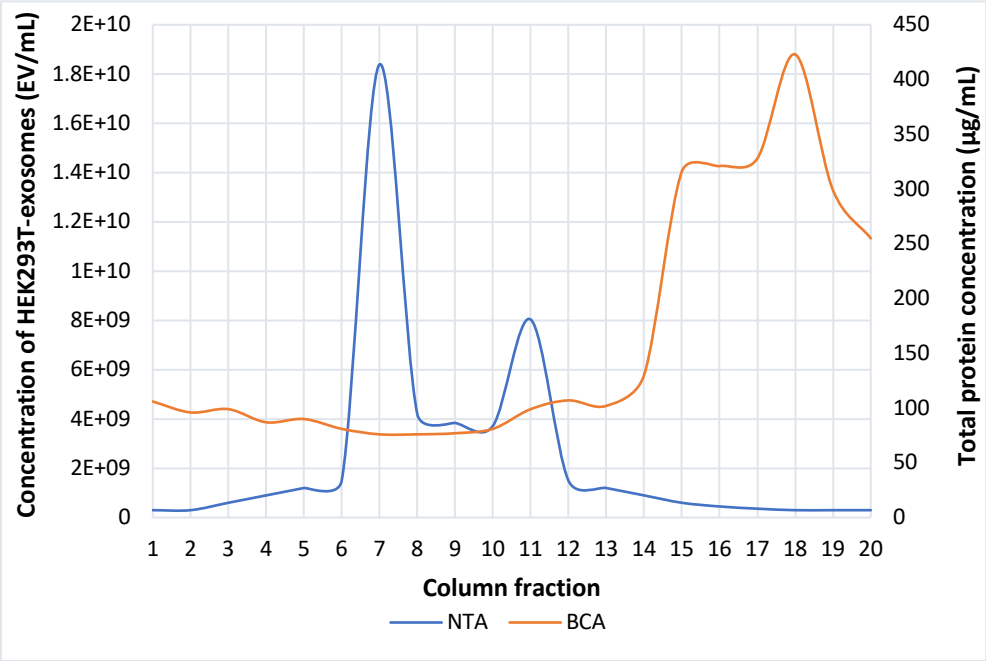

Figure 5.8. Graph showing exosome concentration determined by NTA (blue) and total protein concentration determined by BCA (orange) of the column fractions collected from SEC. The highest exosome concentration determined with NTA was for fraction 7 (1.8 x 10^{10}), whereas the highest total protein content was found in fraction 18 (420 µg/mL).

NTA evaluation revealed that the highest concentrations of HEK293T-derived exosomes were in fractions 6 to 8, whereas the highest levels of total protein concentration by BCA determination was found in fractions 15 to 20.

5.3 Discussion

In this chapter, I attempted to optimise the interaction between HEK293T-derived exosomes and the head portion of mammalian sperm. I did this via exosome functionalisation with a CPP C105Y. The sperm-targeted cell-penetrating peptide C105Y has a proven potential to increase the internalisation of nanomaterials into the sperm, without compromising the membrane integrity or functionality of the sperm (Jones et al., 2013; Barkalina et al., 2015a). Indeed, the synthesis of C105Y-engineered exosomes was driven by its reported ability to enhance the rate of interaction between silica nanoparticles and the sperm head.

Barkalina et al. (2015a) demonstrated that C105Y-functionalized mesoporous silica nanoparticles (MSNPs) exhibited an association efficacy with boar sperm that was 3-4 fold higher than that of non-modified MSNPs; no alterations were detected in any of the sperm parameters evaluated (motility and integrity of the acrosomal apical ridge).

Since HEK293T cells present with a high transfection and growth efficiency, I attempted to functionalise HEK293T-derived exosomes by following the protocol by El-Andaloussi and colleagues that describes an elegant approach through mammalian-cell transfection with a plasmid encoding the sequence of interest fused to *Lamp2a*, to obtain exosomes expressing the cell-targeting moiety (El-Andaloussi et al., 2012). However, prior to cell transfection, ligation of the insert into the pcDNA3.1+/C-(K)/DYK-Lamp2a plasmid was unsuccessful despite several attempts to modify plasmid-to-insert ratios.

The plasmid sequencing results consistently showed features of an undigested vector which could have been due to suboptimal restriction reaction. Sanger sequencing revealed the presence of the multiple cloning site segment that should have been replaced by C105Y. Gel electrophoresis of the digested vector also revealed a digested plasmid with a faint restriction fragment when compared to the linearized plasmid. This inefficient digestion could have been caused by the loss of enzyme activity due to salt inhibition when using spin columns to extract the plasmid DNA. Moreover, an insufficient amount of enzyme (only 4 units per 1µg of DNA) and possible contamination of the enzyme buffer, might have also compromised the plasmid digestion, or perhaps, a plasmid-to-insert ratio of 1:10 was too low, thus requiring a higher quantity of insert. In future attempts to functionalise the HEK293T-derived exosomes, a more simple approach, for example that used by Barkalina et al., (2015a) should be considered, with a C105Y-TMR fluorescent peptide (tetramethylrhodamine-CSIPPEVKFNKPFVYLI-CONH2). This peptide is directly attached to the exosome membrane via the cross-linking of amine groups in the membrane proteins following simple co-incubation. Moreover, while exosomes represent a modifiable tool, their loading capacity remains unknown. In theory, functionalisation should not alter exosome physiochemical properties, and thus allow maximum loading of the selected cargo. Nonetheless, once functionalised, cargo loading into the HEK293T-derived exosomes should be evaluated.

In this study, molecular loading into unmodified HEK293T-derived exosomes with DNA and recombinant mCherry protein was tested as a proof-of-concept for cargo loading and further drug delivery. DNA loading into HEK293T-derived exosomes was carried out by electroporation; loading efficiency, together with the transfer of the pHL-FcHis-mCherry plasmid into boar sperm, were then evaluated by PCR. Unfortunately, neither loading nor the transfer of the plasmid were successful.

First, no mCherry bands were observed in the treated sperm lysates, and even if such band was present in the HEK293T-derived exosome lysates instead, DNA loading into the HEK293T-derived exosomes could not be confirmed due to mCherry amplicon contamination revealed by the presence of this band in some of the negative controls. Moreover, the fact that there was no amplification of the swine leptin sequence in any of the sperm lysates brings to light a problem within the PCR process, that could be caused by insufficient sperm DNA. Therefore, in further optimisation of the PCR step, total DNA quantity should be increased as much as possible.

Protein loading on the other hand, was carried out with previously purified recombinant mCherry protein (34 kDa) with a mild saponification treatment (0.1%). Protein loading was assessed by quantifying total protein in the eluted column fraction lysates. This revealed very low levels of protein in the fractions containing the highest levels of HEK293T-derived exosomes, as determined by NTA. The highest protein content was detected in the later fractions, thus revealing inefficient loading of the mCherry protein. Nonetheless, a concentration of 1000 μg/mL of mCherry protein was incubated with the exosome samples, and the resulting total protein concentration measured was of 500 μg/mL and thus, such a decrease in the protein quantity in the column fractions collected most probably was due to the exosome filtering step through SEC that inevitably results in a significant loss of sample. Both electroporation and saponification techniques were carried out with a direct approach, where the cargo of interest was introduced into the isolated HEK293T-derived exosomes. Plasmid transfection to ensure the expression of the RNA or protein of interest should also be considered, as this offers advantages for loading efficiency and does not compromise the integrity of the exosomes (Lamichhane et al., 2015). Moreover, it is important to consider where the cargo is placed in the exosomes.

One option is intraluminal loading, where the cargo is deposited in suspension in the exosome's cytoplasm; this can be achieved with techniques like electroporation and saponification.

An alternative technique is the anchoring of the molecule to the exosomal membrane; as intended when fusing the cargo of interest to the *Lamp2a* fusion protein in a transfection plasmid. This can also be achieved without the need for cell transfection, by fusing the molecule to a CP05 peptide which has a very strong affinity towards the CD63 tetraspanin (Kooijmans et al., 2016). Nonetheless, any of these options should be chosen according to the most frequent cellular uptake pathway involved in the internalization of the exosomes. For instance, if exosome uptake takes place via membrane fusion suggested for boar sperm and HEK293T-derived exosomes (**Chapter 4**), then cargo loading into the exosomal membrane should be avoided, as this would lead to drug transfer into the recipient cell's plasma membrane (Tian et al., 2010). Moreover, in future studies, other simple approaches to boost exosome delivery to boost exosome delivery should be considered, such as adding a $CaCl_2$ into the culture media, as it has shown to increase the exosome delivery in a dose- and time-dependent manner without impacting cell viability (Kim *et al.,* 2019).

In terms of the nature of the cargo loaded, HEK293T-derived exosomes could also be used as vehicles for artificial drugs such as the gene editing machinery CRISPR/CAS9, to correct genetic mutations in the sperm. Indeed, gene editing of the paternal gene pool is of high interest nowadays, as it is more effectively can avoid mutations from being passed onto the descendant line, and there are less ethical and legal drawbacks than with embryo editing (Cwik, 2020). In a recent publication from De Jong and colleagues (2020), transfected HEK293T cells were used to produce exosomes containing the CAS9 protein as well as the sgRNA guide to target a genetic sequence in the recipient cell for its excision.

The most striking aspect of this publication, is that it developed, for the first time, a reporter system for the visual confirmation of RNA transfer, and therefore, can be used to specifically distinguish between the delivery of mRNA and the expressed protein product that is also present in the engineered exosomes.

Finally, when developing exosomes for drug delivery, descriptive studies need to be conducted, such as the *in vivo* tracking of the delivered cargo, the assessment of its molecular stability within the subcellular structures, and the evaluation of any changes in the cargo bioactivity, in order to validate this tool as an efficient therapeutic treatment (Salunkhe et al., 2020).

5.4 Key Findings

- Functionalisation of HEK293T-exosomes with C105Y to specifically enhance sperm-head targeting unfortunately was not achieved, but this should further be attempted either with indirect approaches such as mammalian-cell transfection or through the direct attachment of a cell-penetrating moiety onto the exosomal surface when aiming to increase the delivery efficiency of therapeutic drugs into the nuclei of sperm.

- Molecular cargo loading of DNA with an mCherry plasmid was more successful with electroporation than with saponification, yet an amplicon contamination in the negative controls could not fully demonstrate the loading of the exogenous plasmid into the HEK293T-derived exosomes.

Further loading of DNA, proteins or artificial drugs should be attempted either by using direct or indirect approaches, to test the efficacy of each technique, as well as their implications for cargo delivery, sub-localisation within the recipient sperm cell, and sustained bioactivity, and the delivered cargo should be quantified for C105Y-functionalised HEK293T-derived exosomes and compared with non-functionalised exosomes, as to verify that surface modification does not hamper exosome-sperm interaction and further transfer of the drugs of interest.

CHAPTER 6

Final Discussion and Future Perspectives

This thesis investigated the use of HEK293T-derived exosomes as a biocompatible and cell-friendly nanocarrier for the delivery of therapeutic compounds into mammalian sperm in the context of ART. The rationale behind this project was to develop a non-invasive alternative to conventional ART techniques, for the treatment of sperm-borne impairments responsible for infertility problems. This novel research tool could have numerous potential applications, spanning across the study of the fundaments of reproductive biology, for its clinical applicability in veterinary science, and future human fertility treatment. The foundations of this project were based upon the industrial scalability of this therapy and wide applicability in a variety of clinical scenarios. Some of these scenarios (depicted in **Figure 6.1**) include SMGT, the supplementation of molecular deficiencies in sperm, gene therapy to correct mutations in the parental line, the delivery of 'nourishing' compounds into *in vitro* tissue culture systems, the enhancement of oocyte-fertilisation, and also the administration of molecular inhibitors for contraceptive purposes. Therefore, the experiments described throughout this thesis essentially aimed to develop a safe, easy-to-produce, and versatile tool for the administration of bioactive molecules capable of traversing tissue barriers and the compact membrane of mammalian sperm to exert desirable effects.

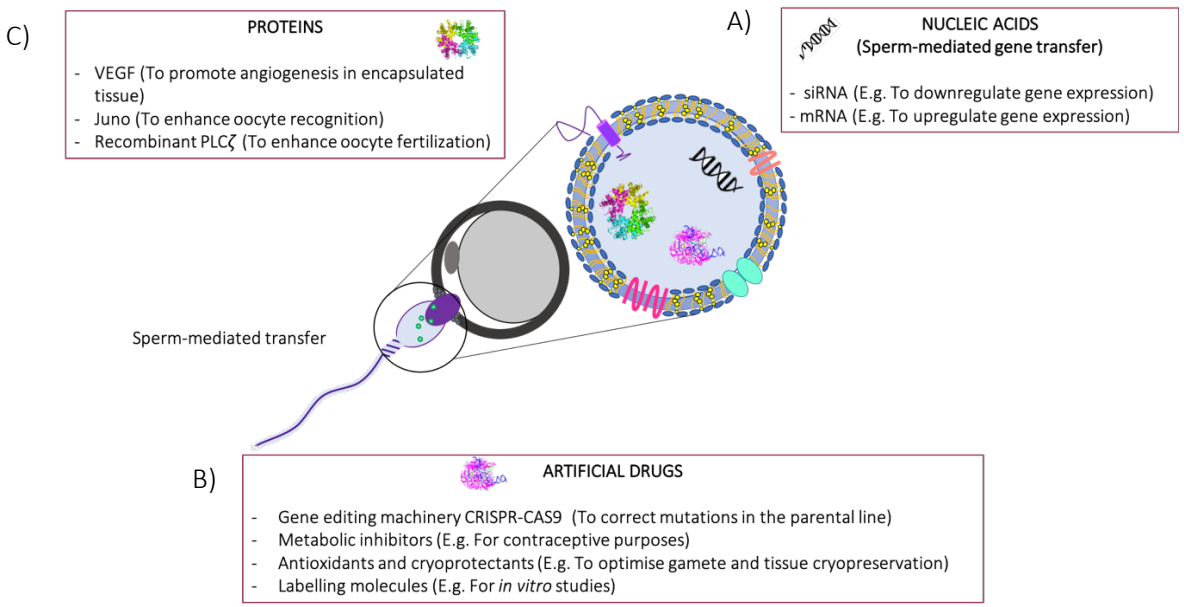

Figure 6.1. Potential clinical and research applications of exosomes as a delivery platform for reproductive purposes. A) Molecular cargo can be intended for sperm-mediated transfer, by transferring nucleic acids (e.g. siRNA) to regulate gene expression in the fertilised oocyte or future embryo. B) Artificial drugs such as CRISPR/CAS9 to correct mutations in the parental line and prevent them from being passed over to the future offspring, or labelling molecules to facilitate imaging of biological processes in *in vitro* studies. C) Proteins such as VEGF to promote angiogenesis in cultured tissue or recombinant proteins that are deficient in the infertile male such as PLCζ.

Exosomes have shown promising results in other fields of medicine, including the delivery of drugs across the blood-brain-barrier, thus rivalling engineered nanotools such as liposomes that have been developed for drug delivery for some time now, but with known side-effects.

The specific choice of exploiting the HEK293T cell line as the source for exosome production was driven by its safety profile in a clinical context (given their lack of carcinogenic and immunogenic effects) and its ease of manipulation that can ultimately allow scalability of production into the industrial setting.

HEK293T-derived exosomes have already been examined and developed for the treatment of multiple diseases, having proven their ease of production, versatile targeting ability and harmlessness for their *in vitro* application with living cells (Li et al., 2016; Rosas et al., 2016; Zhu et al., 2017).

Moreover, HEK293T-derived exosomes owe their popularity to the fact that they can be engineered to boost their compound delivery capabilities (e.g. via their functionalisation with targeting peptides), and therefore at a similar way as it is carried out for pharmaceuticals (such as encapsulated or pegylated drug delivery systems), and more importantly, this cell line allows the mass production of exosomes, and thus the implementation of industrial manufacturing like that for pharmaceuticals. Finally, HEK293T-derived exosomes exhibit loading and delivery abilities, including the possibility to transfer nucleic acids, artificial drugs and larger molecules such as recombinant proteins, into recipient cells. On this basis, I chose to isolate exosomes from HEK293T cells, for their development as nanocarriers with mammalian sperm *in vitro*.

In this thesis, I hypothesised that HEK293T-derived exosomes can provide an alternative to engineered nanotools and conventional ART, by offering a non-invasive and efficient approach for the delivery of therapeutic compounds into mammalian sperm. The overall aim of this thesis was to develop a mammalian-based system for the isolation of exosomes in a scalable manner, that allows versatile applicability for a wide spectrum of clinical scenarios and research applications. To fulfil this aim, HEK293T-derived exosomes were isolated and comprehensively characterised.

The short- and long-term effects of the *in vitro* co-incubation of HEK293T-derived exosomes upon boar sperm functionality including sperm motility, sperm viability, membrane fluidity and mitochondrial membrane potential were then evaluated by CASA and flow cytometry. Exosome-sperm interaction, including surface attachment and internalisation, was then confirmed visually by super-resolutive fluorescence microscopy techniques. Thereafter, qualitative and quantitative approaches were developed for the evaluation of HEK293T-derived exosome uptake, including an in-depth analysis of the molecular mechanisms involved. Finally, a proof-of-concept to enhance sperm-head targeting through functionalisation with a cell-penetrating peptide, as well as molecular cargo loading into the HEK293T-derived

exosomes was described. This study is the first of its kind to develop and investigate the capability of HEK293T-derived exosomes for cargo delivery into mammalian sperm and has led to novel data which may have an impact in the growing field of infertility.

6.1 Biocompatibility of HEK293T-derived Exosomes with Mammalian Sperm

In **Chapter 2**, the UC-based protocol used for the isolation of exosomes from HEK293T cells resulted in a heterogeneous population of EVs in terms of size and morphology, with up to three different vesicle categories that have not been previously described for HEK293T-derived samples. This data illustrates a higher complexity than expected. Nonetheless, this pool of vesicles mostly consisted of high concentrations of exosomes with a size ranging between 30 and 150 nm, and a rounded morphology. Further profiling of the HEK293T-derived exosome samples showed that they had preserved membrane integrity, and are particularly enriched in the cytosolic proteins Alix and Syntenin-1, as well as the transmembrane protein CD9 whose role has been linked with cell adhesion, tethering, and sperm-oocyte recognition. Therefore, the integrity of CD9, especially when it comes to the treatment of mammalian sperm is of special importance, as it may also positively influence the future reproductive outcomes of the sperm treated by these means. More to the point, very low levels of contamination with oncosomes and apoptotic bodies were detected, and thus, the presence of larger but harmless vesicles like microvesicles in these samples did not influence the choice of the HEK293T cell line, nor the isolation protocols used, but rather adds to the multiple traits that make HEK293T-derived exosomes desirable for their use with live sperm.

The safety of this tool with boar sperm was then assessed in **Chapter 3** through the evaluation of functional parameters that are informative of the sperm's capacity to undergo capacitation and acrosome reaction, and therefore, its metabolic competence to fertilise an oocyte. This chapter revealed that neither sperm motility (as assessed by CASA), nor sperm viability, membrane fluidity or mitochondrial membrane potential (as analysed by flow cytometry) were negatively influenced by short or long-term exposure with HEK293T-derived exosomes. Nonetheless, further studies have to be conducted to fully evaluate the safety profile of this therapeutic strategy, such as carrying out an *in vitro* fertilisation study to prove that the sperm treated by these means retain the ability to fertilise competent oocytes that can later give rise to a healthy embryo.

6.2 Optimization of HEK293T-derived Exosomes as Efficient Nanocarriers for Drug Delivery

In **Chapter 4** of this thesis, I visualized the internalisation of HEK293T-derived exosomes in the three portions of boar sperm within 10 minutes of co-incubation, reflecting a spontaneous affinity that was more profound at the sperm tail due to its larger surface area and undulating movement. Moreover, the interaction of nanoparticles with live cells is highly regulated by the electrostatic charge in both systems. Sperm cells have an overall negative surface charge that ranges between -10 and -30 mV (Magdanz et al., 2019), and therefore, electrostatic interactions with positively charged particles are favoured. Nonetheless, the net charge of the sperm membrane fluctuates constantly as metabolic changes take place throughout the maturation and capacitation processes. For instance, the acrosome reaction is accompanied by a reduction in negative charge to facilitate binding to the oocyte's zona pellucida.

In addition, in the study by Magdanz and colleagues (2019), they found particles with a negative charge bound to all three regions of the sperm. Furthermore, the electrostatic charge of the nanoparticles that were bound to the sperm were very similar to that of HEK293T-derived vesicles (around -12 mV) (Marazioti et al., 2019). Therefore, this might explain the affinity of the HEK293T-derived exosomes towards boar sperm, despite their negative zeta potential. Nonetheless, if we aim to target exosome-mediated drug administration onto the sperm head, where the relevant molecules and mechanisms involved in oocyte-fertilisation are harboured, a bioengineering strategy to improve sperm-head targeting by the HEK293T-derived exosomes is clearly required.

In **Chapter 5**, functionalisation of the HEK293T-derived exosomes was attempted by anchoring a positively charged CPP, C105Y, that has an already proven successful targeting ability towards the mammalian sperm head (Jones et al., 2013; Barkalina et al., 2015a). This functionalisation could either be carried out through mammalian cell transfection for higher yields of modified exosomes or with a spontaneous labelling method for the attachment of such moieties by chemical cross-linking (Barkalina et al., 2015a).

Chapter 5 also investigated cargo loading and potential delivery efficiencies by testing different techniques for DNA and recombinant proteins. The uptake mechanisms taking place for the HEK293T-derived exosomes by boar sperm will play a crucial role in delivery efficiency.

As suggested in **Chapter 4**, this interaction most likely happens via membrane fusion, yet, the involvement of accessory molecules that are present in these membranes, such as the gap-junctional protein CONNEXIN-43 as an auxiliary pathway for such a process cannot be excluded. We know that endocytic sorting machinery is required for endocytosis, and therefore, such a route cannot be expected in sperm cells.

Collectively, this data shed light onto intraluminal loading as the method with which cargo delivery into the sperm can be achieved at the highest level. Finally, to enhance cargo delivery, simple strategies, such as the addition of adjuvant reagents into the exosome mixture should be explored.

6.3 The Impact of HEK293T-derived Exosomes in Fertility and Other Clinical Applications

Exosomes derived from HEK293T cells offer a wide range of applications in terms of their purpose, that can range from developing a research platform for the study of reproductive processes to their clinical application as an alternative infertility treatment in embryos, gametes or their nursing tissues (such as Sertoli cells in the case of the male testicular tissues). But more interestingly, this versatile approach can be used with patients from a wide clinical spectrum. Indeed, this thesis provides the first evidence of a mammalian-based system based on a commercial cell line, that provides scalability options, also for manipulation and drug loading, and thus, an efficient source from which to develop an exosome-based treatment for patients difficult to manage such as those with cancer, for whom the administration of exogenously retrieved vesicles is the only safe option as to avoid the re-introduction of the disease. The present thesis developed and tested this non-invasive treatment for the targeting of mature sperm cells.

Male infertility accounts for up to 50% of the global infertility cases (HFEA, 2020), and most of the causes leading to male fertility problems stem from a molecular impairment at the sperm level.

Most of the aetiologies of male infertility remain underexamined, yet studies have found that up to 30% of male infertile problems have a genetic origin (Gunes et al., 2016), and in up to 30% – 80% of the cases, oxidative stress in the sperm is thought to be responsible for the problem (Agarwal et al., 2019, Kurkowska et al., 2020). Therefore, addressing these sperm-borne impairments could have a substantial impact on the prevalence of fertility in as much as half of the global population experiencing some sort of problem to conceive within the first 3 months of attempting (Dunson et al., 2014).

Currently, ART protocols that are used in the clinic to improve fertility outcomes are centred around the female aspect, leading to the misuse of techniques such as ICSI that are invasive for the manipulated gametes (Turner et al., 2020). For these reasons, the main concept for the application of a HEK293T-derived exosome treatment is to correct molecular aberrations in the mature sperm, either directly or indirectly by targeting spermatogonial stem cells in the seminal epithelium via oral or testicular-mediated administration (TMA) of HEK293T-derived exosomes carrying a drug of interest, such as antioxidants (Shateri et al., 2019). In this way, by administering the previously drug-loaded HEK293T-derived exosomes for the targeting of the sperm's precursor cells we can intended to correct and enhance sperm functionality more efficiently, and thus, provide the patient with competence to fertilise oocytes and give rise to healthy offspring following natural intercourse. Nonetheless, as already mentioned, this tool also has the potential to be used in female reproductive tissues, or with those *in vitro* cultured oocytes and embryos to also treat female-related infertility (Barkalina et al., 2015b).

6.4 General Limitations

This thesis describes a non-invasive system based on exosomes for compound delivery into mammalian sperm. However, even though this approach can serve as a proof-of-concept for the management of male infertility, further developments and considerations have to be undertaken to translate this technique from basic research into a clinical context.

The experiments described in this thesis were conducted *in vitro* by using the boar as an animal model. Therefore, this data cannot be extrapolated into the human, nor for a scenario *in vivo*, where the application of this technique might evoke an immune response. Indeed, we must remember that the boar model is not entirely representative of the human, particularly with regards to physiological response.

It is also important to lay out the considerations for deciding to use this tool to *in vivo* rather than *ex vitro*, since only in these means the germ cells are transcriptionally and translationally active, and so delivery of episomal DNA or mRNA is a plausible strategy. These, crucially, are able to *amplify* the response i.e. producing many transcripts from a single DNA template, and many protein molecules from a single transcript.

Moreover, the physicochemical properties relating to membrane fluidity, sperm size and morphology play a crucial role in binding and internalisation rates when developing a nanosized tool. The boar sperm-head is 2 to 3 times larger than that of the human. Such a difference in size entails that exosomes are approximately 40 times smaller relative to the human sperm head, and 120 times smaller when compared to the boar sperm head. Therefore, such a reduction in surface area ratios might be translated into lower exosome-sperm interaction rates. Nonetheless, it is also reasonable to believe that a lower quantity of cargo may be required to replenish a smaller sperm head, and hence, a lower number of exosomes might be required to treat human sperm.

With regards to membrane fluidity, boar sperm possess a more fluid membrane than human (Briz and Fabrega, 2013). Most likely this will enhance a higher exosome uptake for boar sperm, and therefore, may result in reduced internalisation and consequent cargo transfer from HEK293T-derived exosomes into human sperm.

Finally, it is important to consider also studying the influence that other intrinsic mechanisms present during natural conception may exert upon this treatment, such as the presence of male-derived and female-derive EVs that are also involved in the fertilization process.

The specific limitations associated with each set of experiments are discussed in detail in each of the experimental chapters.

6.5 Conclusion and Next Steps

With the increasing trend for infertility to cause a serious impact on global birth rates, both developed and non-developed countries have declared this condition of national interest and established policies that encourage research and development for new treatments. Despite the prevalence of male-related infertility problems that account for up to 50% of infertility cases, male infertility remains underexamined, where current fertility treatments and research are disproportionally skewed towards a female-related perspective. Therefore, there are only limited, or no options, for the successful diagnosis nor treatment of infertile men caused by a potentially treatable problem. I believe that the development of exosome-based delivery systems may provide us with a highly useful tool to develop new ways of studying sperm biology and provide us with new options for the diagnosis and treatment of male fertility.

The concluding remarks drawn from the results obtained in this thesis, and the future steps to be continued are:

1. The mass production of exosomes was achieved with the use of HEK293T cells. HEK293T-derived exosome samples were proven to be enriched with high concentrations of exosomes of high purity, while maintaining their functional integrity for cell adhesion. Thus, this scalable approach can be further developed for the industrial production of HEK293T-derived exosomes as molecular tools by culturing the HEK293T cells in bioreactors to obtain much larger yields of sample.

2. Long-term *in vitro* exposure of boar sperm with HEK293T-derived exosomes did not exert a detrimental impact upon the functionality of boar sperm under capacitating conditions, as per the analysis of sperm motility with CASA, and sperm viability, membrane fluidity and mitochondrial membrane potential via flow cytometry. Nonetheless, further studies should now investigate the extent to which the particular nature of EVs, whether derived from epithelial cell lines, such as HEK293T, or any other sources, has a specific impact upon the ability of sperm to capacitate and undergo AR. Furthermore, the effects upon sperm capacitation that are closely related with sperm motility, such as the phosphorylation of tyrosine residues in sperm tail proteins, and the capacity of treated sperm to fertilise an oocyte should be examined.

3. The visualization of boar sperm samples treated with HEK293T-derived exosomes under high resolution and super-resolution microscopy techniques revealed high affinity of the HEK293T-derived exosomes that binds to the sperm in a spontaneous manner with only 10 minutes of incubation, regardless of the conditions and incubation ratio. Moreover, further quantitative evaluation revealed a steady rate for internalization, as seen by the significantly increasing number of positive sperm cells with time of incubation.

In future experiments specific labelling of the HEK293T-derived exosomes via antibody conjugation for those membrane proteins exclusively present in these exosomes would be ideal, as to avoid overestimating exosome-sperm interaction by counting vesicles carried over from the seminal fluid, or other mammalian cell debris that can inevitably be stained with the WGA-based dyes.

4. It is likely that a protein-mediated pathway may be enhancing membrane fusion as the main uptake mechanism of the HEK293T-derived exosomes by the boar sperm that is absent of endocytic mechanisms, and therefore, further in-depth analysis may shed light onto the role of CONNEXIN-43 as part of the array of membrane proteins present in exosomes derived from HEK293T cells. Hence, efficiency of cargo transfer may greatly vary according to the source used for exosome isolation.

5. Finally, in future work, functionalization of HEK293T-derived exosomes with a cell penetrating peptide (C105Y) is desirable to enhance the targeting towards the sperm head, but also for the targeting of the sperm's precursor cells in the testicular tissue (especially important if administering this treatment orally), as well as to exogenously add chemicals to the culture media to boost exosome delivery to contribute to the delivery of the payload in a much more effective manner.

To summarize, exosomes derived from HEK293T cells can be thought for the non-invasive delivery of agents capable of treating male infertility when it is caused by a molecular impairment at the sperm level or at the level of its precursor cells, by avoiding the use of ART that are detrimental to the gametes.

References

AALBERTS, M., SOSTARIC, E., WUBBOLTS, R., WAUBEN, M. W., NOLTE-'T HOEN, E. N., GADELLA, B. M., STOUT, T. A. & STOORVOGEL, W. 2013. Spermatozoa Recruit Prostasomes in Response to Capacitation Induction. *Biochim Biophys Acta,* 1834**,** 2326-35.

AALBERTS, M., STOUT, T. A. & STOORVOGEL, W. 2014. Prostasomes: Extracellular Vesicles from the Prostate. *Reproduction,* 147**,** R1-14.

AALBERTS, M., VAN DISSEL-EMILIANI, F. M. F., VAN ADRICHEM, N. P. H., VAN WIJNEN, M., WAUBEN, M. H. M., STOUT, T. A. E. & STOORVOGEL, W. 2012. Identification of Distinct Populations of Prostasomes That Differentially Express Prostate Stem Cell Antigen, Annexin A1, and GLIPR2 in Humans1. *Biol Reprod,* 86.

AGARWAL, A., MULGUND, A., HAMADA, A. & CHYATTE, M. R. 2015. A Unique View on Male Infertility Around the Globe. *Reprod Biol Endocrinol,* 13**,** 37.

AGARWAL, A., PANNER SELVAM, M., ARAFA, M., OKADA, H., HOMA, S., KILLEEN, A., BALABAN, B., SALEH, R., ARMAGAN, A., ROYCHOUDHURY, S. & SIKKA, S. 2019. Multi-Center Evaluation of Oxidation-Reduction Potential by the MiOXSYS in Males with Abnormal Semen. *Asian J Androl,* 21**,** 565-569.

AGARWAL, A., SAID, T. M., BEDAIWY, M. A., BANERJEE, J. & ALVAREZ, J. G. 2006. Oxidative Stress in an Assisted Reproductive Techniques Setting. *Fertil Steril,* 86**,** 503-512.

AGRAWAL, A. K., AQIL, F., JEYABALAN, J., SPENCER, W. A., BECK, J., GACHUKI, B. W., ALHAKEEM, S. S., OBEN, K., MUNAGALA, R., BONDADA, S. & GUPTA, R. C. 2017. Milk-Derived Exosomes for Oral Delivery of Paclitaxel. *Nanomedicine,* 13**,** 1627-1636.

AITKEN, R. J., BRONSON, R., SMITH, T. B. & DE IULIIS, G. N. 2013. The Source and Significance of DNA Damage in Human Spermatozoa; a Commentary on Diagnostic Strategies and Straw Man Fallacies. *Mol Hum Reprod,* 19**,** 475-85.

AITKEN, R. J. & DE IULIIS, G. N. 2007. Origins and Consequences of DNA Damage in Male Germ Cells. *Reprod Biomed Online,* 14**,** 727-33.

AL-DOSSARY, A. A., BATHALA, P., CAPLAN, J. L. & MARTIN-DELEON, P. A. 2015. Oviductosome-Sperm Membrane Interaction in Cargo Delivery: Detection of Fusion and Underlying Molecular Players using Three-Dimensional Super-Resolution Structured Illumination Microscopy (SR-SIM). *J Biol Chem,* 290**,** 17710-23.

AL-DOSSARY, A. A., STREHLER, E. E. & MARTIN-DELEON, P. A. 2013. Expression and Secretion of Plasma Membrane Ca2+-ATPase 4a (PMCA4a) During Murine Estrus: Association with Oviductal Exosomes and Uptake in Sperm. *PLoS One,* 8**,** e80181.

ALBANESE, A., TANG, P. S. & CHAN, W. C. 2012. The Effect of Nanoparticle Size, Shape, and Surface Chemistry on Biological Systems. *Annu Rev Biomed Eng,* 14**,** 1-16.

ALTANEROVA, U., BABINCOVA, M., BABINEC, P., BENEJOVA, K., JAKUBECHOVA, J., ALTANEROVA, V., ZDURIENCIKOVA, M., REPISKA, V. & ALTANER, C. 2017. Human Mesenchymal Stem Cell-Derived Iron Oxide Exosomes Allow Targeted Ablation of Tumor Cells via Magnetic Hyperthermia. *Int J Nanomedicine,* 12**,** 7923-7936.

ALVAREZ-ERVITI, L., SEOW, Y., YIN, H., BETTS, C., LAKHAL, S. & WOOD, M. J. 2011. Delivery of siRNA to the Mouse Brain by Systemic Injection of Targeted Exosomes. *Nat Biotechnol,* 29**,** 341-5.

ANDALOUSSI., E. L., MAGER, I., BREAKEFIELD, X. O. & WOOD, M. J. 2013. Extracellular Vesicles: Biology and Emerging Therapeutic Opportunities. *Nat Rev Drug Discov,* 12**,** 347-57.

ANDREU, Z. & YÁÑEZ-MÓ, M. 2014. Tetraspanins in Extracellular Vesicle Formation and Function. *Front Immunol,* 5**,** 442-442.

ARIENTI, G., CARLINI, E. & PALMERINI, C. A. 1997. Fusion of Human Sperm to Prostasomes at Acidic pH. *J Memb Biol,* 155**,** 89-94.

ARMSTRONG, J. P. K., HOLME, M. N. & STEVENS, M. M. 2017. Re-Engineering Extracellular Vesicles as Smart Nanoscale Therapeutics. *ACS Nano,* 11**,** 69-83.

ARVIDSON, G., RONQUIST, G., WIKANDER, G. & ÖJTEG, A.-C. 1989. Human Prostasome Membranes Exhibit very High Cholesterol/Phospholipid Ratios Yielding high Molecular Ordering. *Biochim Biophys Acta (BBA) - Biomembranes,* 984**,** 167-173.

ARYANI, A. & DENECKE, B. 2016. Exosomes as a Nanodelivery System: a Key to the Future of Neuromedicine? *Mol Neurobiol,* 53**,** 818-834.

ASEA, A., JEAN-PIERRE, C., KAUR, P., RAO, P., LINHARES, I. M., SKUPSKI, D. & WITKIN, S. S. 2008. Heat Shock Protein-Containing Exosomes in Mid-Trimester Amniotic Fluids. *J Reprod Immunol,* 79**,** 12-7.

AYERS, L., PINK, R., CARTER, D. R. F. & NIEUWLAND, R. 2019. Clinical Requirements for Extracellular Vesicle Assays. *J Extracell Vesicles,* 8**,** 1593755.

BABAKHANZADEH, E., NAZARI, M., GHASEMIFAR, S. & KHODADADIAN, A. 2020. Some of the Factors Involved in Male Infertility: A Prospective Review. *Int J Gen Med,* 13**,** 29-41.

BÆK, R., SØNDERGAARD, E. K. L., VARMING, K. & JØRGENSEN, M. M. 2016. The Impact of Various Preanalytical Treatments on the Phenotype of Small Extracellular Vesicles in Blood Analyzed by Protein Microarray. *J Immunol Meth,* 438**,** 11-20.

BAHAT, A. & EISENBACH, M. 2006. Sperm Thermotaxis. *Mol Cell Endocrinol,* 252**,** 115-9.

BAIETTI, M. F., ZHANG, Z., MORTIER, E., MELCHIOR, A., DEGEEST, G., GEERAERTS, A., IVARSSON, Y., DEPOORTERE, F., COOMANS, C., VERMEIREN, E., ZIMMERMANN, P. & DAVID, G. 2012. Syndecan-Syntenin-ALIX Regulates the Biogenesis of Exosomes. *Nat Cell Biol,* 14**,** 677-85.

BALZAROTTI, F., EILERS, Y., GWOSCH, K. C., GYNNA, A. H., WESTPHAL, V., STEFANI, F. D., ELF, J. & HELL, S. W. 2017. Nanometer Resolution Imaging and Tracking of Fluorescent Molecules with Minimal Photon Fluxes. *Science,* 355**,** 606-612.

BARKALINA, N., JONES, C. & COWARD, K. 2016. Nanomedicine and Mammalian Sperm: Lessons from the Porcine Model. *Theriogenology,* 85**,** 74-82.

BARKALINA, N., JONES, C., KASHIR, J., COOTE, S., HUANG, X., MORRISON, R., TOWNLEY, H. & COWARD, K. 2013. Effects Of Mesoporous Silica Nanoparticles Upon The Function Of Mammalian Sperm In Vitro. *Nanomed: Nanotechnol, Biol, and Med,* 10**,** 859-70.

BARKALINA, N., JONES, C., TOWNLEY, H. & COWARD, K. 2015a. Functionalization of Mesoporous Silica Nanoparticles with a Cell-Penetrating Peptide to Target Mammalian Sperm In Vitro. *Nanomedicine (Lond),* 10**,** 1539-53.

BARKALINA, N., JONES, C., WOOD, M. J. A. & COWARD, K. 2015b. Extracellular Vesicle-Mediated Delivery of Molecular Compounds into Gametes and Embryos: Learning from Nature. *Human Reprod Update,* 21**,** 627-639.

BATISTA, B. S., ENG, W. S., PILOBELLO, K. T., HENDRICKS-MUÑOZ, K. D. & MAHAL, L. K. 2011. Identification of a Conserved Glycan Signature for Microvesicles. *J Proteome Research,* 10**,** 4624-4633.

BECHOUA, S., RIEU, I., SION, B. & GRIZARD, G. 2011. Prostasomes as Potential Modulators of Tyrosine Phosphorylation in Human Spermatozoa. *Systems Biol Reprod Med,* 57**,** 139-148.

BERNARD, V., KIM, D. U., SAN LUCAS, F. A., CASTILLO, J., ALLENSON, K., MULU, F. C., STEPHENS, B. M., HUANG, J., SEMAAN, A., GUERRERO, P. A., KAMYABI, N., ZHAO, J., HURD, M. W., KOAY, E. J., TANIGUCHI, C. M., HERMAN, J. M., JAVLE, M., WOLFF, R., KATZ, M., VARADHACHARY, G., MAITRA, A. & ALVAREZ, H. A. 2019. Circulating Nucleic Acids Are Associated With Outcomes of Patients With Pancreatic Cancer. *Gastroenterology,* 156**,** 108-118 e4.

BESSE, B., CHARRIER, M., LAPIERRE, V., DANSIN, E., LANTZ, O., PLANCHARD, D., LE CHEVALIER, T., LIVARTOSKI, A., BARLESI, F., LAPLANCHE, A., PLOIX, S., VIMOND, N., PEGUILLET, I., THÉRY, C., LACROIX, L., ZOERNIG, I., DHODAPKAR, K., DHODAPKAR, M., VIAUD, S., SORIA, J.-C., REINERS, K. S., POGGE VON STRANDMANN, E., VÉLY, F., RUSAKIEWICZ, S., EGGERMONT, A., PITT, J. M., ZITVOGEL, L. & CHAPUT, N. 2015. Dendritic Cell-Derived Exosomes as Maintenance Immunotherapy after First Line Chemotherapy in NSCLC. *Oncoimmunology,* 5**,** e1071008-e1071008.

BHASIN, S. 2007. Approach to the Infertile Man. *J Clin Endocrinol Metab,* 92**,** 1995-2004.

BHATTACHARYA, S., HAMILTON, M. P., SHAABAN, M., KHALAF, Y., SEDDLER, M., GHOBARA, T., BRAUDE, P., KENNEDY, R., RUTHERFORD, A., HARTSHORNE, G. & TEMPLETON, A. 2001. Conventional In-Vitro Fertilisation Versus Intracytoplasmic Sperm Injection for the Treatment of Non-Male-Factor Infertility: a Randomised Controlled Trial. *Lancet,* 357**,** 2075-9.

BLAKE, M., GARRISI, J., TOMKIN, G. & COHEN, J. 2000. Sperm Deposition site During ICSI Affects Fertilization and Development. *Fertil Steril,* 73**,** 31-7.

BOBRIE, A., COLOMBO, M., RAPOSO, G. & THERY, C. 2011. Exosome Secretion: Molecular Mechanisms and Roles in Immune Responses. *Traffic,* 12**,** 1659-68.

BONDE, J. P., FLACHS, E. M., RIMBORG, S., GLAZER, C. H., GIWERCMAN, A., RAMLAU-HANSEN, C. H., HOUGAARD, K. S., HOYER, B. B., HAERVIG, K. K., PETERSEN, S. B., RYLANDER, L., SPECHT, I. O., TOFT, G. & BRAUNER, E. V. 2016. The Epidemiologic Evidence Linking Prenatal and Postnatal Exposure to Endocrine Disrupting Chemicals with Male Reproductive Disorders: a Systematic Review and Meta-Analysis. *Hum Reprod Update,* 23**,** 104-125.

BONET, S., CASAS, I., HOLT, W. V. & YESTE, M. 2013. Boar Reproduction. *Springer*.

BONET, S., DELGADO-BERMÚDEZ, A., YESTE, M. & PINART, E. 2018. Study of Boar Sperm Interaction with Escherichia Coli and Clostridium Perfringens in Refrigerated Semen. *Anim Reprod Sci,* 197**,** 134-144.

BORYSHPOLETS, S., PEREZ-CEREZALES, S. & EISENBACH, M. 2015. Behavioral Mechanism of Human Sperm in Thermotaxis: A Role for Hyperactivation. *Hum Reprod,* 30**,** 884-92.

BOULET, S. L., MEHTA, A., KISSIN, D. M., WARNER, L., KAWWASS, J. F. & JAMIESON, D. J. 2015. Trends in use of and Reproductive Outcomes Associated with Intracytoplasmic Sperm Injection. *JAMA,* 313**,** 255-263.

BOURGAIN, C., NAGY, Z., ZUTTER, H., VAN RANST, H., NOGUEIRA, D. & VAN STEIRTEGHEM, A. 1998. Ultrastructure of Gametes after Intracytoplasmic Sperm Injection. *Hum Reprod (Oxford, England),* 13 Suppl 1**,** 107-16.

BOYERS, S. P., DAVIS, R. O. & KATZ, D. F. 1989. Automated Semen Analysis, *Year Book Medical Publishers.*

BÖING, A. N., VAN DER POL, E., GROOTEMAAT, A. E., COUMANS, F. A. W., STURK, A. & NIEUWLAND, R. 2014. Single-Step Isolation of Extracellular Vesicles by Size-Exclusion Chromatography. *J Extracell Vesicles,* 3**,** 23430.

BRAUDE, P., BOLTON, V. & MOORE, S. 1988. Human Gene Expression First Occurs between the Four- and Eight-Cell stages of Preimplantation Development. *Nature,* 332**,** 459-61.

BRAUNDMEIER, A. G., DAYGER, C. A., MEHROTRA, P., BELTON, R. J., JR. & NOWAK, R. A. 2012. EMMPRIN is Secreted by Human Uterine Epithelial Cells in Microvesicles and Stimulates Metalloproteinase Production by Human Uterine Fibroblast Cells. *Reprod Sci (Thousand Oaks, Calif.),* 19**,** 1292-1301.

BREITBART, H. 2002. Intracellular Calcium Regulation in Sperm Capacitation and Acrosomal Reaction. *Mol Cell Endocrinol,* 187**,** 139-44.

BRINK, P. R., VALIUNAS, V., GORDON, C., ROSEN, M. R. & COHEN, I. S. 2012. Can Gap Junctions Deliver? *Biochim Biophys Acta (BBA) - Biomembranes,* 1818**,** 2076-2081.

BRIZ, M. & FABREGA, A. 2013 Boar Spermatozoa Within the Male Genital Tract: The Boar Spermatozoon. In: BONET, S., CASAS, I., HOLT, W. V. & YESTE, M. (eds.) Boar Reproduction: Fundamentals and New Biotechnological Trends. Berlin, Heidelberg: *Springer Berlin Heidelberg*.

BURNETT, L. A., LIGHT, M. M., MEHROTRA, P. & NOWAK, R. A. 2012. Stimulation of GPR30 Increases Release of EMMPRIN-Containing Microvesicles in Human Uterine Epithelial Cells. *J Clin Endocrinol Metab,* 97**,** 4613-22.

BURNOUF, T., AGRAHARI, V. & AGRAHARI, V. 2019. Extracellular Vesicles As Nanomedicine: Hopes And Hurdles In Clinical Translation. *Int J Nanomed,* Volume 14.

BUSSALLEU, E., PINART, E., YESTE, M., BRIZ, M., SANCHO, S., GARCIA-GIL, N., BADIA, E., BASSOLS, J., PRUNEDA, A., CASAS, I. & BONET, S. 2005. Development of a Protocol for Multiple Staining with Fluorochromes to Assess the Functional Status of Boar Spermatozoa. *Microsc Res Tech,* 68**,** 277-83.

CABALLERO, J., FRENETTE, G., D'AMOURS, O., BELLEANNÉE, C., LACROIX-PEPIN, N., ROBERT, C. & SULLIVAN, R. 2012. Bovine Sperm Raft Membrane Associated Glioma Pathogenesis-Related 1-Like Protein 1 (GliPr1L1) is Modified during the Epididymal Transit and is Potentially Involved in Sperm Binding to the Zona Pellucida. *J Cell Physiol,* 227**,** 3876-86.

CABY, M. P., LANKAR, D., VINCENDEAU-SCHERRER, C., RAPOSO, G. & BONNEROT, C. 2005. Exosomal-Like Vesicles are Present in Human Blood Plasma. *Int Immunol,* 17**,** 879-87.

CAMPBELL, J., SAVAGE, A., MADAMIDOLA, O., TAMHANE, K., SORIANO, R., ADYA, A. & BROWN, S. 2013. Progesterone Significantly Enhances the Mobility of Boar Spermatozoa. *Biodiscovery,* 9.

CAMPOS, V. F., DE LEON, P. M., KOMNINOU, E. R., DELLAGOSTIN, O. A., DESCHAMPS, J. C., SEIXAS, F. K. & COLLARES, T. 2011. NanoSMGT: Transgene Transmission into Bovine Embryos using Halloysite Clay Nanotubes or Nanopolymer to Improve Transfection Efficiency. *Theriogenology,* 76**,** 1552-60.

CAMUSSI, G., DEREGIBUS, M. C., BRUNO, S., CANTALUPPI, V. & BIANCONE, L. 2010. Exosomes/Microvesicles as a Mechanism of Cell-to-Cell Communication. *Kidney Int,* 78**,** 838-48.

CARLINI, E., PALMERINI, C. A., COSMI, E. V. & ARIENTI, G. 1997. Fusion of Sperm with Prostasomes: Effects on Membrane Fluidity. *Arch Biochem Biophys,* 343**,** 6-12.

CARLSSON, L., NILSSON, O., LARSSON, A., STRIDSBERG, M., SAHLEN, G. & RONQUIST, G. 2003. Characteristics of Human Prostasomes Isolated from Three Different Sources. *Prostate,* 54**,** 322-30.

CARLSSON, L., PAHLSON, C., BERGQUIST, M., RONQUIST, G. & STRIDSBERG, M. 2000. Antibacterial Activity of Human Prostasomes. *Prostate,* 44**,** 279-86.

CARLSON, B. M. 2019. Chapter 14 - The Reproductive System. *In:* CARLSON, B. M. (ed.) *The Human Body.* Academic Press.

CARNELL-MORRIS, P., TANNETTA, D., SIUPA, A., HOLE, P. & DRAGOVIC, R. 2017. Analysis of Extracellular Vesicles Using Fluorescence Nanoparticle Tracking Analysis. *In:* KUO, W. P. & JIA, S. (eds.) *Extracellular Vesicles: Methods and Protocols.* New York, NY: Springer New York.

CARPI, A., SABANEGH, E. & MECHANICK, J. 2009. Controversies in the Management of Nonobstructive Azoospermia. *Fertil Steril,* 91**,** 963-70.

CARPINTERO-FERNÁNDEZ, P., FAFIÁN-LABORA, J. & O'LOGHLEN, A. 2017. Technical Advances to Study Extracellular Vesicles. *Front Mol Biosci,* 4**,** 79-79.

CASTELLANOS-RIZALDOS, E., GRIMM, D. G., TADIGOTLA, V., HURLEY, J., HEALY, J., NEAL, P. L., SHER, M., VENKATESAN, R., KARLOVICH, C., RAPONI, M., KRUG, A., NOERHOLM, M., TANNOUS, J., TANNOUS, B. A., RAEZ, L. E. & SKOG, J. K. 2018. Exosome-Based Detection of EGFR T790M in Plasma from Non-Small Cell Lung Cancer Patients. *Clin Cancer Res,* 24**,** 2944-2950.

CEBESOY, F. B., AYDOS, K. & UNLU, C. 2006. Effect of Sperm Chromatin Damage on Fertilization Ratio and Embryo Quality Post-ICSI. *Arch Androl,* 52**,** 397-402.

CHAKRABORTY, D., MAITY, A., JHA, T. & MONDAL, N. B. 2014. Spermicidal and Contraceptive Potential of Desgalactotigonin: a Prospective Alternative of Nonoxynol-9. *PLoS One,* 9**,** e107164

CHAMBERS, G. M., WAND, H., MACALDOWIE, A., CHAPMAN, M. G., FARQUHAR, C. M., BOWMAN, M., MOLLOY, D. & LEDGER, W. 2016. Population Trends and Live Birth Rates Associated with Common ART Treatment Strategies. *Hum Reprod,* 31**,** 2632-2641.

CHEN, C., ZONG, S., WANG, Z., LU, J., ZHU, D., ZHANG, Y. & CUI, Y. 2016. Imaging and Intracellular Tracking of Cancer-Derived Exosomes Using Single-Molecule Localization-Based Super-Resolution Microscope. *ACS Appl Mater Interfaces,* 8**,** 25825-25833.

CHEN, X., BA, Y., MA, L., CAI, X., YIN, Y., WANG, K., GUO, J., ZHANG, Y., CHEN, J., GUO, X., LI, Q., LI, X., WANG, W., ZHANG, Y., WANG, J., JIANG, X., XIANG, Y., XU, C., ZHENG, P., ZHANG, J., LI, R., ZHANG, H., SHANG, X., GONG, T., NING, G., WANG, J., ZEN, K., ZHANG, J. & ZHANG, C. Y. 2008. Characterization of MicroRNAs in Serum: A Novel Class of Biomarkers for Diagnosis of Cancer and other Diseases. *Cell Res,* 18**,** 997-1006.

CHEN, H., MRUK, D. D., XIA, W., BONANOMI, M., SILVESTRINI, B. & CHENG, C.-Y. 2016. Effective Delivery of Male Contraceptives Behind the Blood-Testis Barrier (BTB) - Lesson from Adjudin. *Curr Med Chem,* 23**,** 701-713.

CHEN, Y.-S., LIN, E.-Y., CHIOU, T.-W. & HARN, H.-J. 2019. Exosomes in Clinical Trial and their Production in Compliance with Good Manufacturing Practice. *Ci ji yi xue za zhi = Tzu-chi Medical Journal,* 32**,** 113-120.

CHEN, X., ZHENG, Y., LEI, A., ZHANG, H., NIU, H., LI, X., ZHANG, P., LIAO, M., LV, Y., ZHU, Z., PAN, C., DONG, W., CHEN, H., WU, D., LIU, W., HAMER, G., ZENG, S. & ZENG, W. 2020. Early Cleavage of Preimplantation Embryos is Regulated by tRNA(Gln-TTG)-Derived Small RNAs Present in Mature Spermatozoa. *J Biol Chem*.

COATES, A., HESLA, J. S., HURLIMAN, A., COATE, B., HOLMES, E., MATTHEWS, R., MOUNTS, E. L., TURNER, K. J., THORNHILL, A. R. & GRIFFIN, D. K. 2015. Use of Suboptimal Sperm Increases the Risk of Aneuploidy of the Sex Chromosomes in Preimplantation Blastocyst Embryos. *Fertil Sterility,* 104**,** 866-872.

COCUZZA, M., ALVARENGA, C. & PAGANI, R. 2013. The Epidemiology and Etiology of Azoospermia. *Clinics (Sao Paulo),* 68 Suppl 1**,** 15-26.

COLOMBO, M., MOITA, C., VAN NIEL, G., KOWAL, J., VIGNERON, J., BENAROCH, P., MANEL, N., MOITA, L. F., THERY, C. & RAPOSO, G. 2013. Analysis of ESCRT Functions in Exosome Biogenesis, Composition and Secretion Highlights the Heterogeneity of Extracellular Vesicles. *J Cell Sci,* 126**,** 5553-65.

COLOMBO, M., RAPOSO, G. & THERY, C. 2014. Biogenesis, Secretion, and Intercellular Interactions of Exosomes and other Extracellular Vesicles. *Annu Rev Cell Dev Biol,* 30**,** 255-89.

COOPER, T. 2007. The Human Epididymis, Sperm Maturation and Storage. *ANIR-ANHP,* 9**,** 18-24.

COOPER, T. G. 1998. Interactions Between Epididymal Secretions and Spermatozoa. *J Reprod Fertil. Supplement,* 53**,** 119-136.

CORSO, G., HEUSERMANN, W., TROJER, D., GÖRGENS, A., STEIB, E., VOSHOL, J., GRAFF, A., GENOUD, C., LEE, Y., HEAN, J., NORDIN, J. Z., WIKLANDER, O. P. B., EL ANDALOUSSI, S. & MEISNER-KOBER, N. 2019. Systematic Characterization of Extracellular Vesicle Sorting Domains and Quantification at the Single Molecule – Single Vesicle Level by Fluorescence Correlation Spectroscopy and Single Particle Imaging. *J Extracell Vesicles,* 8**,** 1663043.

COSTA VERDERA, H., GITZ-FRANCOIS, J. J., SCHIFFELERS, R. M. & VADER, P. 2017. Cellular uptake of Extracellular Vesicles is Mediated by Clathrin-Independent Endocytosis and Macropinocytosis. *J Control Release,* 266**,** 100-108.

COVARRUBIAS, A. A., YESTE, M., SALAZAR, E., RAMÍREZ-REVECO, A., RODRIGUEZ GIL, J. E. & CONCHA, I. I. 2015. The Wnt1 ligand/Frizzled 3 receptor System Plays a Regulatory Role in the Achievement of the 'In Vitro' Capacitation and Subsequent 'In Vitro' Acrosome Exocytosis of Porcine Spermatozoa. *Andrology,* 3**,** 357-367.

COWARD, K., KUBOTA, H., HIBBITT, O., MCILHINNEY, J., KOHRI, K. & PARRINGTON, J. 2006. Expression of a Fluorescent Recombinant Form of Sperm Protein Phospholipase C Zeta in Mouse Epididymal Sperm by In Vivo Gene Transfer into the Testis. *Fertil Steril,* 85 Suppl 1**,** 1281-9.

COWARD, K., KUBOTA, H. & PARRINGTON, J. 2007. In Vivo Gene Transfer into Testis and Sperm: Developments and Future Application. *Arch Androl,* 53**,** 187-97.

CRAWFORD, G. E. & LEDGER, W. L. 2019. In Vitro Fertilisation/Intracytoplasmic Sperm Injection Beyond 2020. *BJOG,* 126**,** 237-243.

CROSS, N. L. 1996. Effect of Cholesterol and other Sterols on Human Sperm Acrosomal Responsiveness. *Mol Reprod Dev,* 45**,** 212-7.

CROSS, N. L. 1998. Role of Cholesterol in Sperm Capacitation. *Biol Reprod,* 59**,** 7-11.

CROSS, N. L. & MAHASRESHTI, P. 1997. Prostasome Fraction of Human Seminal Plasma prevents Sperm from becoming Acrosomally responsive to the Agonist Progesterone. *Arch Androl,* 39**,** 39-44.

CURRY, M. R., MILLAR, J. D., TAMULI, S. M. & WATSON, P. F. 1996. Surface Area and Volume Measurements for Ram and Human Spermatozoa1. *Biology of Reproduction,* 55**,** 1325-1332.

CWIK, B. 2020. Responsible Translational Pathways for Germline Gene Editing? *Curr Stem Cell Rep***,** 1-8.

DADOUNE, J.P. & DEMOULIN, A. 1993. Structure and functions of the testis. In: THIBAULT, C., LEVASSEUR, M.C. & HUNTER, R.H.F. (eds) *Reproduction in Mammals and Man*. Ellipses, Paris, 27–255

DA SILVEIRA, J. C., VEERAMACHANENI, D. N., WINGER, Q. A., CARNEVALE, E. M. & BOUMA, G. J. 2012. Cell-Secreted Vesicles in Equine Ovarian Follicular Fluid contain miRNAs and Proteins: A Possible New Form of Cell Communication within the Ovarian Follicle. *Biol Reprod,* 86**,** 71.

DAS, J., CHOI, Y. J., SONG, H. & KIM, J. H. 2016. Potential Toxicity of Engineered Nanoparticles in Mammalian Germ Cells and Developing Embryos: Treatment Strategies and Anticipated Applications of Nanoparticles in Gene Delivery. *Hum Reprod Update,* 22**,** 588-619.

DAVIS, C. N., PHILLIPS, H., TOMES, J. J., SWAIN, M. T., WILKINSON, T. J., BROPHY, P. M. & MORPHEW, R. M. 2019. The Importance of Extracellular Vesicle Purification for Downstream Analysis: A Comparison of Differential Centrifugation and Size Exclusion Chromatography for Helminth Pathogens. *PLOS Neglect Trop D,* 13**,** e0007191.

DE JONG, O. G., MURPHY, D. E., MÄGER, I., WILLMS, E., GARCIA-GUERRA, A., GITZ-FRANCOIS, J. J., LEFFERTS, J., GUPTA, D., STEENBEEK, S. C., VAN RHEENEN, J., EL ANDALOUSSI, S., SCHIFFELERS, R. M., WOOD, M. J. A. & VADER, P. 2020. A CRISPR-Cas9-based Reporter System for Single-Cell Detection of Extracellular Vesicle-Mediated Functional Transfer of RNA. *Nat Comm,* 11**,** 1113.

DEY-HAZRA, E., HERTEL, B., KIRSCH, T., WOYWODT, A., LOVRIC, S., HALLER, H., HAUBITZ, M. & ERDBRUEGGER, U. 2010. Detection of Circulating Microparticles by Flow Cytometry: Influence of Centrifugation, Filtration of Buffer, and Freezing. *Vascular Health and Risk Management,* 6**,** 1125-1133.

DIDION, B. A. 2008. Computer-Assisted Semen Analysis and its Utility for Profiling Boar Semen Samples. *Theriogenology,* 70**,** 1374-1376.

DIDIOT, M. C., HALL, L. M., COLES, A. H., HARASZTI, R. A., GODINHO, B. M., CHASE, K., SAPP, E., LY, S., ALTERMAN, J. F., HASSLER, M. R., ECHEVERRIA, D., RAJ, L., MORRISSEY, D. V., DIFIGLIA, M., ARONIN, N. & KHVOROVA, A. 2016. Exosome-mediated Delivery of Hydrophobically Modified siRNA for Huntingtin mRNA Silencing. *Mol Ther,* 24**,** 1836-1847.

DONNELLY, E. T., O'CONNELL, M., MCCLURE, N. & LEWIS, S. E. 2000. Differences in Nuclear DNA Fragmentation and Mitochondrial Integrity of Semen and Prepared Human Spermatozoa. *Hum Reprod,* 15**,** 1552-61.

DOYLE, U., SAMPSON, N., ZENZMAIER, C., SCHWARZLER, P. & BERGER, P. 2012. Seminal Plasma Enhances and Accelerates Progesterone-Induced Decidualisation of Human Endometrial Stromal Cells. *Reprod Fertil Dev,* 24**,** 517-22.

DRAGOVIC, R. A., COLLETT, G. P., HOLE, P., FERGUSON, D. J. P., REDMAN, C. W., SARGENT, I. L. & TANNETTA, D. S. 2015. Isolation of Syncytiotrophoblast Microvesicles and Exosomes and their Characterisation by Multicolour Flow Cytometry and Fluorescence Nanoparticle Tracking Analysis. *Methods (San Diego, Calif.),* 87**,** 64-74.

DRAGOVIC, R. A., SOUTHCOMBE, J. H., TANNETTA, D. S., REDMAN, C. W. G. & SARGENT, I. L. 2013. Multicolor Flow Cytometry and Nanoparticle Tracking Analysis of Extracellular Vesicles in the Plasma of Normal Pregnant and Pre-eclamptic Women1. *Biol Reprod,* 89.

DU, J., SHEN, J., WANG, Y., PAN, C., PANG, W., DIAO, H. & DONG, W. 2016. Boar Seminal Plasma Exosomes Maintain Sperm Function by Infiltrating into the Sperm Membrane. *Oncotarget,* 7**,** 58832-58847.

DUNSON, D. B., BAIRD, D. D. & COLOMBO, B. 2004. Increased Infertility with Age in Men and Women. *Obstet Gynecol,* 103**,** 51-6.

DU, Y. M., ZHUANSUN, Y. X., CHEN, R., LIN, L., LIN, Y. & LI, J. G. 2018. Mesenchymal Stem Cell Exosomes Promote Immunosuppression of Regulatory T Cells in Asthma. *Exp Cell Res,* 363**,** 114-120.

DYER, S., CHAMBERS, G. M., DE MOUZON, J., NYGREN, K. G., ZEGERS-HOCHSCHILD, F., MANSOUR, R., ISHIHARA, O., BANKER, M. & ADAMSON, G. D. 2016. International Committee for Monitoring Assisted Reproductive Technologies World Report: Assisted Reproductive Technology 2008, 2009 and 2010. *Hum Reprod,* 31**,** 1588-609.

DYM, M. 1973. The Fine Structure of the Monkey (Macaca) Sertoli Cell and its Role in Maintaining the Blood-Testis Barrier. *Anat Rec,* 175**,** 639-56.

EBNER, T., SHEBL, O., MOSER, M., MAYER, R. B., ARZT, W. & TEWS, G. 2010. Group Culture of Human Zygotes is Superior to Individual Culture in Terms of Blastulation, Implantation and Life Birth. *Reprod BioMed Online,* 21**,** 762-768.

EGUCHI, T., TAHA, E. A., CALDERWOOD, S. K. & ONO, K. 2020. A Novel Model of Cancer Drug Resistance: Oncosomal Release of Cytotoxic and Antibody-Based Drugs. *Biology (Basel),* 9.

EICHENLAUB-RITTER, U., SHEN, Y. & TINNEBERG, H. R. 2002. Manipulation of the Oocyte: Possible Damage to the Spindle Apparatus. *Reprod Biomed Online,* 5**,** 117-24.

EISENBACH, M. & GIOJALAS, L. C. 2006. Sperm Guidance in Mammals - an Unpaved Road to the Egg. *Nat Rev Mol Cell Biol,* 7**,** 276-85.

EL-ANDALOUSSI, S., LEE, Y., LAKHAL-LITTLETON, S., LI, J., SEOW, Y., GARDINER, C., ALVAREZ-ERVITI, L., SARGENT, I. L. & WOOD, M. J. 2012. Exosome-Mediated Delivery of siRNA In Vitro and In Vivo. *Nat Protoc,* 7**,** 2112-26.

ENJETI, A. K., LINCZ, L. & SELDON, M. 2008. Bio-Maleimide as a Generic Stain for Detection and Quantitation of Microparticles. *Int J Lab Hematol,* 30**,** 196-199.

ESCREVENTE, C., KELLER, S., ALTEVOGT, P. & COSTA, J. 2011. Interaction and Uptake of Exosomes by Ovarian Cancer Cells. *BMC Cancer,* 11**,** 108.

ESCUDIER, B., DORVAL, T., CHAPUT, N., ANDRE, F., CABY, M. P., NOVAULT, S., FLAMENT, C., LEBOULAIRE, C., BORG, C., AMIGORENA, S., BOCCACCIO, C., BONNEROT, C., DHELLIN, O., MOVASSAGH, M., PIPERNO, S., ROBERT, C., SERRA, V., VALENTE, N., LE PECQ, J. B., SPATZ, A., LANTZ, O., TURSZ, T., ANGEVIN, E. & ZITVOGEL, L. 2005. Vaccination of Metastatic Melanoma Patients with Autologous Dendritic Cell (DC) Derived-Exosomes: Results of the First Phase I Clinical Trial. *J Transl Med,* 3**,** 10.

ESHRE CAPRI WORKSHOP GROUP, A. D., ANDERSON R, BHATTACHARYA S, 2017. A Prognosis-Based Approach to Infertility: Understanding the Role of Time. *Hum Reprod,* 32**,** 1556-1559.

ESSELTINE, J. L. & LAIRD, D. W. 2016. Next-Generation Connexin and Pannexin Cell Biology. *Trends Cell Biol,* 26**,** 944-955.

EUROPEAN SOCIETY OF HUMAN REPRODUCTION AND EMBRYOLOGY (ESHRE). ART fact sheet (February 2018). Available at: http://www.eshre.eu/Guidelines-and-Legal/ART-fact-sheet. aspx [Accessed on March 2020].

EXOPHARM. 2021. Preclinical Data from Ostheoarthritis Animal Study (1 April 2021). Available at: https://exopharm.com/wp-content/uploads/2021/04/2196373.pdf [Accessed on May 2021].

EXOCARTA.ORG. 2020. Exocarta - Exosome Database. Available at: <http://exocarta.org/> [Accessed 10 June 2020].

FANALE, D., TAVERNA, S., RUSSO, A. & BAZAN, V. 2018. Circular RNA in Exosomes. *Adv Exp Med Biol,* 1087**,** 109-117.

FARUQU, F. N., XU, L. & AL-JAMAL, K. T. 2018. Preparation of Exosomes for siRNA Delivery to Cancer Cells. *J Vis Exp*.

FAUQUE, P., JOUANNET, P., LESAFFRE, C., RIPOCHE, M. A., DANDOLO, L., VAIMAN, D. & JAMMES, H. 2007. Assisted Reproductive Technology affects developmental kinetics, H19 Imprinting Control Region methylation and H19 gene expression in individual mouse embryos. *BMC Dev Biol,* 7**,** 116.

FERESHTEH, Z., BATHALA, P., GALILEO, D. S. & MARTIN-DELEON, P. A. 2019. Detection of Extracellular Vesicles in the Mouse Vaginal Fluid: Their Delivery of Sperm Proteins that Stimulate Capacitation and Modulate Fertility. *J Cell Physiol,* 234**,** 12745-12756.

FERGUSON, S. W. & NGUYEN, J. 2016. Exosomes as Therapeutics: The Implications of Molecular Composition and Exosomal Heterogeneity. *J Control Release,* 228**,** 179-190.

FERNANDEZ-GAGO, R., DOMINGUEZ, J. C. & MARTINEZ-PASTOR, F. 2013. Seminal Plasma Applied Post-Thawing Affects Boar Sperm Physiology: A Flow Cytometry Study. *Theriogenology,* 80**,** 400-10.

FERRY, L., MERMILLOD, P., MASSIP, A. & DESSY, F. 1994. Bovine Embryos Cultured in Serum-Poor Oviduct-Conditioned Medium need Cooperation to Reach the Blastocyst Stage. *Theriogenology,* 42**,** 445-53.

FRANCHI, A., MORENO-IRUSTA, A., DOMINGUEZ, E. M., ADRE, A. J. & GIOJALAS, L. C. 2020. Extracellular Vesicles from Oviductal Isthmus and Ampulla Stimulate the Induced Acrosome Reaction and Signaling Events Associated with Capacitation in Bovine Spermatozoa. *J Cell Biochem,* 121**,** 2877-2888.

FROLÍKOVÁ, M., MAŇÁSKOVÁ-POSTLEROVÁ, P., ČERNÝ, J., JANKOVICOVÁ, J., ŠIMONÍK, O., POHLOVÁ, A., SEČOVÁ, P., ANTALIKOVA, J. & DVORAKOVA-HORTOVA, K. 2018. CD9 and CD81 Interactions and Their Structural Modelling in Sperm Prior to Fertilization. *Int J Mol Sci,* 19.

FUHRMANN, G., SERIO, A., MAZO, M., NAIR, R. & STEVENS, M. M. 2015. Active Loading into Extracellular Vesicles Significantly Improves the Cellular Uptake and Photodynamic Effect of Porphyrins. *J Control Release,* 205**,** 35-44.

GADELLA, B. M. 2012. Dynamic Regulation of Sperm Interactions with the Zona Pellucida prior to and after Fertilisation. *Reprod Fertil Dev,* 25**,** 26-37.

GADELLA, B. M., TSAI, P. S., BOERKE, A. & BREWIS, I. A. 2008. Sperm Head Membrane Reorganisation during Capacitation. *Int J Dev Biol,* 52**,** 473-80.

GAGO-FUENTES, R., CARPINTERO-FERNANDEZ, P., GOLDRING, M. B., BRINK, P. R., MAYAN, M. D. & BLANCO, F. J. 2014. Biochemical Evidence for Gap Junctions and Cx43 Expression in Immortalized Human Chondrocyte Cell Line: A Potential Model in the Study of Cell Communication in Human Chondrocytes. *Osteoart Cartil,* 22**,** 586-90.

GALLUZZI, L., PALINI, S., STEFANI, S., ANDREONI, F., PRIMITERRA, M., DIOTALLEVI, A., BULLETTI, C. & MAGNANI, M. 2015. Extracellular Embryo Genomic DNA and its Potential for Genotyping Applications. *Future Sci OA,* 1**,** FSO62.

GALOTTO, C., CAMBIASSO, M. Y., JULIANELLI, V. L., VALZACCHI, G. J. R., ROLANDO, R. N., RODRIGUEZ, M. L., CALVO, L., CALVO, J. C. & ROMANATO, M. 2019. Human Sperm Decondensation In Vitro is Related to Cleavage Rate and Embryo Quality in IVF. *J Assis Reprod Gen,* 36**,** 2345-2355.

GANDHAM, S., SU, X., WOOD, J., NOCERA, A. L., ALLI, S. C., MILANE, L., ZIMMERMAN, A., AMIJI, M. & IVANOV, A. R. 2020. Technologies and Standardization in Research on Extracellular Vesicles. *Trends Biotechnol*.

GARCEZ, M. E., DOS SANTOS BRANCO, C., LARA, L. V., PASQUALOTTO, F. F. & SALVADOR, M. 2010. Effects of Resveratrol Supplementation on Cryopreservation Medium of Human Semen. *Fertil Steril,* 94**,** 2118-21.

GARCIA HERREROS, M., APARICIO, I. M., NUNEZ, I., GARCIA-MARIN, L. J., GIL, M. C. & PENA VEGA, F. J. 2005. Boar Sperm Velocity and Motility Patterns under Capacitating and Non-Capacitating Incubation Conditions. *Theriogenology,* 63**,** 795-805.

GARCIA, J. C., DOMINGUEZ, J. C., PENA, F. J., ALEGRE, B., GONZALEZ, R., CASTRO, M. J., HABING, G. G. & KIRKWOOD, R. N. 2010. Thawing Boar Semen in the Presence of Seminal Plasma: Effects on Sperm Quality and Fertility. *Anim Reprod Sci,* 119**,** 160-5.

GARDINER, C., FERREIRA, Y. J., DRAGOVIC, R. A., REDMAN, C. W. & SARGENT, I. L. 2013. Extracellular Vesicle Sizing and Enumeration by Nanoparticle Tracking Analysis. *J Extracell Vesicles,* 2.

GARNER, D. L. & JOHNSON, L. A. 1995. Viability Assessment of Mammalian Sperm using SYBR-14 and Propidium Iodide. *Biol Reprod,* 53**,** 276-84.

GIACOMINI, E., VAGO, R., SANCHEZ, A. M., PODINI, P., ZAROVNI, N., MURDICA, V., RIZZO, R., BORTOLOTTI, D., CANDIANI, M. & VIGANÒ, P. 2017. Secretome of In Vitro Cultured Human Embryos Contains Extracellular Vesicles that are Uptaken by the Maternal Side. *Scientific Reports,* 7**,** 521.

GILAD, S., MEIRI, E., YOGEV, Y., BENJAMIN, S., LEBANONY, D., YERUSHALMI, N., BENJAMIN, H., KUSHNIR, M., CHOLAKH, H., MELAMED, N., BENTWICH, Z., HOD, M., GOREN, Y. & CHAJUT, A. 2008. Serum MicroRNAs are Promising Novel Biomarkers. *PLoS One,* 3**,** e3148.

GILULA, N. B., FAWCETT, D. W. & AOKI, A. 1976. The Sertoli Cell Occluding Junctions and Gap Junctions in Mature and Developing Mammalian Testis. *Dev Biol,* 50**,** 142-68.

GIMONA, M., PACHLER, K., LANER-PLAMBERGER, S., SCHALLMOSER, K. & ROHDE, E. 2017. Manufacturing of Human Extracellular Vesicle-Based Therapeutics for Clinical Use. *Int J Mol Sci,* 18.

GIRÃO, H., CATARINO, S. & PEREIRA, P. 2009. Eps15 Interacts with Ubiquitinated Cx43 and Mediates its Internalization. *Exp Cell Res,* 315**,** 3587-3597.

GOLDBERG, J. M., FALCONE, T. & ATTARAN, M. 2007. In Vitro Fertilization Update. *Cleve Clin J Med,* 74**,** 329-38.

GONDA, A., KABAGWIRA, J., SENTHIL, G. N. & WALL, N. R. 2019. Internalization of Exosomes through Receptor-Mediated Endocytosis. *Mol Can Res,* 17**,** 337-347.

GOODENOUGH, D. A. & PAUL, D. L. 2003. Beyond the Gap: Functions of Unpaired Connexon Channels. *Nat Rev Mol Cell Biol,* 4**,** 285-295.

GOULD, S. J. & RAPOSO, G. 2013. As we Wait: Coping with an Imperfect Nomenclature for Extracellular Vesicles. *J Extracell Vesicles,* 2.

GREIL, A. L., SLAUSON-BLEVINS, K. & MCQUILLAN, J. 2010. The Experience of Infertility: A Review of Recent Literature. *Sociol Health Illn,* 32**,** 140-62.

GRIFFITHS, G. S., GALILEO, D. S., REESE, K. & MARTIN-DELEON, P. A. 2008. Investigating the Role of Murine Epididymosomes and Uterosomes in GPI-linked Protein Transfer to Sperm Using SPAM1 as a Model. *Mol Reprod Dev,* 75**,** 1627-36.

GRIMMER, S., VAN DEURS, B. & SANDVIG, K. 2002. Membrane Ruffling and Macropinocytosis in A431 Cells Require Cholesterol. *J Cell Sci,* 115**,** 2953-62.

GUDBERGSSON, J. M., JOHNSEN, K. B., SKOV, M. N. & DUROUX, M. 2016. Systematic Review of Factors Influencing Extracellular Vesicle Yield from Cell Cultures. *Cytotechnology,* 68**,** 579-92.

GUNES, S., ARSLAN, M. A., HEKIM, G. N. T. & ASCI, R. 2016. The Role of Epigenetics in Idiopathic Male Infertility. *J Assist Reprod Genet,* 33**,** 553-569.

GURUNG, S., PEROCHEAU, D., TOURAMANIDOU, L. & BARUTEAU, J. 2021. The Exosome Journey: From Biogenesis to Uptake and Intracellular Signalling. *Cell Commun Signal,* 19**,** 47.

GUTHRIE, H. D. & WELCH, G. R. 2006. Determination of Intracellular Reactive Oxygen Species and High Mitochondrial Membrane Potential in Percoll-treated Viable Boar Sperm using Fluorescence-Activated Flow Cytometry. *J Anim Sci,* 84**,** 2089-100.

HANEY, M. J., KLYACHKO, N. L., ZHAO, Y., GUPTA, R., PLOTNIKOVA, E. G., HE, Z., PATEL, T., PIROYAN, A., SOKOLSKY, M., KABANOV, A. V. & BATRAKOVA, E. V. 2015. Exosomes as Drug Delivery Vehicles for Parkinson's Disease Therapy. *J Control Release,* 207**,** 18-30.

HANEY, M. J., ZHAO, Y., JIN, Y. S., LI, S. M., BAGO, J. R., KLYACHKO, N. L., KABANOV, A. V. & BATRAKOVA, E. V. 2020. Macrophage-Derived Extracellular Vesicles as Drug Delivery Systems for Triple Negative Breast Cancer (TNBC) Therapy. *J Neuroim Pharmacol,* 15**,** 487-500.

HANSEN, M., KURINCZUK, J. J., MILNE, E., DE KLERK, N. & BOWER, C. 2013. Assisted Reproductive Technology and Birth Defects: A Systematic Review and Meta-Analysis. *Hum Reprod Update,* 19**,** 330-353.

HARDING, C., HEUSER, J. & STAHL, P. 1983. Receptor-Mediated Endocytosis of Transferrin and Recycling of the Transferrin Receptor in Rat Reticulocytes. *J Cell Biol,* 97**,** 329-39.

HARGREAVE, M., JENSEN, A., TOENDER, A., ANDERSEN, K. K. & KJAER, S. K. 2013. Fertility Treatment and Childhood Cancer Risk: A Systematic Meta-Analysis. *Fertil Steril,* 100**,** 150-61.

HARPER, C. V., KIRKMAN-BROWN, J. C., BARRATT, C. L. & PUBLICOVER, S. J. 2003. Encoding of Progesterone Stimulus Intensity by Intracellular [Ca2+] ([Ca2+]i) in Human Spermatozoa. *Biochem J,* 372**,** 407-17.

HARRISON, R. A. 1996. Capacitation Mechanisms, and the Role of Capacitation as seen in Eutherian Mammals. *Reprod Fertil Dev,* 8**,** 581-94.

HARRISON, R. A. 2004. Rapid PKA-catalysed Phosphorylation of Boar Sperm Proteins Induced by the Capacitating Agent Bicarbonate. *Mol Reprod Dev,* 67**,** 337-52.

HARRISON, R. A., ASHWORTH, P. J. & MILLER, N. G. 1996. Bicarbonate/CO2, an Effector of Capacitation, Induces a Rapid and Reversible change in the lipid Architecture of Boar Sperm Plasma Membranes. *Mol Reprod Dev,* 45**,** 378-91.

HEILEMANN, M., VAN DE LINDE, S., SCHUTTPELZ, M., KASPER, R., SEEFELDT, B., MUKHERJEE, A., TINNEFELD, P. & SAUER, M. 2008. Subdiffraction-Resolution Fluorescence Imaging with Conventional Fluorescent Probes. *Angew Chem Int Ed Engl,* 47**,** 6172-6.

HEMLER, M. E. 2005. Tetraspanin Functions and Associated Microdomains. *Nat Rev Mol Cell Biol,* 6**,** 801-11.

HENKEL, R. R. 2011. Leukocytes and Oxidative Stress: Dilemma for Sperm Function and Male Fertility. *Asian J Androl,* 13**,** 43-52.

HEWITSON, L., DOMINKO, T., TAKAHASHI, D., MARTINOVICH, C., RAMALHO-SANTOS, J., SUTOVSKY, P., FANTON, J., JACOB, D., MONTEITH, D., NEURINGER, M., BATTAGLIA, D., SIMERLY, C. & SCHATTEN, G. 1999. Unique Checkpoints During the First Cell Cycle of Fertilization after Intracytoplasmic Sperm Injection in Rhesus Monkeys. *Nat Med,* 5**,** 431-3.

HFEA.GOV.UK. n.d. *HFEA - Human Fertilisation And Embryology Authority*. [online] Available at: <http://www.hfea.gov.uk/> [Accessed 10 June 2020].

HOELKER, M., RINGS, F., LUND, Q., GHANEM, N., PHATSARA, C., GRIESE, J., SCHELLANDER, K. & TESFAYE, D. 2009. Effect of the Microenvironment and Embryo Density on Developmental Characteristics and Gene Expression Profile of Bovine Preimplantative Embryos Cultured In Vitro. *Reproduction,* 137**,** 415-25.

HOEKSTRA, D., DE BOER, T., KLAPPE, K. & WILSCHUT, J. 1984. Fluorescence Method for Measuring the Kinetics of Fusion between Biological Membranes. *Biochemistry,* 23**,** 5675-81.

HOOG, J. L. & LOTVALL, J. 2015. Diversity of Extracellular Vesicles in Human Ejaculates Revealed by Cryo-Electron Microscopy. *J Extracell Vesicles,* 4**,** 28680.

HOSHINO, D., KIRKBRIDE, K. C., COSTELLO, K., CLARK, E. S., SINHA, S., GREGA-LARSON, N., TYSKA, M. J. & WEAVER, A. M. 2013. Exosome Secretion is Enhanced by Invadopodia and Drives Invasive Behavior. *Cell Rep,* 5**,** 1159-68.

HSU, C., MOROHASHI, Y., YOSHIMURA, S., MANRIQUE-HOYOS, N., JUNG, S., LAUTERBACH, M. A., BAKHTI, M., GRONBORG, M., MOBIUS, W., RHEE, J., BARR, F. A. & SIMONS, M. 2010. Regulation of Exosome Secretion by Rab35 and its GTPase-Activating Proteins TBC1D10A-C. *J Cell Biol,* 189**,** 223-32.

ICH.ORG. 2020. ICH- Official Web Site. Available at:<https://www.ich.org/products/guidelines> [Accessed 10 June 2020].

IKAWA, M., INOUE, N., BENHAM, A. M. & OKABE, M. 2010. Fertilization: A Sperm's Journey to and Interaction with the Oocyte. *J Clin Invest,* 120**,** 984-94.

JAIN, T. & GUPTA, R. S. 2007. Trends in the Use of Intracytoplasmic Sperm Injection in the United States. *New England Journal of Medicine,* 357**,** 251-257.

JAMES, P. S., HENNESSY, C., BERGE, T. & JONES, R. 2004. Compartmentalisation of the Sperm Plasma Membrane: A FRAP, FLIP and SPFI Analysis of Putative Diffusion Barriers on the Sperm Head. *J Cell Sci,* 117**,** 6485-95.

JAMUR, M. C. & OLIVER, C. 2010. Permeabilization of Cell Membranes. *Methods Mol Biol,* 588**,** 63-6.

JANG, S. C., KIM, O. Y., YOON, C. M., CHOI, D. S., ROH, T. Y., PARK, J., NILSSON, J., LOTVALL, J., KIM, Y. K. & GHO, Y. S. 2013. Bioinspired Exosome-Mimetic Nanovesicles for Targeted Delivery of Chemotherapeutics to Malignant Tumors. *ACS Nano,* 7**,** 7698-710.

JIMENEZ, I., GONZALEZ-MARQUEZ, H., ORTIZ, R., HERRERA, J. A., GARCII, A., BETANCOURT, M. & FIERRO, R. 2003. Changes in the Distribution of Lectin Receptors During Capacitation and Acrosome Reaction in Boar Spermatozoa. *Theriogenology,* 59**,** 1171-80.

JOHNSTONE, R. M. 2006. Exosomes Biological Significance: A Concise Review. *Blood Cells Mol Dis,* 36**,** 315-21.

JOHNSTONE, R. M., ADAM, M., HAMMOND, J. R., ORR, L. & TURBIDE, C. 1987. Vesicle Formation During Reticulocyte Maturation. Association of Plasma Membrane Activities with Released Vesicles (Exosomes). *J Biol Chem,* 262**,** 9412-20.

JONES, S., LUKANOWSKA, M., SUHORUTSENKO, J., OXENHAM, S., BARRATT, C., PUBLICOVER, S., COPOLOVICI, D. M., LANGEL, Ü. & HOWL, J. 2013. Intracellular Translocation and Differential Accumulation of Cell-Penetrating Peptides in Bovine Spermatozoa: Evaluation of Efficient Delivery Vectors that do not Compromise Human Sperm Motility. *Hum Reprod,* 28**,** 1874-89.

JU, Z., MA, J., WANG, C., YU, J., QIAO, Y. & HEI, F. 2017. Exosomes from iPSCs Delivering siRNA Attenuate Intracellular Adhesion Molecule-1 Expression and Neutrophils Adhesion in Pulmonary Microvascular Endothelial Cells. *Inflammation,* 40**,** 486-496.

JUNG, M., RÜDIGER, K. & SCHULZE, M. 2015. In Vitro Measures for Assessing Boar Semen Fertility. *Reprod Dom Anim,* 50**,** 20-24.

JUNGWIRTH, A., GIWERCMAN, A., TOURNAYE, H., DIEMER, T., KOPA, Z., DOHLE, G., KRAUSZ, C. & EUROPEAN ASSOCIATION OF UROLOGY WORKING GROUP ON MALE, I. 2012. European Association of Urology guidelines on Male Infertility: the 2012 update. *Eur Urol,* 62**,** 324-32.

KALANI, A., KAMAT, P. K., CHATURVEDI, P., TYAGI, S. C. & TYAGI, N. 2014. Curcumin-Primed Exosomes Mitigate Endothelial Cell Dysfunction during Hyperhomocysteinemia. *Life Sci,* 107**,** 1-7.

KANWAR, K. C., YANAGIMACHI, R. & LOPATA, A. 1979. Effects of Human Seminal Plasma on Fertilizing Capacity of Human Spermatozoa. *Fertil Steril,* 31**,** 321-7.

KATZ-JAFFE, M. G., SCHOOLCRAFT, W. B. & GARDNER, D. K. 2006. Analysis of Protein Expression (secretome) by Human and Mouse Preimplantation Embryos. *Fertil Steril,* 86**,** 678-85.

KHALAJ, K., MILLER, J. E., LINGEGOWDA, H., FAZLEABAS, A. T., YOUNG, S. L., LESSEY, B. A., KOTI, M. & TAYADE, C. 2019. Extracellular Vesicles from Endometriosis Patients are Characterized by a Unique miRNA-lncRNA Signature. *JCI Insight,* 4.

KHANDWALA, Y. S., ZHANG, C. A., LU, Y. & EISENBERG, M. L. 2017. The Age of Fathers in the USA is Rising: An Analysis of 168 867 480 births from 1972 to 2015. *Hum Reprod,* 32**,** 2110-2116.

KIELBIK, P., KASZEWSKI, J., DABROWSKI, S., FAUNDEZ, R., WITKOWSKI, B. S., WACHNICKI, L., ZHYDACHEVSKYY, Y., SAPIERZYNSKI, R., GAJEWSKI, Z., GODLEWSKI, M. & GODLEWSKI, M. M. 2019. Transfer of Orally Administered ZnO:Eu Nanoparticles through the Blood-Testis Barrier: the Effect on Kinetic Sperm Parameters and Apoptosis in Mice Testes. *Nanotechnology,* 30**,** 455101.

KIM, D., JEONG, Y. Y. & JON, S. 2010a. A Drug-Loaded Aptamer-Gold Nanoparticle Bioconjugate for Combined CT Imaging and Therapy of Prostate Cancer. *ACS Nano,* 4**,** 3689-96.

KIM, H., KANG, J. Y., MUN, D., YUN, N. & JOUNG, B. 2019. Calcium Chloride Enhances the Delivery of Exosomes. *PLoS One,* 14**,** e0220036.

KIM, T. S., LEE, S. H., GANG, G. T., LEE, Y. S., KIM, S. U., KOO, D. B., SHIN, M. Y., PARK, C. K. & LEE, D. S. 2010b. Exogenous DNA Uptake of Boar Spermatozoa by a Magnetic Nanoparticle Vector System. *Reprod Domest Anim,* 45**,** e201-6.

KOBAYASHI, H., SATO, A., OTSU, E., HIURA, H., TOMATSU, C., UTSUNOMIYA, T., SASAKI, H., YAEGASHI, N. & ARIMA, T. 2007. Aberrant DNA Methylation of Imprinted loci in Sperm from Oligospermic Patients. *Hum Mol Genet,* 16**,** 2542-2551.

KOLIHA, N., WIENCEK, Y., HEIDER, U., JÜNGST, C., KLADT, N., KRAUTHÄUSER, S., JOHNSTON, I. C., BOSIO, A., SCHAUSS, A. & WILD, S. 2016. A Novel Multiplex Bead-Based Platform Highlights the Diversity of Extracellular Vesicles. *J Extracell Vesicles,* 5**,** 29975.

KONG, L., TANG, M., ZHANG, T., WANG, D., HU, K., LU, W., WEI, C., LIANG, G. & PU, Y. 2014. Nickel Nanoparticles Exposure and Reproductive Toxicity in Healthy Adult Rats. *Int J Mol Sci,* 15**,** 21253-69.

KOOIJMANS, S. A. A., ALEZA, C. G., ROFFLER, S. R., VAN SOLINGE, W. W., VADER, P. & SCHIFFELERS, R. M. 2016. Display of GPI-Anchored Anti-EGFR Nanobodies on Extracellular Vesicles Promotes Tumour Cell Targeting. *J Extracellular Vesicles,* 5**,** 31053.

KOWAL, J., TKACH, M. & THERY, C. 2014. Biogenesis and Secretion of Exosomes. *Curr Opin Cell Biol,* 29**,** 116-25.

KRAWETZ, S. 2005. Krawetz SA. Paternal Contribution: New Insights and Future Challenges. Nat Rev Genet 6: 633-642. *Nat Rev. Genetics,* 6**,** 633-42.

KUMAR, M., KUMAR, K., JAIN, S., HASSAN, T. & DADA, R. 2013. Novel Insights into the Genetic and Epigenetic Paternal Contribution to the Human Embryo. *Clinics (Sao Paulo),* 68 Suppl 1**,** 5-14.

KUMAR, N. & SINGH, A. K. 2015. Trends of Male Factor Infertility, an Important Cause of Infertility: A Review of Literature. *J Hum Reprod Sci,* 8**,** 191-6.

KUNZMANN, A., ANDERSSON, B., THURNHERR, T., KRUG, H., SCHEYNIUS, A. & FADEEL, B. 2011. Toxicology of Engineered Nanomaterials: Focus on Biocompatibility, Biodistribution and Biodegradation. *Biochim Biophys Acta,* 1810**,** 361-73.

KURKOWSKA, W., BOGACZ, A., JANISZEWSKA, M., GABRYŚ, E., TISZLER, M., BELLANTI, F., KASPERCZYK, S., MACHOŃ-GRECKA, A., DOBRAKOWSKI, M. & KASPERCZYK, A. 2020. Oxidative Stress is Associated with Reduced Sperm Motility in Normal Semen. *Amer J Men Heal,* 14**,** 1557988320939731-1557988320939731.

LACROIX, R., JUDICONE, C., PONCELET, P., ROBERT, S., ARNAUD, L., SAMPOL, J. & DIGNAT-GEORGE, F. 2012. Impact of Pre-analytical Parameters on the Measurement of Circulating Microparticles: Towards Standardization of Protocol. *J Throm Haemost,* 10**,** 437-446.

LAINSCEK, D., KADUNC, L., KEBER, M. M., BRATKOVIC, I. H., ROMIH, R. & JERALA, R. 2018. Delivery of an Artificial Transcription Regulator dCas9-VPR by Extracellular Vesicles for Therapeutic Gene Activation. *ACS Synth Biol,* 7**,** 2715-2725.

LAMICHHANE, T. N., RAIKER, R. S. & JAY, S. M. 2015. Exogenous DNA Loading into Extracellular Vesicles via Electroporation is Size-Dependent and Enables Limited Gene Delivery. *Mol Pharm,* 12**,** 3650-7.

LANKVELD, D. P., RAYAVARAPU, R. G., KRYSTEK, P., OOMEN, A. G., VERHAREN, H. W., VAN LEEUWEN, T. G., DE JONG, W. H. & MANOHAR, S. 2011. Blood Clearance and Tissue Distribution of PEGylated and Non-PEGylated Gold Nanorods after Intravenous Administration in Rats. *Nanomedicine (Lond),* 6**,** 339-49.

LASSER, C., ALIKHANI, V. S., EKSTROM, K., ELDH, M., PAREDES, P. T., BOSSIOS, A., SJOSTRAND, M., GABRIELSSON, S., LOTVALL, J. & VALADI, H. 2011. Human Saliva, Plasma and Breast Milk Exosomes Contain RNA: Uptake by Macrophages. *J Transl Med,* 9**,** 9.

LAULAGNIER, K., VINCENT-SCHNEIDER, H., HAMDI, S., SUBRA, C., LANKAR, D. & RECORD, M. 2005. Characterization of Exosome Subpopulations from RBL-2H3 cells using Fluorescent Lipids. *Blood Cells, Molecules, and Diseases,* 35**,** 116-121.

LE BOUC, Y., ROSSIGNOL, S., AZZI, S., STEUNOU, V., NETCHINE, I. & GICQUEL, C. 2010. Epigenetics, Genomic Imprinting and Assisted Reproductive Technology. *Ann Endocrinol (Paris),* 71**,** 237-8.

LEAVER, M. & WELLS, D. 2020. Non-Invasive Preimplantation Genetic Testing (niPGT): the Next Revolution in Reproductive Genetics? *Hum Reprod Update,* 26**,** 16-42.

LEITHE, E., KJENSETH, A., SIRNES, S., STENMARK, H., BRECH, A. & RIVEDAL, E. 2009. Ubiquitylation of the Gap Junction Protein Connexin-43 Signals its Trafficking from early Endosomes to Lysosomes in a Process Mediated by Hrs and Tsg101. *J Cell Sci,* 122**,** 3883-3893.

LEE, J. A., SPIDLEN, J., BOYCE, K., CAI, J., CROSBIE, N., DALPHIN, M., FURLONG, J., GASPARETTO, M., GOLDBERG, M., GORALCZYK, E. M., HYUN, B., JANSEN, K., KOLLMANN, T., KONG, M., LEIF, R., MCWEENEY, S., MOLOSHOK, T. D., MOORE, W., NOLAN, G., NOLAN, J., NIKOLICH-ZUGICH, J., PARRISH, D., PURCELL, B., QIAN, Y., SELVARAJ, B., SMITH, C., TCHUVATKINA, O., WERTHEIMER, A., WILKINSON, P., WILSON, C., WOOD, J., ZIGON, R., SCHEUERMANN, R. H. & BRINKMAN, R. R. 2008. MIFlowCyt: The Minimum Information about a Flow Cytometry Experiment. *Cytometry A,* 73**,** 926-30.

LEE, J., KIM, J., JEONG, M., LEE, H., GOH, U., KIM, H., KIM, B. & PARK, J. H. 2015. Liposome-based Engineering of Cells to Package Hydrophobic Compounds in Membrane Vesicles for Tumor Penetration. *Nano Lett,* 15**,** 2938-44.

LEE, Y., EL ANDALOUSSI, S. & WOOD, M. J. 2012. Exosomes and Microvesicles: Extracellular Vesicles for Genetic Information Transfer and Gene Therapy. *Hum Mol Genet,* 21**,** R125-34.

LEE, Y. X. F., JOHANSSON, H., WOOD, M. J. A. & EL ANDALOUSSI, S. 2019. Considerations and Implications in the Purification of Extracellular Vesicles – A Cautionary Tale. *Front Neurosci,* 13.

LENER, T., GIMONA, M., AIGNER, L., BORGER, V., BUZAS, E., CAMUSSI, G., CHAPUT, N., CHATTERJEE, D., COURT, F. A., DEL PORTILLO, H. A., O'DRISCOLL, L., FAIS, S., FALCON-PEREZ, J. M., FELDERHOFF-MUESER, U., FRAILE, L., GHO, Y. S., GORGENS, A., GUPTA, R. C., HENDRIX, A., HERMANN, D. M., HILL, A. F., HOCHBERG, F., HORN, P. A., DE KLEIJN, D., KORDELAS, L., KRAMER, B. W., KRAMER-ALBERS, E. M., LANER-PLAMBERGER, S., LAITINEN, S., LEONARDI, T., LORENOWICZ, M. J., LIM, S. K., LOTVALL, J., MAGUIRE, C. A., MARCILLA, A., NAZARENKO, I., OCHIYA, T., PATEL, T., PEDERSEN, S., POCSFALVI, G., PLUCHINO, S., QUESENBERRY, P., REISCHL, I. G., RIVERA, F. J., SANZENBACHER, R., SCHALLMOSER, K., SLAPER-CORTENBACH, I., STRUNK, D., TONN, T., VADER, P., VAN BALKOM, B. W., WAUBEN, M., ANDALOUSSI, S. E., THERY, C., ROHDE, E. & GIEBEL, B. 2015. Applying Extracellular Vesicles based Therapeutics in Clinical Trials - an ISEV Position Paper. *J Extracell Vesicles,* 4**,** 30087.

LENZI, A., PICARDO, M., GANDINI, L. & DONDERO, F. 1996. Lipids of the Sperm Plasma Membrane: From Polyunsaturated Fatty Acids Considered as Markers of Sperm Function to Possible Scavenger Therapy. *Hum Reprod Update,* 2**,** 246-256.

LEO-MACIAS, A., AGULLO-PASCUAL, E. & DELMAR, M. 2016. The Cardiac Connexome: Non-canonical Functions of Connexin43 and their role in Cardiac Arrhythmias. *Seminars in Cell & Developmental Biology,* 50**,** 13-21.

LEVINE, H., JORGENSEN, N., MARTINO-ANDRADE, A., MENDIOLA, J., WEKSLER-DERRI, D., MINDLIS, I., PINOTTI, R. & SWAN, S. H. 2017. Temporal Trends in Sperm Count: A Systematic Review and Meta-Regression Analysis. *Hum Reprod Update,* 23**,** 646-659.

LEVY, S. & SHOHAM, T. 2005. The Tetraspanin Web Modulates Immune-Signalling Complexes. *Nat Rev Immunol,* 5**,** 136-48.

LIMONI, S. K., MOGHADAM, M. F., MOAZZENI, S. M., GOMARI, H. & SALIMI, F. 2019. Engineered Exosomes for Targeted Transfer of siRNA to HER2 Positive Breast Cancer Cells. *Applied Biochemistry and Biotechnology,* 187**,** 352-364.

LINARES, R., TAN, S., GOUNOU, C., ARRAUD, N. & BRISSON, A. R. 2015. High-Speed Centrifugation Induces Aggregation of Extracellular Vesicles. *J Extracell Vesicles,* 4**,** 29509-29509.

LIU, Q., XU, C., JI, G., LIU, H., MO, Y., TOLLERUD, D. J., GU, A. & ZHANG, Q. 2016. Sublethal Effects of Zinc Oxide Nanoparticles on Male Reproductive Cells. *Toxicol In Vitro,* 35**,** 131-8.

LIU, T., ZHANG, X., DU, L., WANG, Y., LIU, X., TIAN, H., WANG, L., LI, P., ZHAO, Y., DUAN, W., XIE, Y., SUN, Z. & WANG, C. 2019. Exosome-Transmitted miR-128-3p Increase Chemosensitivity of Oxaliplatin-Resistant Colorectal Cancer. *Mol Cancer,* 18.

LIU, Y., LI, D., LIU, Z., ZHOU, Y., CHU, D., LI, X., JIANG, X., HOU, D., CHEN, X., CHEN, Y., YANG, Z., JIN, L., JIANG, W., TIAN, C., ZHOU, G., ZEN, K., ZHANG, J., ZHANG, Y., LI, J. & ZHANG, C. Y. 2015. Targeted Exosome-Mediated Delivery of Opioid Receptor Mu siRNA for the Treatment of Morphine Relapse. *Sci Rep,* 5**,** 17543.

LI, Z., ZHOU, X., WEI, M., GAO, X., ZHAO, L., SHI, R., SUN, W., DUAN, Y., YANG, G. & YUAN, L. 2019. In Vitro and in Vivo RNA Inhibition by CD9-HuR Functionalized Exosomes Encapsulated with miRNA or CRISPR/dCas9. *Nano Letters,* 19**,** 19-28.

LORENZEN, E., FOLLMANN, F., JUNGERSEN, G. & AGERHOLM, J. S. 2015. A Review of the Human vs. Porcine Female Genital Tract and Associated Immune System in the Perspective of using Minipigs as a Model of Human Genital Chlamydia Infection. *Vet Research,* 46**,** 116-116.

LÖTVALL, J., HILL, A. F., HOCHBERG, F., BUZÁS, E. I., DI VIZIO, D., GARDINER, C., GHO, Y. S., KUROCHKIN, I. V., MATHIVANAN, S., QUESENBERRY, P., SAHOO, S., TAHARA, H., WAUBEN, M. H., WITWER, K. W. & THÉRY, C. 2014. Minimal Experimental Requirements for Definition of Extracellular Vesicles and their Functions: A Position Statement from the International Society for Extracellular Vesicles. *J Extracell Vesicles,* 3**,** 26913.

LOUTRADI, K. E., TARLATZIS, B. C., GOULIS, D. G., ZEPIRIDIS, L., PAGOU, T., CHATZIIOANNOU, E., GRIMBIZIS, G. F., PAPADIMAS, I. & BONTIS, I. 2006. The Effects of Sperm Quality on Embryo Development after Intracytoplasmic Sperm Injection. *J Assist Reprod Genet,* 23**,** 69-74.

LV, L. H., WAN, Y. L., LIN, Y., ZHANG, W., YANG, M., LI, G. L., LIN, H. M., SHANG, C. Z., CHEN, Y. J. & MIN, J. 2012. Anticancer Drugs Cause Release of Exosomes with Heat Shock Proteins from Human Hepatocellular Carcinoma Cells that Elicit Effective Natural Killer Cell Antitumor Responses In Vitro. *J Biol Chem,* 287**,** 15874-85.

LY, J. D., GRUBB, D. R. & LAWEN, A. 2003. The Mitochondrial Membrane Potential (deltapsi(m)) in Apoptosis; an Update. *Apoptosis,* 8**,** 115-28.

MACHTINGER, R., LAURENT, L. C. & BACCARELLI, A. A. 2016. Extracellular Vesicles: Roles in Gamete Maturation, Fertilization and Embryo Implantation. *Hum Reprod Update,* 22**,** 182-93.

MAEDA, H., NAKAMURA, H. & FANG, J. 2013. The EPR Effect for Macromolecular Drug Delivery to Solid Tumors: Improvement of Tumor Uptake, Lowering of Systemic Toxicity, and Distinct Tumor Imaging In Vivo. *Advanced Drug Delivery Reviews,* 65**,** 71-79.

MAES, M., DECROCK, E., COGLIATI, B., OLIVEIRA, A., MARQUES, P., ZAIDAN DAGLI, M. L., MENEZES, G., MENNECIER, G., LEYBAERT, L., VANHAECKE, T., ROGIERS, V. & VINKEN, M. 2014. Connexin and Pannexin (hemi)channels in the Liver. *Frontiers in Physiology,* 4.

MAGDANZ, V., GEBAUER, J., SHARAN, P., ELTOUKHY, S., VOIGT, D. & SIMMCHEN, J. 2019. Sperm–Particle Interactions and Their Prospects for Charge Mapping. *Advanced Biosystems,* 3**,** 1900061.

MARAZIOTI, A., PAPADIA, K., KANNAVOU, M., SPELLA, M., BASTA, A., DE LASTIC, A.-L., RODI, M., MOUZAKI, A., SAMIOTAKI, M., PANAYOTOU, G., STATHOPOULOS, G. T. & ANTIMISIARIS, S. G. 2019. Cellular Vesicles: New Insights in Engineering Methods, Interaction with Cells and Potential for Brain Targeting. *Journal of Pharmacology and Experimental Therapeutics,* 370**,** 772-785.

MARCHETTI, C., JOUY, N., LEROY-MARTIN, B., DEFOSSEZ, A., FORMSTECHER, P. & MARCHETTI, P. 2004. Comparison of Four Fluorochromes for the Detection of the Inner Mitochondrial Membrane Potential in Human Spermatozoa and their Correlation with Sperm Motility. *Hum Reprod,* 19**,** 2267-76.

MARCUS, M. E. & LEONARD, J. N. 2013. FedExosomes: Engineering Therapeutic Biological Nanoparticles that Truly Deliver. *Pharmaceuticals (Basel),* 6**,** 659-80.

MARTIN-DELEON, P. A. 2015. Epididymosomes: Transfer of Fertility-Modulating Proteins to the Sperm Surface. *Asian J Androl,* 17**,** 720-5.

MARTIN-DELEON, P. A. 2016. Uterosomes: Exosomal Cargo During the Estrus Cycle and Interaction with Sperm. *Front Biosci (Schol Ed),* 8**,** 115-22.

MARTINEZ, P. & MORROS, A. 1996. Membrane Lipid Dynamics During Human Sperm Capacitation. *Front Biosci,* 1**,** d103-17.

MARTINS-MARQUES, T., ANJO, S. I., PEREIRA, P., MANADAS, B. & GIRÃO, H. 2015. Interacting Network of the Gap Junction (GJ) Protein Connexin43 (Cx43) is Modulated by Ischemia and Reperfusion in the Heart. *Mol Cell Proteomics,* 14**,** 3040-55.

MARTINS-MARQUES, T., PINHO, M. J., ZUZARTE, M., OLIVEIRA, C., PEREIRA, P., SLUIJTER, J. P., GOMES, C. & GIRAO, H. 2016. Presence of Cx43 in Extracellular Vesicles Reduces the Cardiotoxicity of the Anti-Tumour Therapeutic Approach with Doxorubicin. *J Extracell Vesicles,* 5**,** 32538.

MASCARENHAS, M. N., FLAXMAN, S. R., BOERMA, T., VANDERPOEL, S. & STEVENS, G. A. 2012. National, Regional, and Global Trends in Infertility Prevalence Since 1990: A Systematic Analysis of 277 Health Surveys. *PLoS Med,* 9**,** e1001356.

MATA-MARTINEZ, E., DARSZON, A. & TREVINO, C. L. 2018. pH-Dependent Ca(+2) Oscillations Prevent Untimely Acrosome Reaction in Human Sperm. *Biochem Biophys Res Commun,* 497**,** 146-152.

MATHIVANAN, S. & SIMPSON, R. J. 2009. ExoCarta: A Compendium of Exosomal Proteins and RNA. *Proteomics,* 9**,** 4997-5000.

MATSUMOTO, A., TAKAHASHI, Y., NISHIKAWA, M., SANO, K., MORISHITA, M., CHAROENVIRIYAKUL, C., SAJI, H. & TAKAKURA, Y. 2017a. Role of Phosphatidylserine-Derived Negative Surface Charges in the Recognition and Uptake of Intravenously Injected B16BL6-Derived Exosomes by Macrophages. *J Pharm Sci,* 106**,** 168-175.

MATSUMOTO, J., STEWART, T., BANKS, W. A. & ZHANG, J. 2017b. The Transport Mechanism of Extracellular Vesicles at the Blood-Brain Barrier. *Curr Pharm Des,* 23**,** 6206-6214.

MATSUO, H., CHEVALLIER, J., MAYRAN, N., LE BLANC, I., FERGUSON, C., FAURE, J., BLANC, N. S., MATILE, S., DUBOCHET, J., SADOUL, R., PARTON, R. G., VILBOIS, F. & GRUENBERG, J. 2004. Role of LBPA and Alix in Multivesicular Liposome Formation and Endosome Organization. *Science,* 303**,** 531-4.

MAU KAI, C., MAIN, K. M., ANDERSEN, A. N., LOFT, A., SKAKKEBAEK, N. E. & JUUL, A. 2007. Reduced Serum Testosterone Levels in Infant Boys Conceived by Intracytoplasmic Sperm Injection. *J Clin Endocrinol Metab,* 92**,** 2598-603.

MILLER, J. & SMITH, T. 2001. The Effect of Intracytoplasmic Sperm Injection and Semen Parameters on Blastocyst Development In Vitro. *Hum Reprod (Oxford, England),* 16**,** 918-24.

MILUTINOVIC, B., MITIC, N., RONCEVIC, J., GOC, S. & JANKOVIC, M. 2016. Glycome complexity of human seminal plasma high molecular mass components: Evaluation of the contribution of acid-soluble glycoproteins/mucins and extracellular vesicles. *Arch Biochem Biophys,* 609**,** 20-30.

MINCIACCHI, V. R., FREEMAN, M. R. & DI VIZIO, D. 2015. Extracellular vesicles in cancer: exosomes, microvesicles and the emerging role of large oncosomes. *Semin Cell Dev Biol,* 40**,** 41-51.

MINELLI, A., ALLEGRUCCI, C., LIGUORI, L. & RONQUIST, G. 2002. Ecto-diadenosine polyphosphates hydrolase activity on human prostasomes. *Prostate,* 51**,** 1-9.

MITCHELL, P. S., PARKIN, R. K., KROH, E. M., FRITZ, B. R., WYMAN, S. K., POGOSOVA-AGADJANYAN, E. L., PETERSON, A., NOTEBOOM, J., O'BRIANT, K. C., ALLEN, A., LIN, D. W., URBAN, N., DRESCHER, C. W., KNUDSEN, B. S., STIREWALT, D. L., GENTLEMAN, R., VESSELLA, R. L., NELSON, P. S., MARTIN, D. B. & TEWARI, M. 2008. Circulating microRNAs as stable blood-based markers for cancer detection. *Proceedings of the National Academy of Sciences of the United States of America,* 105**,** 10513-10518.

MIYADO, K., YOSHIDA, K., YAMAGATA, K., SAKAKIBARA, K., OKABE, M., WANG, X., MIYAMOTO, K., AKUTSU, H., KONDO, T., TAKAHASHI, Y., BAN, T., ITO, C., TOSHIMORI, K., NAKAMURA, A., ITO, M., MIYADO, M., MEKADA, E. & UMEZAWA, A. 2008. The fusing ability of sperm is bestowed by CD9-containing vesicles released from eggs in mice. *Proceedings of the National Academy of Sciences of the United States of America,* 105**,** 12921-12926.

MOGIELNICKA-BRZOZOWSKA, M., STRZEZEK, R., WASILEWSKA, K. & KORDAN, W. 2015. Prostasomes of canine seminal plasma - zinc-binding ability and effects on motility characteristics and plasma membrane integrity of spermatozoa. *Reprod Domest Anim,* 50**,** 484-91.

MOISYADI, S., KAMINSKI, J. M. & YANAGIMACHI, R. 2009. Use of intracytoplasmic sperm injection (ICSI) to generate transgenic animals. *Comparative Immunology, Microbiology and Infectious Diseases,* 32**,** 47-60.

MONGUIÓ-TORTAJADA, M., GÁLVEZ-MONTÓN, C., BAYES-GENIS, A., ROURA, S. & BORRÀS, F. E. 2019. Extracellular vesicle isolation methods: rising impact of size-exclusion chromatography. *Cell Mol Life Sci,* 76**,** 2369-2382.

MONTECALVO, A., LARREGINA, A. T., SHUFESKY, W. J., STOLZ, D. B., SULLIVAN, M. L. G., KARLSSON, J. M., BATY, C. J., GIBSON, G. A., ERDOS, G., WANG, Z., MILOSEVIC, J., TKACHEVA, O. A., DIVITO, S. J., JORDAN, R., LYONS-WEILER, J., WATKINS, S. C. & MORELLI, A. E. 2012. Mechanism of transfer of functional microRNAs between mouse dendritic cells via exosomes. *Blood,* 119**,** 756-766.

MORELLI, A. E., LARREGINA, A. T., SHUFESKY, W. J., SULLIVAN, M. L., STOLZ, D. B., PAPWORTH, G. D., ZAHORCHAK, A. F., LOGAR, A. J., WANG, Z., WATKINS, S. C., FALO, L. D., JR. & THOMSON, A. W. 2004. Endocytosis, intracellular sorting, and processing of exosomes by dendritic cells. *Blood,* 104**,** 3257-66.

MORETTI, E., MAZZI, L., BONECHI, C., SALVATICI, M. C., IACOPONI, F., ROSSI, C. & COLLODEL, G. 2016. Effect of Quercetin-loaded liposomes on induced oxidative stress in human spermatozoa. *Reprod Toxicol,* 60**,** 140-7.

MORIN, S. J. 2017. Oxygen tension in embryo culture: does a shift to 2% O(2) in extended culture represent the most physiologic system? *Journal of assisted reproduction and genetics,* 34**,** 309-314.

MORISHITA, Y., YOSHIOKA, Y., SATOH, H., NOJIRI, N., NAGANO, K., ABE, Y., KAMADA, H., TSUNODA, S.-I., NABESHI, H., YOSHIKAWA, T. & TSUTSUMI, Y. 2012. Distribution and histologic effects of intravenously administered amorphous nanosilica particles in the testes of mice. *Biochemical and Biophysical Research Communications,* 420**,** 297-301.

MORSE, M. A., GARST, J., OSADA, T., KHAN, S., HOBEIKA, A., CLAY, T. M., VALENTE, N., SHREENIWAS, R., SUTTON, M. A., DELCAYRE, A., HSU, D. H., LE PECQ, J. B. & LYERLY, H. K. 2005. A phase I study of dexosome immunotherapy in patients with advanced non-small cell lung cancer. *J Transl Med,* 3**,** 9.

MOTOMU SHIMAOKA, JUNICHI TAKAGI, A. & SPRINGER, T. A. 2002. Conformational Regulation of Integrin Structure and Function. *Annual Review of Biophysics and Biomolecular Structure,* 31**,** 485-516.

MULCAHY, L. A., PINK, R. C. & CARTER, D. R. F. 2014. Routes and mechanisms of extracellular vesicle uptake. *Journal of extracellular vesicles,* 3**,** 10.3402/jev.v3.24641.

MURAMATSU, T., SHIBATA, O., RYOKI, S., OHMORI, Y. & OKUMURA, J. 1997. Foreign gene expression in the mouse testis by localized in vivo gene transfer. *Biochem Biophys Res Commun,* 233**,** 45-9.

MURPHY, D. E., DE JONG, O. G., BROUWER, M., WOOD, M. J., LAVIEU, G., SCHIFFELERS, R. M. & VADER, P. 2019. Extracellular vesicle-based therapeutics: natural versus engineered targeting and trafficking. *Exp Mol Med,* 51**,** 1-12.

NABI, I. R. & LE, P. U. 2003. Caveolae/raft-dependent endocytosis. *J Cell Biol,* 161**,** 673-7.

NAIR, S. & SALOMON, C. 2018. Extracellular vesicles and their immunomodulatory functions in pregnancy. *Seminars in Immunopathology,* 40**,** 425-437.

NAJAFI, A., TAHERI, R. A., MEHDIPOUR, M., MARTINEZ-PASTOR, F., ROUHOLLAHI, A. A. & NOURANI, M. R. 2019. Improvement of post-thawed sperm quality in broiler breeder roosters by ellagic acid-loaded liposomes. *Poult Sci,* 98**,** 440-446.

NAJAFI, D., TAHERI, R. A., NAJAFI, A., SHAMSOLLAHI, M. & ALVAREZ-RODRIGUEZ, M. 2020. Effect of astaxanthin nanoparticles in protecting the post-thawing quality of rooster sperm challenged by cadmium administration. *Poult Sci,* 99**,** 1678-1686.

NG, Y. H., ROME, S., JALABERT, A., FORTERRE, A., SINGH, H., HINCKS, C. L. & SALAMONSEN, L. A. 2013. Endometrial exosomes/microvesicles in the uterine microenvironment: a new paradigm for embryo-endometrial cross talk at implantation. *PLoS One,* 8**,** e58502.

NGUYEN, H. P., SIMPSON, R. J., SALAMONSEN, L. A. & GREENING, D. W. 2016. Extracellular Vesicles in the Intrauterine Environment: Challenges and Potential Functions. *Biol Reprod,* 95**,** 109.

NIESCHLAG, E., BEHRE, H. M. & NIESCHLAG, S. 2010. *Andrology: Male Reproductive Health and Dysfunction*, Springer Berlin Heidelberg.

NIEUWENHUIZEN, R. P., LIDKE, K. A., BATES, M., PUIG, D. L., GRUNWALD, D., STALLINGA, S. & RIEGER, B. 2013. Measuring image resolution in optical nanoscopy. *Nat Methods,* 10**,** 557-62.

NILSSON, J., SKOG, J., NORDSTRAND, A., BARANOV, V., MINCHEVA-NILSSON, L., BREAKEFIELD, X. O. & WIDMARK, A. 2009. Prostate cancer-derived urine exosomes: a novel approach to biomarkers for prostate cancer. *Br J Cancer,* 100**,** 1603-7.

NOSRATI, R., DRIOUCHI, A., YIP, C. M. & SINTON, D. 2015. Two-dimensional slither swimming of sperm within a micrometre of a surface. *Nature Communications,* 6**,** 8703.

NUDELL, D. M. & LIPSHULTZ, L. I. 2001. Is intracytoplasmic sperm injection safe? Current status and future concerns. *Current Urology Reports,* 2**,** 423-431.

OATES, R. 2012. Evaluation of the azoospermic male. *Asian J Androl,* 14**,** 82-7.

OGAWA, Y., KANAI-AZUMA, M., AKIMOTO, Y., KAWAKAMI, H. & YANOSHITA, R. 2008. Exosome-like vesicles with dipeptidyl peptidase IV in human saliva. *Biol Pharm Bull,* 31**,** 1059-62.

OH, J. S., HAN, C. & CHO, C. 2009. ADAM7 is associated with epididymosomes and integrated into sperm plasma membrane. *Mol Cells,* 28**,** 441-6.

OHNAMI, N., NAKAMURA, A., MIYADO, M., SATO, M., KAWANO, N., YOSHIDA, K., HARADA, Y., TAKEZAWA, Y., KANAI, S., ONO, C., TAKAHASHI, Y., KIMURA, K., SHIDA, T., MIYADO, K. & UMEZAWA, A. 2012. CD81 and CD9 work independently as extracellular components upon fusion of sperm and oocyte. *Biology open,* 1**,** 640-647.

OHNO, S., DRUMMEN, G. P. & KURODA, M. 2016. Focus on Extracellular Vesicles: Development of Extracellular Vesicle-Based Therapeutic Systems. *Int J Mol Sci,* 17**,** 172.

OHNO, S., TAKANASHI, M., SUDO, K., UEDA, S., ISHIKAWA, A., MATSUYAMA, N., FUJITA, K., MIZUTANI, T., OHGI, T., OCHIYA, T., GOTOH, N. & KURODA, M. 2013. Systemically injected exosomes targeted to EGFR deliver antitumor microRNA to breast cancer cells. *Mol Ther,* 21**,** 185-91.

OKSVOLD, M. P., KULLMANN, A., FORFANG, L., KIERULF, B., LI, M., BRECH, A., VLASSOV, A. V., SMELAND, E. B., NEURAUTER, A. & PEDERSEN, K. W. 2014. Expression of B-cell surface antigens in subpopulations of exosomes released from B-cell lymphoma cells. *Clin Ther,* 36**,** 847-862 e1.

OLIVEIRA, R., CHRISTOV, C., GUILLAMO, J. S., DE BOÜARD, S., PALFI, S., VENANCE, L., TARDY, M. & PESCHANSKI, M. 2005. Contribution of gap junctional communication between tumor cells and astroglia to the invasion of the brain parenchyma by human glioblastomas. *BMC cell biology,* 6**,** 7-7.

OLLERO, M., POWERS, R. & ALVAREZ, J. 2000. Variation of docosahexaenoic acid content in subsets of human spermatozoa at different stages of maturation: Implications for sperm lipoperoxidative damage. *Molecular reproduction and development,* 55**,** 326-34.

ORGANIZATION, W. H. 2010. WHO laboratory manual for the examination and processing of human semen.

OSMAN, R. A., ANDRIA, M. L., JONES, A. D. & MEIZEL, S. 1989. Steroid induced exocytosis: the human sperm acrosome reaction. *Biochem Biophys Res Commun,* 160**,** 828-33.

OSORIO-QUEREJETA, I., CARREGAL-ROMERO, S., AYERDI-IZQUIERDO, A., MÄGER, I., A, N. L., WOOD, M., EGIMENDIA, A., BETANZOS, M., ALBERRO, A., IPARRAGUIRRE, L., MOLES, L., LLARENA, I., MÖLLER, M., GOÑI-DE-CERIO, F., BIJELIC, G., RAMOS-CABRER, P., MUÑOZ-CULLA, M. & OTAEGUI, D. 2020. MiR-219a-5p Enriched Extracellular Vesicles Induce OPC Differentiation and EAE Improvement More Efficiently Than Liposomes and Polymeric Nanoparticles. *Pharmaceutics,* 12**,** 186.

PALANISAMY, V., SHARMA, S., DESHPANDE, A., ZHOU, H., GIMZEWSKI, J. & WONG, D. T. 2010. Nanostructural and transcriptomic analyses of human saliva derived exosomes. *PLoS One,* 5**,** e8577.

PALERMO, G., JORIS, H., DEVROEY, P. & VAN STEIRTEGHEM, A. C. 1992. Pregnancies after intracytoplasmic injection of single spermatozoon into an oocyte. *Lancet,* 340**,** 17-8.

PALERMO, G., NERI, Q., TAKEUCHI, T. & ROSENWAKS, Z. 2009. ICSI: where we have been and where we are going. *Seminars in Reproductive Medicine,* 27**,** 191-201.

PALMA, J., YADDANAPUDI, S. C., PIGATI, L., HAVENS, M. A., JEONG, S., WEINER, G. A., WEIMER, K. M., STERN, B., HASTINGS, M. L. & DUELLI, D. M. 2012. MicroRNAs are exported from malignant cells in customized particles. *Nucleic Acids Res,* 40**,** 9125-38.

PALMERINI, C. A., CARLINI, E., NICOLUCCI, A. & ARIENTI, G. 1999. Increase of human spermatozoa intracellular Ca2+concentration after fusion with prostasomes. *Cell Calcium,* 25**,** 291-296.

PALMERINI, C. A., SACCARDI, C., CARLINI, E., FABIANI, R. & ARIENTI, G. 2003. Fusion of prostasomes to human spermatozoa stimulates the acrosome reaction. *Fertil Steril,* 80**,** 1181-4.

PAN, B. T. & JOHNSTONE, R. M. 1983. Fate of the transferrin receptor during maturation of sheep reticulocytes in vitro: selective externalization of the receptor. *Cell,* 33**,** 967-78.

PAN, B. T., TENG, K., WU, C., ADAM, M. & JOHNSTONE, R. M. 1985. Electron microscopic evidence for externalization of the transferrin receptor in vesicular form in sheep reticulocytes. *J Cell Biol,* 101**,** 942-8.

PANDIYAN, N. & JEQUIER, A. M. 1996. Mitotic chromosomal anomalies among 1210 infertile men. *Hum Reprod,* 11**,** 2604-8.

PANTAZIS, A. & CLARK, S. J. 2018. A parsimonious characterization of change in global age-specific and total fertility rates. *PLoS One,* 13**,** e0190574.

PARISH, C. R. 1999. Fluorescent dyes for lymphocyte migration and proliferation studies. *Immunology & Cell Biology,* 77**,** 499-508.

PARK, E.-J., BAE, E., YI, J., KIM, Y., CHOI, K., LEE, S. H., YOON, J., LEE, B. C. & PARK, K. 2010. Repeated-dose toxicity and inflammatory responses in mice by oral administration of silver nanoparticles. *Environmental Toxicology and Pharmacology,* 30**,** 162-168.

PARK, K. H., KIM, B. J., KANG, J., NAM, T. S., LIM, J. M., KIM, H. T., PARK, J. K., KIM, Y. G., CHAE, S. W. & KIM, U. H. 2011. Ca2+ signaling tools acquired from prostasomes are required for progesterone-induced sperm motility. *Sci Signal,* 4**,** ra31.

PAROLINI, I., FEDERICI, C., RAGGI, C., LUGINI, L., PALLESCHI, S., DE MILITO, A., COSCIA, C., IESSI, E., LOGOZZI, M., MOLINARI, A., COLONE, M., TATTI, M., SARGIACOMO, M. & FAIS, S. 2009. Microenvironmental pH is a key factor for exosome traffic in tumor cells. *The Journal of biological chemistry,* 284**,** 34211-34222.

PARRINGTON, J., COWARD, K. & GADEA, J. 2011. Sperm and testis mediated DNA transfer as a means of gene therapy. *Systems biology in reproductive medicine,* 57**,** 35-42.

PASCUCCI, L., COCCÈ, V., BONOMI, A., AMI, D., CECCARELLI, P., CIUSANI, E., VIGANÒ, L., LOCATELLI, A., SISTO, F., DOGLIA, S. M., PARATI, E., BERNARDO, M. E., MURACA, M., ALESSANDRI, G., BONDIOLOTTI, G. & PESSINA, A. 2014. Paclitaxel is incorporated by mesenchymal stromal cells and released in exosomes that inhibit in vitro tumor growth: A new approach for drug delivery. *Journal of Controlled Release,* 192**,** 262-270.

PEREZ-HERNANDEZ, D., GUTIERREZ-VAZQUEZ, C., JORGE, I., LOPEZ-MARTIN, S., URSA, A., SANCHEZ-MADRID, F., VAZQUEZ, J. & YANEZ-MO, M. 2013. The intracellular interactome of tetraspanin-enriched microdomains reveals their function as sorting machineries toward exosomes. *J Biol Chem,* 288**,** 11649-61.

PESCHKA, B., LEYGRAAF, J., VAN DER VEN, K., MONTAG, M., SCHARTMANN, B., SCHUBERT, R., VAN DER VEN, H. & SCHWANITZ, G. 1999. Type and frequency of chromosome aberrations in 781 couples undergoing intracytoplasmic sperm injection. *Human Reproduction,* 14**,** 2257-2263.

PETROS, R. A. & DESIMONE, J. M. 2010. Strategies in the design of nanoparticles for therapeutic applications. *Nat Rev Drug Discov,* 9**,** 615-27.

PETRUNKINA, A. M., WABERSKI, D., BOLLWEIN, H. & SIEME, H. 2010. Identifying non-sperm particles during flow cytometric physiological assessment: a simple approach. *Theriogenology,* 73**,** 995-1000.

PIEHL, L. L., FISCHMAN, M. L., HELLMAN, U., CISALE, H. & MIRANDA, P. V. 2013. Boar seminal plasma exosomes: effect on sperm function and protein identification by sequencing. *Theriogenology,* 79**,** 1071-82.

PIERIK, F. H., VAN GINNEKEN, A. M., DOHLE, G. R., VREEBURG, J. T. & WEBER, R. F. 2000. The advantages of standardized evaluation of male infertility. *Int J Androl,* 23**,** 340-6.

PIOMBONI, P., GOVERNINI, L., GORI, M., PUGGIONI, E., COSTANTINO-CECCARINI, E. & LUDDI, A. 2014. New Players in the Infertility of a Mouse Model of Lysosomal Storage Disease: The Hypothalamus-Pituitary-Gonadal Axis. *Front Endocrinol,* 4.

PISITKUN, T., SHEN, R. F. & KNEPPER, M. A. 2004. Identification and proteomic profiling of exosomes in human urine. *Proc Natl Acad Sci U S A,* 101**,** 13368-73.

POLIAKOV, A., SPILMAN, M., DOKLAND, T., AMLING, C. L. & MOBLEY, J. A. 2009. Structural heterogeneity and protein composition of exosome-like vesicles (prostasomes) in human semen. *Prostate,* 69**,** 159-67.

POMA, A., COLAFARINA, S., FONTECCHIO, G. & CHICHIRICCÒ, G. 2014. Transgenerational effects of NMs. *Adv Exp Med Biol,* 811**,** 235-54.

PONSAERTS, R., DE VUYST, E., RETAMAL, M., D'HONDT, C., VERMEIRE, D., WANG, N., DE SMEDT, H., ZIMMERMANN, P., HIMPENS, B., VEREECKE, J., LEYBAERT, L. & BULTYNCK, G. 2010. Intramolecular loop/tail interactions are essential for connexin 43-hemichannel activity. *The FASEB Journal,* 24**,** 4378-4395.

PONS-REJRAJI, H., ARTONNE, C., SION, B., BRUGNON, F., CANIS, M., JANNY, L. & GRIZARD, G. 2011. Prostasomes: inhibitors of capacitation and modulators of cellular signalling in human sperm. *Int J Androl,* 34**,** 568-80.

PRACTICE COMMITTEES OF THE AMERICAN SOCIETY FOR REPRODUCTIVE MEDICINE AND SOCIETY FOR ASSISTED REPRODUCTIVE TECHNOLOGY, S. P., MARC FRITZ, JEFFREY GOLDBERG, R DALE MCCLURE, ROGER LOBO, MICHAEL THOMAS, ERIC WIDRA, GLENN SCHATTMAN, MARK LICHT, JOHN COLLINS, MARCELLE CEDARS, CATHERINE RACOWSKY, MICHAEL VERNON, OWEN DAVIS, KURT BARNHART, CLARISA GRACIA, KIM THORNTON, WILLIAM CATHERINO, ROBERT REBAR, ANDREW LA BARBERA 2012. Intracytoplasmic sperm injection (ICSI) for non-male factor infertility: a committee opinion. *Fertil Steril,* 98**,** 1395-9.

PRETORIUS, E., FRANKEN, D. R., DE WET, J. & GROBLER, S. 1984. Sperm selection capacity of cervical mucus. *Arch Androl,* 12**,** 5-7.

POPULATION.UN.ORG. 2019. United Nations, Department of Economic and Social Affairs, Population Dynamics. World Population Prospects: the 2019 Revision, Key Findings and Advance Tables; 2019. Available at: <https://population.un.org/wpp/Graphs/Probabilistic/FERT/TOT/947> [Accessed 10 June 2020].

QIN, J., LIU, X., SHENG, X., WANG, H. & GAO, S. 2016. Assisted reproductive technology and the risk of pregnancy-related complications and adverse pregnancy outcomes in singleton pregnancies: a meta-analysis of cohort studies. *Fertil Steril,* 105**,** 73-85.e1-6.

RAMIÓ, L., RIVERA, M. M., RAMÍREZ, A., CONCHA, II, PEÑA, A., RIGAU, T. & RODRÍGUEZ-GIL, J. E. 2008. Dynamics of motile-sperm subpopulation structure in boar ejaculates subjected to "in vitro" capacitation and further "in vitro" acrosome reaction. *Theriogenology,* 69**,** 501-12.

RAMIÓ-LLUCH, L., FERNÁNDEZ-NOVELL, J. M., PEÑA, A., COLÁS, C., CEBRIÁN-PÉREZ, J. A., MUIÑO-BLANCO, T., RAMÍREZ, A., CONCHA, II, RIGAU, T. & RODRÍGUEZ-GIL, J. E. 2011. 'In vitro' capacitation and acrosome reaction are concomitant with specific changes in mitochondrial activity in boar sperm: evidence for a nucleated mitochondrial activation and for the existence of a capacitation-sensitive subpopulational structure. *Reprod Domest Anim,* 46**,** 664-73.

RAMOS-IBEAS, P., HERAS, S., GOMEZ-REDONDO, I., PLANELLS, B., FERNANDEZ-GONZALEZ, R., PERICUESTA, E., LAGUNA-BARRAZA, R., PEREZ-CEREZALES, S. & GUTIERREZ-ADAN, A. 2019. Embryo responses to stress induced by assisted reproductive technologies. *Mol Reprod Dev,* 86**,** 1292-1306.

RAPOSO, G., NIJMAN, H. W., STOORVOGEL, W., LIEJENDEKKER, R., HARDING, C. V., MELIEF, C. J. & GEUZE, H. J. 1996. B lymphocytes secrete antigen-presenting vesicles. *J Exp Med,* 183**,** 1161-72.

RAPOSO, G. & STOORVOGEL, W. 2013. Extracellular vesicles: exosomes, microvesicles, and friends. *J Cell Biol,* 200**,** 373-83.

RATAJCZAK, J., MIEKUS, K., KUCIA, M., ZHANG, J., RECA, R., DVORAK, P. & RATAJCZAK, M. Z. 2006a. Embryonic stem cell-derived microvesicles reprogram hematopoietic progenitors: evidence for horizontal transfer of mRNA and protein delivery. *Leukemia,* 20**,** 847-56.

RATAJCZAK, J., WYSOCZYNSKI, M., HAYEK, F., JANOWSKA-WIECZOREK, A. & RATAJCZAK, M. Z. 2006b. Membrane-derived microvesicles: important and underappreciated mediators of cell-to-cell communication. *Leukemia,* 20**,** 1487-95.

REDMAN, C. W. & SARGENT, I. L. 2007. Microparticles and immunomodulation in pregnancy and pre-eclampsia. *J Reprod Immunol,* 76**,** 61-7.

RESTELLI, L., PAFFONI, A., CORTI, L., RABELLOTTI, E., MANGIARINI, A., VIGANO, P., SOMIGLIANA, E. & PAPALEO, E. 2014. The strategy of group embryo culture based on pronuclear pattern on blastocyst development: a two center analysis. *J Assist Reprod Genet,* 31**,** 1629-34.

RIBEIRO-RODRIGUES, T. M., MARTINS-MARQUES, T., MOREL, S., KWAK, B. R. & GIRÃO, H. 2017. Role of connexin 43 in different forms of intercellular communication – gap junctions, extracellular vesicles and tunnelling nanotubes. *Journal of Cell Science,* 130**,** 3619-3630.

RIENZI, L., UBALDI, F., MARTINEZ, F., IACOBELLI, M., MINASI, M. G., FERRERO, S., TESARIK, J. & GRECO, E. 2003. Relationship between meiotic spindle location with regard to the polar body position and oocyte developmental potential after ICSI. *Human Reproduction,* 18**,** 1289-1293.

RODRIGUEZ-CARO, H., DRAGOVIC, R., SHEN, M., DOMBI, E., MOUNCE, G., FIELD, K., MEADOWS, J., TURNER, K., LUNN, D., CHILD, T., SOUTHCOMBE, J. H. & GRANNE, I. 2019. In vitro decidualisation of human endometrial stromal cells is enhanced by seminal fluid extracellular vesicles. *Journal of extracellular vesicles,* 8**,** 1565262-1565262.

RONQUIST, G. & BRODY, I. 1985. The prostasome: its secretion and function in man. *Biochim Biophys Acta,* 822**,** 203-18.

RONQUIST, G., FABIANI, R., JIN, M., NILSSON, B. O., ELENBRING, K. & HJERTEN, S. 1996. Adherence of Human Prostasomes to Mouse Spermatozoa and Their Displacement by Monoclonal Antibodies as Revealed by Free Zone Electrophoresis. *Archives of Andrology,* 36**,** 101-107.

RONQUIST, G., NILSSON, B. O. & HJERTËN, S. 1990. Interaction Between Prostasomes and Spermatozoa From Human Semen. *Archives of Andrology,* 24**,** 147-157.

ROWE, P. J., COMHAIRE, F. H., HARGREAVE, T. B. & MAHMOUD, A. M. 2000. *WHO manual for the standardized investigation and diagnosis of the infertile male*, Cambridge University Press.

RUISS, R., JOCHUM, S., MOCIKAT, R., HAMMERSCHMIDT, W. & ZEIDLER, R. 2011. EBV-gp350 confers B-cell tropism to tailored exosomes and is a neo-antigen in normal and malignant B cells--a new option for the treatment of B-CLL. *PloS one,* 6**,** e25294-e25294.

RURANGWA, E., KIME, D. E., OLLEVIER, F. & NASH, J. P. 2004. The measurement of sperm motility and factors affecting sperm quality in cultured fish. *Aquaculture,* 234**,** 1-28.

RUSSELL, L. D. & PETERSON, R. N. 1985. Sertoli cell junctions: morphological and functional correlates. *Int Rev Cytol,* 94**,** 177-211.

RUST, M. J., BATES, M. & ZHUANG, X. 2006. Sub-diffraction-limit imaging by stochastic optical reconstruction microscopy (STORM). *Nat Methods,* 3**,** 793-5.

SAADELDIN, I. M., KIM, S. J., CHOI, Y. B. & LEE, B. C. 2014. Improvement of cloned embryos development by co-culturing with parthenotes: a possible role of exosomes/microvesicles for embryos paracrine communication. *Cell Reprogram,* 16**,** 223-34.

SAEZ, F., FRENETTE, G. & SULLIVAN, R. 2003. Epididymosomes and Prostasomes: Their Roles in Posttesticular Maturation of the Sperm Cells. *Journal of Andrology,* 24**,** 149-154.

SAINT-POL, J., GOSSELET, F., DUBAN-DEWEER, S., POTTIEZ, G. & KARAMANOS, Y. 2020. Targeting and Crossing the Blood-Brain Barrier with Extracellular Vesicles. *Cells,* 9.

SALILEW-WONDIM, D., GEBREMEDHN, S., HOELKER, M., THOLEN, E., HAILAY, T. & TESFAYE, D. 2020. The Role of MicroRNAs in Mammalian Fertility: From Gametogenesis to Embryo Implantation. *Int J Mol Sci,* 21.

SALUNKHE, S., DHEERAJ, BASAK, M., CHITKARA, D. & MITTAL, A. 2020. Surface functionalization of exosomes for target-specific delivery and in vivo imaging & tracking: Strategies and significance. *J Control Release,* 326**,** 599-614.

SAN LUCAS, F. A., ALLENSON, K., BERNARD, V., CASTILLO, J., KIM, D. U., ELLIS, K., EHLI, E. A., DAVIES, G. E., PETERSEN, J. L., LI, D., WOLFF, R., KATZ, M., VARADHACHARY, G., WISTUBA, I., MAITRA, A. & ALVAREZ, H. 2016. Minimally invasive genomic and transcriptomic profiling of visceral cancers by next-generation sequencing of circulating exosomes. *Ann Oncol,* 27**,** 635-41.

SANDIN, S., NYGREN, K.-G., ILIADOU, A., HULTMAN, C. M. & REICHENBERG, A. 2013. Autism and Mental Retardation Among Offspring Born After In Vitro Fertilization. *JAMA,* 310**,** 75-84.

SASAKI, S., KOJIMA, Y., KUBOTA, H., TATSURA, H., HAYASHI, Y. & KOHRI, K. 2000. Effects of the gene transfer into sperm mediated by liposomes on sperm motility and fertilization in vitro. *Hinyokika kiyo. Acta urologica Japonica,* 46**,** 591-5.

SATO, M., TAKABAYASHI, S., AKASAKA, E. & NAKAMURA, S. 2020. Recent Advances and Future Perspectives of In Vivo Targeted Delivery of Genome-Editing Reagents to Germ Cells, Embryos, and Fetuses in Mice. *Cells,* 9.

SATO, T., SAKUMA, T., YOKONISHI, T., KATAGIRI, K., KAMIMURA, S., OGONUKI, N., OGURA, A., YAMAMOTO, T. & OGAWA, T. 2015. Genome Editing in Mouse Spermatogonial Stem Cell Lines Using TALEN and Double-Nicking CRISPR/Cas9. *Stem cell reports,* 5**,** 75-82.

SCHINDELL, B., WEBB, A. & KINDRACHUK, J. 2018. Persistence and Sexual Transmission of Filoviruses. *Viruses,* 10**,** 683.

SCHWARZ, A., WENNEMUTH, G., POST, H., BRANDENBURGER, T., AUMULLER, G. & WILHELM, B. 2013. Vesicular transfer of membrane components to bovine epididymal spermatozoa. *Cell Tissue Res,* 353**,** 549-61.

SERMONDADE, N., FAURE, C., FEZEU, L., SHAYEB, A. G., BONDE, J. P., JENSEN, T. K., VAN WELY, M., CAO, J., MARTINI, A. C., ESKANDAR, M., CHAVARRO, J. E., KOLOSZAR, S., TWIGT, J. M., RAMLAU-HANSEN, C. H., BORGES, E., JR., LOTTI, F., STEEGERS-THEUNISSEN, R. P., ZORN, B., POLOTSKY, A. J., LA VIGNERA, S., ESKENAZI, B., TREMELLEN, K., MAGNUSDOTTIR, E. V., FEJES, I., HERCBERG, S., LEVY, R. & CZERNICHOW, S. 2013. BMI in relation to sperm count: an updated systematic review and collaborative meta-analysis. *Hum Reprod Update,* 19**,** 221-31.

SHAMSI, M. B., KUMAR, K. & DADA, R. 2011. Genetic and epigenetic factors: Role in male infertility. *Indian J Urol,* 27**,** 110-20.

SHATERI, H., RANJBAR, A., KHEIRIPOUR, N., GHASEMI, H., POURFARJAM, Y., HABIBITABAR, E., GHOLAMI, H. & MORIDI, H. 2019. Tempol improves oxidant/antioxidant parameters in testicular tissues of diabetic rats. *Life Sciences,* 221**,** 65-71.

SHIGEMOTO-KURODA, T., OH, J. Y., KIM, D. K., JEONG, H. J., PARK, S. Y., LEE, H. J., PARK, J. W., KIM, T. W., AN, S. Y., PROCKOP, D. J. & LEE, R. H. 2017. MSC-derived Extracellular Vesicles Attenuate Immune Responses in Two Autoimmune Murine Models: Type 1 Diabetes and Uveoretinitis. *Stem Cell Reports,* 8**,** 1214-1225.

SHIMAOKA, M., KAWAMOTO, E., GAOWA, A., OKAMOTO, T. & PARK, E. J. 2019. Connexins and Integrins in Exosomes. *Cancers (Basel),* 11.

SHIN, D., LO, K. C. & LIPSHULTZ, L. I. 2005. Treatment options for the infertile male with cancer. *J Natl Cancer Inst Monogr*, 48-50.

SHOUKIR, Y., CHARDONNENS, D., CAMPANA, A. & SAKKAS, D. 1998. Blastocyst development from supernumerary embryos after intracytoplasmic sperm injection: a paternal influence? *Hum Reprod,* 13, 1632-7.

SICILIANO, L., MARCIANO, V. & CARPINO, A. 2008. Prostasome-like vesicles stimulate acrosome reaction of pig spermatozoa. *Reprod Biol Endocrinol,* 6, 5.

SIGISMUND, S., WOELK, T., PURI, C., MASPERO, E., TACCHETTI, C., TRANSIDICO, P., DI FIORE, P. P. & POLO, S. 2005. Clathrin-independent endocytosis of ubiquitinated cargos. *Proceedings of the National Academy of Sciences of the United States of America,* 102, 2760-2765.

SIEW, A., 2014. Current Issues With Nanomedicines. Pharmaceutical Technology. Available at: <http://www.pharmtech.com/current-issues-nanomedicines> [Accessed 10 June 2020].

SILVA, C. P., KOMMINENI, K., OLDENBOURG, R. & KEEFE, D. L. 1999. The first polar body does not predict accurately the location of the metaphase II meiotic spindle in mammalian oocytes. *Fertility and Sterility,* 71, 719-721

SIMON, B., BOLUMAR, D., AMADOZ, A., JIMENEZ-ALMAZAN, J., VALBUENA, D., VILELLA, F. & MORENO, I. 2020. Identification and Characterization of Extracellular Vesicles and Its DNA Cargo Secreted During Murine Embryo Development. *Genes (Basel),* 11.

SIMON, C., GREENING, D. W., BOLUMAR, D., BALAGUER, N., SALAMONSEN, L. A. & VILELLA, F. 2018. Extracellular Vesicles in Human Reproduction in Health and Disease. *Endocr Rev,* 39, 292-332.

SIMPSON, R. J., JENSEN, S. S. & LIM, J. W. 2008. Proteomic profiling of exosomes: current perspectives. *Proteomics,* 8, 4083-99.

SIU, M. K. Y. & CHENG, C. Y. 2004. Dynamic cross-talk between cells and the extracellular matrix in the testis. *BioEssays,* 26, 978-992.

SKIBINSKI, G., KELLY, R. W., HARKISS, D. & JAMES, K. 1992. Immunosuppression by human seminal plasma--extracellular organelles (prostasomes) modulate activity of phagocytic cells. *Am J Reprod Immunol,* 28, 97-103.

SLADE, P., O'NEILL, C., SIMPSON, A. J. & LASHEN, H. 2007. The relationship between perceived stigma, disclosure patterns, support and distress in new attendees at an infertility clinic. *Human Reproduction,* 22, 2309-2317.

SMITH, Z. J., LEE, C., ROJALIN, T., CARNEY, R. P., HAZARI, S., KNUDSON, A., LAM, K., SAARI, H., IBAÑEZ, E. L., VIITALA, T., LAAKSONEN, T., YLIPERTTULA, M. & WACHSMANN-HOGIU, S. 2015. Single exosome study reveals subpopulations distributed among cell lines with variability related to membrane content. *Journal of extracellular vesicles,* 4, 28533-28533.

SNOW-LISY, D. C., SABANEGH, E. S., SAMPLASKI, M. K. & LABHASETWAR, V. 2015. Anatomical Targeting Improves Delivery of Unconjugated Nanoparticles to the Testicle. *The Journal of Urology,* 194, 1155-1161.

SOARES, A. R., MARTINS-MARQUES, T., RIBEIRO-RODRIGUES, T., FERREIRA, J. V., CATARINO, S., PINHO, M. J., ZUZARTE, M., ISABEL ANJO, S., MANADAS, B., P G SLUIJTER, J., PEREIRA, P. & GIRAO, H. 2015. Gap junctional protein Cx43 is involved in the communication between extracellular vesicles and mammalian cells. *Scientific reports,* 5, 13243-13243.

SOHEL, M. M., HOELKER, M., NOFERESTI, S. S., SALILEW-WONDIM, D., THOLEN, E., LOOFT, C., RINGS, F., UDDIN, M. J., SPENCER, T. E., SCHELLANDER, K. & TESFAYE, D. 2013. Exosomal and Non-Exosomal Transport of Extra-Cellular microRNAs in Follicular Fluid: Implications for Bovine Oocyte Developmental Competence. *PLoS One,* 8**,** e78505.

SOKOLOVA, V., LUDWIG, A. K., HORNUNG, S., ROTAN, O., HORN, P. A., EPPLE, M. & GIEBEL, B. 2011. Characterisation of exosomes derived from human cells by nanoparticle tracking analysis and scanning electron microscopy. *Colloids Surf B Biointerfaces,* 87**,** 146-50.

SONG, S., GHOSH, J., MAINIGI, M., TURAN, N., WEINERMAN, R., TRUONGCAO, M., COUTIFARIS, C. & SAPIENZA, C. 2015. DNA methylation differences between in vitro- and in vivo-conceived children are associated with ART procedures rather than infertility. *Clin Epigenetics,* 7**,** 41.

SPEYER, B., O'NEILL, H., SAAB, W., SESHADRI, S., CAWOOD, S., HEATH, C., GAUNT, M. & SERHAL, P. 2019. In assisted reproduction by IVF or ICSI, the rate at which embryos develop to the blastocyst stage is influenced by the fertilization method used: a split IVF/ICSI study. *Journal of assisted reproduction and genetics,* 36**,** 647-654.

SPIELMANN, N. & WONG, D. T. 2011. Saliva: diagnostics and therapeutic perspectives. *Oral diseases,* 17**,** 345-354.

SRINIVASAKUMAR, N., OGRA, P. & FLANAGAN, T. 1991. Characteristics of fusion of respiratory syncytial virus with HEp-2 cells as measured by R18 fluorescence dequenching assay. *Journal of virology,* 65**,** 4063-4069.

STEGMAYR, B. & RONQUIST, G. 1982. Promotive effect on human sperm progressive motility by prostasomes. *Urol Res,* 10**,** 253-7.

STEPTOE, P. C. & EDWARDS, R. G. 1978. Birth after the reimplantation of a human embryo. *Lancet,* 2**,** 366.

STRAUSS, K., GOEBEL, C., RUNZ, H., MOBIUS, W., WEISS, S., FEUSSNER, I., SIMONS, M. & SCHNEIDER, A. 2010. Exosome secretion ameliorates lysosomal storage of cholesterol in Niemann-Pick type C disease. *J Biol Chem,* 285**,** 26279-88.

SUÁREZ, H., GÁMEZ-VALERO, A., REYES, R., LÓPEZ-MARTÍN, S., RODRÍGUEZ, M. J., CARRASCOSA, J. L., CABAÑAS, C., BORRÀS, F. E. & YÁÑEZ-MÓ, M. 2017. A bead-assisted flow cytometry method for the semi-quantitative analysis of Extracellular Vesicles. *Scientific Reports,* 7**,** 11271.

SULLIVAN, R., FRENETTE, G. & GIROUARD, J. 2007. Epididymosomes are involved in the acquisition of new sperm proteins during epididymal transit. *Asian J Androl,* 9**,** 483-91.

SUN, D., ZHUANG, X., XIANG, X., LIU, Y., ZHANG, S., LIU, C., BARNES, S., GRIZZLE, W., MILLER, D. & ZHANG, H. G. 2010. A novel nanoparticle drug delivery system: the anti-inflammatory activity of curcumin is enhanced when encapsulated in exosomes. *Mol Ther,* 18**,** 1606-14.

SUN, G. H., LIN, Y. C., GUO, Y. W., CHANG, S. Y. & LIU, H. W. 2000. Purification of GP-83, a glycoprotein secreted by the human epididymis and conjugated to mature spermatozoa. *Mol Hum Reprod,* 6**,** 429-34.

SUN, H., GONG, T. T., JIANG, Y. T., ZHANG, S., ZHAO, Y. H. & WU, Q. J. 2019. Global, regional, and national prevalence and disability-adjusted life-years for infertility in 195 countries and territories, 1990-2017: results from a global burden of disease study, 2017. *Aging (Albany NY),* 11**,** 10952-10991.

SUN, X. L., WANG, J. L., PENG, Y. P., GAO, Q. Q., SONG, T., YU, W., XU, Z. P., CHEN, Y. & DAI, Y. T. 2018. Bilateral is superior to unilateral varicocelectomy in infertile males with left clinical and right subclinical varicocele: a prospective randomized controlled study. *Int Urol Nephrol,* 50**,** 205-210.

SWAIN, J. E. 2019. Controversies in ART: can the IVF laboratory influence preimplantation embryo aneuploidy? *Reproductive BioMedicine Online,* 39**,** 599-607.

SZEBENI, J. 2001. Complement activation-related pseudoallergy caused by liposomes, micellar carriers of intravenous drugs, and radiocontrast agents. *Crit Rev Ther Drug Carrier Syst,* 18**,** 567-606.

TAN, L., WU, H., LIU, Y., ZHAO, M., LI, D. & LU, Q. 2016. Recent advances of exosomes in immune modulation and autoimmune diseases. *Autoimmunity,* 49**,** 357-365.

TANIGAWA, M., MIYAMOTO, K., KOBAYASHI, S., SATO, M., AKUTSU, H., OKABE, M., MEKADA, E., SAKAKIBARA, K., MIYADO, M., UMEZAWA, A. & MIYADO, K. 2008. Possible involvement of CD81 in acrosome reaction of sperm in mice. *Mol Reprod Dev,* 75**,** 150-5.

TANNETTA, D., DRAGOVIC, R., ALYAHYAEI, Z. & SOUTHCOMBE, J. 2014. Extracellular vesicles and reproduction-promotion of successful pregnancy. *Cell Mol Immunol,* 11**,** 548-63.

TAPIA, J., MACIAS-GARCIA, B., MIRO-MORAN, A., ORTEGA-FERRUSOLA, C., SALIDO, G., PEÑA, F. & APARICIO, I. 2012. The Membrane of the Mammalian Spermatozoa: Much More Than an Inert Envelope. *Reproduction in Domestic Animals,* 47**,** 65-75.

TARIO, J. D., JR., HUMPHREY, K., BANTLY, A. D., MUIRHEAD, K. A., MOORE, J. S. & WALLACE, P. K. 2012. Optimized staining and proliferation modeling methods for cell division monitoring using cell tracking dyes. *Journal of visualized experiments : JoVE***,** e4287-e4287.

TEMCHURA, V. V., TENBUSCH, M., NCHINDA, G., NABI, G., TIPPLER, B., ZELENYUK, M., WILDNER, O., UBERLA, K. & KUATE, S. 2008. Enhancement of immunostimulatory properties of exosomal vaccines by incorporation of fusion-competent G protein of vesicular stomatitis virus. *Vaccine,* 26**,** 3662-72.

TEIXEIRA, F. G., CARVALHO, M. M., PANCHALINGAM, K. M., RODRIGUES, A. J., MENDES-PINHEIRO, B., ANJO, S., MANADAS, B., BEHIE, L. A., SOUSA, N. & SALGADO, A. J. 2017. Impact of the Secretome of Human Mesenchymal Stem Cells on Brain Structure and Animal Behavior in a Rat Model of Parkinson's Disease. *Stem Cells Transl Med,* 6**,** 634-646.

TERADA, Y., LUETJENS, C. M., SUTOVSKY, P. & SCHATTEN, G. 2000. Atypical decondensation of the sperm nucleus, delayed replication of the male genome, and sex chromosome positioning following intracytoplasmic human sperm injection (ICSI) into golden hamster eggs: does ICSI itself introduce chromosomal anomalies? *Fertility and Sterility,* 74**,** 454-460.

TESARIK, J., MENDOZA, C. & GRECO, E. 2002. Paternal effects acting during the first cell cycle of human preimplantation development after ICSI. *Hum Reprod,* 17**,** 184-9.

THERY, C., AMIGORENA, S., RAPOSO, G. & CLAYTON, A. 2006. Isolation and characterization of exosomes from cell culture supernatants and biological fluids. *Curr Protoc Cell Biol,* Chapter 3**,** Unit 3 22.

THERY, C., BOUSSAC, M., VERON, P., RICCIARDI-CASTAGNOLI, P., RAPOSO, G., GARIN, J. & AMIGORENA, S. 2001. Proteomic analysis of dendritic cell-derived exosomes: a secreted subcellular compartment distinct from apoptotic vesicles. *J Immunol,* 166**,** 7309-18.

THÉRY, C., OSTROWSKI, M. & SEGURA, E. 2009. Membrane vesicles as conveyors of immune responses. *Nat Rev Immunol,* 9**,** 581-93.

THERY, C., WITWER, K. W., AIKAWA, E., ALCARAZ, M. J., ANDERSON, J. D., ANDRIANTSITOHAINA, R., ANTONIOU, A., ARAB, T., ARCHER, F., ATKIN-SMITH, G. K., AYRE, D. C., BACH, J. M., BACHURSKI, D., BAHARVAND, H., BALAJ, L., BALDACCHINO, S., BAUER, N. N., BAXTER, A. A., BEBAWY, M., BECKHAM, C., BEDINA ZAVEC, A., BENMOUSSA, A., BERARDI, A. C., BERGESE, P., BIELSKA, E., BLENKIRON, C., BOBIS-WOZOWICZ, S., BOILARD, E., BOIREAU, W., BONGIOVANNI, A., BORRAS, F. E., BOSCH, S., BOULANGER, C. M., BREAKEFIELD, X., BREGLIO, A. M., BRENNAN, M. A., BRIGSTOCK, D. R., BRISSON, A., BROEKMAN, M. L., BROMBERG, J. F., BRYL-GORECKA, P., BUCH, S., BUCK, A. H., BURGER, D., BUSATTO, S., BUSCHMANN, D., BUSSOLATI, B., BUZAS, E. I., BYRD, J. B., CAMUSSI, G., CARTER, D. R., CARUSO, S., CHAMLEY, L. W., CHANG, Y. T., CHEN, C., CHEN, S., CHENG, L., CHIN, A. R., CLAYTON, A., CLERICI, S. P., COCKS, A., COCUCCI, E., COFFEY, R. J., CORDEIRO-DA-SILVA, A., COUCH, Y., COUMANS, F. A., COYLE, B., CRESCITELLI, R., CRIADO, M. F., D'SOUZA-SCHOREY, C., DAS, S., DATTA CHAUDHURI, A., DE CANDIA, P., DE SANTANA, E. F., DE WEVER, O., DEL PORTILLO, H. A., DEMARET, T., DEVILLE, S., DEVITT, A., DHONDT, B., DI VIZIO, D., DIETERICH, L. C., DOLO, V., DOMINGUEZ RUBIO, A. P., DOMINICI, M., DOURADO, M. R., DRIEDONKS, T. A., DUARTE, F. V., DUNCAN, H. M., EICHENBERGER, R. M., EKSTROM, K., EL ANDALOUSSI, S., ELIE-CAILLE, C., ERDBRUGGER, U., FALCON-PEREZ, J. M., FATIMA, F., FISH, J. E., FLORES-BELLVER, M., FORSONITS, A., FRELET-BARRAND, A., et al. 2018. Minimal information for studies of extracellular vesicles 2018 (MISEV2018): a position statement of the International Society for Extracellular Vesicles and update of the MISEV2014 guidelines. *J Extracell Vesicles,* 7**,** 1535750.

TIAN, T., WANG, Y., WANG, H., ZHU, Z. & XIAO, Z. 2010. Visualizing of the cellular uptake and intracellular trafficking of exosomes by live-cell microscopy. *J Cell Biochem,* 111**,** 488-96.

TIAN, T., ZHU, Y. L., HU, F. H., WANG, Y. Y., HUANG, N. P. & XIAO, Z. D. 2013. Dynamics of exosome internalization and trafficking. *J Cell Physiol,* 228**,** 1487-95.

TIAN, Y., LI, S., SONG, J., JI, T., ZHU, M., ANDERSON, G. J., WEI, J. & NIE, G. 2014. A doxorubicin delivery platform using engineered natural membrane vesicle exosomes for targeted tumor therapy. *Biomaterials,* 35**,** 2383-2390.

TRUMMER, A., DE ROP, C., TIEDE, A., GANSER, A. & EISERT, R. 2009. Recovery and composition of microparticles after snap-freezing depends on thawing temperature. *Blood Coagulation & Fibrinolysis,* 20.

TONG, M. & CHAMLEY, L. W. 2015. Placental extracellular vesicles and feto-maternal communication. *Cold Spring Harb Perspect Med,* 5**,** a023028.

TORO, E., FERNÁNDEZ, S., COLOMAR, A., CASANOVAS, A., ÁLVAREZ, J. G., LÓPEZ-TEIJÓN, M. & VELILLA, E. 2009. Processing of semen can result in increased sperm DNA fragmentation. *Fertility and Sterility,* 92**,** 2109-2112.

TOURNAYE, H. 2012. Male factor infertility and ART. *Asian J Androl,* 14**,** 103-8.

TRAJKOVIC, K., HSU, C., CHIANTIA, S., RAJENDRAN, L., WENZEL, D., WIELAND, F., SCHWILLE, P., BRÜGGER, B. & SIMONS, M. 2008. Ceramide triggers budding of exosome vesicles into multivesicular endosomes. *Science,* 319**,** 1244-7.

TROIANO, L., GRANATA, A. R., COSSARIZZA, A., KALASHNIKOVA, G., BIANCHI, R., PINI, G., TROPEA, F., CARANI, C. & FRANCESCHI, C. 1998. Mitochondrial membrane potential and DNA stainability in human sperm cells: a flow cytometry analysis with implications for male infertility. *Exp Cell Res,* 241**,** 384-93.

TSAI, P.-S., GARCIA-GIL, N., VAN HAEFTEN, T. & GADELLA, B. M. 2010. How Pig Sperm Prepares to Fertilize: Stable Acrosome Docking to the Plasma Membrane. *PLOS ONE,* 5**,** e11204.

TULLOCH, W. S. 1955. Varicocele in subfertility; results of treatment. *Br Med J,* 2**,** 356-8.

TURNER, K. A., RAMBHATLA, A., SCHON, S., AGARWAL, A., KRAWETZ, S. A., DUPREE, J. M. & AVIDOR-REISS, T. 2020. Male Infertility is a Women's Health Issue-Research and Clinical Evaluation of Male Infertility Is Needed. *Cells,* 9**,** 990.

VALADI, H., EKSTRÖM, K., BOSSIOS, A., SJÖSTRAND, M., LEE, J. J. & LÖTVALL, J. O. 2007. Exosome-mediated transfer of mRNAs and microRNAs is a novel mechanism of genetic exchange between cells. *Nat Cell Biol,* 9**,** 654-9.

VALAPALA, M. & VISHWANATHA, J. K. 2011. Lipid raft endocytosis and exosomal transport facilitate extracellular trafficking of annexin A2. *J Biol Chem,* 286**,** 30911-25.

VAN ASSCHE, E., BONDUELLE, M., TOURNAYE, H., JORIS, H., VERHEYEN, G., DEVROEY, P., VAN STEIRTEGHEM, A. & LIEBAERS, I. 1996. Cytogenetics of infertile men. *Human Reproduction,* 11**,** 1-26.

VAN DER POL, E., BÖING, A. N., HARRISON, P., STURK, A. & NIEUWLAND, R. 2012. Classification, functions, and clinical relevance of extracellular vesicles. *Pharmacol Rev,* 64**,** 676-705.

VAN NIEL, G., PORTO-CARREIRO, I., SIMOES, S. & RAPOSO, G. 2006. Exosomes: a common pathway for a specialized function. *J Biochem,* 140**,** 13-21.

VAN RUMSTE, M. M., EVERS, J. L. & FARQUHAR, C. M. 2004. ICSI versus conventional techniques for oocyte insemination during IVF in patients with non-male factor subfertility: a Cochrane review. *Hum Reprod,* 19**,** 223-7.

VELANDO, A., TORRES, R. & ALONSO-ALVAREZ, C. 2008. Avoiding bad genes: oxidatively damaged DNA in germ line and mate choice. *Bioessays,* 30**,** 1212-9.

VERSTEGEN, J., IGUER-OUADA, M. & ONCLIN, K. 2002. Computer assisted semen analyzers in andrology research and veterinary practice. *Theriogenology,* 57**,** 149-79.

VIAUD, S., PLOIX, S., LAPIERRE, V., THERY, C., COMMERE, P. H., TRAMALLONI, D., GORRICHON, K., VIRAULT-ROCROY, P., TURSZ, T., LANTZ, O., ZITVOGEL, L. & CHAPUT, N. 2011. Updated technology to produce highly immunogenic dendritic cell-derived exosomes of clinical grade: a critical role of interferon-gamma. *J Immunother,* 34**,** 65-75.

VICENTE-CARRILLO, A., ALVAREZ-RODRIGUEZ, M. & RODRIGUEZ-MARTINEZ, H. 2017. The CatSper channel modulates boar sperm motility during capacitation. *Reprod Biol,* 17**,** 69-78.

VILELLA, F., MORENO-MOYA, J. M., BALAGUER, N., GRASSO, A., HERRERO, M., MARTINEZ, S., MARCILLA, A. & SIMON, C. 2015. Hsa-miR-30d, secreted by the human endometrium, is taken up by the pre-implantation embryo and might modify its transcriptome. *Development,* 142**,** 3210-21.

VLASSOV, A. V., MAGDALENO, S., SETTERQUIST, R. & CONRAD, R. 2012. Exosomes: current knowledge of their composition, biological functions, and diagnostic and therapeutic potentials. *Biochim Biophys Acta,* 1820**,** 940-8.

VOJTECH, L., WOO, S., HUGHES, S., LEVY, C., BALLWEBER, L., SAUTERAUD, R. P., STROBL, J., WESTERBERG, K., GOTTARDO, R., TEWARI, M. & HLADIK, F. 2014. Exosomes in human semen carry a distinctive repertoire of small non-coding RNAs with potential regulatory functions. *Nucleic Acids Res,* 42**,** 7290-304.

WAGNER, V., DULLAART, A., BOCK, A. K. & ZWECK, A. 2006. The emerging nanomedicine landscape. *Nat Biotechnol,* 24**,** 1211-7.

WAHLGREN, J., DE L KARLSON, T., BRISSLERT, M., VAZIRI SANI, F., TELEMO, E., SUNNERHAGEN, P. & VALADI, H. 2012. Plasma exosomes can deliver exogenous short interfering RNA to monocytes and lymphocytes. *Nucleic acids research,* 40**,** e130-e130.

WANG, J., JIANG, Q., FALETI, O. D., TSANG, C.-M., ZHAO, M., WU, G., TSAO, S.-W., FU, M., CHEN, Y., DING, T., CHONG, T., LONG, Y., YANG, X., ZHANG, Y., CAI, Y., LI, H., PENG, M., LYU, X. & LI, X. 2020. Exosomal Delivery of AntagomiRs Targeting Viral and Cellular MicroRNAs Synergistically Inhibits Cancer Angiogenesis. *Molecular Therapy - Nucleic Acids,* 22**,** 153-165.

WANG, W.-H., MENG, L., HACKETT, R. J., ODENBOURG, R. & KEEFE, D. L. 2001. The spindle observation and its relationship with fertilization after intracytoplasmic sperm injection in living human oocytes. *Fertility and Sterility,* 75**,** 348-353.

WANG, X., SHARMA, R. K., GUPTA, A., GEORGE, V., THOMAS, A. J., FALCONE, T. & AGARWAL, A. 2003. Alterations in mitochondria membrane potential and oxidative stress in infertile men: a prospective observational study. *Fertil Steril,* 80 Suppl 2**,** 844-50.

WARD, W. S. 2010. Function of sperm chromatin structural elements in fertilization and development. *Mol Hum Reprod,* 16**,** 30-6.

WARD, W. S. 2011. Regulating DNA supercoiling: sperm points the way. *Biol Reprod,* 84**,** 841-3.

WATSON, D. C., YUNG, B. C., BERGAMASCHI, C., CHOWDHURY, B., BEAR, J., STELLAS, D., MORALES-KASTRESANA, A., JONES, J. C., FELBER, B. K., CHEN, X. & PAVLAKIS, G. N. 2018. Scalable, cGMP-compatible purification of extracellular vesicles carrying bioactive human heterodimeric IL-15/lactadherin complexes. *J Extracell Vesicles,* 7**,** 1442088.

WEBBER, J. & CLAYTON, A. 2013. How pure are your vesicles? *J Extracell Vesicles,* 2**,** 10.3402/jev.v2i0.19861.

WIKLANDER, O. P., NORDIN, J. Z., O'LOUGHLIN, A., GUSTAFSSON, Y., CORSO, G., MÄGER, I., VADER, P., LEE, Y., SORK, H., SEOW, Y., HELDRING, N., ALVAREZ-ERVITI, L., SMITH, C. I., LE BLANC, K., MACCHIARINI, P., JUNGEBLUTH, P., WOOD, M. J. & ANDALOUSSI, S. E. 2015. Extracellular Vesicle In Vivo Biodistribution is Determined by Cell Source, Route of Administration and Targeting. *J Extracell Vesicles,* 4**,** 26316.

WINTERS, B. R. & WALSH, T. J. 2014. The Epidemiology of Male Infertility. *Urol Clin North Am,* 41**,** 195-204.

WITTE, T. S. & SCHÄFER-SOMI, S. 2007. Involvement of Cholesterol, Calcium and Progesterone in the Induction of Capacitation and Acrosome Reaction of Mammalian Spermatozoa. *Anim Reprod Sci,* 102**,** 181-93.

WITWER, K. W., SOEKMADJI, C., HILL, A. F., WAUBEN, M. H., BUZAS, E. I., DI VIZIO, D., FALCON-PEREZ, J. M., GARDINER, C., HOCHBERG, F., KUROCHKIN, I. V., LOTVALL, J., MATHIVANAN, S., NIEUWLAND, R., SAHOO, S., TAHARA, H., TORRECILHAS, A. C., WEAVER, A. M., YIN, H., ZHENG, L., GHO, Y. S., QUESENBERRY, P. & THERY, C. 2017. Updating the MISEV Minimal Requirements for Extracellular Vesicle Studies: Building Bridges to Reproducibility. *J Extracell Vesicles,* 6**,** 1396823.

WITWER, K. W. & THERY, C. 2019. Extracellular Vesicles or Exosomes? On Primacy, Precision, and Popularity Influencing a Choice of Nomenclature. *J Extracell Vesicles,* 8**,** 1648167.

WU, Y., ZHOU, H., FAN, X., ZHANG, Y., ZHANG, M., WANG, Y., XIE, Z., BAI, M., YIN, Q., LIANG, D., TANG, W., LIAO, J., ZHOU, C., LIU, W., ZHU, P., GUO, H., PAN, H., WU, C., SHI, H., WU, L., TANG, F. & LI, J. 2015. Correction of a Genetic Disease by CRISPR-Cas9-Mediated Gene Editing in Mouse Spermatogonial Stem Cells. *Cell Res,* 25**,** 67-79.

YAN, I. K., SHUKLA, N., BORRELLI, D. A. & PATEL, T. 2018. Use of a Hollow Fiber Bioreactor to Collect Extracellular Vesicles from Cells in Culture. *Methods Mol Biol,* 1740**,** 35-41.

YANAGIMACHI, R. 1994. Mammalian fertilization. *The Physiology of Reproduction*.

YESTE, M. 2013. Boar Spermatozoa Within the Oviductal Environment (II): Sperm Capacitation. *In:* BONET, S., CASAS, I., HOLT, W. V. & YESTE, M. (eds.) *Boar Reproduction: Fundamentals and New Biotechnological Trends.* Berlin, Heidelberg: Springer Berlin Heidelberg.

YESTE, M., FERNÁNDEZ-NOVELL, J. M., RAMIÓ-LLUCH, L., ESTRADA, E., ROCHA, L. G., CEBRIÁN-PÉREZ, J. A., MUIÑO-BLANCO, T., CONCHA, II, RAMÍREZ, A. & RODRÍGUEZ-GIL, J. E. 2015. Intracellular Calcium Movements of Boar Spermatozoa during 'In Vitro' Capacitation and Subsequent Acrosome Exocytosis follow a Multiple-Storage Place, Extracellular Calcium-Dependent Model. *Andrology,* 3**,** 729-47.

YIN, K., WANG, S. & ZHAO, R. C. 2019. Exosomes from Mesenchymal Stem/Stromal Cells: a New Therapeutic Paradigm. *Biomark Res,* 7**,** 8.

YOSHIDA, A., MIURA, K. & SHIRAI, M. 1997. Cytogenetic Survey of 1,007 Infertile Males. *Urol Int,* 58**,** 166-76.

YOSHIDA, S., HIYOSHI, K., ICHINOSE, T., TAKANO, H., OSHIO, S., SUGAWARA, I., TAKEDA, K. & SHIBAMOTO, T. 2009. Effect of Nanoparticles on the Male Reproductive System of Mice. *Int J Androl,* 32**,** 337-42.

YOU, Y. & IKEZU, T. 2019. Emerging roles of Extracellular Vesicles in Neurodegenerative Disorders. *Neurobiol Dis,* 130**,** 104512.

ZABEO, D., CVJETKOVIC, A., LÄSSER, C., SCHORB, M., LÖTVALL, J. & HÖÖG, J. L. 2017. Exosomes Purified from a Single Cell Type have Diverse Morphology. *J Extracell Vesicles,* 6**,** 1329476.

ZHANG, J., LI, S., LI, L., LI, M., GUO, C., YAO, J. & MI, S. 2015. Exosome and Exosomal MicroRNA: Trafficking, Sorting, and Function. *Genom Proteom Bioinform,* 13**,** 17-24.

ZHANG, W., ZHANG, J., CHENG, L., NI, H., YOU, B., SHAN, Y., BAO, L., WU, D., ZHANG, T., YUE, H. & CHEN, J. 2018. A Disintegrin and Metalloprotease 10-Containing Exosomes Derived from Nasal Polyps Promote Angiogenesis and Vascular Permeability. *Mol Med Rep,* 17**,** 5921-5927.

ZHOU, W., STANGER, S. J., ANDERSON, A. L., BERNSTEIN, I. R., DE IULIIS, G. N., MCCLUSKEY, A., MCLAUGHLIN, E. A., DUN, M. D. & NIXON, B. 2019. Mechanisms of Tethering and Cargo Transfer during Epididymosome-Sperm Interactions. *BMC Biol,* 17**,** 35.

ZHUANG, X., XIANG, X., GRIZZLE, W., SUN, D., ZHANG, S., AXTELL, R. C., JU, S., MU, J., ZHANG, L., STEINMAN, L., MILLER, D. & ZHANG, H. G. 2011. Treatment of Brain Inflammatory Diseases by Delivering Exosome Encapsulated Anti-Inflammatory Drugs from the Nasal Region to the Brain. *Mol Ther,* 19**,** 1769-79.

ZIGO, M., MAŇÁSKOVÁ-POSTLEROVÁ, P., ZUIDEMA, D., KERNS, K., JONÁKOVÁ, V., TŮMOVÁ, L., BUBENÍČKOVÁ, F. & SUTOVSKY, P. 2020. Porcine model for the study of sperm capacitation, fertilization and male fertility. *Cell and Tissue Research,* 380**,** 237-262.

ZITVOGEL, L., REGNAULT, A., LOZIER, A., WOLFERS, J., FLAMENT, C., TENZA, D., RICCIARDI-CASTAGNOLI, P., RAPOSO, G. & AMIGORENA, S. 1998. Eradication of Established Murine Tumors Using a Novel Cell-Free Vaccine: Dendritic Cell-Derived Exosomes. *Nat Med,* 4**,** 594-600.

Appendix I

NTA Graphs Displaying the Differences in Size and Concentration Profiles of HEK293T-derived Exosomes Processed in Different Ways

I.I The Effect of Freeze/Thaw cycles

For long-term storage for no more than 3 months, HEK293T-derived exosomes are frozen at –80ºC. Upon their use with the samples, the frozen HEK293T-derived samples are thawed at RT. These free/thaw cycle has been reported to be detrimental for the vesicles' membrane integrity (Dey-Hazra et al., 2010), and therefore, the use of fresh samples is recommended when possible (Thery et al., 2006).

A graph displaying the size and concentration profiles of a sample of HEK293T-derived exosomes before and after freezing (fresh and thawed respectively) is provided in **Figure A.I.I**. As seen in the graph, the fresh sample had double the concentration than after undergoing a freeze/thaw cycle, and mode size of the vesicles present was also smaller, suggesting that free/thawing may disrupt the physicochemical properties of the membrane in such a way that it becomes more fluid and therefore prone to fuse with other vesicles forming larger ones, or caused by aggregation via lipid rafts in the membrane as previously described in (Trummer et al., 2009), however, this effect does not severly impact the integrity of the samples as recognised in most studies, thus samples can be used for up to 4 freeze-thaw cycles (LACROIX et al., 2012, Bæk et al., 2016).

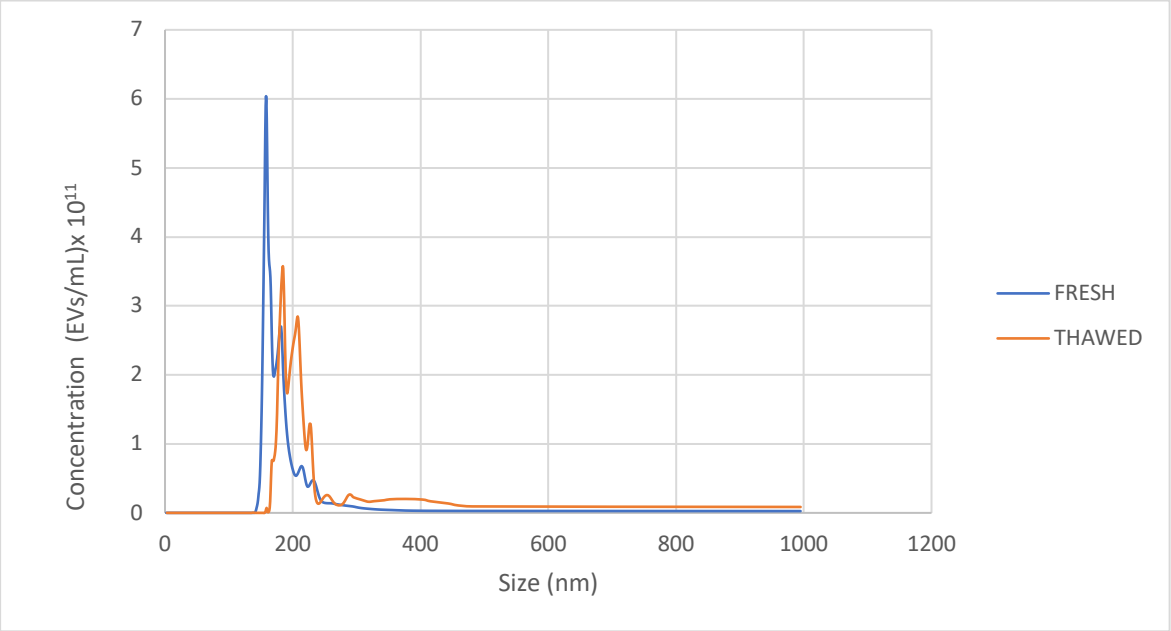

Figure A.I.I. NTA graph displaying the concentration (Y-axis) and size (x-axis) profiles of a HEK293T-derived sample before undergoing a freezing/thawing cycle. The fresh sample (blue curve) has a maximum concentration of 6.1 x 10^{11} EVs/mL and a mode size of 163 nm. The thawed sample (orange curve) has a maximum concentration of 3.6 x 10^{11} EVs/mL and a modal size of 200 nm.

I.II. The Effect of SEC washing step

For the fluorescence visualization of the HEK293T-derived exosomes under HRCM, Bio-Maleimide (BODIPY FL N-(2-aminoethyl) maleimide dye was used as described in **Chapter 4.4.1.** Following the labelling step, the HEK293T-derived samples were filtered through an Exo-spin column (Cell Guidances, UK) that combines precipitation with SEC to remove unbound dye, and therefore, as previously described, lower yields are expected from this additional washing step (Monguió-Tortajada et al., 2019). Graphs displaying the size and concentration profiles of thawed BODIPY-labelled and un-labelled HEK293T-derived exosomes to compare the effects of this treatment are provided in **Figure A.I.II**.

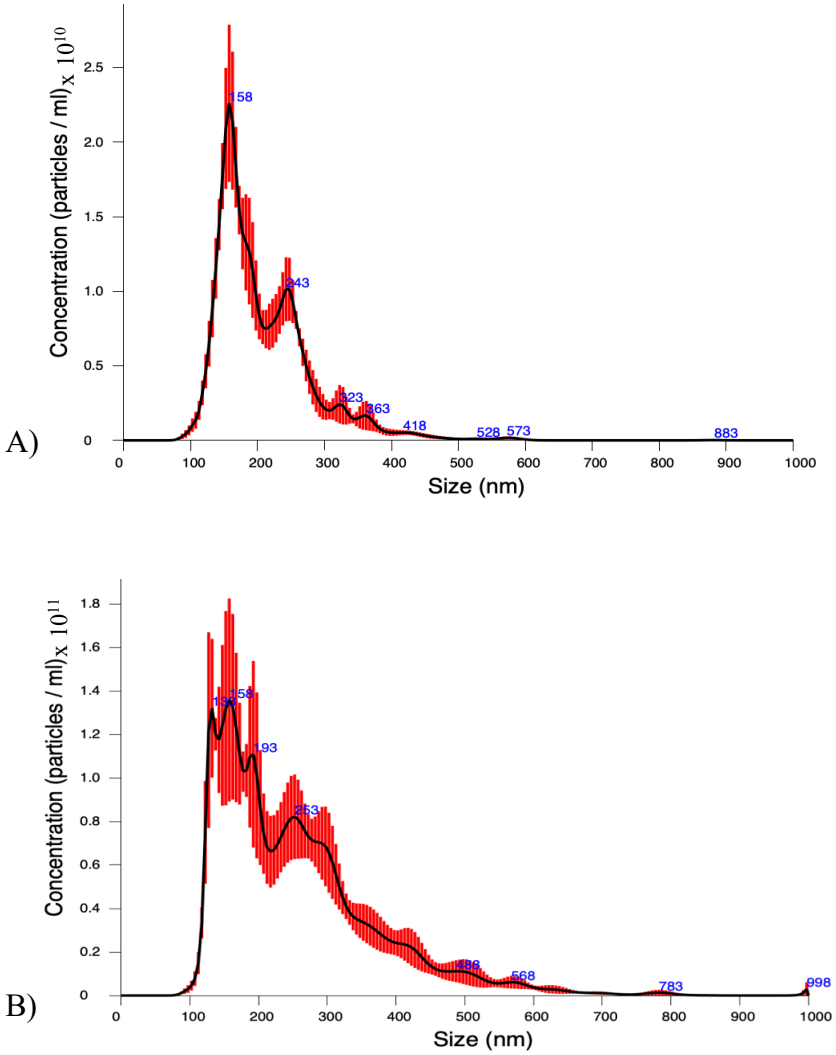

Figure A.I.II. NTA graphs displaying the concentration (Y-axis) and size (x-axis) profiles of A) BODIPY-labelled HEK293T-derived exosomes after undergoing SEC, exhibiting a concentration of 2.2 x 10^{10} EV/mL and mode size of 158 nm. B) unlabeled HEK293T-derived exosomes without undergoing SEC, displaying a concentration of 1.38 x 1011 EV/mL and mode size of 150 nm.

As it can be seen, the graph in **Figure A.I.II.A** displaying the profile of the BODIPY-exosomes after their washing up through a SEC column is more sharp; displays one bigger peak of an exosome population of 158 nm and as well as a considerably smaller peak for an exosome population of 243 nm. The HEK293T-derived samples that have been isolated with UC compared to those that undergo an additional SEC step, present many more different populations of vesicles as represented by several peaks in **Figure A.I.II.B**, and also a higher concentration of exosomes (the population of size 158 nm) as expected.

Appendix II

Visual Evidence of Capacitation and Acrosome Reaction in Boar Sperm Samples Co-Incubated with HEK293T-derived Exosomes under Capacitating Conditions

As part of the analysis to show that the sperm have undergone capacitation and have fully acrosome reacted *in vitro* there is a visual technique based on the staining with lectins (Jimenez et al., 2003). The authors of this paper identified a change in the distribution of surface carbohydrates in boar spermatozoa during capacitation and AR which can be labelled with Wheat-germ agglutinin. Therefore, further confirmation that the boar sperm samples that I have co-incubated with the HEK293T-derived exosomes under capacitating conditions have indeed undergone the full capacitation process, including acrosome reaction adding to the functional analyses carried out to show this in **Chapter 3**, as it can be seen in the image below taken with the TIRFM for the condition 100:1 at 5 h post-incubation in one of the experiments carried out for the visual localization of CD9, within the fixed boar sperm samples (labelled with AlexaFluor647 post-fixation) and the HEK293T-derived exosomes in **Chapter 4.4.2**. In this figure a clear enzymatic degradation and release of content can be seen at the level of the sperm head, as a result of the AR that has fully taken place (white arrow).

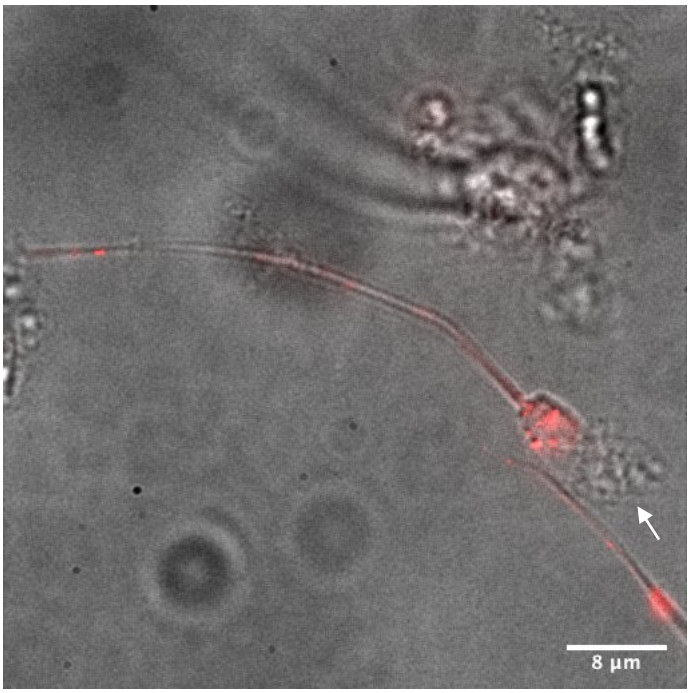

Figure A.II. TIRFM image showing boar sperm labelled with AlexaFluor647 post fixation, after 5 h of co-incubation with HEK293T-derived exosomes at a ratio of 100:1. Image shows evidence of AR as indicated by the white arrow next to the sperm head that has released its content due to the enzymatic degradation.

Appendix III

Technical Limitations of Sperm Imaging under Super-Resolution Microscopy (TIRFM/dSTORM)

There are many challenges encountered when imaging sperm cells with super-resolution microscopy. Unlike the majority of live cells, sperm cells are constantly swimming; when fixed, most sperm will possess a wavy flagellum. This, combined with the rounded morphology of the sperm head, creates certain limitations when imaging these cells under a microscope. This complication is even more evident when attempting to visualize exosome attachment since exosome-cell interaction relies upon imaging flat cells on the surface of the slide. For this reason, in the experiments in **Chapter 4.4.1** for the visualization of exosome-sperm interaction I have only been able to image sperm cells that were lying flat on the slide during fixation as they follow a slither motion; inevitably, this means that only a small number of sperm are suitable for this analysis (Nosrati et al., 2015). Hence, a quantitative analysis for exosome-sperm internalization would be a biased approach, because even when lying on the slide, these cells are not totally flat and cannot be imaged consistently across their entire axis. Therefore, out of caution, all I can provide at present is the quantification of exosome-sperm interaction involving both exosome attachment and internalization, as it is based upon positive sperm cells (those presenting at least one exosome, either attached or internalized) in order to give a more reliable measurement for exosome internalization, yet this analysis must be taken with caution since it presents a small sample size (n) of 20–50 sperm cells per time point.

Appendix IV

Research Output

Original research paper:

- **Vilanova-Perez T**, Jones C, Balint S, Dragovic R, L Dustin M, Yeste M, Coward K. 'Exosomes derived from HEK293T cells interact in an efficient and non-invasive manner with mammalian sperm *in vitro*' Nanomedicine (Lond). 2020 Aug;15(20):1965-1980.

Oral presentations at national and international conferences:

- "Capabilities of HEK293T-derived Exosomes for Mammalian Sperm" at Fertility 2021, online. (*Invited speaker*).
- "Development and Evaluation of Safety and Capabilities of HEK293T Cell-Derived Exosomes as a Non-Invasive Delivery Tool for Mammalian Sperm Cells" at ISEV 2019, Kyoto.
- "Exosomes for mammalian sperm cells: Assessing the impact of this novel tool for future clinical applications" at Fertility 2019, Birmingham. (*Awarded a prize for the best oral presentation by the Society of Fertility and Reproduction*).
- "Development of a Versatile Exosome-based Platform for the Delivery of Molecular Compounds to Mammalian Sperm" at BAS annual meeting 2018, London.

Poster presentations:

- "Exosomes derived from Human Embryonic Kidney 293T Cells as a Non-Invasive Delivery Tool for Mammalian Sperm" at Annual Oxford Developmental Symposium, 2019, Oxford.
- "Exosomes, a Bio-Compatible Delivery Platform for Mammalian Sperm Cells: a Non-Invasive Approach for the Transfer of Therapeutic Compounds" at ESHRE 2018, Barcelona.

Grants:

- St. Peter's College Foundation Student Awarded by St. Peter's College Alumni Fund, 2020
- Gustav Born Scholarship granted by St. Peter's College, 2019
- Travelling grant by the Society of Reproduction and Fertility, 2018